Molecular and cellular basis of Exogen and Anagen induction

Claire Alexandra Higgins

MOLECULAR AND CELLULAR BASIS OF EXOGEN AND ANAGEN INDUCTION

A Thesis Submitted In Part Requirement For
The Degree of Doctor of Philosophy

CLAIRE ALEXANDRA HIGGINS

Department of Biological and Biomedical Sciences
University Of Durham

2007

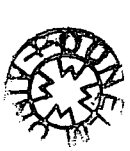

This thesis is entirely the result of my own work. It has not been accepted for any other degree and is not being submitted for any other degree.

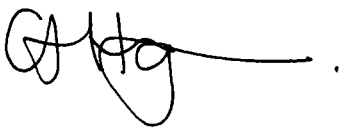

Claire Alexandra Higgins

September 2007

Acknowledgements

First and foremost I would like to thank my supervisors Professor Colin Jahoda and Dr Gillian Westgate for their support throughout. To Colin for giving me the opportunity to join his lab and for providing me with solid guidance and thoughtful criticism throughout. Also, to Gill for all the interesting discussions, and for the constant motivation. I'd like to thank people who have helped me along the way so thanks to Mr Dudley Ferdinando, Mr Tony Weaver and Mrs Christine Richardson for their help with all the different microscopy machines, and for all the hours spent teaching me to use them. Thankyou to Mrs Nikki Dunbar who sectioned the paraffin embedded human skin sections for me and to Professor Desmond Tobin for kindly giving me the dermal papilla cell line. Thanks to Professor Angela Christiano for enabling me to visit her lab to complete the microarray work, to Mr Vladan Miljkovic who carried out the hybridisation and scanning of the GeneChips, and to Dr Hisham Bazzi for helping me make sense of the results. Thanks to everyone in Lab 8 who were not just colleagues but friends also, and who made my time in Durham so enjoyable-the gym sessions, the basketball, the trips to the botanical gardens, and the picnics on rowing boats will all be fondly remembered. In addition to the social side I have to say thanks to Dr Gavin Richardson and Dr James Waters for their help with the sphere work and to Mrs Heather Crawford, Miss Beth Arnott and Mr Preyesh Parmar for helping me learn all the cell culture techniques. Thanks to Gavin for all the hours he spent in the basement at Newcastle University helping me pluck whiskers whilst I made him suffer listening to Manu Chao. My time spent in Bedford during my PhD was brief although I made some good friends there who will be fondly remembered, and rowing up and down the river every night with Claire, Vicky and Lydia kept me busy and was particularly enjoyable. Special thanks have to go to my parents who not only throughout my PhD, but throughout my whole academic career so far have been very supportive, believing in my abilities even when I was doubting myself. I also have to say thanks to Andy, who has been there when I needed to take my mind of the work, but also not been phased by the hours and hours that I spent at my desk by myself. Lastly, thankyou to the Biotechnology and Biological Sciences Research Council and to my industrial sponser for funding the project, without which the work could not have been carried out.

Abstract

The hair follicle has the unique capacity to pass through periods of growth, regression and rest before regenerating itself to restart the cycle. This dynamic cycling capacity enables animals to change their coats, and for hair length to be controlled at different body sites. While progress has been made on some of the outstanding questions in hair follicle biology, many of the cellular and molecular mechanisms involved in driving hair follicle cycling remain undiscovered. The first section of work in this thesis reports on the dermal papilla, an essential component of the hair follicle with a key role in follicle regeneration. Using hanging drop cultures spheres of human dermal papilla cells were created, and the expression of cytoskeletal and extracellular matrix components characteristic of intact papillae were analysed using immunohistochemistry and real time PCR. I found evidence that over time the gene and protein expression profiles of the papilla cell spheres became more representative of intact dermal papillae, although differences were seen between papilla cells strains derived from different individuals. I then demonstrated the inductive capability of human dermal papilla cells using this spherical model in an amputated follicle assay. This data provides some of the first evidence that cultured human dermal papilla cells can retain inductive capacity without having to be combined with other cell types. This induction phenomenon may also have relevance to anagen initiation and cycling. The second section of this thesis was concentrated on the process of club fibre shedding, now widely recognised as a phase of the follicle cycle known as exogen. The vibrissa follicle, with its predictable timing of club fibre loss, was first developed as a new model for exogen, and the structural and adhesive changes associated with the progression towards club fibre release were analysed using SEM and TEM. Combined with plucking experiments these showed club loss to be gradual process. The expression of proteins involved in cell adhesion, differentiation, communication and digestion, all potential mediators of fibre loss were examined around "young" and "old" club fibres using immunohistochemistry. To further assess the mechanism of exogen, and to search for signalling molecules microarray technology was utilised, enabling the identification of 75 genes that were associated with the process. Group analysis highlighted a particular role for proteases and their inhibitors in the retention and final release of the club fibre. Moreover, immunofluorescent analysis of the

results from the microarray identified a process of differentiation, specific to the cell layer surrounding the club fibre prior to club fibre release. This data provides evidence that the process of exogen is progressive, associated with maturation of the cells surrounding the club fibre, and terminating with the release of the club fibre. The processes involved in club fibre release are becoming more widely recognised as an important aspect of the hair cycle and this thesis is one of the first comprehensive pieces of work that analyses club retention and release as an active phase.

Table of Contents

List of Figures

List of Tables

List of Graphs

List of Abbreviations

a-SMA	Alpha Smooth Muscle Actin
ADAM	A disintegrin and a metalloprotease domain
Acth	Adrenocorticotropic hormone
Aqp5	Aquaporin 5
bHLH	Basic Helix Loop Helix
BDMA	Benzyldimethylamine
BMP	Bone Morphogenetic Protein
BSA	Bovine Serum Albumin
Cea	Carcinoembryonic antigen
Ctsl	Cathepsin-L
Cav2	Caveolin 2
CTE	Chronic Telogen Effluvium
CFI	Complement Factor I
cDNA	Complementary deoxyribonucleic acid
Cx26	Connexin 26
Cx30	Connexin 30
Cx43	Connexin 43
CRH	Corticotropin Releasing Hormone
dNTP	Deoxynucleoside triphosphate
DNA	Deoxyribonucleic acid
DP	Dermal Papilla
Dsg1	Desmoglein 1
Dsg3	Desmoglein 3
DAPI	Diamino-2-phenylindole
DEPC	Diethylpyrocarbonate
DDSA	Dodeoenyl succinic anhydride
EE	Early Exogen
EGF	Epidermal Growth Factor
EtOH	Ethanol
EDTA	Ethylenediamine tetraacetic acid
ECM	Extracellular Matrix

FADD	Fas death domain
FBS	Fetal Bovine Serum
FCS	Fetal Calf Serum
Fetub	Fetuin Beta
FGF	Fibroblast Growth Factor
FGF2	Fibroblast Growth Factor 2
GJB6	Gap Junction Beta 6
GAPDH	Glyceraldehyde 3-phosphate dehydrogenase
H&E	Haematoxylin and Eosin
HPA	Hypothalamic-Pituitary-Adrenal
ID3	Inhibitor of Differentiation 3
IRS	Inner Root Sheath
IL18	Interleukin 18
IF	Intermediate Filament
KLK5	Kallikrein 5
KLK7	Kallikrein 7
KLK8	Kallikrein 8
K14	Keratin 14
K6	Keratin 6
K6hf	Keratin 6 hair follicle
KAPs	Keratin Associated Proteins
KAP	Kidney Androgen Regulated Protein
LE	Late Exogen
MMP	Matrix Metalloprotease
mRNA	Messenger ribonucleic acid
MEM	Minimal Essential Medium
NCBI	National Centre for Biotechnology Information
Nrp2	Neuropilin 2
ORS	Outer Root Sheath
PBS	Phosphate Buffered Saline
PAI2	Plasminogen Activator Inhibitor 2
PCR	Polymerase Chain Reaction
PCNA	Proliferative Cell Nuclear Antigen

PI	Propidium Iodide
Pcsk5	Proprotein convertase subtilisin/kexin type 5
Prlr	Prolactin Receptor
Er	Repeated Epilation
RT-PCR	Reverse Transcriptase-Polymerase Chain Reaction
RT	Reverse Transcription
Rpm	Revolutions per minute
RNA	Ribonucleic acid
Rc	Rough Coat
RER	Rough Endoplasmic Reticulum
S100a4	S100 calcium binding protein a4
S100a6	S100 calcium binding protein a6
S100a8	S100 calcium binding protein a8
S100a9	S100 calcium binding protein a9
SEM	Scanning Electron Microscopy
Shh	Sonic Hedgehog
Spon-1	Spondin-1
SCCE	Stratum Corneum Chymotryptic Enzyme
SCTE	Stratum Corneum Tryptic Enzyme
Strep-AP	Streptavidin-Alkaline Phosphatase
SDC1	Syndecan 1
TUNEL	Terminal deoxynucleotidyl transferase-mediated dUTP-biotin nick end labelling
3D	Three-Dimensional
TIMP3	Tissue Inhibitor of Metalloprotease 3
TACE	TNFa converting enzyme
TGF	Transforming Growth Factor
TGFß	Transforming Growth Factor Beta
TA	Transit Amplifying
TEM	Transmission Electron Microscopy
TS	Trichilemma Sac
TK	Trichilemmal Keratin
TAE	Tris Acetate EDTA

TBS	Tris Buffered Saline
TNFa	Tumour Necrosis Factor alpha
2D	Two-Dimensional
Tnfsfr11b	Tumour Necrosis Factor Super Family Receptor 11b
VEGF	Vascular Endothelial Growth Factor

Chapter 1: General Introduction

1.1: Hair follicle morphology and the hair cycle

1.1.1: Morphogenesis and the hair cycle

During embryogenesis, morphogenesis of hair follicles occurs, predominantly controlled through reciprocal interactions between the mesenchymal and epithelial components of the skin (Hardy 1992). Throughout its lifetime the hair follicle renews itself in a cyclic fashion, transitioning through phases of active growth, regression and rest before regenerating to start the cycle again (Dry 1926; Chase 1954; Kligman 1959). This process of regeneration makes the hair follicle a unique and dynamic structure. During these three phases, respectively termed anagen, catagen and telogen, the lower portion of the follicle goes through cyclic changes, whilst the upper region of the follicle, including the sebaceous gland remains permanent (Dry 1926). The dynamic cycling ability of the hair follicle enables animals to change their coats dependent on season, and control the length of body hair from site to site (Stenn and Paus 2001). There are two mechanisms involved in the control of coat changes. The first process is the shedding of the old coat, whilst the second is the initiation of new fibre growth, to grow either a winter or summer coat. The process of shedding the old fibre has recently been proposed as a distinct phase (Stenn et al. 1998). In keeping with current terminology this phase has been described as the 'exogen' phase.

1.1.2: The Vibrissa follicle as a model system

The mystacial pad of whiskered mammals is one of the many locations on the body where vibrissa follicles, a subset of 'sinus follicles' are found. In addition to being highly adapted sensory follicles, they produce the largest fibres on the body. An outer collagen capsule surrounds and protects vibrissa follicles, distinguishing them from pelage follicles (Young and Oliver 1976). Moreover, vibrissa follicles contain both ring and cavernous sinuses, proposed to be sensory adaptations (Stephens et al. 1973). Three particular features of vibrissa follicles make them a popular model for use in research. The first is their large size which enables quantitative measurements and experimental manipulations relatively simple procedures to carry out. The second feature is their patterning, with follicles arranged in a consistent, well defined

positions on the mystacial pad (Danforth 1925). The third feature of vibrissa follicles, which makes them a popular model to work with, is the consistency of their growth cycle. This allows for follicles to be selected at precise stages to analyse aspects of the hair cycle, including exogen.

With regard to the follicle patterning, each follicle position was originally identified and named by Danforth. However, throughout this thesis the nomenclature used for labelling vibrissae has been taken from the labelling system defined by Oliver (1966a). Follicles are arranged in ventral to dorsal columns, numbered A to F respectively, and in posterior to anterior rows. The posterior to anterior rows are labelled from 1 to 5, a system which enables the identification of individual follicles with respect to their location (Figure 1.1). Moreover, corresponding locations on both the left and the right mystacial pads mirror each other in terms of their size and cycle stage (Ibrahim and Wright 1975). Whilst ventro-dorsal columns are relatively similar in terms of fibre length, they decrease in length along the horizontal axis (Ibrahim and Wright 1975). This is reflected in fibre growth rates which, although constant within follicles for the duration of anagen, decrease in growth rate postero-anteriorly (Ibrahim and Wright 1975).

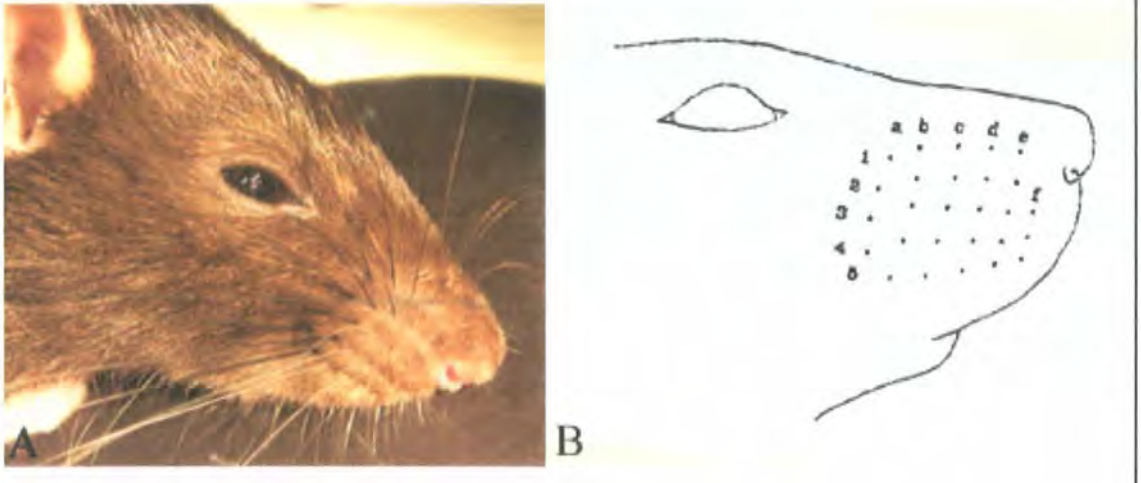

Figure 1. 1: The mystacial pad of a rat.
On a mystacial pad, vibrissa follicles are arranged in ventral-dorsal and posterior-anterior rows (A). These are labelled A-F and 1-5 respectively (B). Cartoon taken from Oliver, 1969.

1.1.3: Hair follicle morphology in anagen

At the base of the follicle is located the dermal papilla; an onion shaped mesenchymal component that protrudes up into the base of the hair follicle, separated from the epithelial component of the follicle by a basement membrane. The dermal papilla, a derivative of the embryonic dermal condensation is believed to retain some embryonic characteristics, especially that of induction (Oliver 1967). Continuing out around the base of the follicle are the cells of the dermal sheath. These also maintain inductive capabilities into adulthood and are progenitors in dermal papilla regeneration after removal of the lower follicle (Oliver 1966a; Horne and Jahoda 1992; Jahoda et al. 1992a). The epithelial component of the follicle that surrounds the base of the dermal papilla is the germinative matrix. These cells are the immediate precursors of the hair fibre. Below an imaginary line known as the 'Line of Auber', which falls across the widest section of the dermal papilla, the matrix is predominately undifferentiated yet highly proliferative (Auber 1952) (Figure 1.2). Above this line, in response to signalling from the dermal papilla the matrix cells begin to differentiate, initially forming precursor cells of the different follicle lineages. As these precursors migrate upwards they undergo specialised programmes of differentiation to form seven different epithelial lineages of the follicle (Legue and Nicolas 2005) (Figure 1.3). As the three central lineages, the medulla, the cortex and the cuticle form the hair fibre this fulfils the primary function of the follicle during anagen which is to produce a hair. Whilst the duration of anagen determines the length of the fibre, the size of the dermal papilla parallels fibre diameter (Van Scott and Ekel 1958; Ibrahim and Wright 1982; Elliott et al. 1999).

Surrounding the hair fibre are the three cell layers of the Inner Root Sheath (IRS), composed of the IRS cuticle which is adjacent to the hair cuticle, Huxley's layer and Henle's layer (Sengel 1976). The IRS undergoes a complex programme of differentiation in the anagen follicle with Henle's layer terminally differentiating shortly after formation. Further up the follicle, the cuticle differentiates followed lastly by differentiation in Huxley's layer, with all three layers undergoing desmosomal remodelling with terminal differentiation (Donetti et al. 2004). At the level of the isthmus, the IRS is degraded by proteolytic enzymes enabling the hair

shaft to enter the hair canal and emerge from the skin surface without injury. After IRS degradation, the companion layer, which moves up the follicle alongside the IRS and hair shaft, undergoes a specialised apoptosis mediated by keratinisation in the isthmus of the follicle (Tanaka et al. 1998). The Outer Root Sheath (ORS), the one lineage not formed from the matrix at the base of the follicle undergoes trichilemmal keratinisation where it faces the uncovered hair shaft (Pinkus et al. 1981) (Figure 1.2).

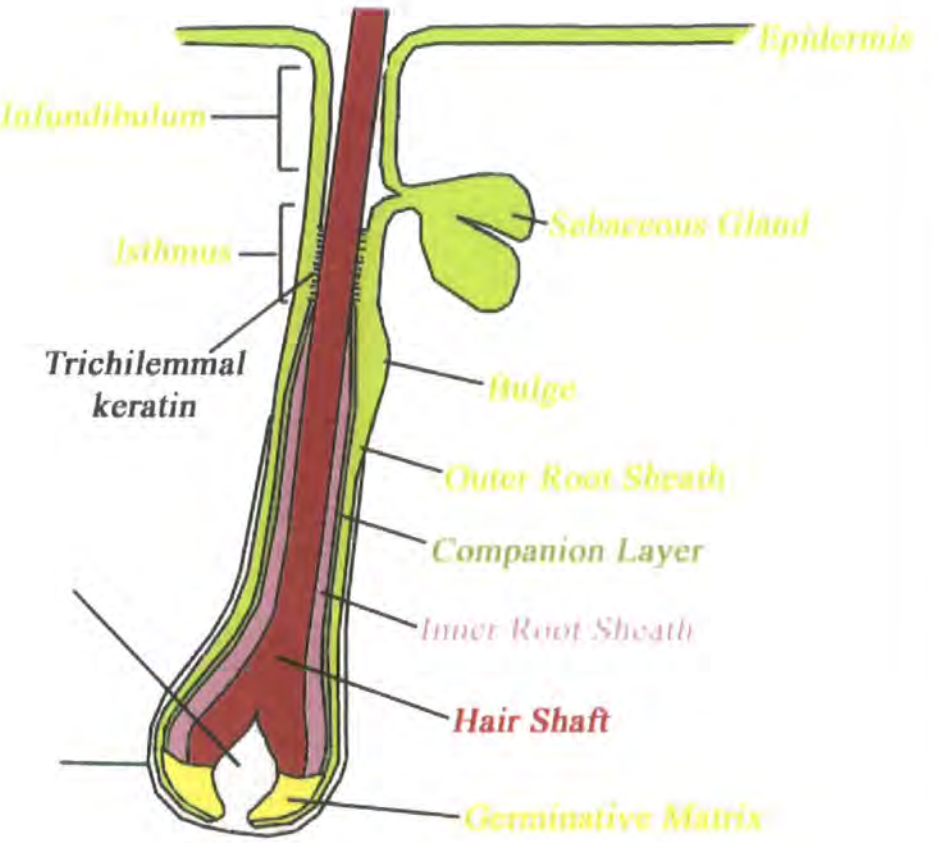

Figure 1. 2: Morphology of a hair follicle in anagen

Hair follicles are composed of several concentric layers which surround the hair shaft, forming the epithelial compartment of the follicle. At the base of the follicle sits the dermal papilla, which plays an important role in the initiation of hair growth through epithelial-mesenchymal interactions.

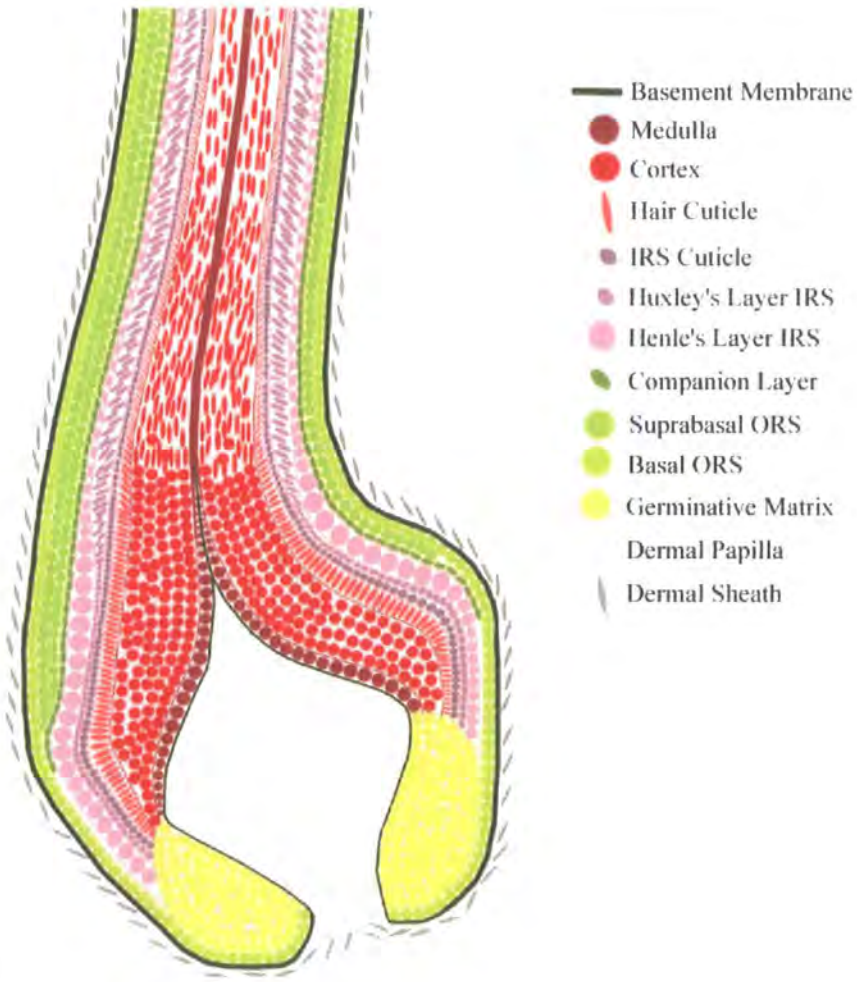

Figure 1. 3: Lineages of the hair follicle

The ORS is unique as it derived from downward growth from the bulge region of the follicle. This is in comparison to the remaining epithelial lineages of the hair follicle, from the companion layer through to the medulla which are derived from upwards growth from the germinative matrix at the base of the follicle, and are encased by the ORS. This is in response to signalling from the dermal papilla.

The companion layer was named after studies by Orwin in the Romney wool follicle identified a morphologically unique layer (Orwin 1971). It was originally described as the innermost layer of the ORS (Ito 1986; 1988). However, unlike ORS cells, companion layer cells do not express large amounts of glycogen nor do companion layer cells possess trichohyaline granules, which distinguishes them from the IRS (Rothnagel and Roop 1995). More recently, it has been demonstrated that this layer

more closely resembles the IRS than the ORS, both morphologically and biochemically (Winter et al, 1998) and that it originates from the upper germinative matrix in line with the IRS (Gu and Coulombe 2007). Nevertheless, it is regarded as the slippage plane between the ORS and IRS which allows progression of the IRS and hair shaft up the follicle during anagen. The companion layer remains attached to the IRS via structures termed 'Flugelzellen', described in human, marsupial and mouse hairs, which extend from Huxley's layer through Henle's layer and link to the companion layer through numerous desmosomes (Clemmensen et al. 1991; Langbein et al. 2002; Alibardi 2004; Gu and Coulombe 2007). These tightly bind the companion layer to the IRS, so that it accompanies the IRS and hair shaft as they move up the follicle. In addition to morphological differences, the companion layer is distinct from the ORS and IRS immunohistochemically, reflecting an individual program of differentiation. It has a unique keratin profile from the surrounding IRS or ORS, expressing a companion layer specific keratin, Keratin 6 hair follicle (K6hf) (Winter et al. 1998; Wang et al. 2003) recently renamed K75 (Schweizer et al. 2006). Electron microscopy studies have indicated the presence of a barrel of transversely orientated intermediate filaments which lie on the inner side of the companion layer, thought to provide support for the IRS, protecting it from the compressive forces of the expanding ORS (Ito 1989). The importance of the structural support provided by the companion layer is demonstrated by alterations in K6. Transgenic expression of a mutated K6a gene in mice results in disturbed intermediate filament organisation (Rothnagel et al. 1994; Wojcik et al. 1999). This compromises hair shaft structure and can lead to alopecia (Rothnagel et al. 1994; Wojcik et al. 1999)

The ORS compartment of the anagen follicle surrounds the companion layer and at the follicle neck, merges into the basal layer of the epidermis (Chase 1954). It is distinct from the other epithelial components as it does not derive by upwards growth from the germinative matrix, but rather directly from the bulge, a stem cell niche in the permanent portion of the follicle (Cotsarelis et al. 1990). The bulge is a cluster of cells, identifiable in rodents due to its prominent morphology (Cotsarelis et al. 1990). Up until recently the location of the bulge in human follicles was unclear, as it is not morphologically distinct like the bulge in rodent pelage follicles. However, identification of unique bulge markers in the human follicle has enabled the human

anagen bulge to be defined as a distinct region (Lyle et al. 1999; Ohyama et al. 2006). In vibrissa follicles the cells of the bulge are believed to be derived from the neural crest (Sieber-Blum et al. 2004; Wong et al. 2006) whilst in trunk skin neural crest derivatives are restricted to glial and melanocyte lineages (Wong et al. 2006). Bulge cells have stem cell potential, demonstrated in lineage studies showing them to be capable of forming all epithelial cell types of the follicle (Morris et al. 2004).

1.1.4: Morphological aspects of the hair cycle

Hair follicle cycling is driven in response to continuing interactions between the mesenchymal compartments and the epithelial components of the follicle, with a complex array of signals and genes involved (Botchkarev and Kishimoto 2003; Rendl et al. 2005). There are also distinct morphological changes associated with the transition through the hair cycle, as the follicle progresses through the cycle stages anagen, catagen and telogen (Figure 1.4).

The duration of anagen, the period of active hair growth of the follicle and hair fibre production is dependent on a variety of factors that vary with body site and species (Kligman 1959). In mouse pelage the anagen phase, which has been subdivided into six substages termed anagen I-VI (Chase *et al*, 1951) has a duration of approximately 1-3 weeks compared to human scalp where anagen can last several years (Kligman 1961).

The beginning of anagen (as observed in mouse skin) is associated with an increase in dermal papilla cell number, due mainly to an influx of dermal sheath cells that have been actively proliferating. This increase in cell number, associated with an increase in both cell size and extracellular matrix material, doubles the volume of the dermal papilla (Tobin et al. 2003). Signalling from the dermal papilla is critical in determining the fate of the overlying epithelial cells, which form the hair shaft surrounded by various supporting lineages, although the exact mechanisms for this positional information flow are not known. At the end of anagen the lower epithelial component of the follicle degenerates and enters the catagen phase of the cycle. Catagen, which is the transition between the active and the resting stages of the hair

cycle has been further divided into eight sub-phases starting with late anagen taking the follicle through to telogen (Muller-Rover et al. 2001).

At the initiation of catagen the dermal papilla is transformed to a relatively quiescent cluster of cells, with a 45% reduction in cell volume due to both the loss of extracellular matrix material and cell numbers (Tobin et al. 2003). The dermal papilla withdraws its fibroblast projections from the basement membrane (Derweet et al. 1982) but rather than undergoing apoptosis to decrease cell number (Lindner et al. 1997) papilla cells migrate out into the connective tissue sheath, where some cells are apoptotic whilst others are 'lost' (Tobin et al. 2003), perhaps into the dermis to replace dermal fibroblasts (Jahoda 2003). Evidence for this loss and recruitment of dermal papilla cells has been documented in mouse skin, although it has yet to be found in human skin.

In most follicles types, with the exception of vibrissae, the initiation of catagen is characterised by a cessation of mitotic activity in the matrix cells of the bulb, replaced by programmed cell death (Lindner et al. 1997). In all follicles the production of medulla cells stops early in catagen and the remaining hair precursor cells differentiate to form the base of the hair shaft, (Roth 1965; Parakkal 1970; Pinkus et al. 1981) now termed a 'club' fibre. The club fibre is formed from cortical and cuticle cells only, with no medulla cells present. IRS differentiation is also arrested with the IRS predominant and thickened just above the level of the club base (Muller-Rover et al. 2001). Orwin, (1967) observed a flattened double layer of cells continuous with the apparent demarcated IRS around the base of the forming club fibre. This raises the question of which cells of the follicle become finally associated with the club fibre. As the club fibre migrates up the follicle, a germ capsule, derived from ORS cells and termed the 'trichilemma sac' forms around the base of the club fibre. The dermal papilla, still in the subcutaneous fat layer of the skin is separated from the club fibre by an epithelial strand, around which is a thickened convoluted basement membrane, termed the glassy membrane, a characteristic feature of catagen follicles (Parakkal 1970). In catagen, apoptosis in the epithelial strand (Lindner et al. 1997) is proposed by Stenn to create an 'apoptotic force' that draws the dermal papilla up to just beneath the club fibre in the dermis (Stenn et al. 1998), leaving

behind a trailing connective tissue sheath called the streamer or stele. Once the dermal papilla is adjacent to the club fibre and secondary hair germ, the follicle has entered the resting phase, telogen.

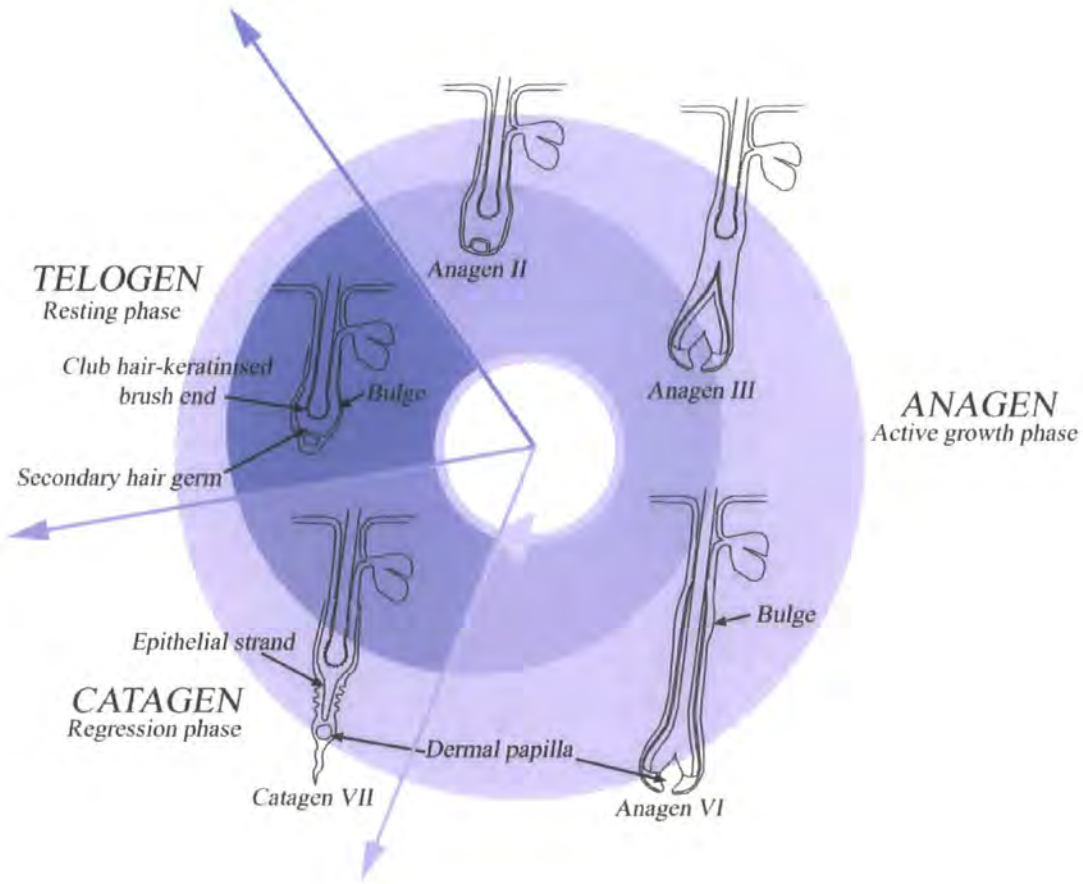

Figure 1. 4: The mouse pelage hair cycle

During the hair cycle, the lower half of the follicle undergoes complex structural rearrangements, as it is destroyed during the catagen phase but reformed during anagen. Catagen and anagen are separated by telogen, often described as the resting phase of the cycle. The initiation of anagen is characterised by the downward growth of the follicle to surround the dermal papilla. After this initiation, epithelial cells derived from the germinative matrix move upwards undergoing complex differentiation programmes to form the lineages of the hair follicle, which is still elongating down into the subcutis layer of the skin. Catagen is a destructive phase, characterised by release of the hair fibre which moves up the hair follicle. During telogen, signalling from the dermal papilla to the secondary hair germ initiates the start of the new hair cycle, the beginning of anagen.

In human follicles the catagen phase lasts approximately two weeks across most body sites and follicle types (Kligman 1959). However, the duration of telogen varies with body site with the phase lasting approximately three months in scalp follicles (Price and Griffiths 1985). This is in contrast to trunk follicles where the duration of telogen is much longer, lasting approximately twice the duration of the anagen phase (Saitoh et al. 1970; Seago and Ebling 1985). Whilst in humans the loss of the club fibre usually occurs before the new anagen fibre has emerged above the skin surface (Rook and Dawber 1982) club fibres in other mammals are mostly retained through the entire next cycle (Dry 1926).

During telogen, dermal papilla cells are morphologically rounded, with high nuclear to cytoplasmic ratios (Tobin et al. 2003), whilst the secondary hair germ is located at the periphery of the follicle bulb during this cycle stage. The initiation of the anagen phase from telogen is believed to be regulated in a similar manner to morphogenesis of the follicle, with the signal being initiated in the mesenchymal component of the follicle; the dermal condensation during morphogenesis and the dermal papilla during anagen initiation. Whilst the predetermination hypothesis believes the signal is directed to the secondary hair germ (Panteleyev et al. 2001), the bulge activation hypothesis originally proposed that the signal acts upon the bulge (Cotsarelis et al. 1990; Sun et al. 1991). This bulge activation hypothesis was later refined proposing that the signal acts upon the secondary hair germ (Ito et al. 2004). However, the origin of this secondary hair germ, which has a role in anagen initiation, is under dispute. The predetermination hypothesis of anagen initiation proposes that the secondary hair germ is derived from a population of germinative cells in the bulb of the follicle, that are sustained through the degenerative catagen phase of the follicle (Panteleyev et al. 2001). It proposes that this germ population is derived from the bulge progenitors in the previous anagen cycle stage, a viewpoint supported by the localisation of two K19 stem cell reservoirs in the human anagen follicle both in the bulge and the bulb of the follicle (Commo et al. 2000). However, the refined bulge hypothesis proposes that the secondary hair germ is formed at the termination of catagen, as a subset of bulge cells (Ito et al. 2004). Although secondary hair germ cells are biochemically distinct from the bulge they are able to replenish the bulge

population after depletion (Ito et al. 2002). This suggests that the secondary hair germ and bulge populations are closely related.

Bulge cells are capable of forming all epithelial lineages of the follicle (Morris et al. 2004). In a follicle with a short anagen duration such as mouse pelage the proliferative capacity of the germinative matrix is sufficient to sustain the follicle through its growth phase. However, in follicles with a longer anagen duration such as the human scalp follicle, or in specialised vibrissa follicles it is believed there is a continuous migration of precursor cells from the bulge down the ORS, which replenish the population of germinative matrix cells at the base of the follicle (Oshima et al. 2001). This stem cell trafficking theory, proposed by Oshima *et al* is supported in the both vibrissae and human follicles by the clonagenic potential of ORS cells at all heights of the follicle (Rochat et al. 1994; Oshima et al. 2001).

1.1.5: The hair cycle in the Vibrissa follicle

Although the anagen phase is similar in vibrissa and pelage follicles, vibrissae are distinct from pelage follicles as the duration of catagen and telogen make only a brief contribution to the cycle, being less than three days in total (Ibrahim and Wright 1975). Moreover, unlike pelage follicles which shorten during catagen, no upward movement of the papilla is observed in vibrissa follicles (Young and Oliver 1976). Unique also to vibrissae, is their predictability of timing throughout the cycle. Vibrissa follicles often have two fibres, a retained club fibre and a growing fibre. As fibres grow to a predetermined length (Dry 1926), the relative lengths of the two fibres can be compared to specifically identify follicles at various cycle stages. Moreover, follicles can be specifically selected a time points right through from club fibre formation through to club fibre release to analyse this aspect of the hair follicle.

1.2: Molecular Basis of the Hair Cycle

Cross talk between the dermal and epithelial compartments of the follicle during hair follicle cycling mediates aspects of hair cycling. Various signalling molecules have been implicated in controlling different aspects of the hair follicle cycle. Whilst the

transforming growth factor beta (TGFß) family has been implicated with a role in the anagen-catagen transition the Wnt/ß-catenin and Sonic Hedgehog (Shh) signalling pathways have been shown to have functions in the reactivation of the follicle in the telogen-anagen transition. After the telogen-anagen transition the Wnt/ß-catenin, Bone Morphogenetic Protein (BMP) and Notch signalling pathways are believed to contribute in the transition of matrix cells to a terminally differentiated hair follicle lineage (reviewed by Blanpain and Fuchs 2006). During anagen initiation the dermal papilla cells expresses the BMP-inhibitor Noggin, also permissive for Lef1 expression and Wnt signalling.

The cross talk between the mesenchymal and epithelial components has been studied extensively and in the adult follicle is thought to be modulated by proteoglycans, acting to enhance or inhibit the activities of growth stimulators (Botchkarev and Kishimoto 2003). During the hair cycle, there are large changes in the volume of the dermal papilla, largely as a result of alterations to the extracellular matrix components between cells. The chondroitin sulfate proteoglycans versican and bamacan, which are highly expressed in the anagen papilla, decrease during the transition to catagen becoming virtually absent in the telogen dermal papilla (Couchman et al. 1990; du Cros et al. 1995; Harris and Jahoda 2001; Soma et al. 2005). In contrast the proteoglycan perlecan is expressed in the dermal papilla throughout the hair cycle (Couchman et al. 1990). Various roles in signal transduction or the sequesterisation of signals are proposed for this family of proteoglycan molecules (Botchkarev and Kishimoto 2003).

1.2.1: The Dermal Papilla

A key component of the hair follicle, the dermal papilla has been implicated with a fundamental role in hair follicle cycle transitions, with the initial signal for anagen initiation believed to arise here. The dermal papilla is derived from the dermal condensation during hair follicle development and is believed to retain some embryonic characteristics. This is evidenced by the ability of dermal papilla from rodent and human follicles to retain inductive capabilities when isolated from the remaining follicle, and to induce new fibre formation (Oliver 1967; Jahoda et al.

2001). Moreover, rodent dermal papillae have been demonstrated to induce *de novo* follicle formation (Jahoda 1992).

Dermal papillae can be readily dissected and propagated to form cell cultures, thus expanding the dermal papilla cell population. In culture, dermal papilla cells propagated from vibrissa follicles retain elements of embryogenesis, and are able to aggregate into a clump that appears morphologically similar to a mesenchymal aggregation (Jahoda and Oliver 1984c). The inductive capabilities of cultured dermal papilla cells, isolated from rodent vibrissa and pelage follicles, demonstrates the retained embryonic properties of these cells (Jahoda et al. 1984; Horne et al. 1986; Jahoda et al. 1993). There is also evidence that dermal papilla cells have stem cell like potential as evidenced by their capacity to differentiate into bone, adipocyte, skeletal and neuronal lineages in culture (Jahoda et al. 2003; Richardson et al. 2005; Rufaut et al. 2006).

Although often exploited in research, cultured dermal papilla cells are limited in their function as a representative model of the dermal papilla. Key differences between dermal papilla cells *in vivo* and *in vitro* are seen in both alpha smooth muscle actin (aSMA) expression and in their mitotic activity (Jahoda and Oliver 1984c; Jahoda et al. 1991). Moreover, cultured dermal papilla cells have a limited lifespan in culture (Messenger et al. 1986), and over time lose their previously mentioned inductive capabilities.

1.3: Exogen: A new phase of the hair cycle

Molecular factors regulating the transition between the key stages of the hair cycle, anagen, catagen and telogen are well documented in the literature (Paus et al. 1999; Muller-Rover et al. 2001; Stenn and Paus 2001; Stenn 2005; Alonso and Fuchs 2006; Blanpain and Fuchs 2006). However, more recently, a fourth stage in the hair cycle has been proposed relating to the loss of club hairs from the follicle (Figure 1.5). Although considered to be independent from the rest of the hair cycle, this stage was termed 'exogen' by Stenn, in context with the accepted hair terminology (Stenn et al. 1998; Milner et al. 2002). This stage relates to the loss of the club fibre from the

follicle, with 'exogen' describing an active process involving the signals for shaft release, in addition to shaft release itself. As well as exogen, the term 'teloptosis' has been introduced into hair terminology, derived from the Greek for 'falling off', and relates to both a loss of cellular adhesion in the cells surrounding the club fibre and the subsequent loss of the fibre (Pierard-Franchimont and Pierard 2001). Although the signals that regulate transitions through the hair cycle are well known, currently there has been no signal detected that initiates exogen.

Although the loss of club fibres occurs in the vast majority of all hairy mammals, very little is known about this stage of the hair cycle. There are still two schools of thought on the process of hair shedding; the first being that hair shedding is a passive process caused by a physical force exerted by the next growing fibre which dislodges the club fibre (Segall 1918; Kligman 1961). Evidence supporting this notion also comes from the observation that in mice, several small fibres can be present in a follicle at one time, whilst with larger fibres, fewer are present, indicating that limited space in the epithelial sac may influence the retention of club fibres (Dry 1926). In contrast, in humans, it is considered to be unusual for club fibres to be retained through subsequent anagen phases (Rook and Dawber 1982).

A second, and perhaps more compelling proposal, is that hair shedding, or exogen is an active process with specific signals controlling the breakdown of cellular adhesion between the club fibre and its surrounding epithelial sac, leading to the release of the hair shaft from the follicle some time after telogen is completed (Stenn et al. 1998; Milner et al. 2002). Evidence for this includes the accumulation of a large number of vellus telogen hairs on the face seen with the condition *Trichostasis spinulosa* (Chung et al. 1998), or the absence of club fibres in telogen follicles leaving them empty as seen in trichograms of human scalp (Courtois et al. 1994; 1995), and in several breeds of domestic sheep (Auber and Burns 1947). These observations suggest that more than just a mechanical stimulus from a new growing fibre is required to trigger exogen. This argument is also based on the observation that the timing of exogen can be controlled, as in the seasonal moult of animals, or entered prematurely, as seen in cases of immediate telogen release (Headington 1993), a type of telogen effluvium seen with treatments such as minoxidil (Bamford 1987; Bardelli and Rebora 1989).

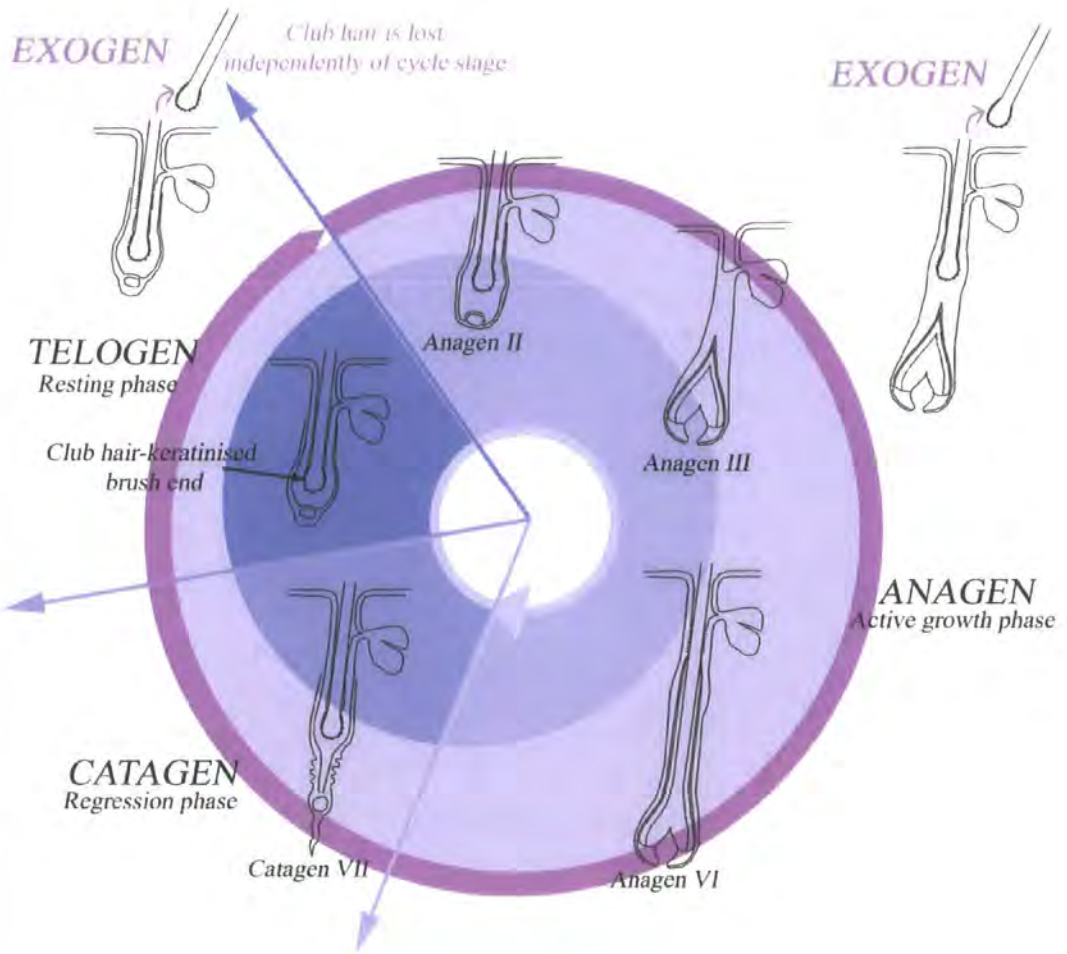

Figure 1. 5: A new stage of the hair cycle; Exogen

Exogen was introduced into hair cycle terminology in 1998 (Stenn et al. 1998). It refers to the active release of the club fibre from its epithelial sac and is regarded to be independent from the rest of the hair cycle stages. In humans some consider that exogen occurs during the transition from telogen to anagen, or in early anagen, before the tip of the new anagen fibre reaches the scalp skin surface. However, phototrichogram technology is not developed to identify vellus fibres, and hence the tips of new growing fibres alongside a retained club fibre would be difficult to identify. In contrast, in mice it is usual for club fibres to be retained from previous growth cycles, and for the growing fibre to be visualised next to them. Shedding peaks in mouse pelage follicles are thought to be coupled to anagen (Milner et al. 2002). However, the only follicle in which exogen is a relatively predictable event is the vibrissa follicle, where the club fibre is retained through the next anagen phase, but lost prior to the onset of catagen (Dry 1926; Ibrahim and Wright 1975).

1.3.1: Formation and anchorage of the club fibre in its epithelial sac

The stimulus for entry into catagen, and hence the formation of a club hair, can occur several months before exogen occurs, with variations in the duration of club fibre retention dependent on species and body site (Johnson 1972; Randall and Ebling 1991). If not to be shed, but actively retained, club fibres are firmly anchored in the follicle, with the force required to remove them being similar to that required to extract an anagen fibre from its follicle (Chapman 1992).

A developing club fibre is characterised by a brush like appearance at is proximal end, which is due to an electron dense non-nucleated layer, termed 'trichilemmal keratin' forming the base of the fibre (Maurer 1895). The trichilemmal cells are not derived from the hair fibre itself (Vandevelde and Allaerts 1984) but rather form an envelope around the base of the fibre and are described as 'fused' onto the club fibre, although the mechanism by which this occurs is not yet understood (Pinkus et al. 1981). Many electron dense processes of the trichilemmal keratin layer are seen to extend outwards and in-between the cells of the surrounding ORS, and along with numerous desmosomal contacts in this location, are thought to secure the club fibre in place (Pinkus 1969; Pinkus et al. 1981). The dogma is that the trichilemmal keratin layer of the club fibre originates from the surrounding ORS (Pinkus et al. 1981). However, some researchers have described this layer as IRS derived (Lavker et al. 1998) and hence the origin of the trichilemmal keratin remains unclear. Moreover, the innermost layer of ORS cells that surrounds the club fibre has many similarities with the companion layer of the growing fibre. Whether this layer is a cycle derived manifestation of the companion layer or if it is independently formed is unclear. Throughout this thesis, the term '$\underline{\text{companion}}^{CL}$' will be used to distinguish this innermost layer surrounding the club fibre from the companion layer of the anagen follicle.

On analysing club fibres after they have been shed Kligman observed variations in the amounts of material attached to club ends (Kligman 1961). Kligman concluded that the majority of club fibres shed appeared to have no sheath attached, although a few were seen with epithelial sacs. The latter were regarded as prematurely shed fibres, whilst those with no sheath attached were considered to be mature clubs, ready

for natural shedding (Kligman 1961). More recently, differences between club fibres have been characterised, with distinctions between retained clubs (termed telogen clubs) and exogen club fibres being identified in both human scalp and mouse pelage follicles (Milner et al. 2002; Van Neste et al. 2007). Exogen clubs, as described by these authors are analogous to Kligman's mature club fibres. It has been shown that exogen club fibres from mouse pelage follicles have very few cells attached, which lack cytological detailing and have destroyed intercellular attachments. In contrast, plucked telogen club fibres have many surrounding cells that have prominent nuclei and abundant cytoplasms. The loss of cytological detailing in the cells surrounding exogen club fibres is thought to be indicative of a proteolytic degradation mediated release (Milner et al. 2002).

1.3.2: The importance of a club fibre

In 1972, Johnson described the changing coat properties of small animals in relation to hormonal and seasonal factors, and it is clear from this early work that the production of a stable telogen phase in the absence of hair shedding is important in many mammals. The simplest shedding cycle observed is the seasonal moult which can occur once or twice a year, enabling animals to change their coat thickness or colour quickly for summer or winter (Ryder 1965; Johnson 1972). In mammals with a seasonal moult, the retention of the telogen club hair in the skin between moults is essential as this forms the majority of the coat, protecting the animal from heat loss, trauma, infestation and sunlight (Johnson 1972; Stenn and Paus 2001). In laboratory rats and mice which are domesticated and lack a seasonal influence, telogen club shedding and hair growth cycles are observed in waves along the length of the body and are continuous throughout the year (Ebling and Johnson 1964). With both seasonal and non-seasonal animals, stable telogen follicles with 1-2 club hairs are found in adjacent sites. Change occurs over substantial areas of the coat in a wave pattern, without loss of the covering of hair indicating that club hairs can be retained for long periods and throughout one or more hair cycles. In contrast, man has what is described as an irregular, mosaic shedding pattern, where each individual follicle acts independently of those surrounding it (Chase 1954; Kligman 1959).

Whilst moult waves are obvious in animals, seasonal shedding is also observed in humans with a spring and autumn moult being observed on the thigh in some individuals, whilst just one moult cycle, during autumn is observed on the scalp (Randall and Ebling 1991). Instead of a noticeable moult, humans tend to lose hairs from all over the scalp so that they appear to retain a full head of hair (Harrison and Sinclair 2002). This is important since in humans hair is a social signature and required for both sun protection and camouflage (Stenn and Paus 2001). Of 100,000 follicles on the average scalp, approximately 4-14% of follicles are in telogen with 1% in catagen and the remaining follicles in anagen (Rook 1965). In contrast, the torso and thigh have up to 50% of hairs in telogen, where a light covering of vellus-like hairs from follicles with short anagen durations are found (Seago and Ebling 1985; Blume et al. 1991; Randall and Ebling 1991).

In man, especially on the scalp, the retention of telogen club hairs is of little consequence until the factors driving hair loss conditions such as male and female pattern hair loss lead to excessive hair shedding. Premature hair loss and excessive hair shedding in humans can have many negative psychological and psycho-social effects (Cash 1992; Cash et al. 1993; Cash 1999; Williamson et al. 2001; Schmidt 2003; Hadshiew et al. 2004; Hunt and McHale 2005). Moreover, in animals, the premature loss of club fibres can be disastrous. Understanding the relevant retention mechanisms of the telogen club fibre and the controls and triggers for exogen could be invaluable in identifying therapeutic routes to stabilise the shedding process and retard telogen effluvium.

1.4: Mouse models revealing information on club formation and retention and release

In order to analyse the process of exogen, and to decide upon a route of study, mice exhibiting alterations relating to club fibre development and retention were analysed. A variety of transgenic, knockout and naturally occurring mutant mice show altered club fibre formation, retention and release. Information drawn from them, in context with the other literature was used to decide upon areas that may be important in the context of exogen, and merited further investigation within this thesis.

Type II wool IF transgenic mouse

A cyclical hair loss phenotype is observed in transgenic mice that overexpress a wool *type II intermediate filament* (IF) in their hair cortex (Powell and Rogers 1990). These mice first exhibit hair loss at 19 days corresponding with the onset of telogen (Dry 1926), and thereafter show progressive hair re-growth and hair loss (Figure 1.6). Structural analysis of the hair fibres shed from these mice showed that club fibres were broken just above the club shaped end rather than being shed completely. Analysis of the keratin composition in hairs from these mice showed a decrease of sulphur protein and tyrosine protein groups (Powell and Rogers 1990), constituents that form the keratin associated proteins (KAPs) which act as a matrix to embed IF proteins (Powell et al. 1986). The authors hypothesised that an alteration in the keratin constituents of the hair fibres leads to enhanced fragility of club fibre ends, whilst anagen hairs are seemingly not broken (Powell and Rogers 1990).

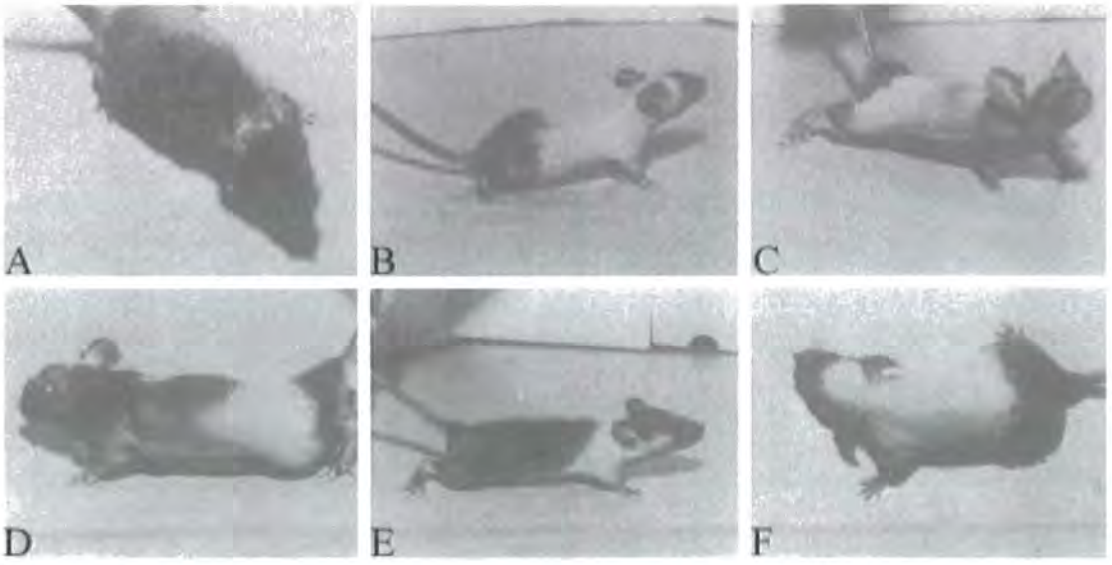

Figure 1. 6: Cyclic hair loss in the type II wool IF transgenic mouse

Consecutive photographs show the wave like pattern of hair loss (A-C) in an anterior of the ventral and dorsal regions towards the tail. Regrowth occurs in the same direction (D-E), succeeded by a subsequent hair loss cycle (F). Pictures taken from Powell and Rogers, 1990).

Cathepsin-L knockout mouse

Cathepsin-L (Ctsl) is a lysosomal protease with functions in maintaining a balance between proliferation and terminal differentiation of the epidermis. Mice generated with a targeted disruption of the *ctsl* gene, which is co-allelic with the *furless* mutation with a similar phenotype (Green 1954), have a pathological phenotype of the epidermis due to epidermal thickening, whilst also exhibiting cyclical hair loss. This corresponds with hair loss in the telogen stage of the hair cycle (Roth et al. 2000). The loss of the lysosomal protease Ctsl seems to disturb hair cycling causing prolonged catagen, yet a truncated telogen phase (Roth et al. 2000). Normal terminal differentiation is observed within the IRS although the subsequent sloughing of the IRS in the isthmus is delayed. *Ctsl-/-* mice also exhibit a default during club fibre development which results in a defective anchorage and subsequent premature loss of the club fibre (Tobin et al. 2002). Club fibres in these mice are distinct from the wild-type as they have a poorly formed trichilemmal keratin layer, and therefore an absence of anchoring rootlets and desmosomal contacts (Tobin et al. 2002). TEM of club fibres from *Ctsl-/-* mice also show the persistence of Huxley's layer of the IRS in the club fibre, which has failed to keratinise (Tobin et al. 2002).

Notch-1 transgenic mouse

Mice with overexpression of *Notch-1* in the IRS, driven by an involucrin promoter, exhibit club fibre shedding, although it is associated with the onset of the anagen phase of the hair cycle (Uyttendaele et al. 2004). Moreover, vibrissa follicles prematurely lose their club fibres and only exhibit one fibre, a growing fibre in the Notch-1 transgenic mouse (Uyttendaele et al. 2004), when it is usual for vibrissae to have both a growing and a club fibre positioned alongside each other (Young and Oliver 1976). *Notch-1*, implicated with a role in the commitment of keratinocytes to terminally differentiate (Rangarajan et al. 2001; Okuyama et al. 2004), delays differentiation of the IRS when overexpressed in transgenic mice whilst causing premature differentiation in the suprabasal epidermis (Uyttendaele et al. 2004). Transgenic mice overexpressing *Notch-1* have defective development of club fibres, with a resultant club fibre lacking the usual anchoring protrusions (Figure 1.7) seen on the trichilemmal comb surrounding the fibre (Uyttendaele et al. 2004). However,

these club fibres do not fall during telogen but rather with the onset of the anagen wave of growth of the follicle giving rise to an anagen wave of hair shedding (Uyttendaele et al. 2004).

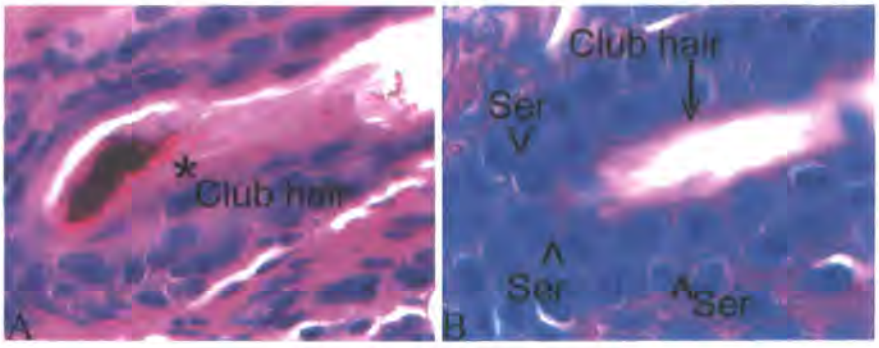

Figure 1. 7: Club fibre formation in the *Notch-1* transgenic mouse

Club fibres formed during the catagen phase of a pelage hair follicle in a *Notch-1* transgenic mouse are improperly formed, and are not surrounded by the usual trichilemmal keratin comb (A). This is in contrast to the trichilemmal keratin anchoring serratations (Ser) observed surrounding club fibres from control mice (B). (Pictures taken from Uyttendaele et al, 2004)

Msx2 knockout mouse

Kilgman stated that cases of telogen effluvium were as a result of premature anagen termination or catagen onset which results in the defective formation of a club fibre (Kligman 1961). Although not always the case, premature entry into catagen often results in a hair loss phenotype, an example of which is seen in the *Msx2* knockout mouse, where a cyclical hair loss phenotype is observed in a synchronised wave along the body, corresponding with club fibre formation (Ma et al. 2003). Follicles in this mouse have a shortened anagen phase, and prematurely enter catagen which is then prolonged (Satokata et al. 2000). Msx2 is a member of the homeobox family, involved in signal transduction and is required for proper differentiation of the hair shaft and surrounding cuticle (Ma et al. 2003). Although no morphological differences were seen in the shed club fibres between *Msx2*-/- mice and wildtype mice, defects during club fibre formation were proposed to cause the resultant hair loss observed (Ma et al. 2003).

Stratifin mutant mouse

Of interest with regard to club fibre loss are mice with a mutation in Stratifin, which underlies the repeated epilation (*Er*) phenotype seen in heterozygous *Er/+* mice (Herron et al. 2005; Li et al. 2005). Mice with a mutation in Stratifin typically lose their hair at the end of the growth phase (Herron et al. 2005). The timing of hair loss is concurrent with the onset of club fibre formation although no work has been published confirming if club fibres are lost in this mouse, or relating to the structure of club fibres in mice with a Stratifin mutation. Stratifin, an epithelial cell marker is a member of the conserved 14-3-3 protein family, and has a proposed role regulating epidermal differentiation (Olsen et al. 1995; Rufaut et al. 1999; Herron et al. 2005). In an induced cycle in the wool follicle, messenger Ribonucleic acid (mRNA) expression of Stratifin has been localised throughout the epidermal portion of the anagen follicle, being downregulated during the telogen phase (Rufaut et al. 1999). A hypothesised role of Stratifin in regulating the differentiation of trichocytes in the wool follicle has been proposed, mediated in part through protein kinase C (Rufaut et al. 1999). This suggests that a mutation in Stratifin would lead to a structurally weakened club fibre, in terms of trichilemmal anchorage protrusions or in regards to the strength of the fibre itself.

Hairless mutant mouse

Mice with a mutation in the hairless gene show normal hair morphogenesis but lose their hair prematurely coinciding with the onset of club fibre formation (Orwin et al. 1967). This is attributed to a combination of reasons, the first being loss of anchorage due to the continued presence of a thick IRS surrounding the club fibre and therefore no trichilemmal keratin layer to anchor the club fibre (Orwin et al. 1967; Panteleyev et al. 1999). Uncharacteristic disintegration of the ORS in the isthmus region allows the unanchored club fibre to move up the follicle, whilst a dilated infundibulum allows final loss of the club fibre. Thus it would seem that all these factors contribute to fibre retention. In comparison to mice with a mutation in hairless, knockout mice exhibit both hair loss and wrinkling of the skin with 14 genes implicated in terminal differentiation, including Caspase 14, Neuropsin, and Connexin 43, upregulated in their epidermis (Potter et al. 2001). The *hairless* gene encodes a zinc transcription

factor that acts as a transcriptional corepressor for thyroid hormone receptors (Potter et al. 2001). In the wildtype mouse, *hairless* is expressed throughout the IRS during anagen decreasing with terminal differentiation of Huxley's layer, and in the trichilemmal keratin during club fibre formation in catagen, decreasing on the completion of club fibre formation (Panteleyev et al. 2000)

Rough coat mutant mouse

The rough coat (*Rc*) is a spontaneous mutation observed in C57BL/6J mice. These mice exhibit a hair loss phenotype with shedding during catagen and telogen phases to give a sparse hair appearance. However, the hair is not lost in a wave, corresponding to the onset of various cycle domain stages seen in the C57BL/6J mice, but instead the mouse suffers from diffuse loss all over its back (Hayashi et al. 2004). Hair also appears dishevelled, and with age the mice become nude (Hayashi et al. 2004). The gene mutated in Rough Coat mice is believed to encode a cell adhesion molecule, Myelin protein zero like-3 (Cao et al. 2007). Moreover, circulating calcium levels are higher in the mutant mouse than in the wildtype (Hayashi et al. 2004) which may indicate that alterations in keratinocyte differentiation either within or surrounding the club fibre during its formation may be of importance, in addition to cell adhesion.

Desmoglein 3 knockout mouse

Loss of desmosomal integrity can lead to premature exogen as indicated by the Desmoglein 3 (*Dsg3*) null mouse (Koch et al. 1998), with the *Dsg3* allele being co-allelic with the *balding* mutation locus (Koch et al. 1997), a mouse with a similar hair loss phenotype (Sundberg 1994). The *Dsg3*-/- mouse exhibits cyclical hair loss, corresponding with the onset of the telogen phase when the club fibre is formed. In this mouse, the desmosomes between the suprabasal keratinocytes surrounding the club fibre and the basal layer of the outer root sheath split (Figure 1.8), resulting in ineffective mooring of the club fibre and premature club fibre loss (Koch et al. 1998). In mouse pelage hair, the suprabasal ORS cells surrounding the club fibre do not express Desmoglein 1 (*Dsg1*). However, transgenic expression of *Dsg1*, driven by a Keratin 14 (K14) promoter, protects against the cyclical hair loss phenotype usually

seen in *Dsg3-/-* mice (Hanakawa et al. 2002). In contrast, in humans, Dsg1 is seen in the suprabasal ORS surrounding the club hair (Wu et al. 2003), perhaps explaining why hair loss is not a prominent clinical phenotype seen in people with Pemphigus Vulgaris, a disease in which the body produces autoantibodies against Dsg3.

Although the loss of Dsg3 and desmosomal integrity seen in the *Dsg3* null mouse does not explain the mechanism of exogen, it suggests that desmosomal contacts are important in retaining the telogen club fibre within its associated epithelial sac.

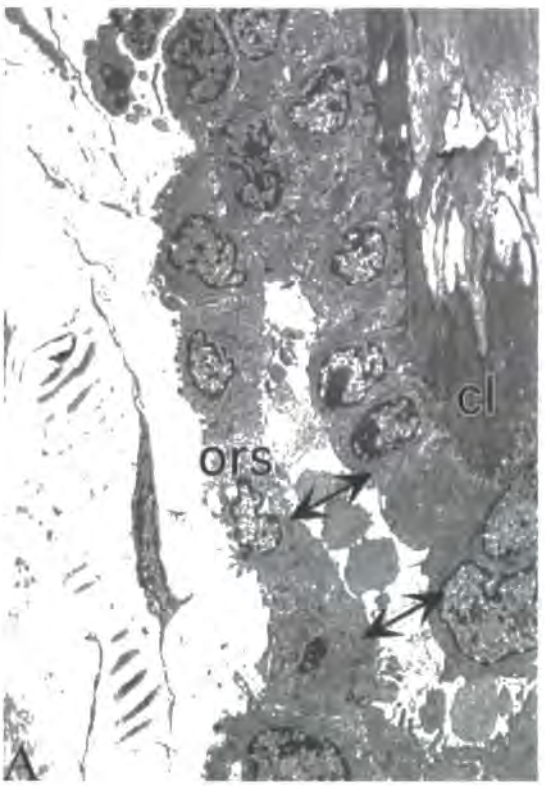

Figure 1. 8: Club fibre loss in *Dsg3* null mice

In the *Dsg3* null mouse, desmosomal integrity is lost and splitting is observed (double arrows) between the inner layer of keratinocytes surrounding the club fibre (cl), the companion^{CL}, and the remaining ORS. This results in premature hair loss, corresponding with club fibre formation. Club fibres are also distinguishable from club fibres from control mice as they have a layer of cells still attached to them. No loss of anagen hairs is observed. (Picture taken from Koch et al, 1998)

Bcl-x_L transgenic mouse

Although normally not expressed in the hair follicle, expression of the anti-apoptotic gene *Bcl-x_L* in the ORS, driven by a K14 promoter appears to reduce the length of anagen, whilst increasing the length of telogen in mouse pelage folliles (Pena et al. 1999). Of interest and relevant to exogen is the observation that club fibres in these mice appear to be retained for longer than in their wildtype counterparts (Pena et al.

1999), which suggests that a programmed cell death could be involved in the release of the club fibre from its epithelial sac.

1.4.1: Summary of Mouse Models

With the various mouse models the aspect of the club fibre mainly affected is its formation as seen in Table 1.1. In addition to formation, other aspects of the club fibre affected were retention and release, highlighting these three aspects of the club fibre as potential areas for further research.

Table 1. 1: Summary of mouse models that give an insight into club formation, retention and release

Mouse Model	Function of protein	Relevance to Club fibre	Aspect of Club fibre affected	References
Type II wool IF transgenic	Structural component of cells	Over expression affects the composition of IF in the club fibre causing weakening and breakage.	FORMATION	(Powell and Rogers 1990)
Cathepsin-L knockout	Proteolytic function. Important in IRS differentiation	Knockout causes defective trichilemmal keratin formation resulting in defective retention and premature loss.	FORMATION	(Roth et al. 2000; Tobin et al. 2002)
Notch-1 transgenic	Function regulating epidermal differentiation. Within hair follicle regulates IRS differentiation	Overexpression driven by the involucrin promoter delays IRS differentiation. Club fibres do not possess a trichilemmal keratin layer and therefore have defective retention in the ORS.	FORMATION	(Uyttendaele et al. 2004)
Msx-2 knockout	Involved in signal transduction (HOX). Required for hair shaft and cuticle differentiation	Premature hair loss is observed in the knockout mouse. No visible defects are seen in shed fibres from this mouse although the knockout affects club fibre formation.	FORMATION	(Ma et al. 2003)
Stratifin Mutation	Regulates epidermal differentiation	Knockout results in defective club fibre retention and release and is observed corresponding with club fibre formation.	FORMATION	(Herron et al. 2005; Li et al. 2005)
Hairless mutation	Transcriptional co-repressor. Regulates terminal differentiation in the epidermis and IRS	Club fibres in this mouse have no trichilemmal keratin layer as a result of the continued presence of undifferentiated IRS surrounding the fibre, preventing trichilemmal keratin formation.	FORMATION	(Orwin et al. 1967; Panteleyev et al. 1998; Panteleyev et al. 1999)
Rough coat mutation	Cell Adhesion molecule	Club fibre shedding corresponds with club fibre formation.	FORMATION/ RETENTION	(Hayashi et al. 2004)
Desmoglein 3 knockout	Desmosomal component-role in cellular adhesion	Club fibre appears normal in this mouse although the innermost layer of cells surrounding the fibre lack functional desmosomes resulting in splitting between the cells and early release of the club fibre.	RETENTION	(Koch et al. 1998)
Bcl-x_L transgenic	Anti-apoptotic function	Expression driven by the Keratin 14 promoter causes delayed release of the club fibre-potentially by preventing cell death in the cells surrounding the club fibre.	RELEASE	(Pena et al. 1999)

1.4.2: Cellular activities during exogen progression

Currently, there is no information as to any signals that initiate exogen, nor is there evidence that shedding can be spontaneously triggered. This raises the question of whether exogen is a gradual process or a sudden event. The mouse models of exogen do not give any indication as to the signalling, if there is any, which is involved in mediating exogen. However, they do highlight three aspects of the club fibre; its formation, retention and its release, which may all have influences on exogen. Based on the mouse models and other literature, Figure 1.9 shows a proposed progression of the club fibre from its formation through to its release. The mouse models highlighted that the formation of the club fibre, in particular the surrounding trichilemmal keratin is important for club fibre retention, as an improperly formed club fibre can be prematurely released. Moreover, the disruption of genes with functions regulating differentiation of the IRS, or terminal differentiation of the epidermis appear to affect the structure of the trichilemmal keratin. This highlights the structure of the club fibre as an important feature in its retention, and research into the structural aspects of the club fibre may shed further light in this area. Whilst the structure of the trichilemmal keratin is important for retention of the club fibre, adhesion complexes, such as desmosomes appear important for anchorage. Only one mouse model, the Bcl-x_L transgenic, gave an insight into club fibre release. This transgenic demonstrated that programmed cell death in the cells surrounding the club fibre may be of importance for the release of the club fibre.

From the literature and mouse models, it appears that the club fibre is retained at a cellular level through adhesion complexes such as desmosomes, and that the fibre is released from its trichilemma sac after breakdown of the surrounding cells. Milner (2002), observed cytoplasmic breakdown in the cells surrounding shed exogen club fibres and subsequently suggested that club fibre release is mediated through proteolytic degradation. This indicates that the adhesive properties of the trichilemma sac, and the proteolytic activity within the sac are major activities associated with the retention and release of the club fibre, and merit further research.

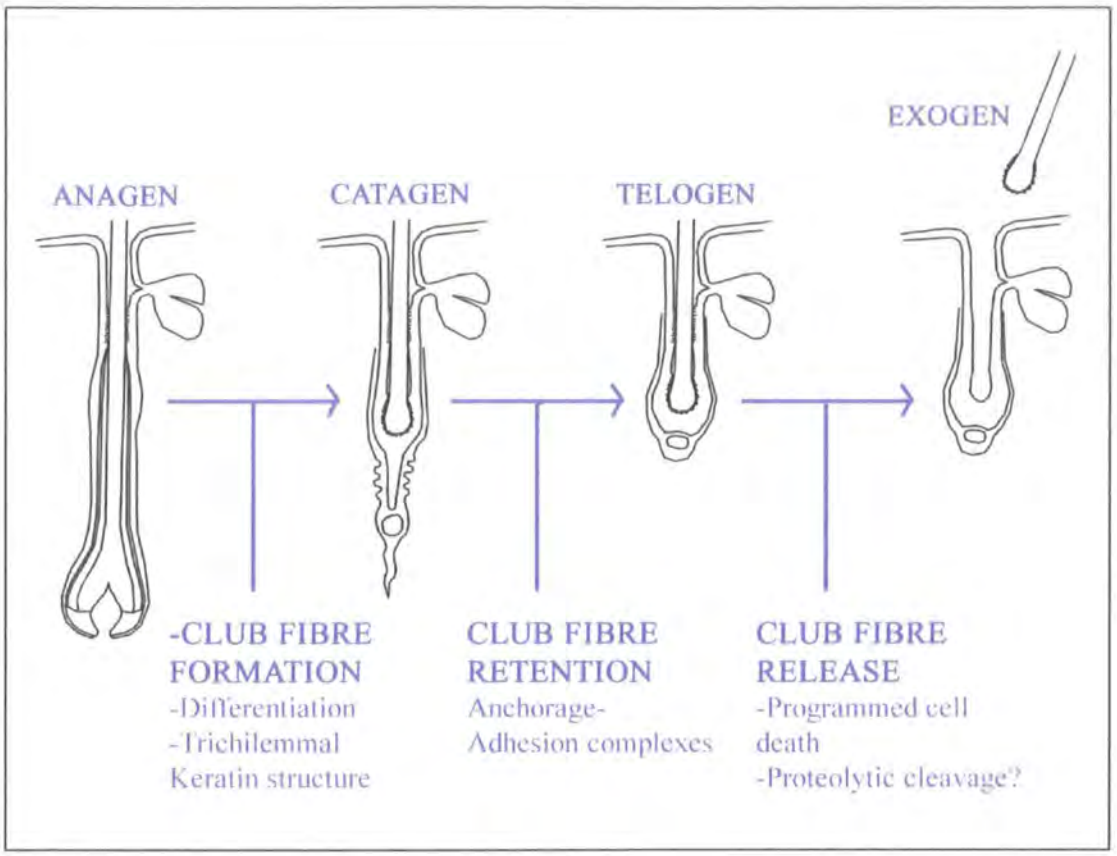

Figure 1. 9: Progression of the club fibre through to exogen

A schematic of the stages of club fibre formation, retention and release giving an insight into various factors important for each of these three stages.

1.5: Aims

During the hair cycle, there are two key elements that affect the density of hair covering the scalp. One is the re-initiation of the follicle into anagen from the latent stage, telogen which causes the growth of a new fibre. The second is the loss of the old club fibre, or exogen as the stage is termed, which when premature can cause noticeable hair thinning. The aims of this thesis were decided with these two elements of the hair cycle in mind, with the understanding that if one could understand these processes in more detail than they could be more effectively targeted for therapeutic intervention. The first aim was carried out partially in the laboratories of my industrial sponsor and partially in the School of Biological and Biomedical Sciences at Durham University. However, aims II-V were carried out in the entirely in the laboratories at the School of Biological and Biomedical Sciences at Durham University. The aims are outlined below.

I. Human dermal papilla cells do not normally aggregate when in culture. However, in hanging drop cultures these cells aggregate together and form a dermal sphere (personal communication, Richardson, 2005). The first aim of this thesis was to analyse and further characterise this new method of cell culture, and to investigate if spheres were more akin to an *in vivo* dermal papilla than cultured dermal papilla cells.

II. The second aim was to investigate the potential of pre-aggregated human dermal papilla cells to behave like an *in vivo* dermal papilla, by analysing their inductive capacity.

III. The second section of work within this thesis is related to exogen. Currently, there is no suitable model with which to study this process of the hair cycle. The first aim within this section was to analyse the vibrissa follicle as a suitable model with which to investigate exogen. This model was also used to address the question of whether exogen is a gradual or sudden event.

IV. The fourth aim within this thesis was to investigate the process of club fibre formation and retention. The mouse models highlighted the structure of the

trichilemmal keratin as an important feature during the formation of the club fibre. They also identified adhesive complexes which are important for club fibre retention. The vibrissa model was utilised with its predictive exogen stage to investigate club fibre formation and retention based on structural and adhesive changes of the club fibre and the surrounding trichilemma sac.

V. The fifth aim was to identify and validate novel changes associated with club fibre formation, retention and release. Currently, the signals that regulate exogen, if there are any, are unknown. Moreover, little is known about the cellular activities involved in exogen. Microarray technology was used to detect and investigate novel gene changes associated with club fibre formation, retention and release.

Chapter 2: Characterisation of a 3D model of dermal papilla cell culture

2.1: Introduction

2.1.1: Cell based models of hair follicle components

As hair follicle cycling involves complex and continuing epithelial-mesenchymal interactions, both ORS and dermal papilla cells have been widely exploited in hair research in identifying, understanding and manipulating the signalling within and between these two follicle compartments. Both ORS and dermal papilla cells can be readily dissected and propagated in culture providing an accessible system in which to study signalling within these systems (Jahoda and Oliver 1981; Messenger 1984; Limat and Noser 1986; Magerl et al. 2002).

Dermal papilla cells represent a specialised dermal cell population, distinct from interfollicular dermal fibroblasts in terms of their molecular signature, with unique *in vitro* characteristics (Jahoda and Oliver 1981; Messenger et al. 1986). A key difference between dermal papilla cells *in vivo* and *in vitro* is seen with the expression of aSMA. *In vivo* aSMA is expressed within the dermal sheath only, although in culture dermal papilla cells from rat vibrissa, rat pelage and human follicles express this antigen, indicative perhaps of a de-differentiation event that is occurring within these cells in culture (Jahoda et al. 1991). The mitotic activity of dermal papilla cells *in vitro*, albeit lower than dermal fibroblasts (Jahoda and Oliver 1984c) is also a key difference from *in vivo*, where only 2% of papilla cells are proliferative, these being during the initiation of anagen (Tobin et al. 2003). Moreover, in culture dermal papilla cell lines senesce between 5-10 passages whilst dermal fibroblasts are able to grow for approximately 15-20 passages (Messenger et al. 1986).

An interesting feature of rat vibrissa and canine dermal papilla cells is their ability to aggregate in culture, into a clump that appears morphologically similar to a mesenchymal aggregation. It has been suggested that these aggregates are analogous to mesenchymal condensations, which would indicate that dermal papilla cells retain characteristics of follicular embryogenesis through to adult life (Jahoda and Oliver 1984c; Bratka-Robia et al. 2002). This aggregative behaviour has also been reported in human dermal papilla cells by some groups (Messenger et al. 1986; Chui et al. 1996), although contrasting information, showing no aggregation of human dermal

papilla cells has also been presented (Withers 1987). Currently, pronounced aggregation of human dermal papilla cultures has not been observed in our laboratory (personal communication, Jahoda, 2007). However, these different observations may be due to differences in techniques between the different laboratories.

In culture systems, both ORS and dermal papilla cells differ in their morphology, behaviour and biosynthetic activity from their *in vivo* status. This is a particular limitation of the regular two dimensional (2D) culture system, and hence researchers have attempted to develop more organotypic three dimensional (3D) models of these cells to try and model *in vivo* compartments of the hair follicle more accurately (Noser and Limat 1987). In an endeavour to more accurately recapture the interactions between the mesenchymal and epithelial compartments of the hair follicle *in vitro*, cell culture models have been developed with mixed or layered outer root sheath and dermal papilla cells isolated from human scalp (Havlickova et al. 2004).

The signalling between the mesenchymal and epithelial components has been studied extensively and in the adult follicle is thought to be modulated by proteoglycans, acting to enhance or inhibit the activities of growth stimulators (Botchkarev and Kishimoto 2003). The extracellular matrix of the papilla contains abundant proteoglycans, including perlecan, bamacan, syndecan 1 (SDC1) and versican (Couchman et al. 1990; Couchman 1993; du Cros et al. 1995; Bayer-Garner et al. 2002). Interestingly, the expression of versican is lost with increasing passage number in dermal papilla cell cultures, and this has been linked with the loss of inductive capabilities of the cells (Kishimoto et al. 1999). Studies have been presented that detail the maintenance of versican expression *in vitro* (Shimizu and Morgan 2004; Kim et al. 2006), thought to be a way of maintaining the anagen characteristics and inductive capabilities of these cells (Shimizu and Morgan 2004).

2.1.2: Amputated Follicle Induction Assay

In the telogen stage of the hair cycle, the follicle remodels itself into a structure similar to that of the developing hair peg as seen during morphogenesis (Chase 1954; Hardy 1992). The initiation of the growth phase and subsequent elongation of the follicle shares many similarities with the processes of morphogenesis. In particular,

the dermal papilla, derived from the mesenchymal condensation during morphogenesis, plays a crucial role in anagen initiation due to its interactions with the epithelial components of the follicle. Studies into hair follicle regeneration and induction may shed light on aspects of hair follicle cycling and anagen initiation, potentially fundamental for hair restoration therapy.

The vibrissa follicle is a popular model with which to analyse aspects of hair follicle formation and follicle cycling due to its large size and finely tuned cyclical timing. In 1966, Oliver first demonstrated that the dermal papilla and end bulb could spontaneously regenerate and induce a new fibre after surgical amputation of up to a third of the lower follicle, if transplanted ectopically onto a kidney capsule (Oliver 1966b; a; c). Similar to the original vibrissae regeneration experiments carried out by Oliver, the regeneration of amputated human follicles has also been observed after subcutaneous grafting of amputated follicles onto athymic nude mice and SCID mice (Jahoda et al. 1996; Hashimoto et al. 2001; Tang et al. 2002). Perhaps more relevant for transplantation studies is the work by Kim and Choi demonstrating the ability of human scalp follicles with their bulbs removed to regenerate and grow fibres after autologous grafting (Kim and Choi 1995). This suggests that the regeneration process in hair follicles is universal across species. However, unlike hair follicles, regeneration is not a process that is common to all appendages as demonstrated in feather follicles with amputated bulbs, that lack the ability to regenerate after surgical removal of their base (Lillie and Wang 1941; Wang 1943; Lillie and Wang 1944).

With hair follicles, the regeneration of the dermal papilla is believed to be due to the migration and conversion of dermal sheath cells from the remaining follicle (Oliver 1966a; Horne and Jahoda 1992; Jahoda et al. 1992a). It is generally considered that the epithelial component of the follicle is regenerated from the stem cells of the bulge after removal of the lower follicle (Tang et al. 2002).

In the vibrissae, after the removal of more than the lower third of the follicle regeneration does not occur (Oliver 1966c) and subsequently this model has been used as an amputated follicle assay to analyse end bulb and fibre induction with dermal component of the follicle (Figure 2.1). Using this induction assay both isolated rat vibrissa dermal papillae and dermal sheath have been shown to induce

hair growth when placed in contact with the amputated follicle epithelium (Oliver 1967; Horne and Jahoda 1992). Cultured vibrissa dermal papilla cells at a low passage produce a similar result, whilst late passage dermal papilla cells lose this ability (Jahoda et al. 1984; Horne et al. 1986). However, if the dermal papilla cells are maintained, for example by culturing in Fibroblast Growth Factor (FGF) containing medium (Matsuzaki and Yoshizato 1998) or in keratinocyte conditioned medium, this increases both the lifespan and inductive capabilities of dermal papilla cells at higher passages (Inamatsu et al. 1998). Inductive capabilities of late passage dermal papilla and sheath cells can also be restored by co-transplantation with germinative cells although both by themselves are unable to induce fibre formation (Reynolds and Jahoda 1996).

In culture, the ability of dermal papilla cells to induce end bulb and fibre formation diminishes with increasing passage number. However, if intact dermal papilla isolated 20 days after the cessation of hair growth in an organ culture system are implanted onto amputated follicles that would otherwise not grow, they are able to induce fibre formation in these follicles (Robinson et al. 2001). This indicates that the cessation of hair growth, usually observed after 10 days in culture (Philpott et al. 1991) is not due to the inactivation of the dermal papilla (Robinson et al. 2001).

More recently, fibre growth and end bulb formation after implantation of intact dermal papillae from human donors onto amputated vibrissa follicles has been demonstrated after grafting onto kidney capsules (Jahoda et al. 2001). This is exciting with regard to potential therapeutic strategies for hair loss although induction of fibre growth using cultured human dermal papilla cells has not yet been successfully reported using this assay. In addition to interspecies transplants, cultured tooth papillae from both humans and rats have been shown to induce fibre formation in the amputated follicle assay highlighting the cross-appendage qualities of dermal papillae (Reynolds and Jahoda 2004). This relates back to an early series of interclass recombination experiments which analysed appendage morphogenesis (Dhouailly and Sengel 1972; 1973). These indicated that the signal for appendage formation is derived from the dermis although the nature of the resulting appendage is dictated by the epidermis. Moreover, cross-appendage and interspecies recombinations have

showed that the signalling during appendage formation is evolutionarily conserved (Dhouailly and Sengel 1972; 1973).

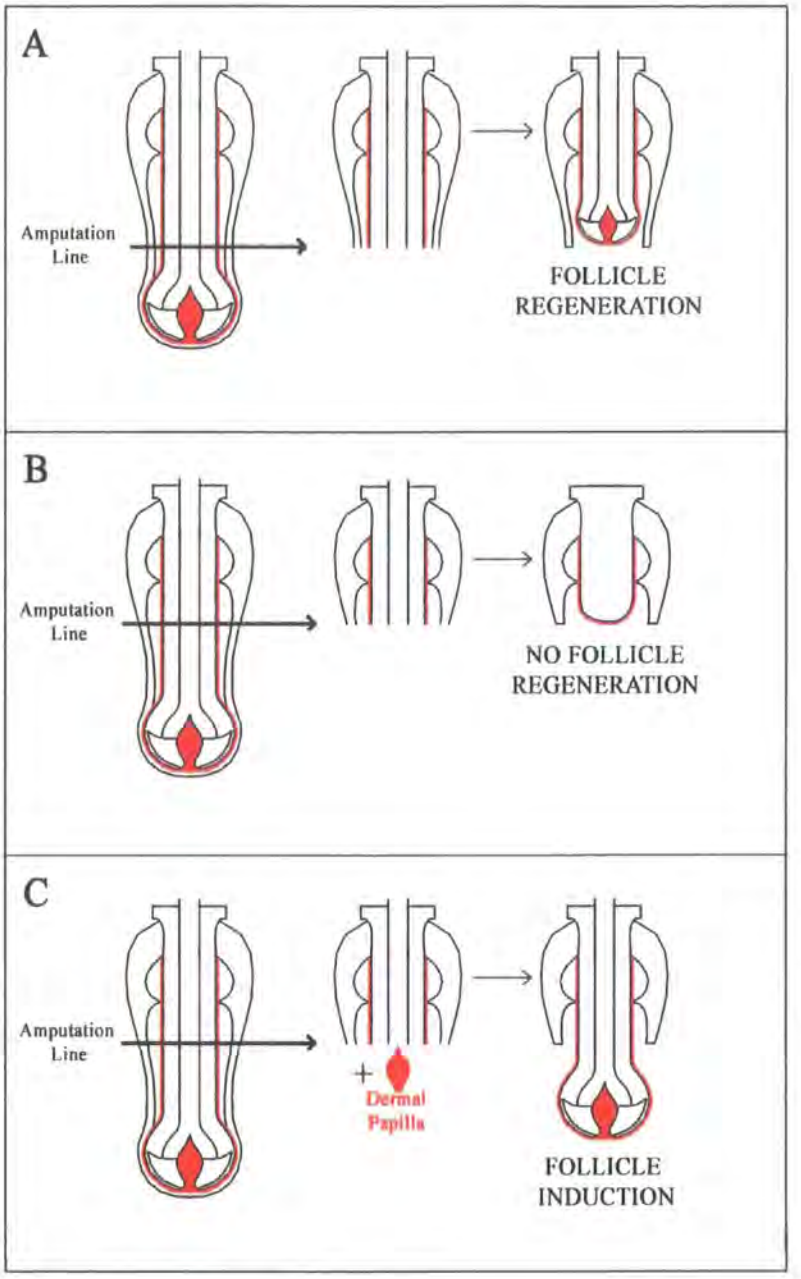

Figure 2. 1: The amputated follicle assay

After amputation of the lower third of the vibrissa follicle, regeneration of the end bulb and dermal papilla occurs, followed by fibre growth (A). However, after amputation of more than the lower third of the follicle, no regeneration occurs (B). Subsequently, follicles which have been amputated above their lower third have been used to evaluate the hair inducing capabilities of dermal components such as the dermal papilla, which can cause end bulb formation and fibre induction when placed against the exposed epithelial portion of the amputated and inactivated follicle (C).

2.1.3: Aims

During the hair cycle, a key process is the initiation of hair growth in the telogen to anagen transition. The molecular signals that regulate this are well described and are considered to originate in the dermal papilla (reviewed by Alonso and Fuchs 2006). However, currently the 2D culture model of dermal papilla cells has certain limitations, distinguishing it from *in vivo* dermal papillae. Nevertheless, when human dermal papilla cells are grown in hanging drop cultures they aggregate together to form dermal spheres, which appear morphologically akin to dermal papilla (personal communication, Richardson, 2005). Potentially, dermal spheres may be more representative of *in vivo* dermal papilla than regular 2D cultured dermal papilla cells.

The aim within this chapter of this thesis was to analyse and characterise this hanging drop method of cell culture to determine if dermal spheres were able to behave like an *in vivo* dermal papilla, both in terms of cellular expression patterns, but also with regards to their inductive capabilities. The proliferation and aSMA profiles of spheres were analysed, as these are two profiles that are noticeably different between plated dermal papilla cells and *in vivo* dermal papilla. Thus, selecting to analyse the spheres with proliferation and aSMA markers would determine if spheres were more akin to *in vivo* dermal papillae than 2D cultured cells. Cellular adhesion was selected as an area to analyse, as an obvious change occurring during the formation of a sphere was the increase in cell-cell contact. Proteoglycans were also selected as a family of molecules to investigate within spheres. There are dynamic changes in the size of the dermal papilla during the hair cycle, due partly to changes in the synthesis of proteoglycans. Proteoglycans are also believed to modulate signalling between cells of the dermal papilla both during development and the hair cycle. It therefore was important to analyse the proteoglycan profile of the spheres to determine if they were representative of a particular cycle stage or developmental time point.

Finally, within this chapter the aim was to see if spheres were not only morphologically akin to intact dermal papillae but whether they could behave like them also. Therefore, spheres were used in the amputated follicle assay to see if they were capable of inducing new fibre growth.

2.2: Methods

2.2.1: Cell culture

2.2.1.1: Growth conditions

Dermal papilla cells were cultured in Minimal Essential Medium (MEM) (Sigma) containing 10% Fetal Bovine Serum (FBS) (Sigma). Cells were brought up after being frozen and were grown in T25 flasks (Nunc), and were fed every three days. All cell cultures were maintained in a 37°C incubator, containing 5% CO_2.

Cells were mainly grown without antibiotics or fungizides. However, if used, the antibiotic Gentamicin (Gibco BRL) and the fungizone Amphotericin B (Sigma) were used at 50μg/ml and 0.5μg/ml respectively.

Six cell lines were used to form dermal spheres; DP1 through to DP6. Although little information was known about these cell lines, any relevant information is documented in Table 2.1.

Cell line DP1 was purchased from PromoCell who obtained skin samples from patients with informed consent, and anonymised. Cell line DP2 was established at Bradford University from hair follicle cells taken from discarded skin samples taken at The Yorkshire Clinic, Bradford, West Yorkshire. This specimen was obtained under a general ethical approval for Professor Desmond Tobin. Cell lines DP1 and DP2 were used at Unilever, Colworth. They were brought in under the Human Tissue Act. Cell lines DP3-DP6 were established and used at Durham University. All human samples at Durham were obtained from the Royal Victoria Hospital, Newcastle. All hair follicle cells were from discarded skin samples taken from patients with informed consent, and anonymised. These specimens were obtained under the COREC multi-centre ethical approval for Professor Colin Jahoda, project entitled: "Skin and hair follicles for skin replacement/stem cell research."

Table 2. 1: Dermal papilla cell lines used for analysis

Dermal Papilla cell line	Age of donor	Sex of donor	Body site	Passage number analysed
DP1	47	♂	Scalp	P5
DP2	56	♀	Scalp	P5
DP3	-	♂		P5-P6
DP4	-	♂		P5-P6
DP5	-	-	Scalp	P5-P6
DP6	89	♂	Beard	P7-P8

2.2.1.2: Passaging of cells

On reaching confluence, cells were passaged. They were first washed in warmed Phosphate buffered saline (PBS) (made from PBS tablets-Sigma). This was then removed and 1ml Trypsin-EDTA (Invitrogen) was added to detach the cells from the underlying plastic. Detachment was visualised under a microscope, and once the majority of cells were detached, the flask was gently tapped to ensure complete removal. Trypsin activity was stopped by adding 4mls 10% FBS in MEM to the flask. The suspended cells were then removed from the flask and centrifuged for 5 minutes at 1000rpm in a 50ml falcon tube to pellet the cells. The excess media was poured off, and the pellet of cells resuspended in 1ml 10% FBS in MEM by gentle pipeting. This suspension was spilt between 2 x T25 flasks, each containing 4mls of MEM supplemented with 10% FBS.

2.2.1.3: Sphere formation

Dermal papilla cells were washed with warmed PBS then trypsinised with 1ml Trypsin-EDTA. Trypsinisation was inhibited by adding 4mls MEM containing 10% FBS and the cell suspension was centrifuged in a 50ml falcon tube for 5 minutes at 1000rpm. After centrifugation the excess media was poured off and the cell pellet resuspended in 5mls serum free MEM to wash. The cell suspension was then centrifuged again for 5 minutes at 1000rpm, after which time the excess media was poured off leaving the remaining pellet. The pellet was resuspended in 1ml MEM containing 10% FBS, and 20µl removed for counting the cell number on a

haemocytometer. After counting, an appropriate volume of MEM with 10% FBS was added to dilute the cells to 300cells/μl.

10μl drops of cell suspension were pipetted onto an inverted bacteriological dish lid (VWR) using a 10μl pipette, to give 3000 cells per droplet (Figure 2.2A). Approximately 50 drops were placed onto each bacteriological dish, 0.7cm apart from one another. The base of the bacteriological dish was either filled with PBS, or PBS soaked filter paper was placed in the base, and the top quickly turned back over onto the filled base. The 10μl drops remained in place as hanging drops. Bacteriological dishes were then stacked for placing into the incubator. However, the top plate contained PBS only, with no hanging drops (Figure 2.2C). After incubation, the stacked bacteriological dishes were left undisturbed for between one and five days until further analysis. During this time, the dermal papilla cells in the hanging drops aggregated and formed spheres which could be viewed with the naked eye. Spheres were photographed on a JVC camera attached to a stereo dissection microscope (Nikon).

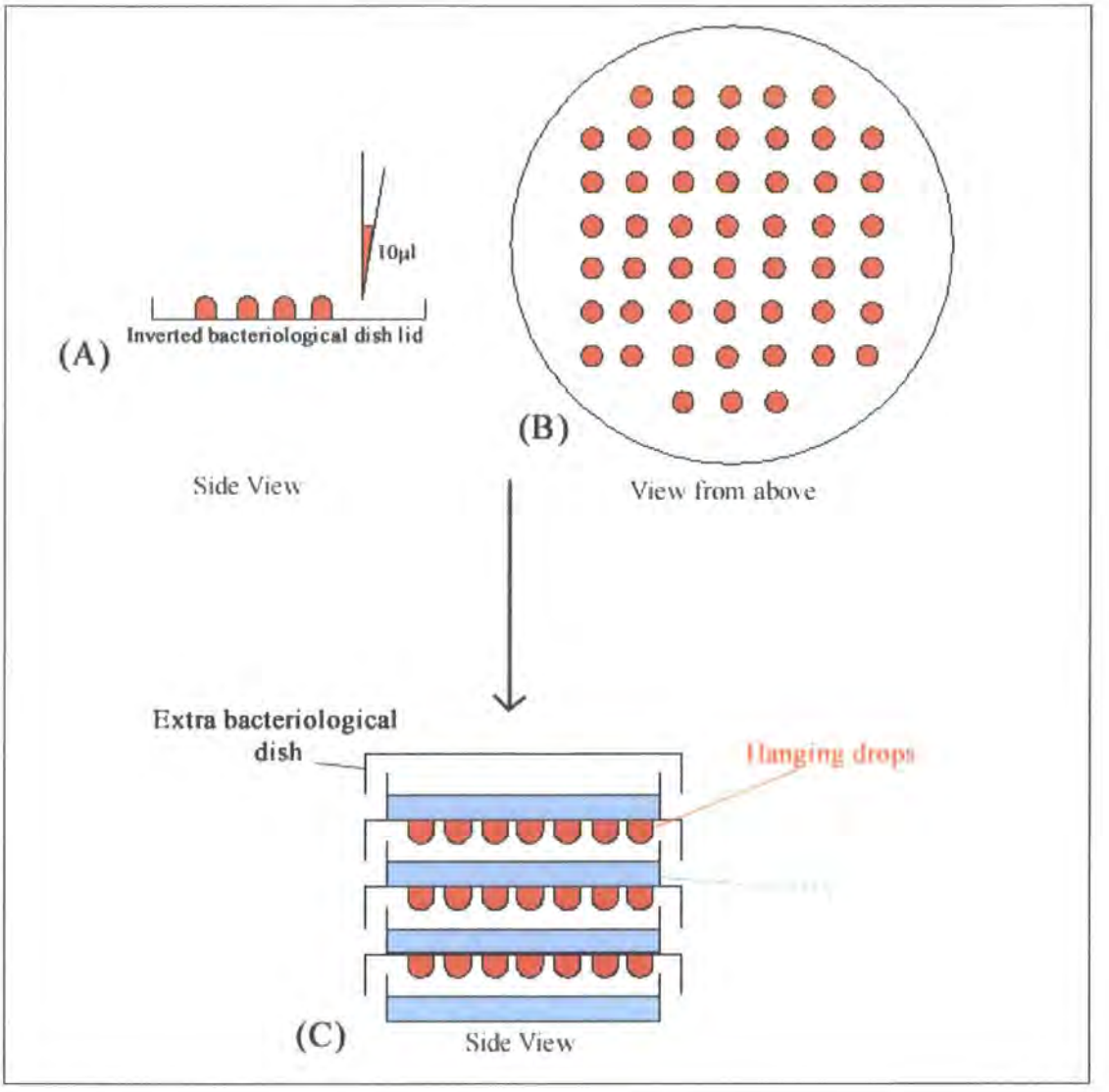

Figure 2. 2: Schematic for making hanging drop cultures

10µl volumes of dermal papilla cell suspensions were pipetted onto an inverted bacteriological dish lid (A) so that each lid contained 50 drops (B). The lids were then inverted and placed back onto the bacteriological dish base, containing PBS. Dishes were stacked, with the top dish free from any cells (C). The stack of bacteriological dishes was then incubated at 37°C where sphere formation occurred in the hanging drop cultures.

2.2.1.4: Preparation of plated cells

After trypsinisation, washing and counting of dermal papilla cells was carried as previously described for sphere formation in Section 2.2.1.3. Cells were diluted

appropriately to give a concentration of 40,000 cells/ml in MEM supplemented with 10% FBS.

For preparation of cells for immunofluorescent analysis, 250µl of cell suspension was added to each well of a 4-well plate, giving a density of 10,000 cells in the well. Wells contained glass coverslips with a diameter of 10mm (VWR) that had previously been baked at 200°C for 2 hours in a dry oven. Cells were incubated until they were approximately 80% confluent, after which time they were fixed and processed for immunofluorescent detection.

For preparation of cells for Ribonucleic acid (RNA) extraction, 1.5mls cell suspension, containing 75,000 cells was added to each of 2x35mm dishes, contained inside a bacteriological dish. Cells were incubated until they were approximately 80% confluent, after which RNA was extracted from the cells using the TRIzol isolation method.

2.2.2: Transmission electron microscopy

After 30 hours, or 120 hours (5 days) in culture, spheres created from cell line DP1 were harvested together in a 1.5ml microcentrifuge tube for preparation for transmission electron microscopy (TEM). After removal from the incubator, spheres were fixed in 2.5% glutaraldehyde (Agar Aids) in 0.1M sodium cacodylate buffer pH 7.4 for approximately 45 minutes. After initial fixation the samples were washed in 3 changes of buffer solution, each wash lasting 5 minutes. Post fixation was in 1% osmium tetroxide (Agar Aids) in 0.1M sodium cacodylate buffer pH 7.4 for 30 minutes. The spheres were then transferred to 1% aqueous uranyl acetate for staining for 1 hour. After staining, spheres were dehydrated through ascending grades of ethanol (70%, 90%, 100%), with 3 changes, each lasting 5 minutes in each ethanol grade. They were then transferred to 100% acetone, acting as an ante-medium between the alcohols and resin. Spheres were then soaked in a 50:50 mixture of Araldite epoxy resin and acetone for 30 minutes, after which time they were transferred to fresh resin and left to soak overnight. After infiltration of the resin overnight, spheres were transferred into a final resin change, orientated to the end of

the resin block and left for 12 hours. After this time, spheres were polymerised into the resin blocks for 2 days at 60°C.

A ribbon of ultrathin sections, with a gold colouration, was cut on a Reichert Ultracut E using a Diatome diamond knife. Sections were floated onto double distilled H_20, and collected onto 400 thin copper mesh discs. They were stained for 10 seconds with lead citrate then washed with double distilled H_20.

All the sections were examined and photographed using a Jeol 1200 EX transmission electron microscope operated at 100KV.

2.2.3: Preparation of cells and spheres for immunofluorescent detection

2.2.3.1: Embedding and sectioning of spheres

After 30, 54 or 78 hours in cell culture, intact spheres were gathered together into one large droplet. Spheres were then picked up carefully into a 200µl pipette tip (Starlabs), and embedded into Oct compound (Agar aids). They were then stored at -80°C until required for cryostat sectioning.

Spheres embedded in Oct compound were sectioned into 7µm sections on a Leica 3050S cryostat. The sections were thawed onto Superfrost Plus microscope slides (VWR) and left to air dry for 1 hour.

2.2.3.2: Plating of spheres

After 30 hours in culture, 8-12 spheres from each of the cell lines DP3, DP4 and DP6 were plated back down into 4 well plates with glass coverslips at the bottom using a 10µl pipette tip (Starlabs). The 4 well plates contained MEM supplemented with 10% FBS. The plated spheres were put into an incubator and were not disturbed for 7 days, after which time they had formed explants. Explants were processed for immunofluorescent analysis the same way that the 2D cultures were treated.

2.2.3.3: Cell Fixation

Spheres created from cell lines DP1 and DP2 were not sectioned on a cryostat, but rather fixed immediately in 100% ice cold methanol for 10 minutes after removal from the incubator. They were fixed in a 1.5ml microcentrifuge tube, during which time they sank to the bottom of the tube. After fixation, they were washed three times in PBS (Appendix 1) and transferred to a fresh PBS droplet in a bacteriological dish.

Frozen spheres from cell lines DP3-DP6 were sectioned on a cryostat and air dried. After drying, sections were fixed onto slides using ice cold methanol fixation for 10 minutes. Slides were then air dried for 5 minutes, then rehydrated in PBS washes (3 x 5 minutes).

Cells and spheres plated onto glass coverslips were washed once, gently in PBS before being fixed to the glass using ice cold methanol for 10 minutes. Methanol was removed, and the cells allowed to air dry before being rehydrated and washed in PBS (3 x 5 minutes).

2.2.3.4: Immunofluorescent analysis

An indirect labelling approach was adopted for all fluorescent analysis of dermal cell spheres. Effectively, a primary antibody against the antigen of interest was incubated with sections. A second antibody, conjugated with a flurophore was then introduced that was specific for the first antibody.

After the PBS washes after the fixation step, non-specific antibody binding was blocked by incubating the sections and spheres for 30 minutes with 2% Bovine Serum Albumin (BSA) (Sigma) in PBS. Whilst the block solution was being incubated, primary antibodies against the antigens of interest were prepared at optimised dilutions in PBS (Table 2.2). The blocking solution was removed, and an appropriate volume of primary antibody was added to each section or cell chamber. Sections were then covered in small strips of Parafilm and incubated in a humidified chamber overnight at 4°C. Spheres were transferred to fresh drops of diluted primary antibody, in a bacteriological dish inside a humidified chamber.

The following morning, unattached primary antibody was removed with PBS washes (3 x 5 minutes). Slides were blotted dry with Kimwipe tissues around sections, leaving sections covered in PBS. Appropriate secondary antibodies (specific for the host in which the primary antibody was raised) were diluted to the optimised dilution in PBS (Table 2.3), and 20µl of diluted antibody was applied to each section. Secondary antibodies were covered with Parafilm and left for 1 hour at room temperature in a dark humidified chamber. Spheres were transferred to a fresh drop of diluted secondary antibody after the PBS washes. After antibody labelling, unattached secondary antibody was removed by washing in PBS (3 x 5 minutes). Glass coverslips (VWR) were mounted using an anti-photobleaching media, Vectashield mounting medium containing the nuclear stain Propidium Iodide (PI) (Vector Laboratories). Spheres were mounted on slides, using ring spacers (Invitrogen) between the slide and the coverslip so as not to flatten the spheres. Coverslips were sealed using nail varnish and kept in the fridge until visualisation.

To evaluate non-specific binding, monoclonal primary antibodies were substituted with PBS, whilst polyclonal primary antibodies were substituted with an appropriately diluted isotype control (Sigma).

Spheres from cell lines DP1 and DP2 were visualised and photographed on a Leica TCS SP confocal whilst sectioned spheres from DP3-DP6 were visualised on a BioRad MicroRadiance confocal. Plated cells were visualised and photographed on a Leica Axio Imager. The number of spheres from each cell line detected with various antibodies is shown in Table 2.4.

Table 2. 2: Primary antibodies and appropriate information

Antibody name	Manufacturer	Host	Working dilution
Anti Proliferating cell nuclear antigen (PCNA)	DAKO	Mouse	1/50
Anti alpha smooth muscle actin (aSMA)	Sigma	Mouse	1/400
Anti Connexin 43 (Cx43)	Sigma	Mouse	1/2000
Anti beta-catenin	Transduction Laboratories	Mouse	1/100
Anti Versican (CSPG2)	Developmental Studies Hybridoma Bank	Mouse	Neat
Anti Syndecan 1 (SDC1)	Chemicon	Mouse	1/300
Anti Bamacan (CSPG6)	Bethyl Laboratories	Rabbit	1/200
Anti Perlecan (HSPG)	Santa Cruz	Rabbit	1/75
Anti Fibronectin	Sigma	Rabbit	1/400
Anti Inhibitor of differentiation 3 (Id3)	Santa Cruz	Rabbit	1/100

Table 2. 3: Secondary antibodies and appropriate information

Antibody name	Manufacturer	Working dilution
Goat anti Mouse Alexafluor 488	Molecular Probes	1/400
Goat anti Rabbit Alexafluor 488	Molecular Probes	1/400

Table 2. 4: Experimental Repeats of staining in dermal spheres

	DP1	DP2	DP3	DP4	DP5	DP6
Alpha Smooth Muscle Actin	5	5	6	8	8	9
Proliferating Cell Nuclear Antigen	5	5	7	8	10	9
Connexin 43	-	-	7	8	8	8
B-catenin	5	5	7	8	8	9
Versican	-	-	8	8	8	8
Syndecan 1	5	5	7	8	9	7
Bamacan	5	5	8	8	10	8
Perlecan	5	5	6	8	8	8
Fibronectin	-	-	7	8	9	9
Inhibitor of differentiation 3	-	-	6	8	7	8

2.2.4: Molecular Biology techniques

2.2.4.1: RNA extraction-TRIzol

TRIzol (Invitrogen) was used to isolate RNA from dermal papilla cells, both from those plated in 35mm dishes, and those formed into spheres. To isolated RNA from plated cells, media was first removed from the 1x35mm dish then 1ml TRIzol was added. A pipette tip was used to scrape the cells which were then transferred to a 1.5ml microcentrifuge tube. To isolate RNA from dermal spheres in hanging drop cultures, 3 plates worth of spheres (150 spheres) were combined in a 1.5ml microcentrifuge tube after 30 hours in culture. Excess media was then pipetted off

and replaced with 1ml TRIzol. TRIzol is a mono-phasic solution of phenol and guanidine isothiocyanate, which maintains the integrity of RNA, while disrupting cells and dissolving cell components. Once cells were in the microcentrifuge tubes with 1ml TRIzol, 200µl Chloroform (Sigma) was added, and the tubes were shaken vigarously for 30 seconds, followed by a 3 minute sit at room temperature. After centrifugation at 13000rpm for 15 minutes at 4°C the solutions had separated into a lower organic and an upper aqueous phase. RNA remained exclusively in the aqueous phase and was removed and transferred to a new microcentrifuge tube using a 200µl pipette. After separation of the aqueous phase, the RNA was precipitated out by the addition of 500µl isopropanol (Sigma) and left for 10 minutes at room temperature. Following precipitation, RNA was pelleted by centrifugation at 13000rpm for 10 minutes at 4°C. 1ml 70% ethanol was then used to wash the RNA, which was pelleted again by centrifugation at 5000rpm for 15 minutes at 4°C. After removal of the ethanol using a 200µl pipette, the pellet was air dried then resuspended in 10µl DEPC treated distilled water.

2.2.4.2: Removal of contaminating DNA from isolated RNA

To the 10µl of resuspended RNA isolated in step 2.2.4.1, 1µl 10X DNase buffer (Sigma) and 1µl DNase 1 (Sigma) were added to remove contaminating Deoxyribonucleic acid (DNA). The DNase buffer consisted of 200mM Tris-HCL, pH 8.3 and 20mM $MgCl_2$. Reactions were carried out in a 1.5 ml microcentrifuge tube for 15 minutes at room temperature. To stop the reaction, 1µl 50mM EDTA (Sigma) was added, and the tubes heated at 70°C for 10 minutes before being placed onto ice. The high temperature denatures the RNA secondary structure, whilst the EDTA inactivates the DNase 1 by chelating its calcium and magnesium ions.

2.2.4.3: Reverse transcription

1µl of isolated, DNA free RNA was used on a Nano Drop ND-1000 Spectrophotometer (Labtech) to quantify the amount of RNA isolated from plated cells and spheres. Next 1µg of RNA was added to 1µl of $Oligo(dT)_{12\text{-}18}$ (Invitrogen) and 1µl 10mM dNTP mix (Invitrogen) in a microcentrifuge tube. Samples were made up to a volume of 13µl with DEPC treated distilled water and incubated on a

heat block at 65°C for 5 min to disrupt the secondary structure of the RNA. During this time a master mix containing 4µl 5X First strand buffer (250mM Tris-HCL pH8.3, 375mM KCL, 15 $MgCl_2$), and 2µl 0.1M DDT per reaction. After the initial incubation the RNA was briefly chilled on ice before adding 6µl of the master mix. The tube contents were then incubated at 42°C for 2 minutes to optimise the temperature for the reaction. 1µl of SuperScript™ II Reverse Transcriptase (Invitrogen) was then added to the RNA, and mixed by pipetting. RNA was incubated for 50 minutes at 42°C. Immediately after this incubation step the sample was incubated at 70°C for 15 minutes to heat inactivate the Reverse Transcriptase enzyme. Resultant complementary deoxyribonucleic acid (cDNA) samples were stored at -20°C until required as a template for amplification in a real-time polymerase chain reaction (PCR).

2.2.4.4: Real-time Polymerase Chain Reaction

The 20µl cDNA created in Step 2.2.4.3 was diluted 1 in 10 to 200µl using DEPC treated distilled water and used for real-time PCR to determine expression levels of the gene of interest. Specific primers for the cDNA sequence of the gene of interest in human (Table 2.5) were designed covering an intron-exon boundary, to ensure that no contaminating genomic DNA would affect the results. cDNA sequences were obtained from the National Centre for Biotechnology Information (NCBI). As $Oligo(dT)_{12\text{-}18}$ was used in the reverse transcription step rather than random primers, primers were designed within 2000 base pairs of the poly-A tail.
Standards for use in real-time PCR were created by running an initial PCR with excess cDNA, and diluting this 10^{-2}, 10^{-4}, 10^{-6}, 10^{-8} and 10^{-10} in DEPC treated distilled water. The same set of standards was kept for all reactions.

Real-time PCR was carried out in a Mini Opticon (BIORAD) thermal cycler, using a SYBR green ready made supermix provided by Sigma. Each reaction was made up on ice and consisted of 12.5µl SYBR green supermix, 2µl cDNA (previously diluted 1/10) and 0.3µM of both forward and reverse primers for the gene of interest. Reactions were made up to 20µl using DEPC treated distilled water and placed into the thermal cycler. All reactions were carried out in triplicate.

The Mini Opticon thermal cycler was programmed to heat the reaction to 94°C for 5 minutes before commencing with the repeated sequence of 94°C for 30 seconds, annealing temperature (see Table 2.5) for 30 seconds, 72°C for 40 seconds. Fluorescence readings were taken after every repeated cycle at 72°C. The repeated sequence was cycled 40 times, after which time the thermal cycler increased the temperature from 72°C up to 95°C, taking a fluorescence reading every 0.2°C. The temperature at which fluorescence signal peaks, is the melting temperature of the PCR product. Controls were carried out using DEPC treated distilled water instead of cDNA. Standards of all dilutions were run alongside the real-time PCR reactions containing sample DNA. The resulting standard data was used to generate a standard profile for each reaction. A negative control containing water rather than cDNA was also run with each reaction setup. cDNA samples were run in triplicate and the mean of the three results used for comparison with other samples. Opticon monitor software was used to obtain the real-time PCR results from the thermal cycler, with the threshold for reactions being set to 0.025. Microsoft excel was used to tabulate data, and to generate graphs of the results. Error bars were calculated based on the standard deviation of the results from the mean result.

Real time PCR was only carried out on plated cells and spheres from cell lines, DP1, DP2, DP4 and DP5 due to limitations of cell numbers.

Table 2. 5: Primer pairs for real time PCR

Primer Pairs	Sequence	Annealing temperature (°C)	Product Size (base-pairs)
Glyceraldehyde-3-phosphate dehydrogenase Forward Glyceraldehyde-3-phosphate dehydrogenase Reverse	CCA GGT GGT CTC CTC TGA CT CCT CTT CAA GGG GTC TAC AT	57	311
Ki67 antigen Forward Ki67 antigen Reverse	AGG CAC TTT GGA AGG TGT GAG G CAA GGA GGG TTG TGT AGA AGT GG	55	388
Alpha Smooth Muscle Actin-Forward Alpha Smooth Muscle Action Reverse	ATC TAT GAG GGC TAT GCC TTG C GCA ACT CGT AAC TCT TCT CAA GG	57	235
SYNDECAN 1 Forward SYNDECAN 1 Reverse	AAG GCC AGG TTC TCC GTT AGC GAA GGC ACA GAG ATT CGA GCC	57	284
BAMACAN Forward BAMACAN Reverse	AGA ACT TGG ATC ACT TCC CCA GG TGC CAC CAG GTA CTA ACT TCT GG	57	322
PERLECAN Forward PERLECAN Reverse	AAG GAG ACC TGT GTG AGC ACG AGG CTC CTG GAG AAG ACA TGG	55	262

2.2.5: Induction analysis

2.2.5.1: Vibrissae follicle dissection

For dissection purposed, PVG black hooded rats (B&K Universals) were sacrificed by asphyxiation according to UK Home Office guidelines. Sterile equipment was used when dissecting follicles from the mystacial pad.

To dissect follicles an incision was made parallel to the dorsal row of follicles (A4-F5) followed by another parallel to the posterior row of follicles using sharp dissection scissors (Fine Surgical Tools) (see Figure 2.3). The skin next to the most posterior row was then clamped using artery forceps (Fine Surgical Tools) and the skin rolled back to reveal the follicles. No.4 watchmakers forceps (Sigma) were used to removed connective tissue from around the follicle allowing it to stand up perpendicular to the back of face pad. The watchmakers forceps were then used to grip individual follicles around their neck region, where the base of the follicle joined the skin, and pull them out in one smooth motion.

After removal, follicles were placed in bacteriological dishes containing MEM supplemented with 0.5 µg/ml Amphotericin B and 50µg/ml Gentamycin.

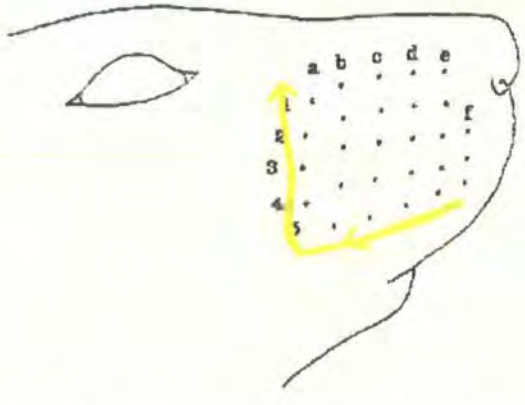

Figure 2. 3: Incision lines for dissection of follicles from the mystacial pad
Prior to isolating follicles the mystacial pad of the rat had to be incised and peeled back. Initially, an incision was made from just below follicle F5 through to A4 using dissection scissors. An incision was then made in the dorsal to ventral direction from A4 through to A1.

2.2.5.2: Operations

All animal operations were performed under home office project licence (Developmental and stem cell biology of skin) approval to Professor Colin Jahoda, by researchers with personal licence approval, Dr Gavin Richardson and Dr James Waters.

Under a Stereo dissection microscope (Nikon) previously dissected vibrissa follicles were transversely sectioned above the nerve entry point on the collagen capsule (Figure 2.4), and the hair fibres removed. They were then inserted into a 1% Geys Agar (see Appendix 1) containing 10% Fetal Calf Serum (FBS) (Sigma) in 60mm Organ culture dishes (BD Falcon). After removal from the incubator, spheres were placed into the space created by the removal of the fibres (Figure 2.4). Only spheres created from cell line DP4 were used for operational procedures.

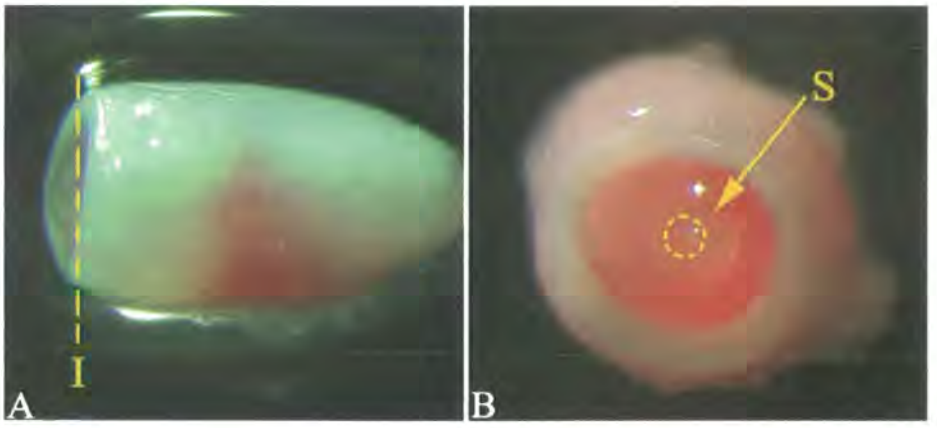

Figure 2. 4: Incision point of the vibrissa follicle and insertion of the sphere
The vibrissa follicle was sectioned above the nerve entry point, half way up the collagen capsule (I) using a sterile No.15 scalpel blade (A). The fibre was removed and the sphere (S) inserted in the space created after the removal of the fibre (B).

ICRF-Nude mice were used as hosts for the follicles, which were grafted onto the kidneys under anaesthetic. Mice were individually anesthetised using 5% Haloethane in Oxygen, at a gas flow rate of 1-2 litres per minute in induction chambers.

Anaesthesia was maintained with 2.5% Haloethane and Oxygen through a gas mask. An incision was made in their left flank, and their kidneys exposed. A small incision was made in the kidney capsule using a No.11 scalpel blade (Swann Morton) and the amputated follicles combined with spheres inserted under the capsule. Nine follicles were inserted onto the kidneys of 3 mice, with 3 on each kidney. After grafting, kidneys were inserted back into position and the incision on the flank sutured. The kidney capsule grafting method is similar to that described by Higgins *et al*, (1989).

Intact dermal papillae, isolated from vibrissa follicles were used as positive controls. As negative controls, spheres were created from interfollicular dermal fibroblasts and used in place of spheres created from dermal papilla cells.

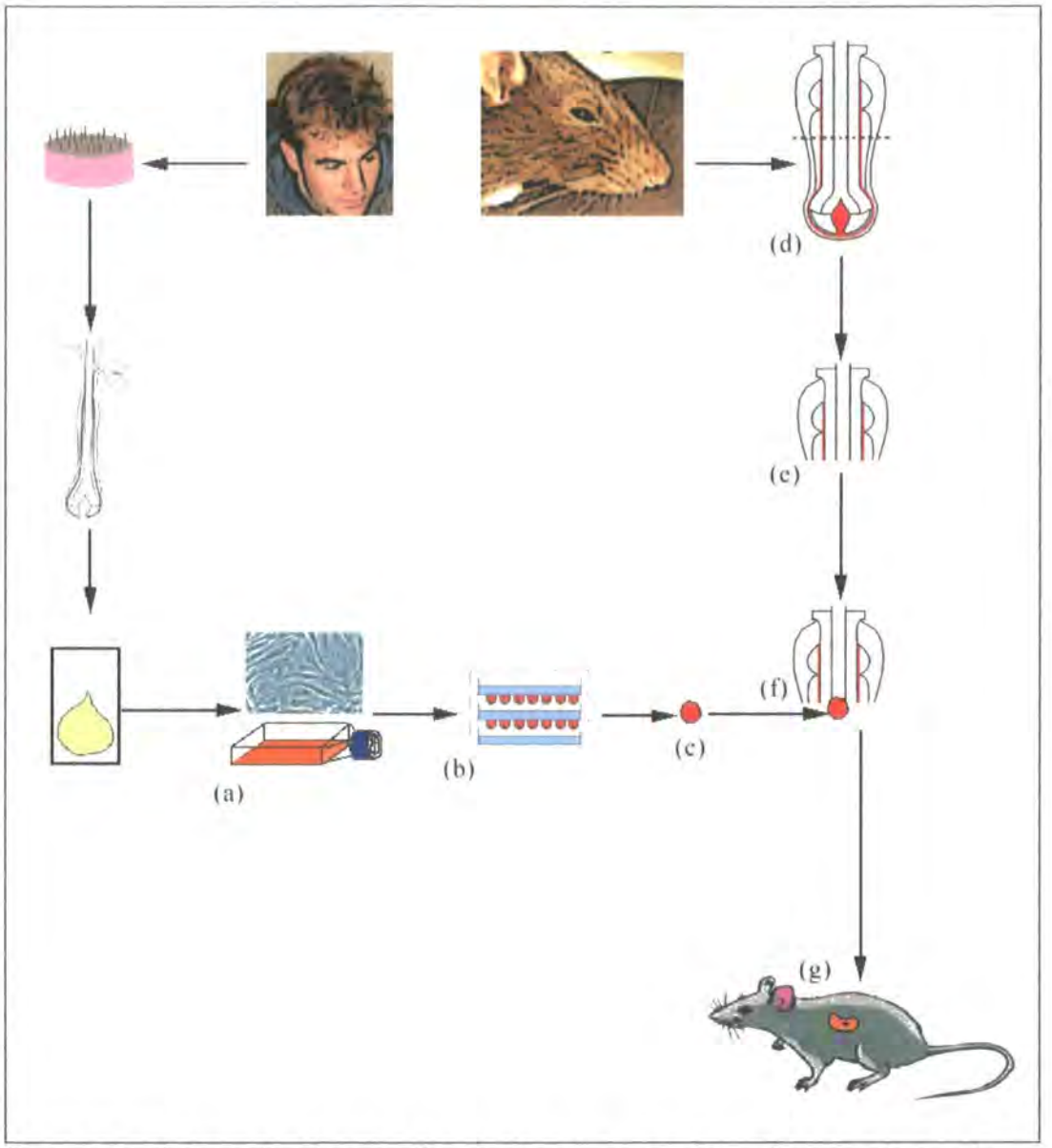

Figure 2. 5: Schematic diagram illustrating the procedures for creating and implanting dermal spheres into amputated vibrissa follicles that are then grafted onto the kidney of nude mice

Dermal papilla cells cultures, derived from previously isolated dermal papilla from human donors were cultured in T25 flasks (a) before the formation of hanging drop cultures (b). The hanging drop culture procedure enabled the dermal papilla cells to form aggregated dermal spheres (c). Vibrissa follicles that had been isolated from the mystacial pad of a PVG rat (d) were transected, inactivating the follicle (e). The dermal sphere from 'c' was then placed in contact with the epithelium in the hair shaft cavity of the inactivated vibrissa follicle (f) and grafted onto the kidney of a nude mouse (g) for 6 weeks incubation.

2.2.5.3: Amputated follicle assay analysis-Immunofluorescence

6 weeks after the initial operations, nude mice were sacrificed by asphyxiation according to UK Home Office guidelines. The kidney, complete with embedded follicles was then removed. Photographs were taken using a JVC camera attached to a stereo dissection microscope. The follicles were separated from the kidney and orientated longitudinally in Oct compound for freezing at -80°C where they were stored until sectioning.

Post operation follicles were cut into 7μm sections on a Leica 3050S cryostat, and thawed onto Superfrost Plus microscope slides (VWR). Fixation was carried out as described for the cell spheres in section 2.2.3.3. However, staining was carried out using a three step process, the antibodies and appropriate dilutions of which can be seen in Table 2.6. The blocking step and primary antibody step were as described in 2.2.3.4. However, after washing to remove unbound primary antibody, the secondary antibody, a linker antibody was applied. This linker antibody, (raised against mouse, the species in which the primary antibody was raised) was a biotinylated sheep anti mouse secondary (Zymed) and was diluted 1/300 in PBS. After a 45 minute incubation at room temperature, unbound secondary antibody was removed by washing slides 3 times in PBS (3 x 5 minutes). A tertiary detection step was then carried out. Streptavidin conjugated to Cytochrome 3 (Jackson laboratories) was diluted 1/500 in PBS and applied to the slides for 45 minutes. The streptavidin bound to the biotin label of the secondary antibody. After 45 minutes, unbound Stretavidin was washed off in 3 PBS washes. Glass coverslips were mounted using Vectashield mounting medium containing the nuclear stain diamino-2-phenylindole (DAPI) (Vector laboratories). Coverslips were sealed using nail varnished. The labelled follicles were visualised and photographed on a Zeiss Axio Imager.

Table 2. 6: Antibodies used for immunofluorescence in amputated follicle analysis

Antibody	Manufacturer	Host	Working Dilution
Anti Versican	Developmental Studies Hybridoma Bank	Mouse	Neat
Anti alpha smooth muscle actin	Sigma	Mouse	1/400
Anti beta-catenin	Transduction Laboratories	Mouse	1/100
Anti Mouse Biotinylated	Zymed	Sheep	1/300

2.2.5.4: Amputated follicle assay analysis-Haematoxylin and Eosin Staining

Frozen sections (7μm) were cut as described above (Section 2.2.5.3) and allowed to air dry for haematoxylin and eosin staining (H&E). Slides were washed briefly in PBS before immersing them in Mayer's haematoxylin solution (Sigma) for 10 min. Slides were subsequently washed in running tap water to remove excess haematoxylin before dipping them 3 times into a bluing solution (Bethyl Laboratories) to blue nuclei. They were washed briefly again in tap water before immersing them in 70% alcohol for 1 minute. They were them immersed in an eosin counter stain (0.5% in 70% alcohol) (Sigma) for 1 minute before taking them through increasing grades of alcohol to dehydrate (70%, 90%, 100%, 30 seconds agitating in each grade). Slides were then immersed in 100% alcohol for 1 minute before being transferred three changes of Histoclear, No 1 (Agar aids), with 1 minute in each change. Glass coverslips were mounted over sections using a synthetic resin, DPX (Agar aids) and left to dry at room temperature. Sections were visualised on a Leica Axio Imager.

2.2.6: Immunohistochemistry of human skin

Immunohistochemistry was carried out on human skin from four different doners to determine the expression of SDC1 throughout the hair cycle. 5μm paraffin sections of scalp tissue, processed and sectioned by Nicki Dunbar at Unilever Colworth were dewaxed and rehydrated by serial incubation in xylene (3 x 5 minutes), 100% ethanol (3 x 5 minutes), 70% ethanol (5 minutes), and finally in H_2O (5 minutes). Antigen retrieval was not required to detect the antigen of interest, SDC1 and therefore tissue sections were washed in Tris buffered saline (TBS) (see Appendix 1), in 3 x 5 minute washes, and taken through to the blocking step immediately.

Non-specific binding of the primary antibody was blocked by incubating sections with 5% sheep serum (Sigma), diluted in TBS for 30 minutes prior to antibody incubation. The blocking serum was subsequently removed and the sections incubated with the primary antibody SDC1 (Chemicon), diluted 1/300 in TBS overnight at 4°C in a humidity chamber. After primary antibody incubation, unbound antibody was removed by washing the slides in TBS (3 x 5 minutes). A secondary antibody, Sheep anti-mouse, conjugated with biotin (Zymed) was diluted 1/300 and incubated on the sections for 45 minutes at room temperature. Following a wash step, samples were subsequently incubated with a Streptavidin-Alkaline Phosphatase (Strep-AP) (Invitrogen) diluted 1/400 in TBS. Strep-AP was incubated on samples for 30 minutes, after which time unbound complex was washed off in TBS (3 x 5 minutes). Intestinal Alkaline phosphatase was detected using Fast Red (Sigma) in TBS, which complexes to form a red precipitate at the reaction site. Fast red contains Levisimol which inhibits all alkaline phosphatase activity with the exception of intestinal alkaline phosphatase. The reaction was inhibited by washing the slides in tap water for 30 seconds. Sections were then counterstained in Gills Haematoxylin No.3 (Sigma) for 10 seconds, then washed in running tap water for 5 minutes. Whilst the slides were washing, the aqueous mounting medium Glycergel (DAKO) was melted by placing in a beaker of previously boiled water. After washing, coverslips were mounted using liquid Glycergel and left to harden at room temperature. As a negative control, slides were incubated with the primary antibody substituted with TBS. Results were visualised and photographed on a Leica DMRB microscope.

2.3: Results:

2.3.1: Optimisation of sphere formation

The DP6 cell line was initially grown in MEM supplemented with antibiotics. Spheres derived from these cells took as long as 72 hours to form complete spheres, whilst matching cells in MEM free of antibiotics had formed complete spheres after only 30 hours in hanging drops. After this optimisation, all spheres were created from cell lines free from antibiotics for at least 48 hours prior to sphere formation. All plated cells were also grown free from antibiotics.

Initially, hanging drops were created using a cell suspension from the cell line DP1. Spheres were only formed if the hanging drops were placed over a dish containing PBS. In hanging drop cultures placed over PBS soaked filter paper, the dermal papilla cells did not aggregate into a sphere, but rather were visible spread over the base of the membrane of the hanging drop. Therefore, after this section of the results, all spheres discussed were formed by suspending dermal papilla cells in hanging drops over PBS.

2.3.2: Morphology of dermal spheres

TEM was carried out on the first dermal papilla cell line, DP1 only. After 30 hours in culture the majority of cells within spheres appeared viable (Figure 2.6A), with only a few cells appearing to be undergoing apoptosis. In contrast, after 5 days in culture with no medium change, few cells and nuclei were distinguishable, with many lipid droplets visible instead.

At 30 hours, cells within the sphere were well compacted, with only a little extracellular space between cells. Although close, and with membranes from adjacent cells touching frequently, no evidence of visible cell junctions was detected. However, communication between cells was visible in the form of vesicular transport, with large numbers of vesicles seen interconnected with the cell membrane, and within the cytoplasm (Figure 2.6C, D). Also, within the cytoplasm, large numbers of rough endoplasmic reticulum (RER) were observed, along with high numbers of

10nm filaments (Figure 2.6E). Cells in the centre of the sphere appeared more spherical in shape, whilst those at the edge of the sphere were flattened and elongated (Figure 2.6F).

Although TEM was not carried out on other cell lines apart from DP1, the nuclear counterstaining patterns of DP3-6 gave an insight into the morphology of spheres created from these cell lines. Spheres from DP3 and DP4 had continuous rounded nuclei present throughout the entire sphere. However, in contrast, spheres from DP5 and DP6 had rounded nuclei in the centre of the sphere, whilst they exhibited flattened elongated nuclei in 3-4 cell layers around the edge of the sphere.

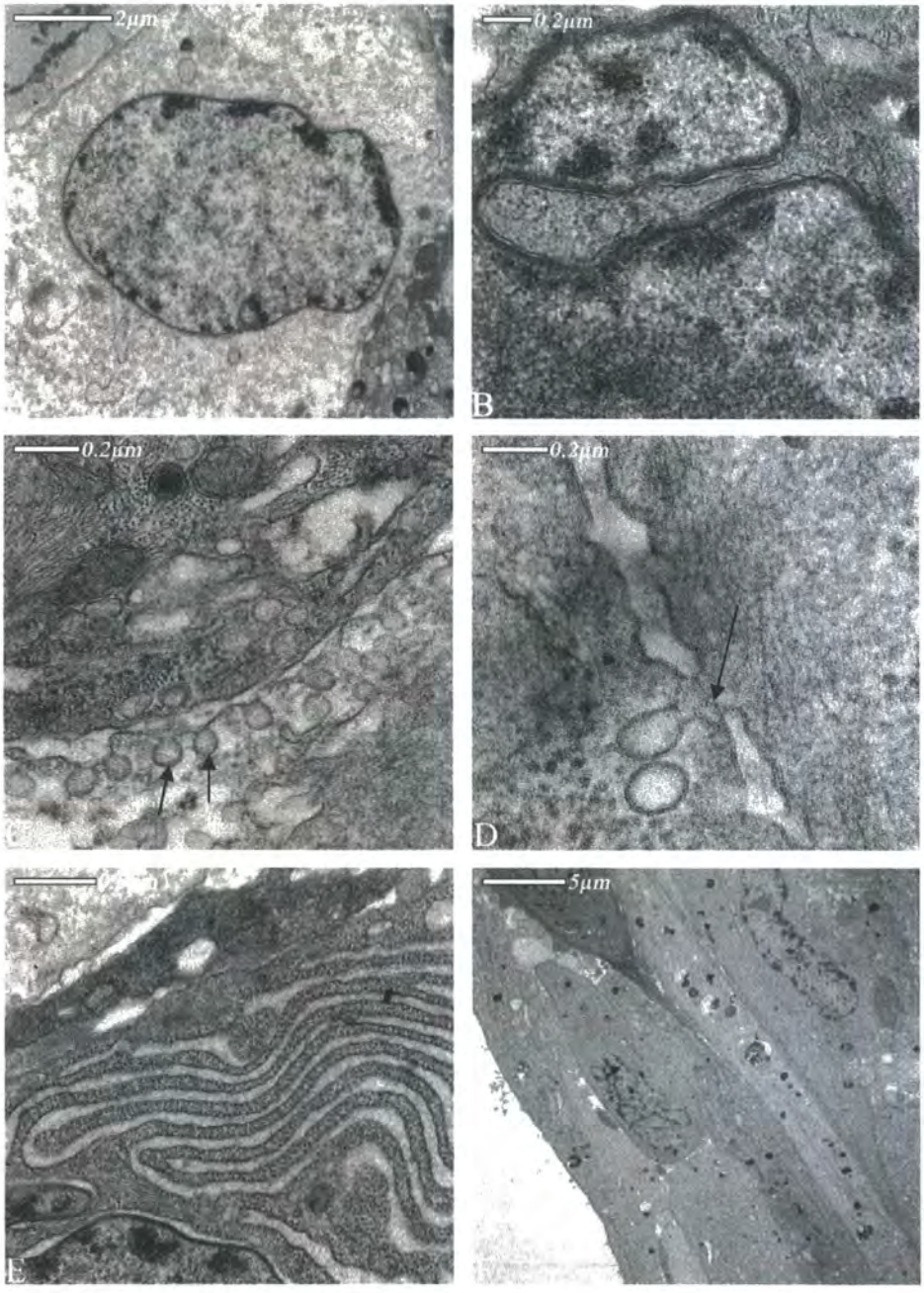

Figure 2. 6: Transmission electron microscopy of DP1 spheres

Intact, healthy cell nuclei are visible (A) within dermal spheres, complete with nuclear pores within the nuclear envelope (B). Numerous numbers of 10nm filaments are seen within cells, in addition to transport vesicles (arrows), which are visible in cells adjacent to one another (C). Transport vesicles are also visible making contact with the cell membrane (arrow), linking adjacent cells, and indicative of cellular transport (D). Large amounts of RER are visible in the cytoplasm of dermal cells within spheres (E). Whilst the cells and nuclei in the centre of the sphere are rounded, the cells at the edge appear flattened and elongated (F).

2.3.3: Comparisons between plated dermal cells and dermal spheres

The PCNA and aSMA expression in spheres was showed and compared to that of plated cells. The results are described in sections 2.3.3.1 and 2.3.3.2, a summary of which can be seen below in Tables 2.7 and 2.8.

Table 2. 7: Protein expression of PCNA and aSMA in plated cells and spheres from different dermal papilla cell lines

	DP1	DP2	DP3	DP4	DP5	DP6
PCNA 2D culture	Present	Present	Present	Present	Present	Present
PCNA 3D culture	Absent	Abse nt	Absent	Absent	Absent	Absent
aSMA 2D culture	Present	Present	Present	Present	Present	Present
aSMA 3D culture	Present at edge only	Present at edge only	Strong in centre, weak on edge	Present at 30 hrs Decreased by 78 hrs	Present at 30 hrs. Absent on outer edge after 78 hrs	Present at 30 hrs Decreased by 78 hrs

Table 2. 8: Gene expression of Ki67 and aSMA in plated cells and spheres from different dermal papilla cell lines

	DP1	DP2	DP3	DP4	DP5	DP6
Ki67 2D culture	High	High	N/A	High	High	N/A
Ki67 3D culture	V.Weak	V.Weak	N/A	V.Weak	V.Weak	N/A
aSMA 2D culture	High	High	N/A	High	High	N/A
aSMA 3D culture	Weak	Weak	N/A	Weak	Weak	N/A

2.3.3.1: Proliferation

PCNA was detected in the nuclei of plated dermal papilla cells, from all cell lines investigated. However, this was in contrast to expression in dermal papilla cell spheres, in which PCNA was absent, as can be seen in Table 2.7 and Figure 2.7. This observation was supported by real time PCR results (Graph 2.1) which showed negligible *Ki67* gene expression in 3D sphere cultures compared to strong expression observed in 2D plated cell cultures (Table 2.8).

2.3.3.2: Alpha Smooth Muscle Actin expression

In cell lines under investigation, aSMA was detected in interwoven microfilament bundles, giving a distinctive fibrillar pattern (Figures 2.8A, B). aSMA was present in all 2D cultures analysed at both the protein and the gene level. In the 3D spheres created from cell lines DP1 and DP2, analysed as whole spheres aSMA was only present at the edge of the sphere. However, in sectioned spheres, created from cell lines DP3-6, aSMA was present after 30 hours in culture. In DP3 spheres, expression remained after 78 hours in culture. However, in DP4-6, aSMA expression had decreased after 78 hours in culture (Figures 2.8E, F). Intriguingly, in all the cell lines analysed with real time PCR, gene expression of *aSMA* was noticeably weaker in 3D cultures than in 2D cultures after 30 hours in culture (Graph 2.2).

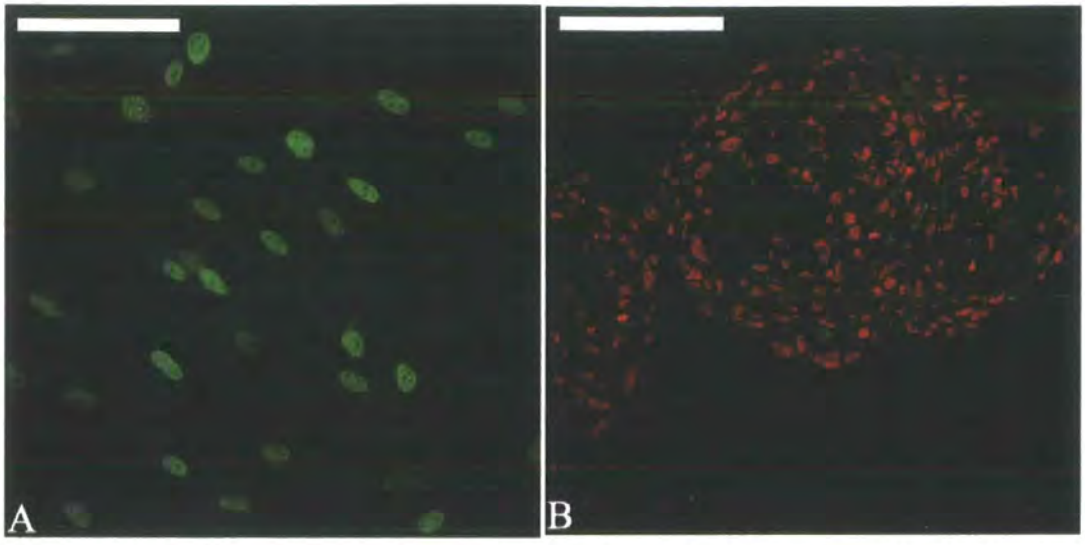

Figure 2. 7: Proliferation of plated cells and dermal spheres from the DP1 cell line

PCNA expression was present in the nuclei of dermal papilla cells in 2D cultures from all 6 cell lines examined, as shown in the DP1 cell line in A. However, its absence in 3D sphere cultures was noticeable (B).

Green-PCNA; Red-PI nuclear counterstain; Scale Bars-100μm

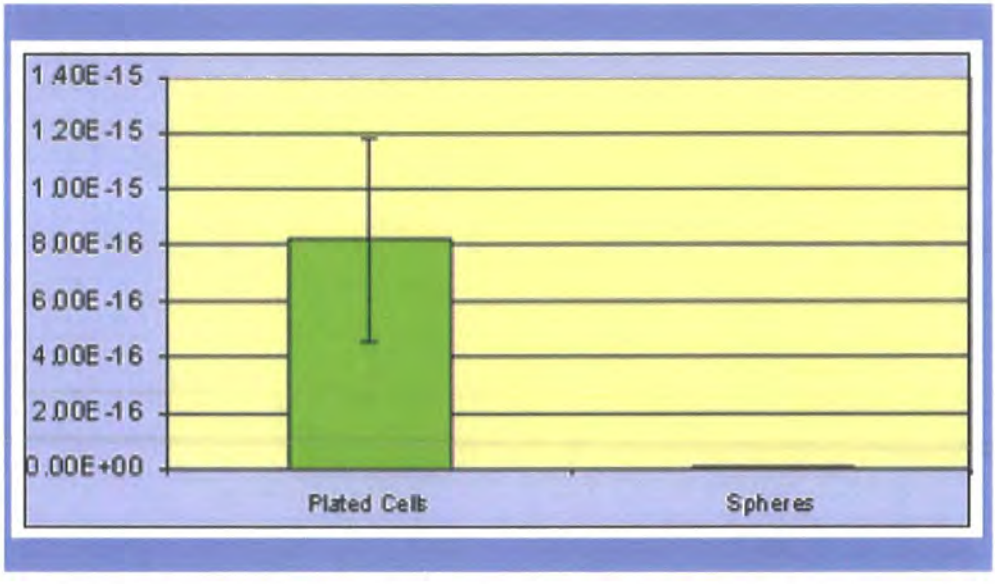

Graph 2. 1: Real time PCR analysis of *Ki67* expression in 2D and 3D dermal papilla cell cultures

The observed change in proliferation between 2D and 3D cell cultures was also recaptured at the gene level, as indicated by the real-time PCR results which showed *Ki67* expression in 2D plated cell cultures but an absence in 3D dermal sphere cultures.

Figure 2. 8: aSMA expression in 2D and 3D cultures of human dermal papilla cells

Plated dermal papilla cells exhibited a distinctly fibrillar pattern of staining, as in microfilament bundles throughout cells (A, B). In dermal spheres created from the DP4 cell line aSMA was present throughout spheres after 30 hours in culture (C). By 78 hours in culture the intensity of staining had decreased significantly (E). A similar phenomenen was seen in the spheres created from the DP5 cell line which after 30 hours in culture exhibited strong aSMA expression throughout (D). After 78 hours in cultures, spheres created from the DP5 cell line had lost aSMA expression in the several flattened cell layers at the periphery of the sphere, although expression remained in the centre (F).

A, C, E: 2D and 3D cell cultures of cell line DP4
B, D, F: 2D and 3D cell cultures of cell line DP5

Green: aSMA,
Red: PI nuclear counterstain

Scale Bars: 100μm

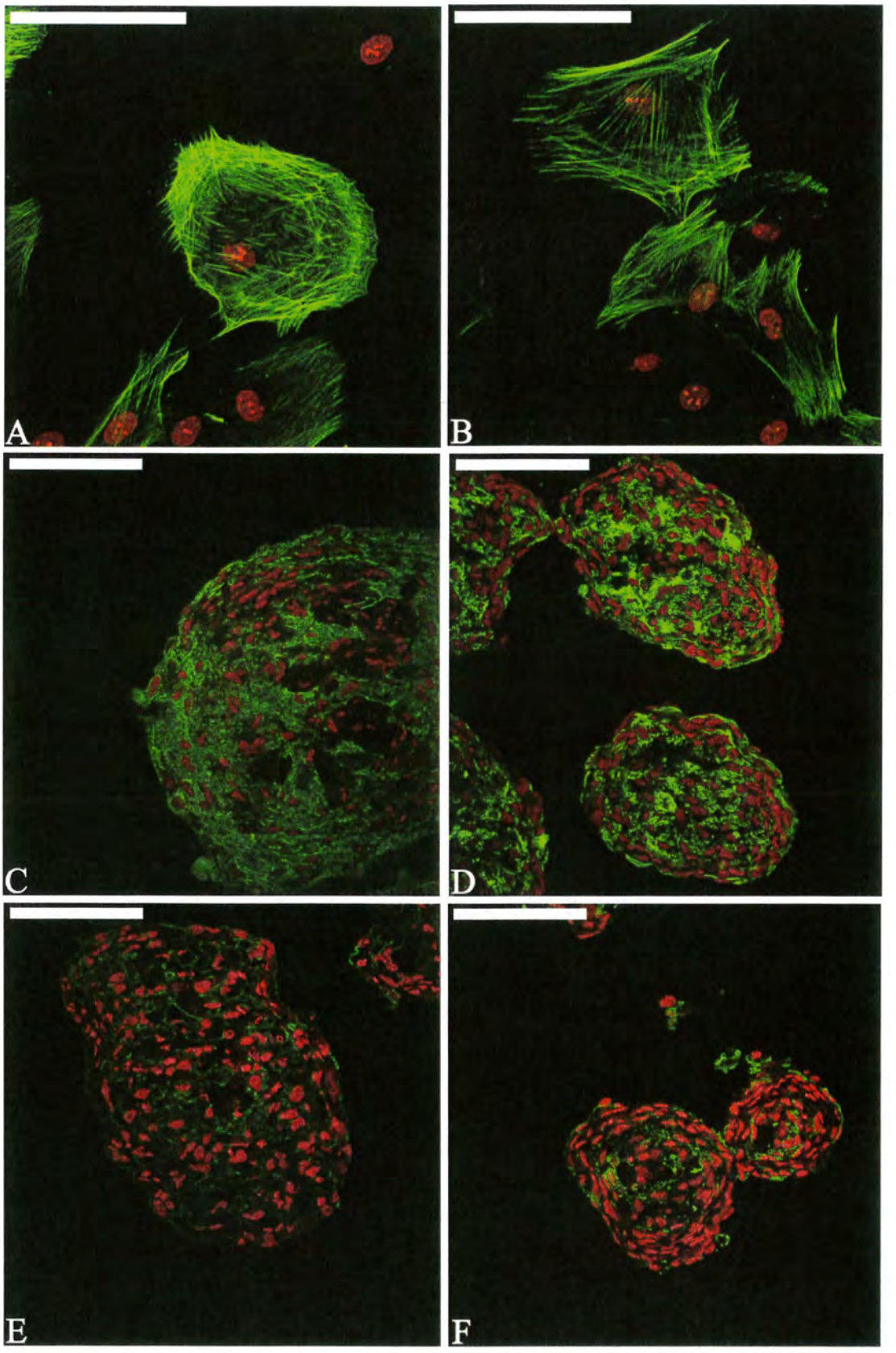
A
B
C
D
E
F

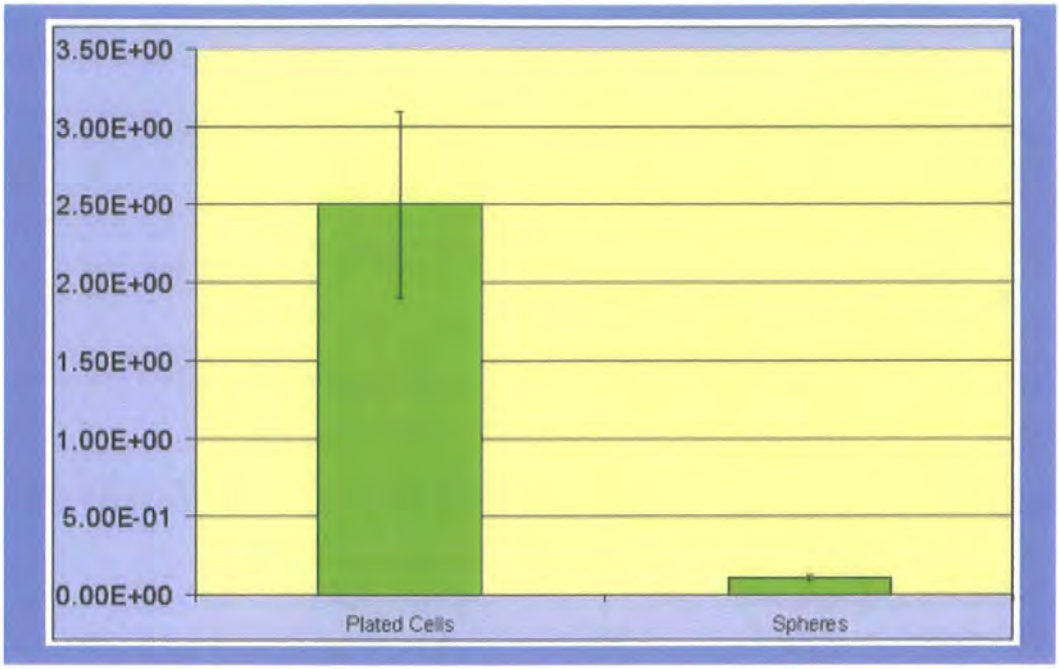

Graph 2. 2: *aSMA* expression in 2D and 3D dermal papilla cell culture from cell line DP4

Real time PCR was used to analyse transcriptional activity of *aSMA* expression in both 2D plated cultures and 3D sphere cultures of dermal papilla cells. There was a decrease in expression in the transition from 2D to 3D. The graph here shows the results for the DP4 cell line. These results were repeated in all cell lines analysed with real time PCR.

2.3.4: Junctional expression

2.3.4.1: Connexin 43

Connexin 43 (Cx43) expression was analysed in cell lines DP3-DP6 only. Punctate Cx43 expression was seen throughout the plated dermal papilla cell cultures, at points of cell contact between cells (Figure 2.9A), with increased expression observed in more confluent areas. Clustering of Cx43 staining was also observed in the cytoplasm localised around the nucleus. Noticeably in spheres, Cx43 expression was observed in a bright punctate staining pattern at the cell membrane; a pattern of fluorescence indicative of gap junctional channels (Figures 2.9, C, E). This profile of Cx43 staining was observed in all DP cells investigated.

2.3.4.2: ß-catenin

ß-catenin expression was analysed in all 6 dermal papilla cell lines under investigation. Expression in 2D cultures was weak, and was visible only at points of contact between cells (Figure 2.9B). However, in 3D cultures ß-catenin expression was dramatically increased, and prominent staining was observed throughout spheres. ß-catenin was present uniformly at the cell membrane, surrounding all cells within the spheres (Figure 2.9D, F). This profile of ß-catenin expression was observed in all DP cell lines investigated.

Figure 2. 9: Connexin 43 and ß-catenin expression in 2D and 3D human dermal papilla cells

Cx43 expression was punctate and visible at gap junctional channels where cell-cell contacts were present. In plated 2D cell cultures Cx43 expression was distributed around the periphery of cells, whilst some perinuclear staining was also present (arrow) (A). Similarly, ß-catenin was present at points of cell-cell contact, appearing almost continuously around the periphery of cells (B). In sphere formations, Cx43 was present throughout the sphere (C), as was ß-catenin, notably present in higher quantities in dermal spheres when compared to flattened cells (D). The punctate nature of Cx43 staining is apparent in spheres at higher magnifications, although no perinuclear staining was observed (E). The higher magnification of ß-catenin in dermal spheres shows an almost uniform presence around the periphery of the cells (F).

Green: A, C, E: Cx43; B, D, F: ß-catenin
Red: PI nuclear counterstain
Scale Bars: 50 μm

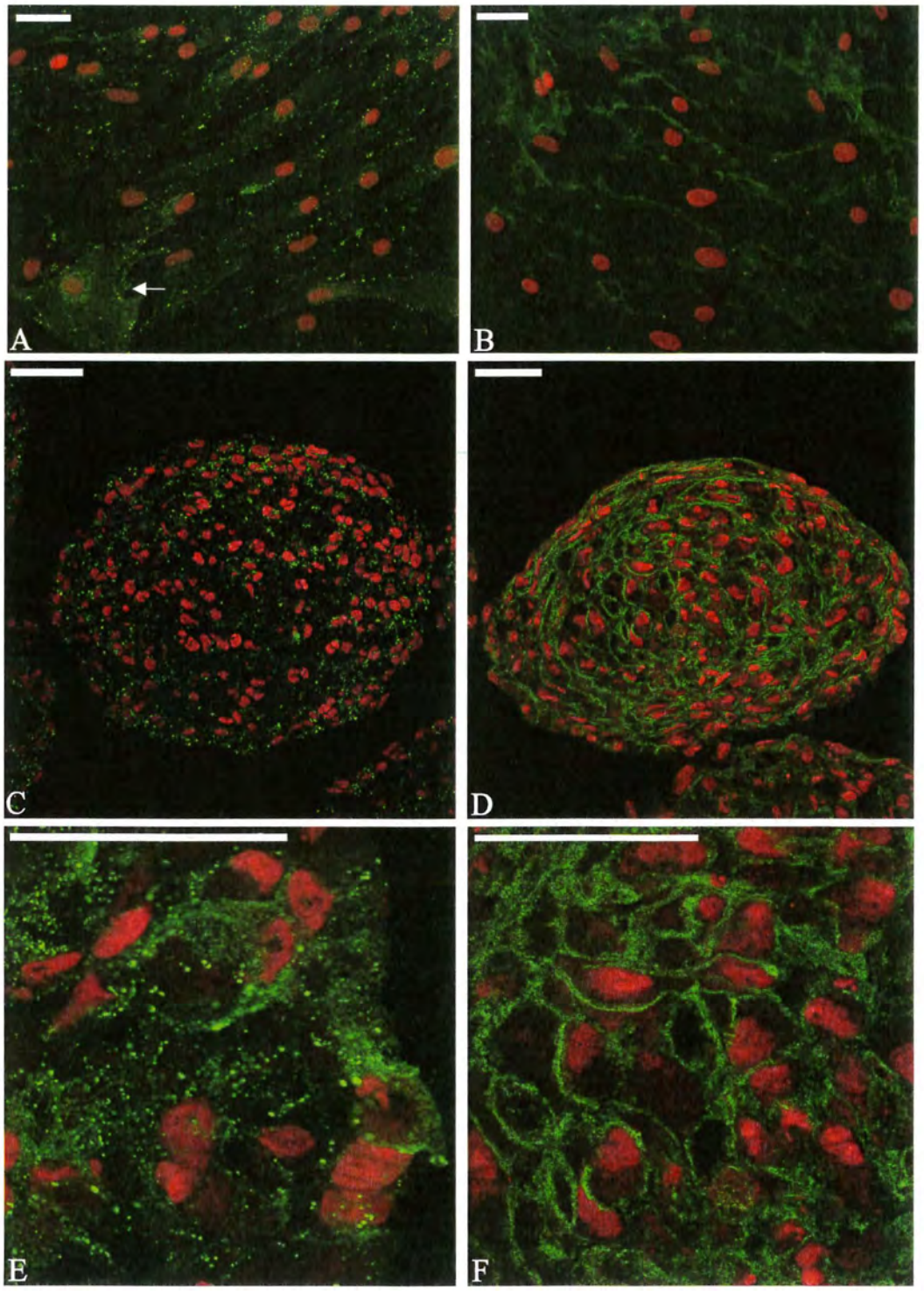
A
B
C
D
E
F

2.3.5: Proteoglycan Expression Profile

The proteoglycan expression profile within 2D and 3D cultures was analysed in the 6 different dermal papilla cell lines. The results are described in sections 2.3.5.1-2.3.5.4 and are outlined below in Table 2.9.

Table 2. 9: Proteoglycan expression profile in 2D and 3D dermal papilla cultures from different cell lines

	DP1	DP2	DP3	DP4	DP5	DP6
Versican 2D Cultures	Absent	Absent	Absent	Absent	Absent	Absent
Versican 3D Cultures	Absent	N/A	Absent	Absent	Weak	Weak
SDC1 2D Cultures	Strong	Weak	Absent	Few strong cells, otherwise absent	Few strong cells, otherwise absent	Absent
SDC1 3D Cultures	Strong	Absent	Absent	Absent	Present at the outer edge of sphere	Present in the centre of sphere only
Bamacan 2D Cultures	Strong	Strong	Weak/Absent	Weak/Absent	Strong	Strong
Bamacan 3D Cultures	Moderate	Strong	Weak/Absent	Weak/Absent	Weak	Strong
Perlecan 2D Cultures	Strong	Strong	Strong	Strong	Strong	Strong
Perlecan 3D cultures	Strong	Strong	Strong	Strong	Strong	Strong

2.3.5.1: Versican

Versican expression was absent in all plated cell lines examined, as might have been anticipated as they were all passage 5 and above (Figure 2.10A). However,

expression of versican was detected in dermal spheres created from both the DP5 and DP6 cell lines (Figure 2.10B, C). Nevertheless, it was absent from all remaining spheres from cell lines DP1-4. In the DP5 and DP6 cell lines, versican expression was extracellular, and observed in a granular pattern.

2.3.5.2: Syndecan 1

SDC1 was analysed in all 6 dermal papilla cell lines with immunofluorescence, and in 4 of the 6 cell lines with real-time PCR. At the protein level however, expression was variable between cell lines as indicated in Table 2.9. Expression was strongest in the DP1 cell line, although it was observed at varying intensities in different individual cells (Figure 2.11A1). Expression was not present in all of the dermal papilla cells from this first cell line-approximately three quarters possessed the antigen. Moreover, in the spheres created with this cell line, SDC1 appeared throughout as shown in Figure 2.11A2. Within the majority of cells, expression was fibrillar, with occasional granular patterning also observed.

In the DP2 cell line, very weak SDC1 was detectable in the occasional plated cell (Figure 2.11B1) whilst in the DP3 cell line no SDC1 was seen in 2D cultures (Figure 2.11C1). Moreover, no expression was detected in spheres created from either of these cell lines (Figures 2.11B2, C2). In both the DP4 and DP5 cell lines, occasional cells in 2D cultures were strikingly fluorescent, indicative of strong SDC1 expression (Figures 2.11D1, E1). However, in spheres created from the DP4 cell line no SDC1 was visible (Figure 2.11D2). In contrast, spheres created from the DP5 cell line exhibited SDC1 expression, although this decreased in the centre of the sphere with increasing time in culture, remaining only at the outer edge of the sphere after 78 hours (Figure 2.11E2). In both the DP4 and DP5 cell lines, gene expression of *SDC1* was analysed by real time PCR (Graphs 2.3C, D). These results indicated a decrease in *SDC1* transcription upon sphere formation in the DP4 cell line. This change is similar to that observed at the protein level. Moreover, in the DP5 cell line, real time PCR showed expression of *SDC1* in 2D cultures to have increased upon 3D sphere formation, again, repeating the observed result at the protein level for this cell line.

In the DP6 cell line, plated cells contained no SDC1 expression whilst spheres had large amounts of SDC1 throughout (Figures 2.11F1, F2). With time in culture this expression decreased at the outer edge of the sphere, remaining only in the centre of the sphere after 78 hours in the hanging drop. This was in stark contrast to the observed results from DP5 cell line spheres.

2.3.5.3: Bamacan

Bamacan expression was analysed in all 6 dermal papilla cell lines with immunofluorescence and, like SDC1, its pattern of expression varied between cell lines. The observed expression pattern was punctate, with both cytoplasmic and nuclear expression visible. However, nuclear expression was more intensive than that visible in the cytoplasm. In the DP1 cell line, strong expression in the plated cells decreased upon sphere formation, though it still remained present, as shown in Figure 2.12A1 and A2. In contrast, DP2 plated cells showed bright staining for bamacan, which became intensified upon sphere formation. These trends were repeated at the gene level using real time PCR for both the DP1 and DP2 cell lines as can be seen in Graph 2.4A and B.

Compared with DP1 and DP2, the DP3 and DP4 cell lines both exhibited weak bamacan expression in plated cells, whilst there was also weak or no bamacan expression in dermal spheres created from these 2 cell lines. Interestingly, the DP5 cell line, which displayed strong bamacan expression throughout plated cells (Figure 2.12E1), showed restricted expression upon sphere formation, with bamacan only visible within cells in the centre of the spheres. Expression was absent from the cells at the periphery of the spheres (Figure 2.12E2). In the DP6 cell line, strong expression in the plated cells was maintained in the 3D spherical cultures, in which cells showed both strong perinuclear and cytoplasmic expression (Figure 2.12F1, F2). Perinuclear staining of proteoglycans may indicate that the pool of protein is still undergoing post-translational modifications in the Golgi complex, prior to being exported into the extracellular matrix. At the gene level, both 2D plated, and 3D sphere cultures from the cell line DP4 showed negligible transcriptional expression compared to the other cell lines. Both plated cells and spheres from the DP5 had high

levels of expression, with no significant difference observed between the two culture conditions as shown in Graphs 2.4C and D.

2.3.5.4: Perlecan

Perlecan antigen was present in all dermal papilla cell lines investigated, in both plated cells and spheres. In all cells lines, perlecan expression appeared disorganised, and was visible as coarse intracellular granules and fibrils, with more intense fibrillar staining visible around the nucleus (Figure 2.13A). In spheres, perlecan expression was more consistent, displaying an extracellular pattern throughout (Figure 2.13C). Real-time PCR indicated that there was very little difference in *perlecan* gene expression between plated cells and dermal spheres in all 4 cell lines analysed with this method (Graph 2.5).

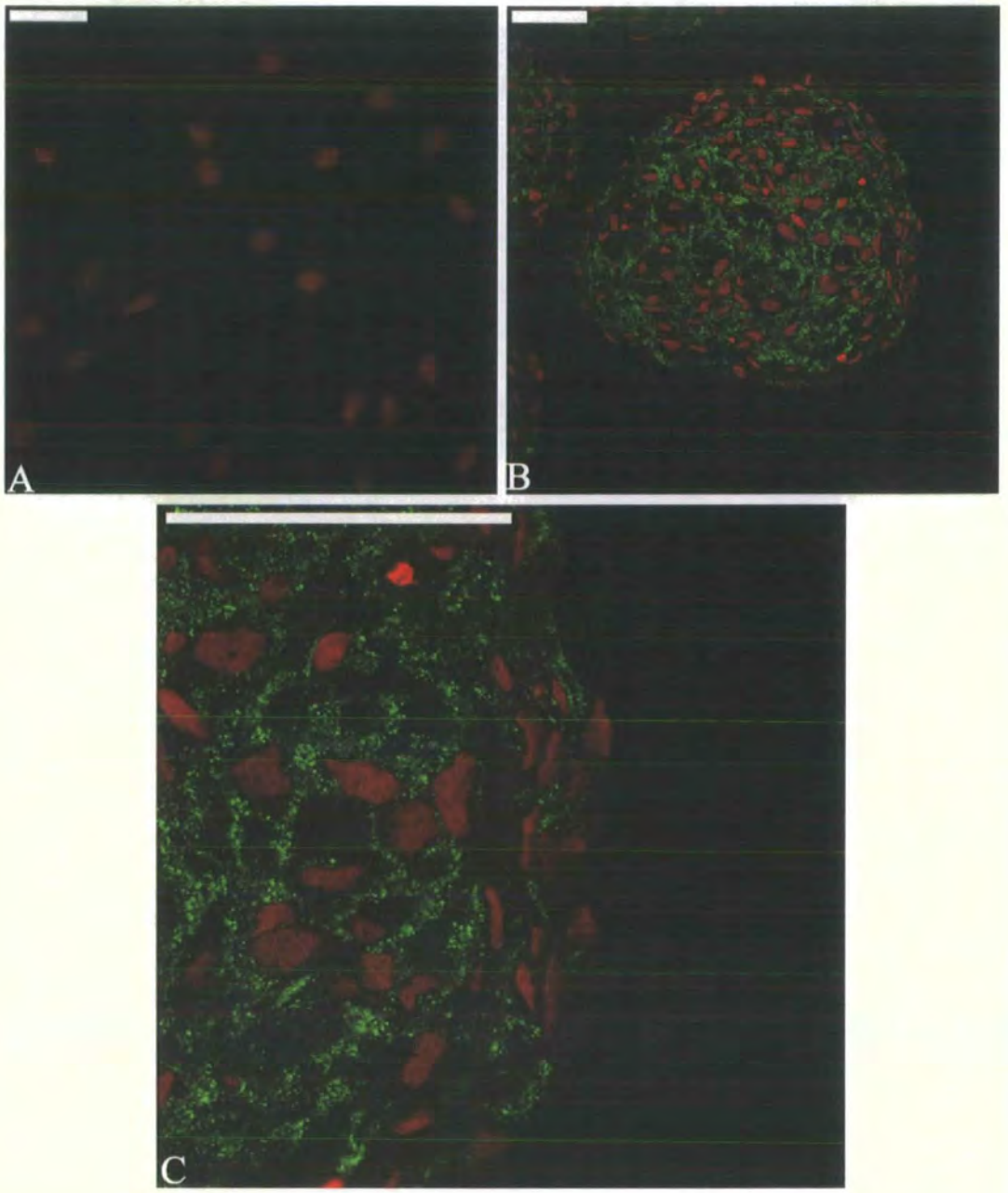

Figure 2. 10: Versican expression in 2D and 3D cell cultures from human dermal papilla cell line DP6

Veriscan was not expressed in monolayer dermal papilla cells from cells which were at passage 8 (A). Upon sphere formation, versican expression was apparent around the dermal papilla cells (B). A higher magnification of spheres showed that the versican expression was granular, in the extracellular space surrounding cells (C).

Green: Versican, Red: PI nuclear counterstain

Scale Bars: 50μm

Figure 2. 11: Syndecan 1 expression 2D and 3D cell cultures of human dermal papilla cells

SDC1 was present in a fibrillar pattern, with occasional granular staining. SDC1 was strongest in cell line DP1, where bright staining was detected in the majority of plated dermal papilla cells (A1). In addition, in spheres created from this cell line SDC1 staining was present throughout the sphere (A2). Weak SDC1 was present in occasional plated cells from the DP2 cells line (B1) although expression was not observed in spheres (B2). In the DP3 cell line no SDC1 expression was observed in either plated cells (C1) or spheres (C2). In contrast, in the DP4 cell line, very bright cells were occasionally observed in plated cells (D1) whilst no SDC1 was present in spheres created from this cell line (D2). In the DP5 cell line bright staining was visible in a small number of plated cells (E1) whilst in the spheres expression was visible at the periphery only (E2). In contrast, plated dermal papilla cells from the DP6 cell line expressed no SDC1 expression (F1) whilst SDC1 was present in the centre of spheres created with this cell line, being absent from the periphery (F2).

Green: SDC1
Red: PI nuclear counterstain
Blue: DAPI nuclear counterstain

Scale Bars: 100μm

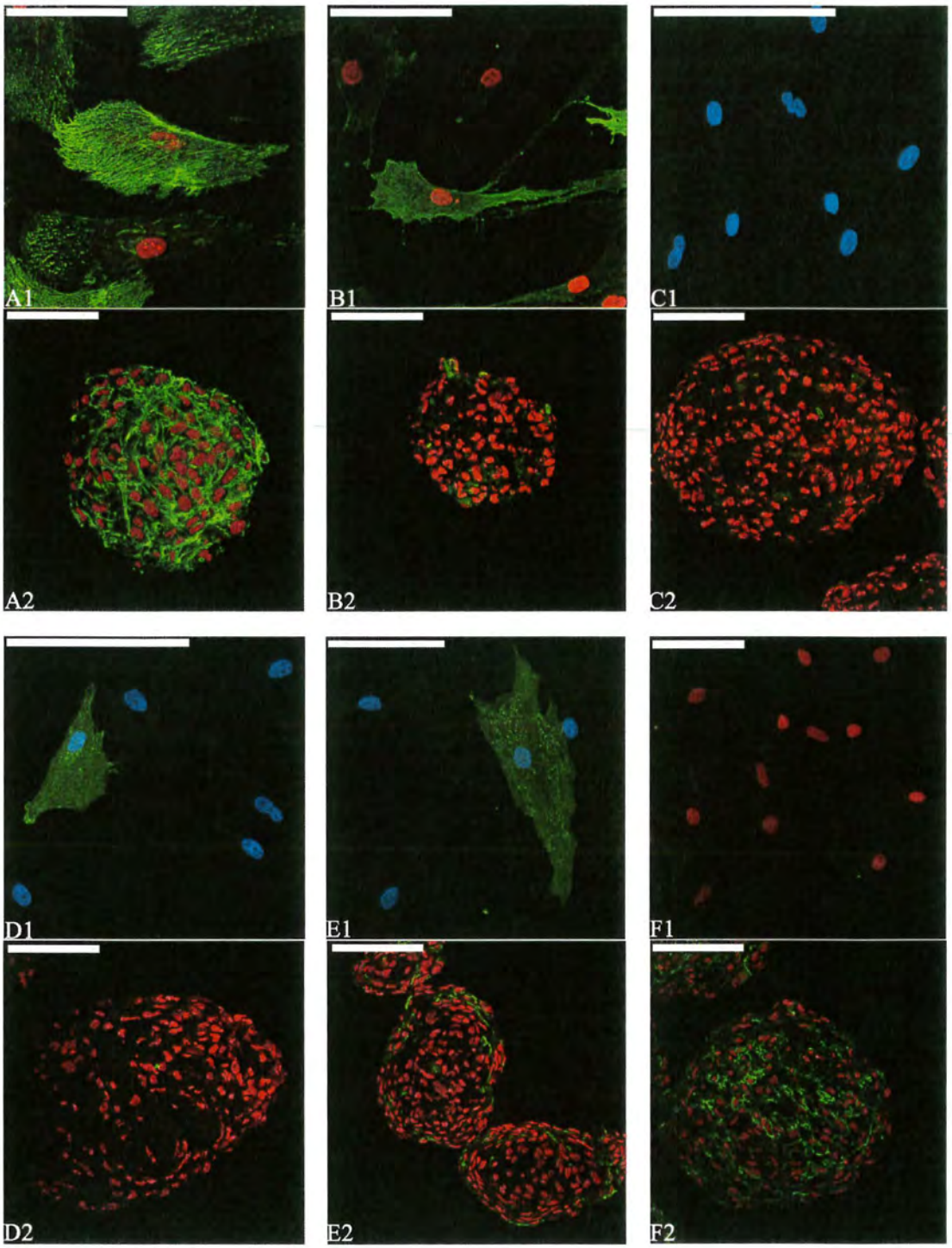
A1
B1
C1
A2
B2
C2
D1
E1
F1
D2
E2
F2

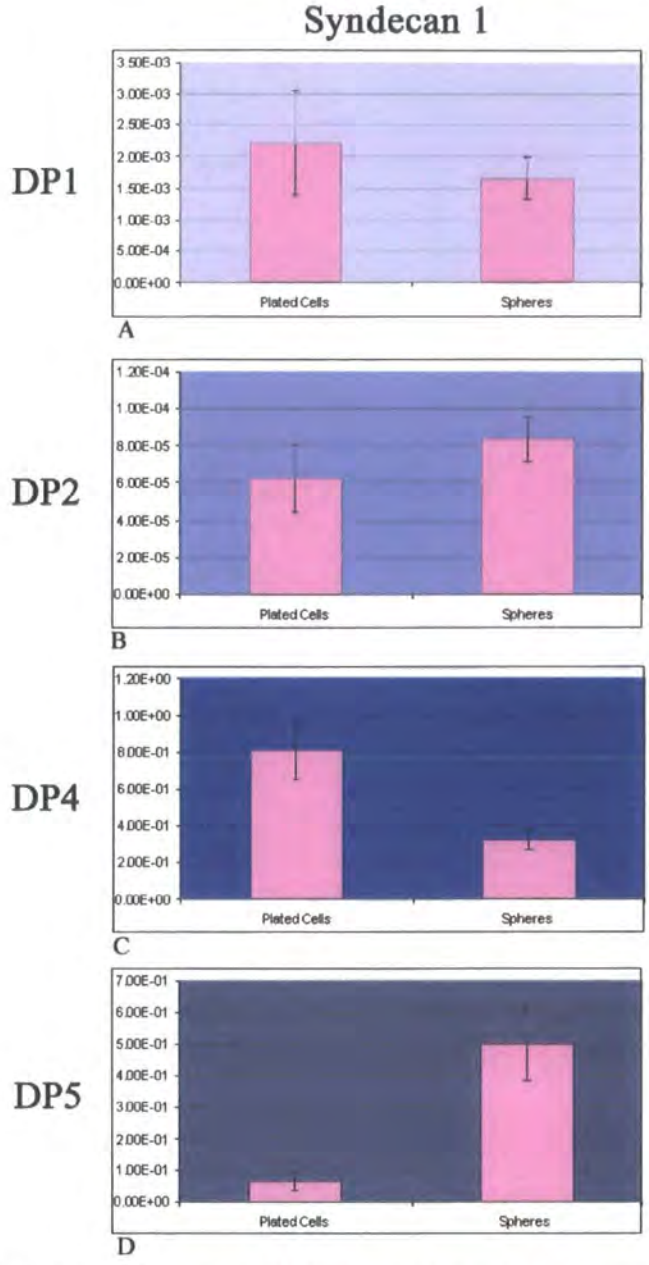

Graph 2. 3: Transcriptional profile of *Syndecan 1* in 2D and 3D dermal papilla cells cultures

Gene expression of *SDC1* was evaluated using Real-time PCR on cDNA created from the DP1, DP2, DP4 and DP5 cell lines. No significant difference was seen between plated cells and dermal spheres from the DP1 (A) and DP2 (B) cell lines. However, a decrease of *SDC1* gene expression was observed with the formation of dermal spheres from plated cells in the DP4 cell line (C). In contrast, an increase was observed upon sphere formation from plated cells in the DP5 cell line (D).

Figure 2. 12: Bamacan expression 2D and 3D cell cultures of human dermal papilla cells

Bamacan expression within plated dermal papilla cells was punctate, with staining following the same pattern as cytoskeletal filaments within cells. Nuclear expression was also present, which was brighter than the observed cytoplasmic staining. In the DP1 cell line, both strong cytoplasmic and nuclear bamacan expression was observed in plated cells (A1), which decreased upon sphere formation (A2). In contrast, both plated cells from cell line DP2 (B1) and spheres both were highly positive for Bamacan (B2). Comparatively, weak bamacan expression was seen in the DP3 cell line, in both plated cells (C1) and spheres (C2). A similar observation was seen in the DP4 cell line, where both plated cells (D1) and spheres (D2) exhibited low bamacan expression. The DP5 cell line showed relatively strong bamacan expression in plated cells (E1). In spheres, this expression appeared restricted to the nuclei of cells in the centre of the spheres, being absent at the periphery, noticeable due to the change in nuclei colour from yellow to red towards the sphere periphery (E2). In the DP6 cell line, both nuclear and cytoplasmic expression of bamcan was observed in plated cells (F1). Moreover, this was recapitulated in spheres where strong nuclear and cytoplasmic expression was present (F2).

Green: Bamacan
Red: PI nuclear counterstain
Blue: DAPI nuclear counterstain

Scale Bars: 100μm

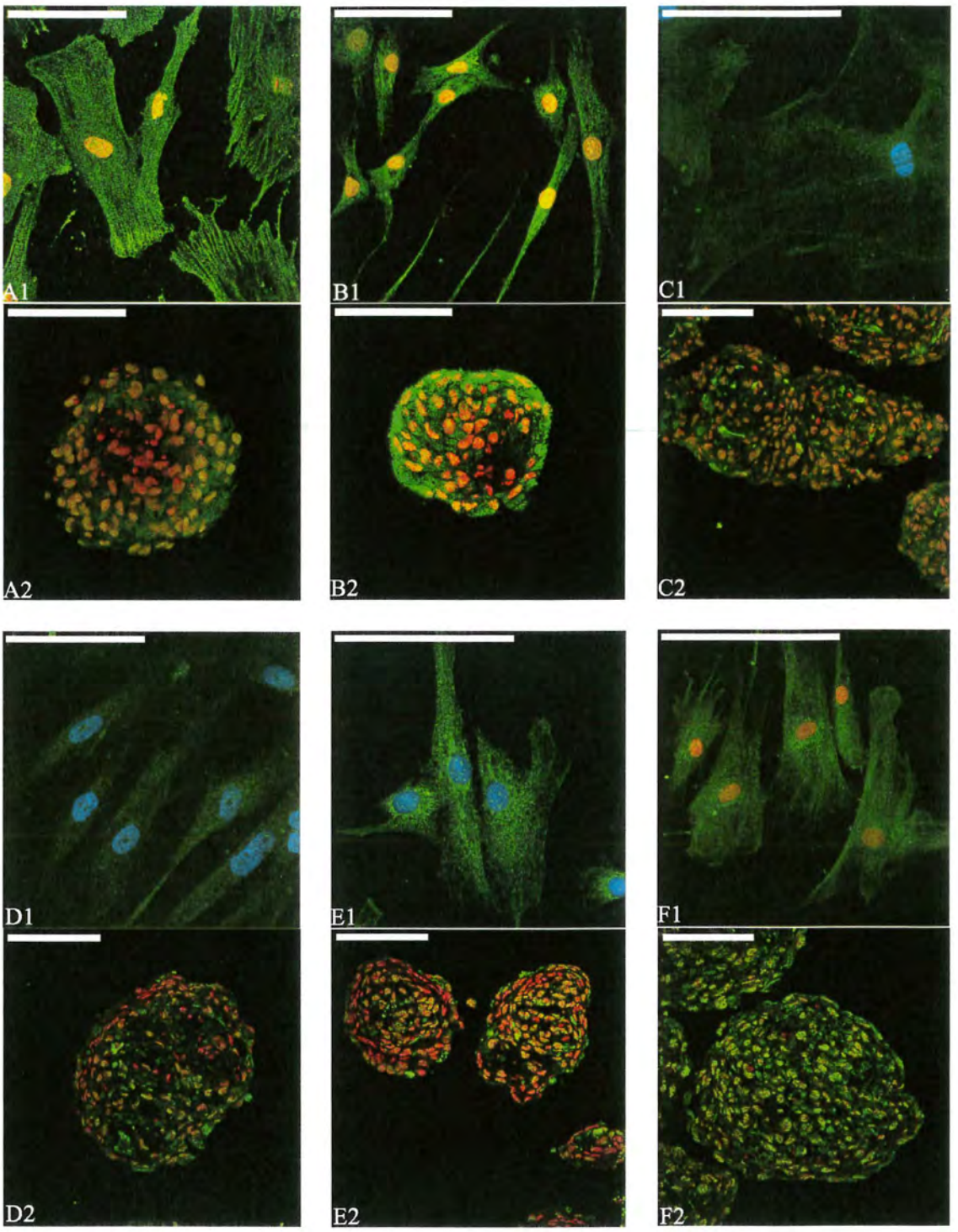
A1
B1
C1
A2
B2
C2
D1
E1
F1
D2
E2
F2

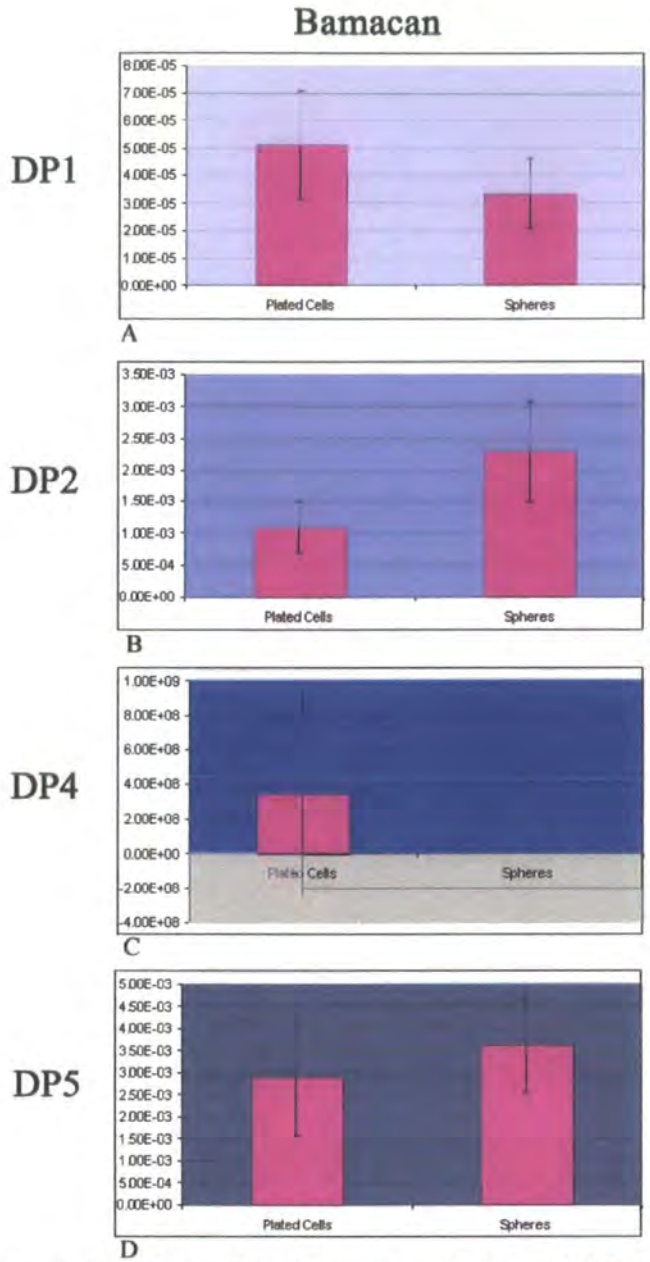

Graph 2. 4: Transcriptional profile of *Bamacan* in 2D and 3D human dermal papilla cultures

Gene expression of *bamacan* was evaluated using Real-time PCR on cDNA created from the DP1, DP2, DP4 and DP5 cell lines. Whilst a slight decrease in *bamacan* expression was observed in cell line DP1, this was not significant (A). However, an increase in transcriptional expression was observed upon sphere formation, when compared to plated cells from the DP2 cells line (B). Negligible transcriptional expression was observed in the DP4 cell line, in both plated cells and spheres (C). However, relatively strong expression was observed in the DP5 cell line, although with no significant difference, as indicated by the error bars, seen between plated cells and dermal spheres.

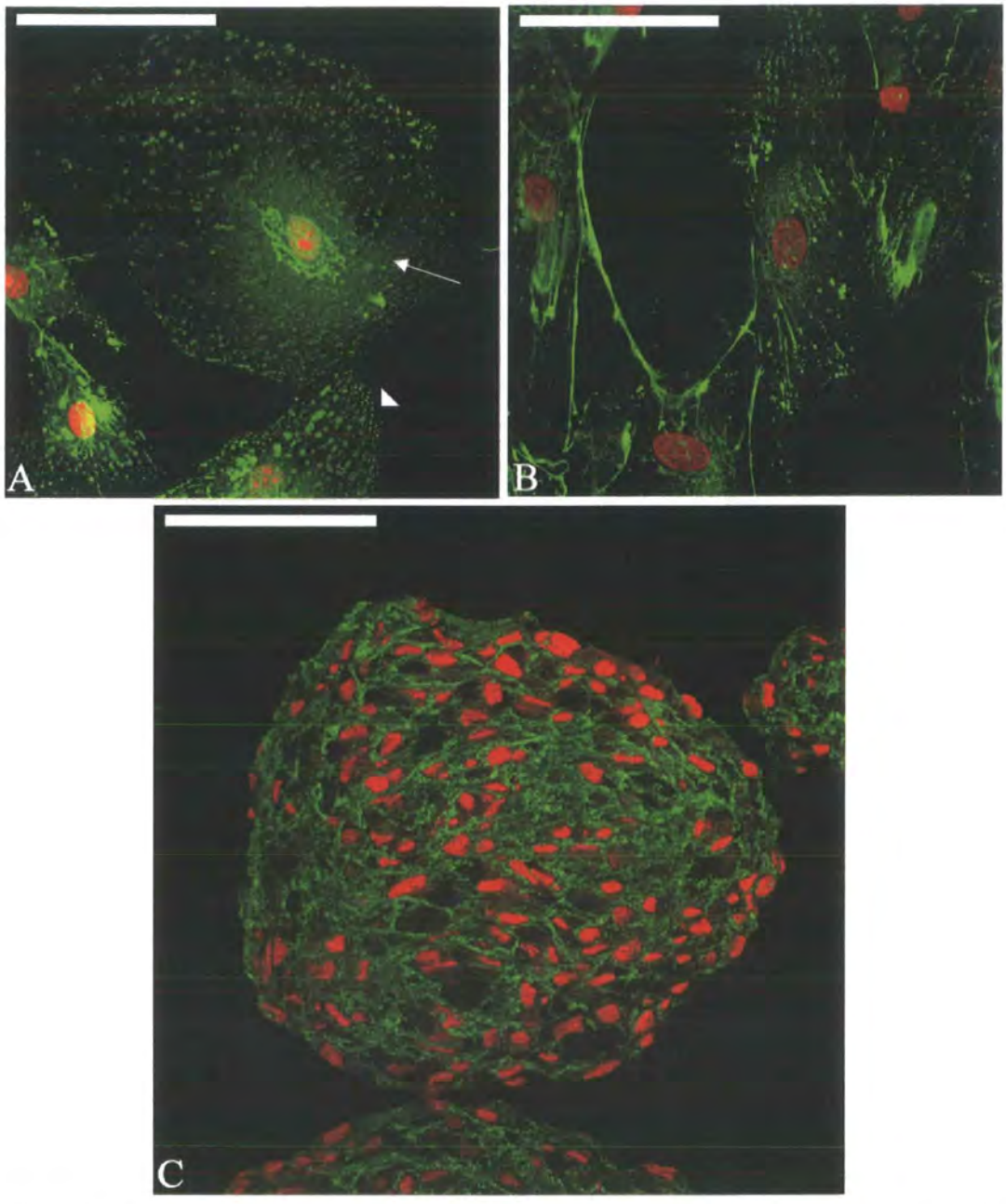

Figure 2. 13: Perlecan expression 2D and 3D cell cultures of dermal papilla cells

Perlecan expression was visible in a similar pattern within all cell lines under investigation. In addition to expression within large intracellular granules (arrowhead), expression was also fibrillar, with more intense staining seen surrounding cell nuclei (arrow) (A). Fibrillar expression was also seen throughout cells, appearing disorganised in arrangement (B). Upon sphere formation, perlecan was consistently visible throughout the entire sphere, appearing in the extracellular matrix surrounding cells (C).

Green: Perlecan; Red: PI nuclear counterstain

Scale Bars: 100μm

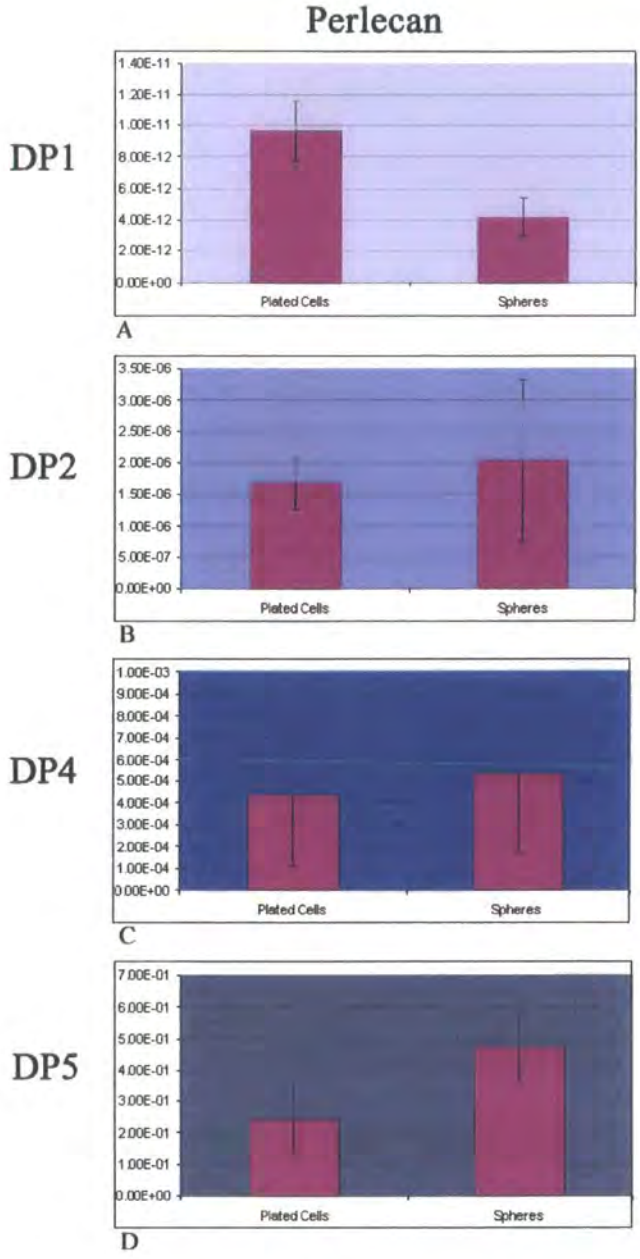

Graph 2. 5: Transcriptional profile of *Perlecan* in 2D and 3D dermal papilla cells cultures

Gene expression of *perlecan* was evaluated using Real-time PCR on cDNA created from the DP1, DP2, DP4 and DP5 cell lines. A slight decrease was observed upon the formation of dermal spheres from the DP1 cell line (A). However, DP2 (B) and DP4 (C) cell lines showed no significant differences between plated cells and dermal spheres. In the DP5 cell line (D), a slight increase in expression was observed upon sphere formation.

2.3.6: Additional expression profiles

2.3.6.1: Fibronectin expression in 2D and 3D cultures

Fibronectin expression was analysed in cell lines DP3-DP6. Strong fibronectin was observed throughout, in both 2D plated cells and 3D sphere cultures. Staining was of a typical fibrillar pattern, appearing disorganised in plated cells (Figure 2.14A, B). Large intracellular granules also were positive for fibronectin. Upon sphere formation fibronectin expression was observed more uniformly in the extracellular matrix between cells (Figure 2.14C, D). This expression profile was observed in all cell lines analysed.

2.3.6.2: Id3 expression in 2D and 3D cultures

Inhibitor of differentiation (Id3) expression was analysed in cell lines DP1, and DP3-DP6. However, the observed staining patterns for Id3 were variable between the different DP cell lines under analysis. All low passage plated cells had similar patterns of staining, with Id3 being expressed in cell nuclei, at varying intensities throughout (Figure 2.15A). In the DP6 cell line, which was of a higher passage number, Id3 was expressed in all cell nuclei. Patterns of Id3 expression appeared to vary much more between cell lines after sphere formation with distinct trends arising. Spheres created from the DP1, DP3 and DP4 cell lines contained ID3 expression throughout, which increased in intensity with time in culture. The DP5 and DP6 spheres appeared to have divided into compartments composed of the centre of the sphere and the flattened cells around the periphery of the sphere (Figures 2.15E, F). In the DP5 cell line, Id3 expression was restricted to the nuclei of cells in the centre of the sphere. By contrast, in the DP6 cell line Id3 expression was restricted to the flattened cells at the edge of the sphere.

2.3.6.3: Id3 expression in explanted dermal spheres

Plated spheres from cell lines DP3, DP4 and DP6 were all analysed for Id3 expression using immunofluorescence. The cells closest in proximity to the explanted spheres had strong nuclear expression of Id3. Immediately surrounding the explants no cytoplasmic expression of Id3 was visible (Figure 2.16A). However, as

cells moved further away from the explanted sphere there was a transition from nuclear to cytoplasmic expression. Nuclear expression of Id3 was lost, with cytoplasmic expression becoming visible in small numbers of cells initially. As cells reached further distances from the explanted spheres, granular cytoplasmic expression of Id3 was evident in almost every cell, with a distinct absence of expression visible in cell nuclei (Figure 2.16D).

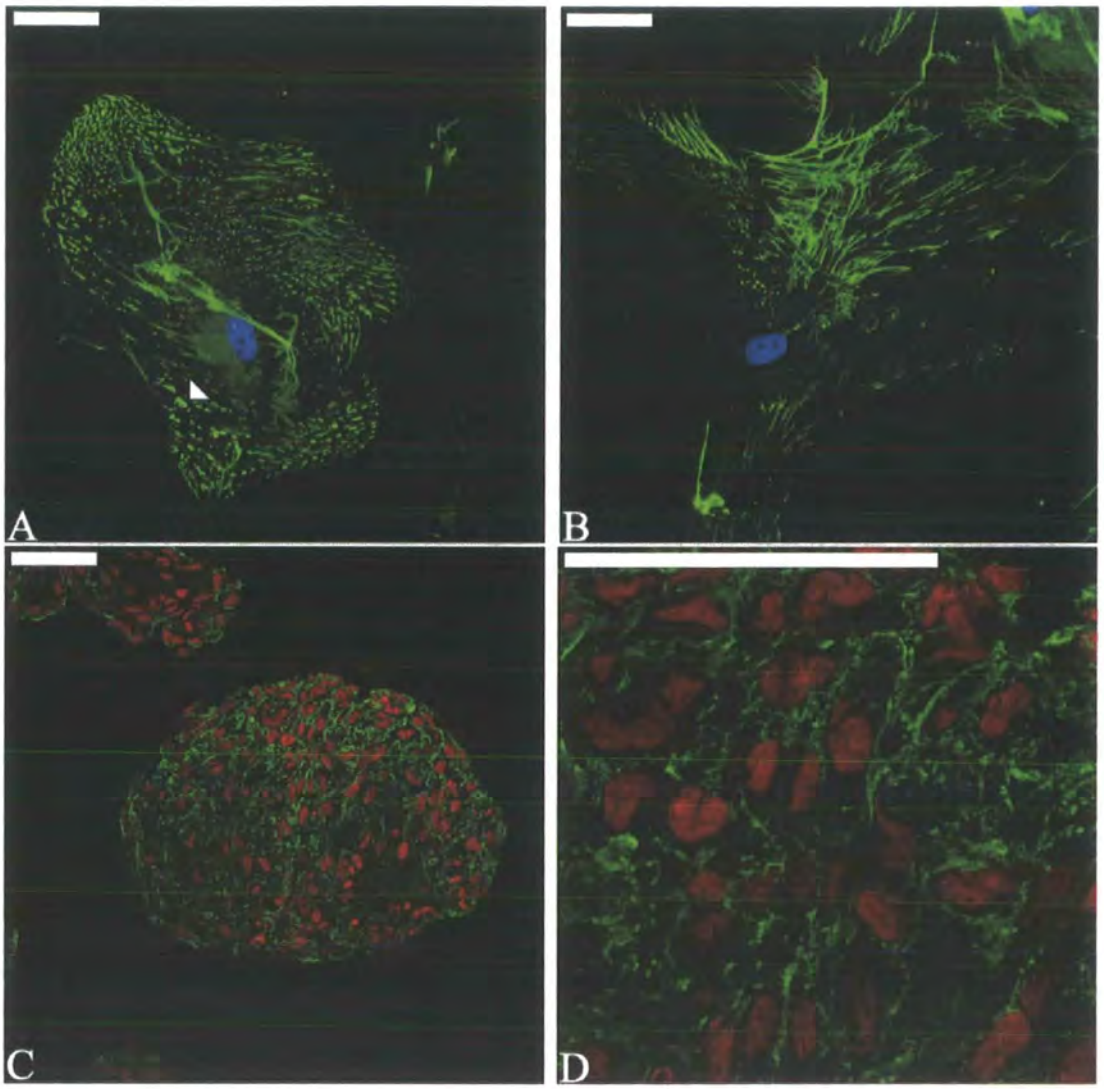

Figure 2. 14: Fibronectin expression in 2D and 3D cell cultures of dermal papilla cell lines

Within dermal papilla cells, fibronectin was visible in course intracellular granules (arrowhead) (A) in addition to being in a typical fibrillar pattern (B). Upon sphere formation expression became more uniform throughout spheres (C), whilst higher magnification shows fibronectin is present surrounding cells (D).

Green: Fibronectin

Red: PI nuclear counterstain

Blue: DAPI nuclear counterstain

Scale Bars: 50μm

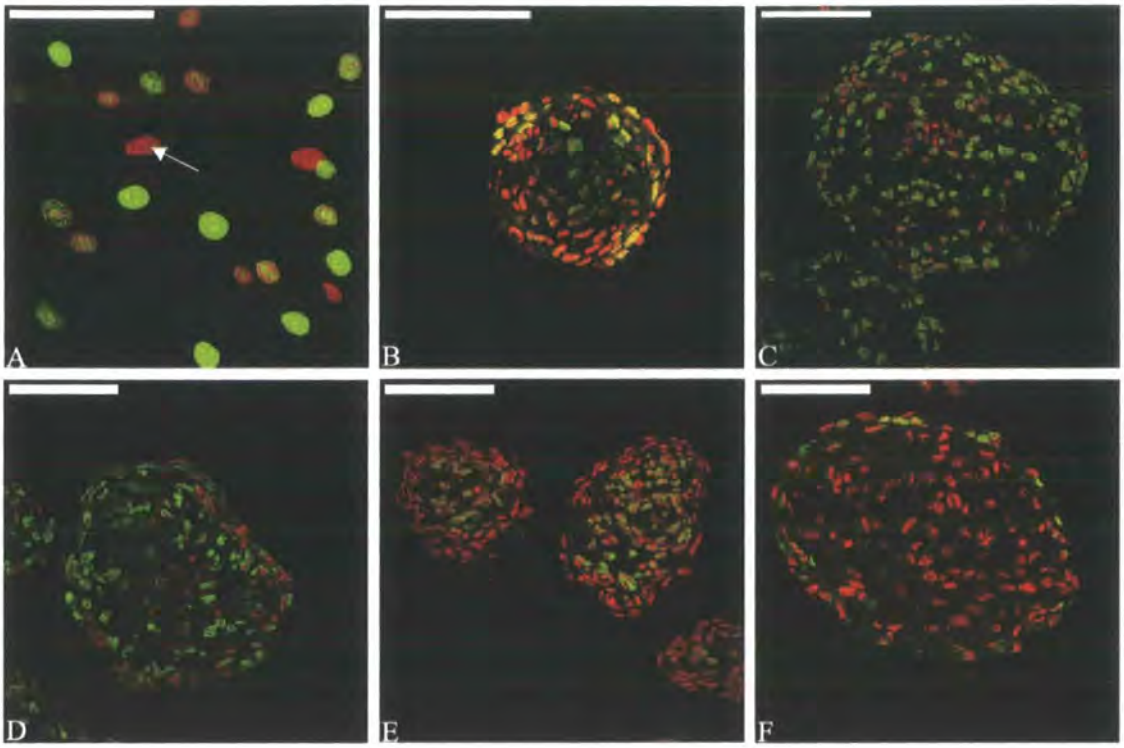

Figure 2. 15: Id3 expression in 2D and 3D cell cultures of dermal papilla cell lines

Plated dermal papilla cells at passage 5 showed Id3 expression within cell nuclei, which varied in intensity from cell to cell, even being absent (arrow) from some (A). In dermal spheres, Id3 expression was variable dependent on the cell line under analysis. Spheres from cell line DP1 (B), DP3 (C) and DP4 (D) all showed relatively consistent levels of Id3 throughout the sphere. In contrast, in spheres from DP5, Id3 was present in the nuclei of cells in the centre of the sphere although was absent from cells at the periphery (E). The opposite expression pattern was observed in spheres from cell line DP6, where Id3 was present in the flattened cells at the periphery of the sphere, but was absent from the centre (F).

Green: Id3

Red: PI nuclear counterstain

Scale bars: 100μm

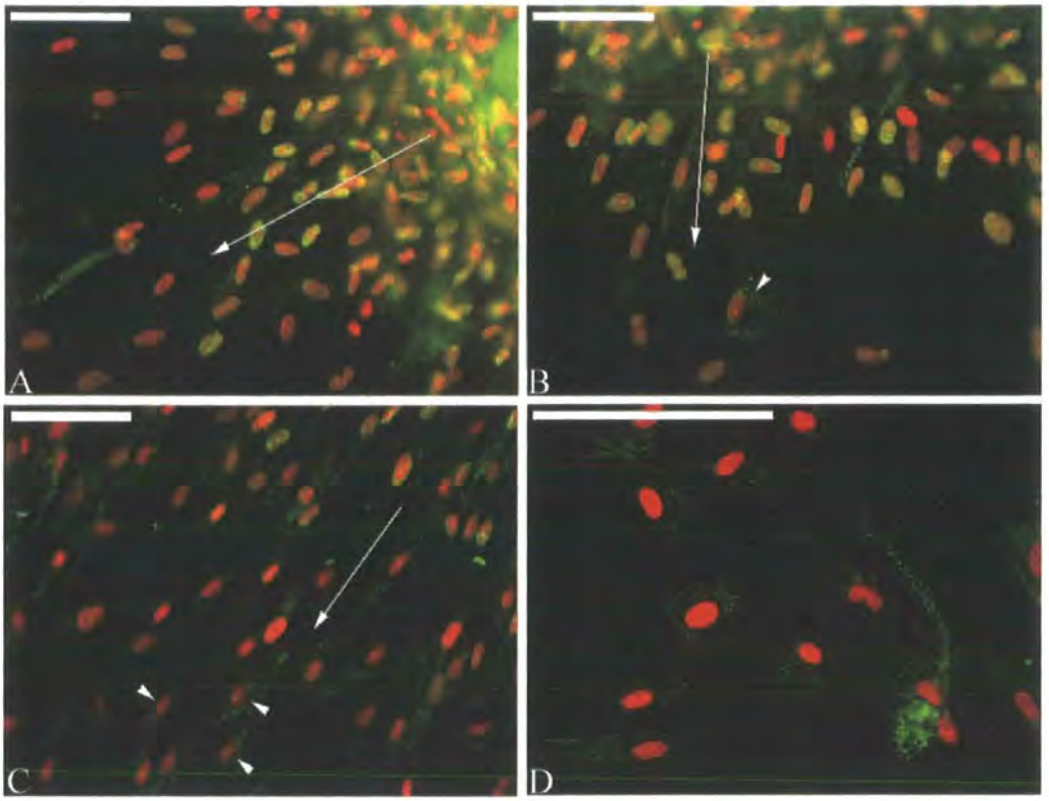

Figure 2. 16: Id3 expression in dermal spheres after explantation

After explantation Id3 expression in dermal papilla cells was initially nuclear (A) although with movement away from the explanted sphere in the direction of the arrows, occasional cells were seen with granular cytoplasmic Id3 expression (arrowhead) (B). With continue movement from the explanted sphere cytoplasmic expression became more obvious (arrowheads) with loss of expression in cell nuclei (C). The absense of expression in nuclei at distances from the explanted spheres was noticeable as nuclei were distinctly red with PI, with no contribution from the green Id3 stain. There, cytoplasmic expression of Id3 was evident with a granular appearance (D).

Green: Id3

Red: PI nuclear counterstain

Scale Bars: 100μm

2.3.7: Operations-Implantation results

Six weeks after the grafting of amputated rat vibrissa follicles with implanted dermal papilla spheres from cell line DP4 onto nude mouse kidneys, host animals were sacrificed and the kidneys removed. Grafts appeared well vascularised and kidney capsules appeared healthy. Initial observation of the grafted follicles revealed small white hairs emerging from two of the follicle specimens (Figure 2.17A). However, a subsequent more detailed examination of follicle sections cut on a cryostat revealed fine hair fibres, in eight out of the nine follicle specimens. In the remaining specimen no fibre was observed. In the negative controls, in which spheres created from dermal fibroblasts (rather than dermal papilla spheres) were implanted onto follicles no fibres were seen emerging from the follicles (Figure 2.17C). Subsequent more detailed examination of control follicles by sectioning and staining with H&E staining revealed no papilla, end bulb or fibre formation. In contrast, the positive controls, in which rat vibrissae dermal papilla were implanted onto amputated follicles, large black fibres were observed emerging from the tips of the grafted follicles, similar in appearance to a vibrissae-type fibre (Figure 2.17D).

In the eight operational specimens with fine hair fibres present, six had visible associated papilla after cryostat sectioning, with a new follicle bulb complete with an epithelial matrix visible. Three of these six had their new bulb structures below the end bulb amputation line (Figure 2.18B) of the capsule whilst two had their new end bulb lying in parallel with the amputation line. The remaining specimen had what appeared to be a catagen papilla above the line of amputation. Two follicles had small club fibres lying alongside the growing fibre, indicative of a full hair cycle transition (Figure 2.18D). Club fibres had club shaped ends, characteristic of human scalp or pelage clubs, rather than a pointed end which is characteristic of vibrissa club fibres. All follicles were positive for versican in the location of the newly formed dermal papilla as shown in Figure 2.19A, with the exception of the follicle entering catagen which showed reduced versican staining intensity.

In follicles with an associated bulb structure and new fibre aSMA and ß-catenin expression were also analysed. aSMA was visible in the dermal sheath of the new bulb but intriguingly, was also visible at the top of the new dermal papilla (Figure

2.19B). Strong ß-catenin expression was observed in the new epithelial matrix and trichocytes surrounding the dermal papilla (Figure 2.19C).

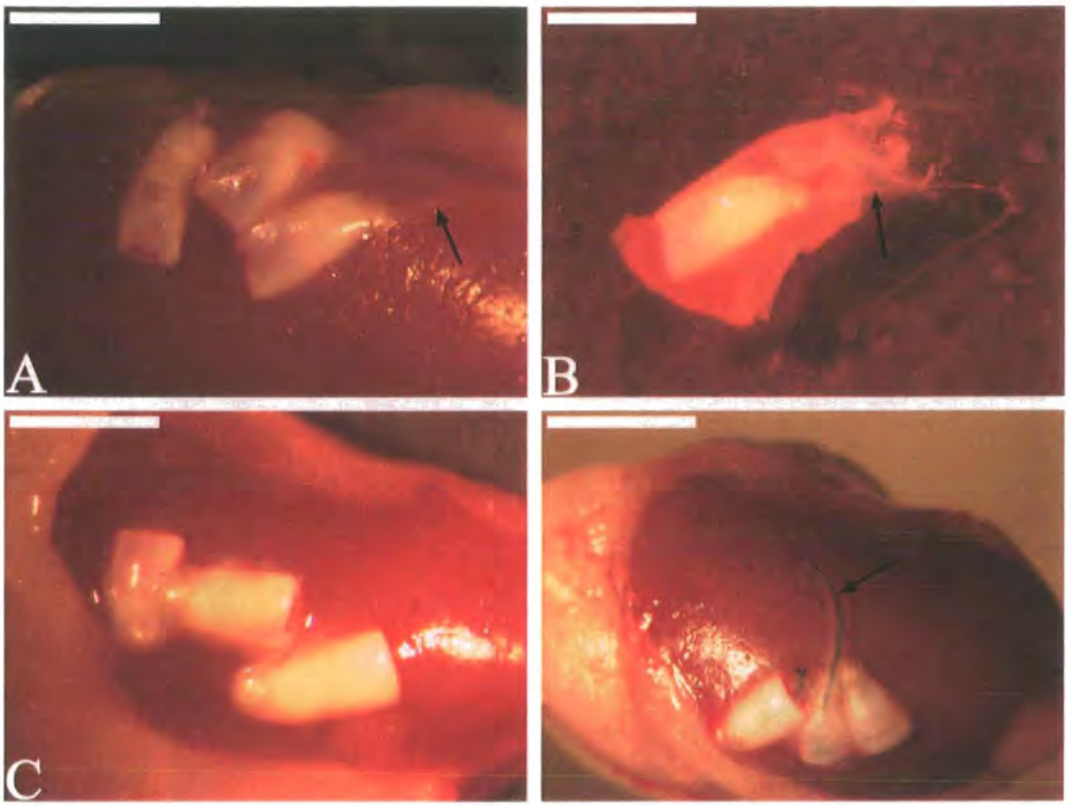

Figure 2. 17: Amputated follicles six weeks after grafting onto a nude mouse kidney

After six weeks grafted onto a nude mouse kidney, follicles that had previously been inactivated by amputation but implanted with a dermal papilla sphere in contact with their exposed epithelium showed growth of fine white fibres (arrow). The fibre (arrow) visible in A was more distinct after dissection from the underlying kidney (B). In the negative controls, where follicles were implanted with spheres created from dermal fibroblasts, no new hair fibres were produced (C). In contrast, the positive controls, where follicles were implanted with rat vibrissa papilla, contained large pigmented, vibrissae-like fibres (arrow) (D).

Scale bars: 2mm

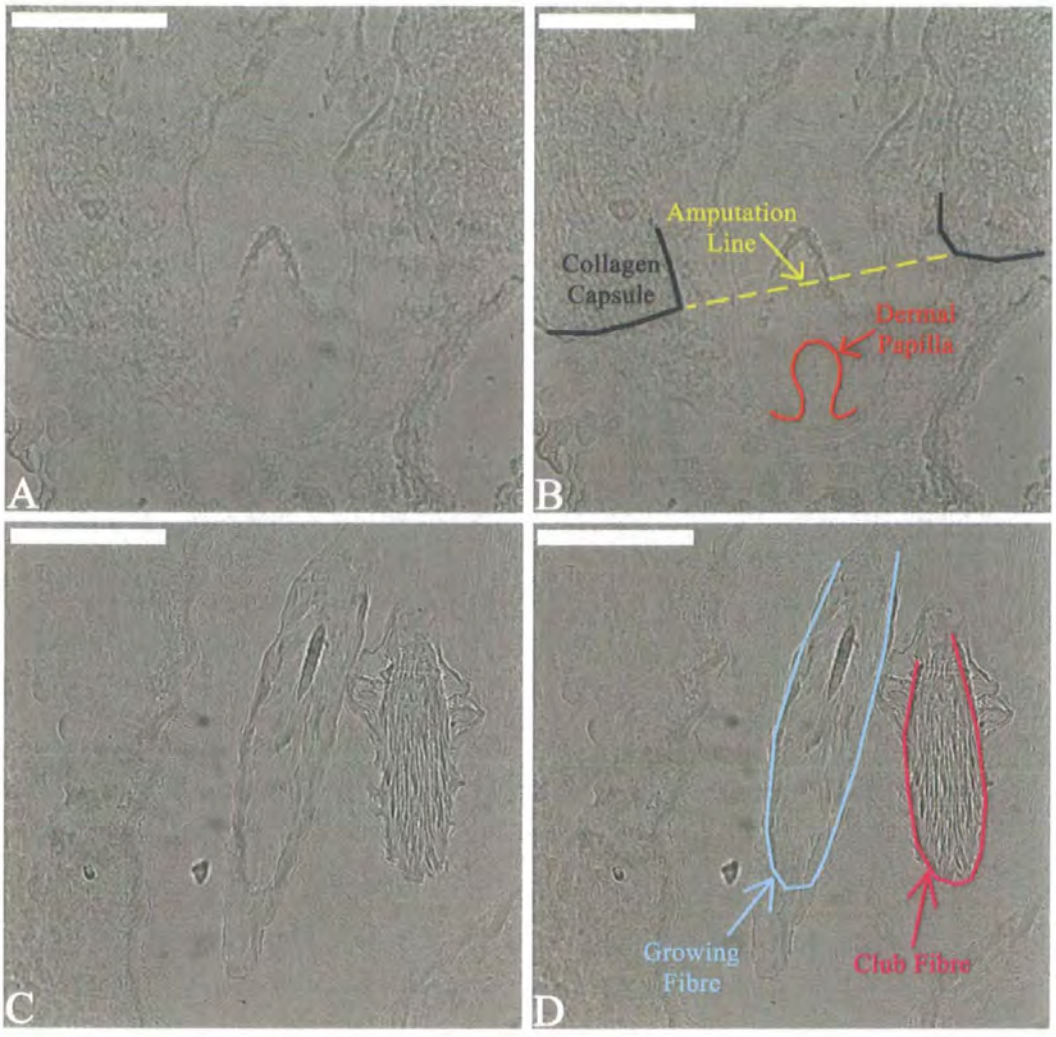

Figure 2. 18: Phase contrast of regenerated end bulbs and fibre growth

Five of the six regenerated follicles, that had visibly associated growing fibres, showed regeneration of the new end bulb, with an associated matrix and dermal papilla below the line of amputation of the previous follicle (A/B). Fibres were visible growing the length of the fibre whilst two follicles contained club fibres adjacent to the new growing fibre. Club fibres had club shaped ends rather than the pointed end characteristic of vibrissa club fibres (C/D).

Scale Bars: 200μm

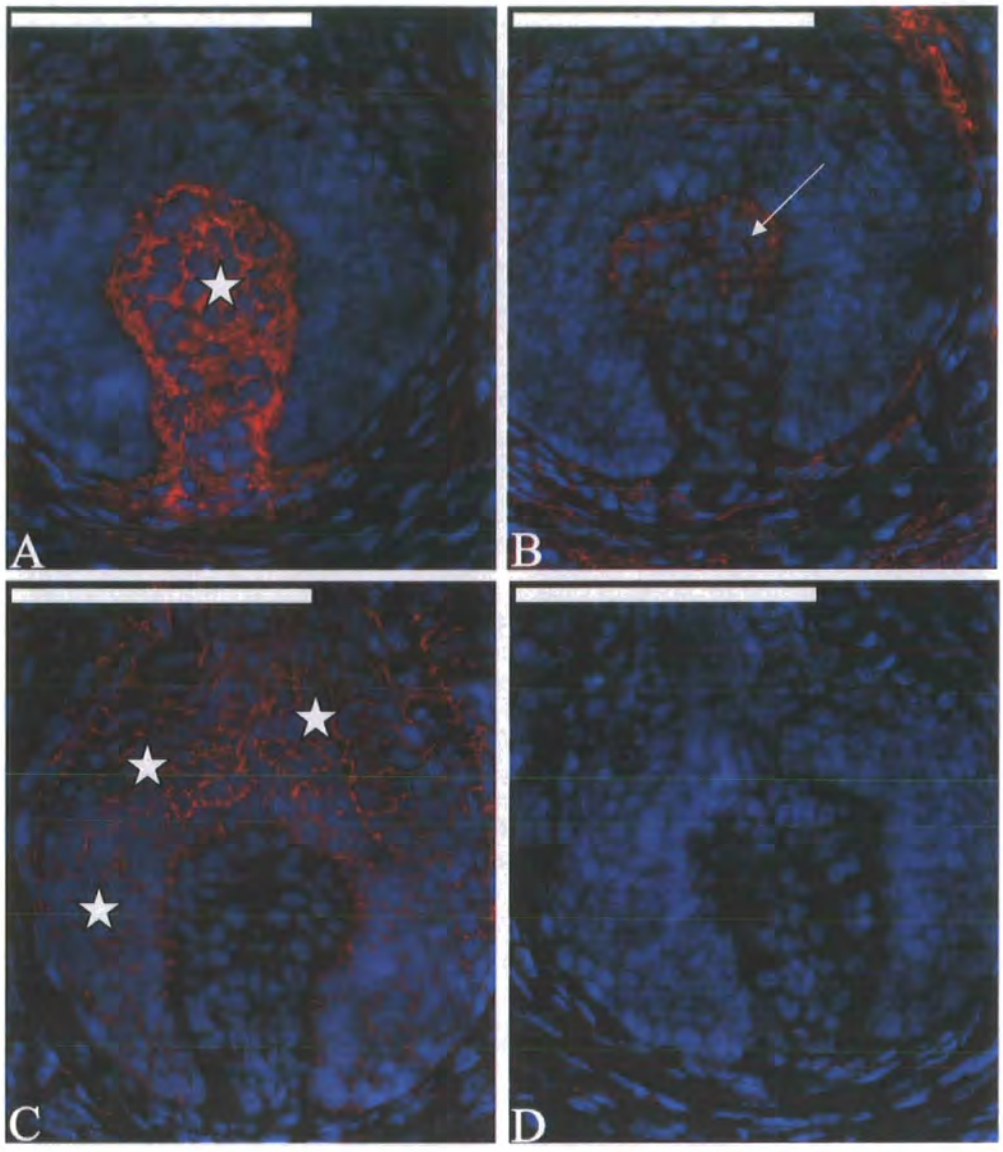

Figure 2. 19: Expression profile of regenerated end bulbs

The dermal papilla of a regenerated end bulb showing prominent versican expression throughout the extracellular matrix surrounding cells. Expression was visible in the neck of the dermal papilla, including in the dermal papilla itself (star) (A). aSMA expression was visible at the apical tip of the papilla (arrow), in addition to the dermal sheath (B). ß-catenin expression was evident in the matrix surrounding dermal papilla (stars), in addition to the trichocytes and presumptive epithelial lineages of the follicle (C). The negative control, where PBS was substituted for the primary antibody showed no specific staining (D).

Red: Antigen of interest, Blue: DAPI nuclear counterstain

Scale Bars: 100μm

2.3.8: Immunohistochemistry- Syndecan 1 on human skin

Immunohistochemistry on 5μm sections of human scalp skin showed the expression of the proteoglycan SDC1 at various points during the hair cycle. During anagen, expression was prominent in the epithelial portion of the hair follicle, in the extracellular matrix between ORS cells through to the basal layer of the follicle. Expression of SDC1 weakened in the suprabasal ORS in the isthmus region of the follicle. In the dermal portion of the follicle expression was not detected in the upper dermal papilla but only in the dermal sheath and the neck of the papilla during anagen (Figure 2.20). However, during telogen positive labelling was seen in the dermal papilla (Figure 2.21).

Figure 2. 20: Immunohistochemistry of Syndecan 1 in anagen hair follicles from human scalp skin

A: Cartoon of an anagen hair follicle showing lines relevant to sections through follicle in B-F.
B: A longitudinal section through an anagen end bulb shows expression of SDC1 in the neck of the dermal papilla. Expression however, is absent from the main body of the dermal papilla.
C: In the isthmus of the follicle, expression of SDC1 is restricted to the less differentiated ORS cells, being absent from the cells adjacent to the IRS, where the beginning of the sloughing process is apparent.
D: Expression of SDC1 is apparent in the basal and suprabasal ORS of the follicle midway down its length.
E: In the lower half of the follicle, where the hair fibre is undergoing differentiation, SDC1 is visible in the extracellular matrix surrounding cells of the suprabasal and basal ORS.
F: In a transverse section though an anagen dermal papilla, the absence of SDC1 expression is evident.

Pink: SDC1
Blue: Gill's Haematoxylin
Scale Bars: 200μm

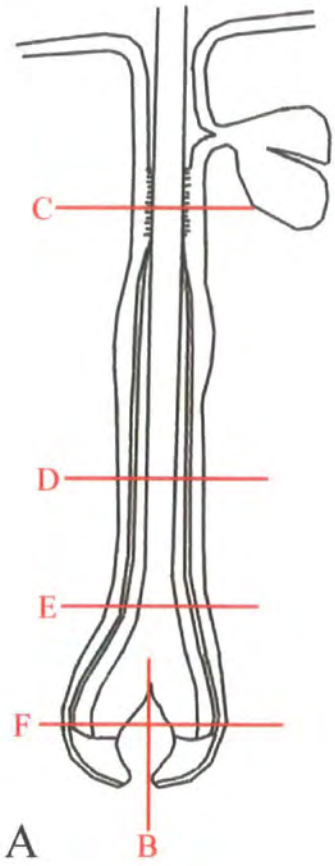
C
D
E
F
A
B

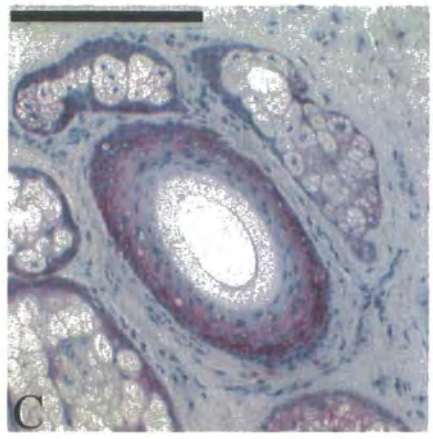
C

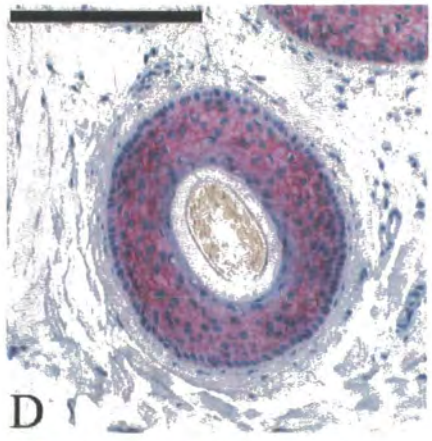
D

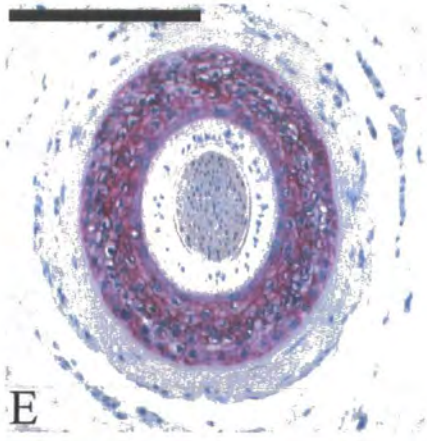
E


B

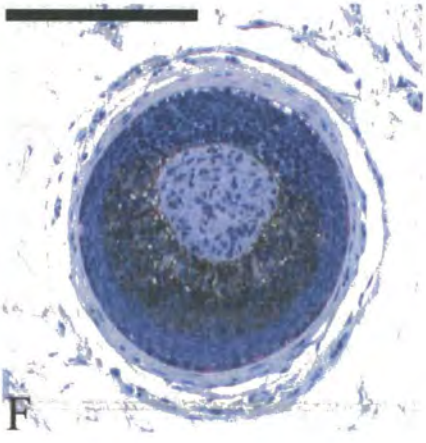
F

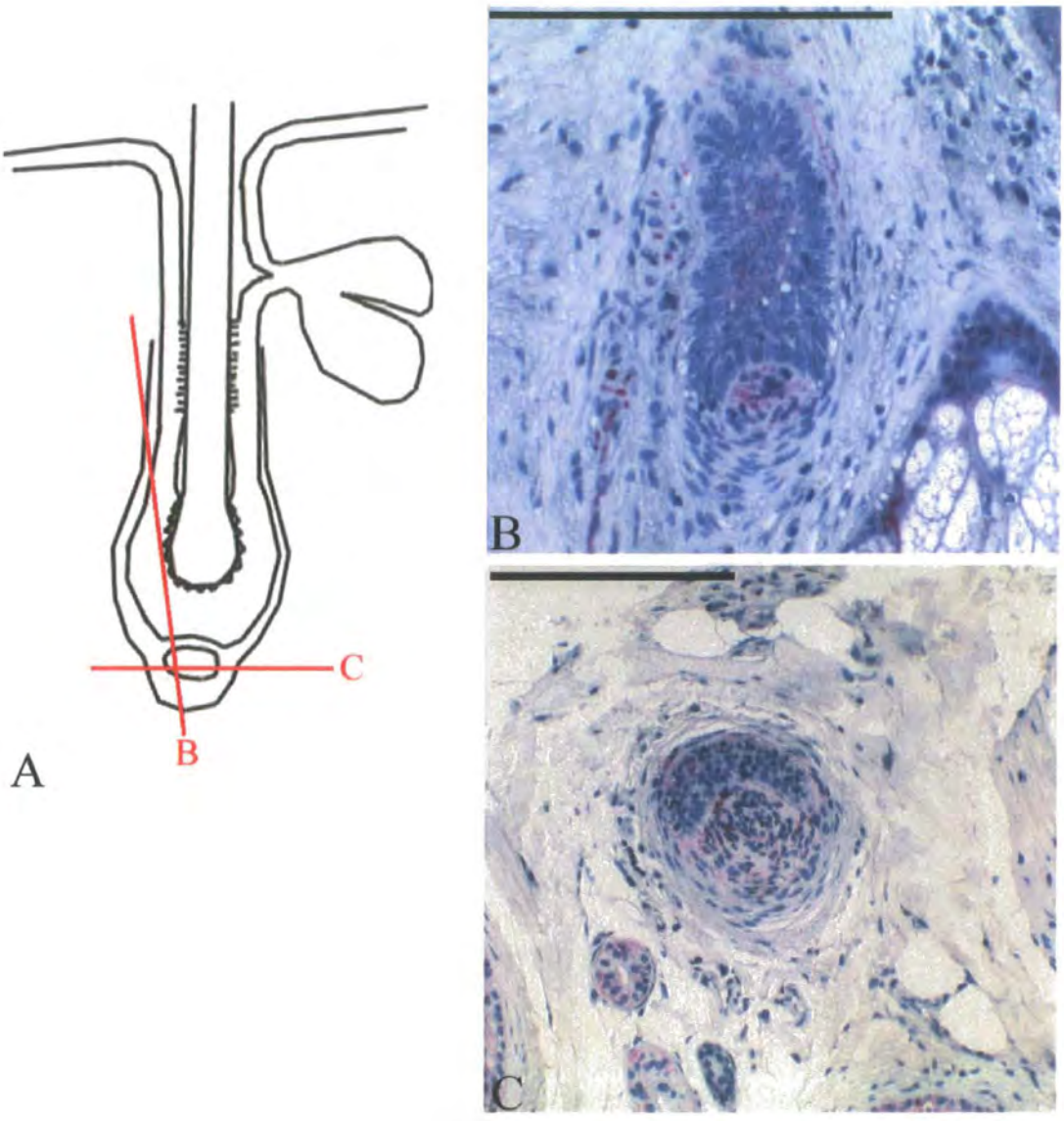

Figure 2. 21: Immunohistochemistry of Syndecan 1 in telogen hair follicles from human scalp skin

A: Cartoon of a telogen hair follicle showing lines relevant to sections through follicle in B and C.

B: Longitudinal section through a telogen hair follicle showing expression of SDC1 within the dermal papilla.

C: Transverse section through a telogen dermal papilla which shows weak SDC1 expression throughout.

Pink: SDC1; Blue: Gill's Haematoxylin

Scale Bars: 200μm

2.4: Analysis and Discussion

2.4.1: Dermal Spheres as a new informative culture model

2.4.1.1: Sphere Viability

After 30 hours in culture spheres appeared viable with a spread of healthy cells as judged by their nuclear architecture. In contrast, spheres after 5 days in culture were obviously distressed, with large lipid globules in between the cells and in place of cells, potentially due to a lack of nutrients reaching the centre of the sphere. Therefore, if this method of cell culture is to become a routine method of culturing dermal papilla cells, the protocol needs to be developed to prolong the viability of cells once they are in spheres. Changing the medium every three days may help.

Although no physical junctions were detected with TEM, there were obvious points of cell contact between cells. Moreover, the appearance of membrane bound vesicles both at the cell membrane and within the cytoplasm of adjacent cells indicates that a communication network in the form of vesicular transport is occurring between dermal papilla cells within the spheres. The large amounts of RER present within cell cytoplasms is also indicative of a large amount of synthetic activity occurring within cells, which in terms of cycle stage is more representative of cells in anagen rather than the telogen, which are relatively quiescent. However, in terms of proximity, cells within the spheres were much closer together than would be observed in an adult anagen dermal papilla *in vivo* (see Figure 2.22). Thus, the spheres may have more in common with either a telogen dermal papilla or a dermal condensation, which have little extracellular material and therefore have cells in close contact with each other (Nanba et al. 2003). TEM was only carried out on one sphere cell line that was distinct from the others due to its high SDC1 expression. SDC1 is a unique proteoglycan as it is expressed specifically during telogen and in the dermal condensation during the early stages of hair follicle morphogenesis only (Trautman et al. 1991) and thus, TEM of the other cell lines may have demonstrated different results.

It is interesting as to why spheres do not form well when formed in media supplemented with antibiotics. Antibiotics disrupt potassium channels as a way of preventing fungal growth. The signalling via potassium channels may be linked to the ability of dermal papilla cells to communicate to form spheres. However, this discrepancy may also help to explain why variations in results are often seen when analysing the effects of minoxidil, a potassium channel opener, on dermal papilla cells (Nakaya et al. 1994; Hamaoka et al. 1997). If potassium channels are required for dermal sphere formation, it would be interesting to investigate the effects of minoxidil on spheres, to see if there are any differences from the effects demonstrated with 2D cell cultures.

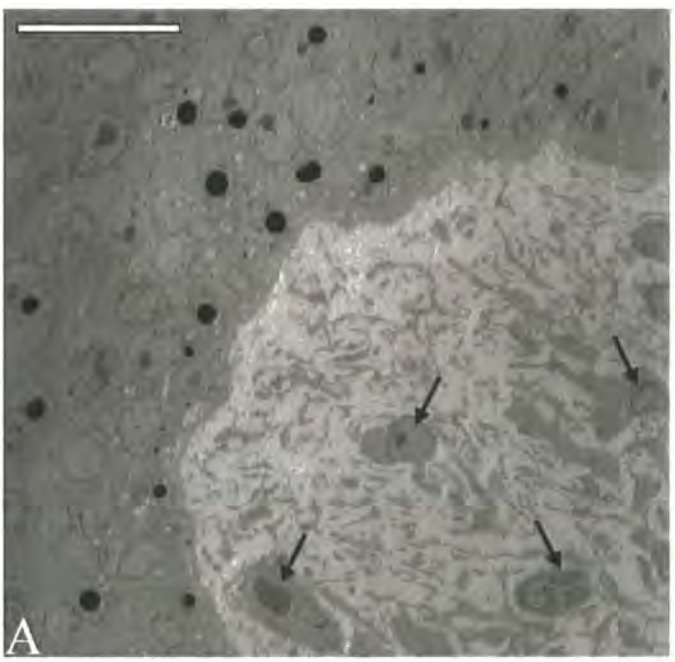

Figure 2. 22: Transmission electron microscopy images of a human hair follicle dermal papilla

A dermal papilla *in vivo* contains cells (arrows) that are spaced at large distances from each other, with the intercellular space filled with extracellular matrix. Long extensions protrude from cells, perhaps to maintain physical cellular contact with the other cells of the dermal papilla. (Image kindly taken and donated by Tony Weaver, Unilever Colworth). Scale Bar: 200μm

2.4.1.2: Differences between cells and spheres

When analysing differences between plated cells and dermal spheres, the latter show many unique features, the most notable perhaps being the reduced proliferation compared to plated cells, a finding evidenced at both protein and gene expression levels. The regular proliferation of dermal papilla cells in culture is a distinguishing feature between them and *in vivo* intact dermal papillae which show approximately 2% proliferation, and only at the initiation of anagen (Tobin et al. 2003). Therefore, the reduced proliferation in spheres is relevant when discussing the benefits of a spherical cell model of dermal papillae over plated 2D cultured papilla cells. Another interesting observation in dermal spheres is the loss of aSMA expression compared to plated cells at the gene level. This is not recapitulated immediately at the protein level in all cell lines although is observed with increased time in culture allowing similarities between dermal spheres and intact dermal papillae to be drawn. In cultured cells, the switching on of aSMA expression has been suggested to represent a de-differentiation event to form a more sheath like phenotype in culture (Jahoda et al. 1991). Therefore, the reduction in gene expression during sphere formation is perhaps indicative of the beginning of a differentiation process to a more papilla-like phenotype that occurs during sphere formation, distinguishing spheres from plated cells.

Another change between plated cells and spheres, detected through fluorescence is the increase in expression of cell junctional markers Cx43 and ß-catenin. Although cell junctions were not visible in the samples prepared for TEM, protein expression of Cx43 and ß-catenin was striking in spheres. In plated cells the gap junction marker Cx43 was expressed in a punctate manner at both points of cell-cell contact and surrounding cell nuclei whilst the adherens junction component ß-catenin was expressed weakly at points of cell contact only. The obvious increase in cell to cell contact in the sphere formation has resulted in an increase of these cell junction markers at points of contact between cells. The presence of Cx43 at junctions represents an increase in gap junctional channels, possibly indicating a greater potential of cells within spheres to communicate with each other whilst the increased expression of ß-catenin may be indicative of reinforced adherens junction cell contacts present within dermal spheres. Interestingly, junctions were not seen with

the TEM in spheres, although junctional markers were present as visualised with immunofluorescence. During hair follicle morphogenesis, expression of cadherin-11 is visualised in a uniform pattern in the dermal condensation at E15, prior to junction formation (Nanba et al. 2003). By P1, the expression pattern is of a more dotted distribution, representative of cadherin-11 at adherens junctions (Nanba et al. 2003). Similarly, in the dermal spheres ß-catenin was uniformly distributed at the cell membrane and so junction formation may have not yet occurred during the time points analysed within this thesis. Nevertheless, spheres are relatively stable structures, beneficial as they can be easily manipulated without creating disruption to the sphere.

Expression of Cx43 is seen in the adult anagen hair follicle (Iguchi et al. 2003) although ß-catenin is absent. However, ß-catenin expression in dermal spheres may reflect the appearance of this molecule in dermal condensations during hair follicle morphogenesis, where ß-catenin is expressed in cadherin based junctions in the papilla during follicle development (Nanba et al. 2003). This, in context with the close proximity of cells, a feature of dermal condensations, leads to the suggestion that the dermal spheres are more representative of dermal condensations seen during development. This suggestion is in line with the early proposals that aggregates of dermal papilla cells formed in culture retain characteristics of embryonic dermal condensations (Jahoda and Oliver 1984c; Messenger et al. 1986; Chui et al. 1996; Bratka-Robia et al. 2002). Supporting this proposal is the re-expression of versican in two of the cell lines investigated. Versican expression in cells in culture is believed to be representative of a cells inductive potential (Kishimoto et al. 1999). Moreover, versican expression, and thus inductive potential is usually lost with increasing time in culture. The re-expression of versican in dermal spheres indicates that the spheres have more inductive capabilities than plated cells in culture that have lost expression of versican, and in this way are similar to original dermal condensates (Kishimoto et al. 1999).

2.4.1.3: Differences between spheres

With the exception of SDC1, bamacan, versican and Id3, only slight differences were perceived in expression patterns between the various plated cell lines under

examination. However, upon sphere formation, small differences became exaggerated, with notable differences in morphology and expression observed between cell lines. Unfortunately, little is known about the origin of cell lines, both in terms of the age and sex of donors, but also of body site origin. The body origin of cell lines may be of relevance as distinct differences are often observed in dermal papilla cell lines of different origin, for example between scalp and beard follicles (Thornton et al. 1993; Rutberg et al. 2006).

A particularly interesting difference seen between spheres was morphological, with cell lines DP1, DP5 and DP6 exhibiting flattened cells at their edges with central cells appearing more rounded. Moreover, the inversed expression patterns observed between spheres from DP5 and DP6 cell lines are noticeable. The SDC1 expression profiles indicated that the DP5 cell line exhibited a more sheath-like phenotype in the flattened cells at the edge of the DP5 sphere, with a papilla phenotype centrally. This is compared to the sheath-like "profile" in the centre of the DP6 spheres with papilla characteristics observed at the periphery of the spheres. This is intriguing as morphologically, the spheres from these different cell lines appear similar, with differences in their expression profiles only. The development of a sheath-papilla relationship intrinsic to the sphere is of interest, although the ability of some cell lines to form compartmented spheres compared to others is perplexing. During the initiation and early stages of anagen the papilla increases in size partly due to an influx of dermal sheath cells that differentiate into a papilla lineage. In comparison, after anagen VI the papilla begins to diminish in cell number due to the migration of cells to the dermal sheath (Tobin et al. 2003), probably associated with a dedifferentiation process. These observations indicate that dermal papilla and dermal sheath are very similar and depending on external influences, are able to change into each other. The different observed morphologies within spheres may be indicative of dermal papilla cells within the sphere undergoing differentiation, or dedifferentiation. The ability of dermal papilla cells to differentiate or dedifferentiate may be reflective of either the age of the donor or the passage of the cell line in culture, with cells behaving as they would at the termination of anagen. Differences in the expression profile of dermal papilla cells has previously been observed between early and late passage cultures (O'Shaughnessy et al. 2004). Moreover, the donor age of tissue

within these experiments was very broad and may be an explanation as to why many differences were observed between cell lines.

An interesting feature observed was that re-expression of versican after sphere formation was only observed in spheres with an intrinsic sheath-papilla relationship, perhaps relevant of a more advanced signalling within and between cells in these spheres. As indicated by the TEM, vesicular transport is occurring between papilla cells in the sphere, evidence that the cells are viable and communicating with each other.

Differences observed between the other proteoglycans studied also revealed interesting patterns. SDC1, a proteoglycan expressed in the telogen dermal papilla and in the dermal condensation during the early stages of hair follicle morphogenesis (Trautman et al. 1991), is coincidentally lost with the onset of bamacan expression in both adult and developing follicles (Couchman et al. 1990). In spheres SDC1 was noticeably expressed in three cell lines with an absence in the remaining cell lines. The correlation between SDC1 gene and protein expression levels also suggests that the control of SDC1 is largely at the transcriptional level. Less striking differences between cell lines were observed with the proteoglycan bamacan, which *in vivo* is expressed during the anagen stage of the adult growth cycle and in the later stages of hair follicle morphogenesis coinciding with the downgrowth of the hair peg (Couchman et al. 1990). In contrast, perlecan which is expressed in all stages of the hair cycle and throughout morphogenesis (Couchman et al. 1990) was expressed uniformly throughout in all spheres analysed.

The expression of Id3, an inhibitor of differentiation, within spheres again highlights the differences in spheres created from different cell lines. Id3 is expressed in the dermal condensation throughout hair follicle development, whilst in the adult pelage hair follicle expression is greatest in the dermal papilla and lower dermal sheath during mid anagen and telogen, being lost in other cycle stages (O'Shaughnessy et al. 2004). In the cell lines with uniformly shaped spheres, Id3 was expressed throughout, increasing with time in culture concurrent with the hypothesis that these cell lines were created from dermal papilla in mid-anagen. However, the altered expression within cell lines DP5 and DP6, in which expression is restricted to the inside and the

outside of the spheres respectively is more puzzling. This does not support nor challenge the original observation that the cell cultures may have been derived from various cycle stages but more raises the intriguing prospect that there may be intrinsic stage cycling within the spheres.

Interestingly, in the spheres that were plated down again in culture and cells allowed to grow out, Id3 expression was initially nuclear, changing to cytoplasmic with increasing distance from the plated spheres. Cytoplasmic expression of Id3 within papilla cells is thought to represent a de-differentiation process (O'Shaughnessy et al. 2004). As discussed earlier, formation of spheres involves a differentiation process, concurrent with the loss of aSMA gene expression but it seems that the cells within the sphere can quickly revert back to their previous state when plated back down into a single layer in culture. Moreover, loss of nuclear Id3 expression after explantation of dermal papilla usually occurs after the first passage (O'Shaughnessy et al. 2004) although loss here was immediate, highlighting a difference between spheres and dermal papillae.

2.4.1.4: Usefulness of the dermal sphere model

Benefits may be derived from the use of dermal spheres as they partially resemble and intact dermal papilla. For this reason, they may be useful for screening possible anagen initiators, or to look at the effects of epithelial signalling on the dermal papilla rather than cells. However, in comparison to plated cells, spheres show a limited life span once formed in culture, compromising their usefulness as a model. Perhaps more relevant with regards to analysing response of dermal papilla cells to anagen initiators would be to use confluent, aggregated cultures rather than low confluence ones. However, this limits the usefulness of cells derived from human donors, which lack an aggregative ability. More analysis of spheres is required, as factors such as sphere size may influence lifespan.

Conceivably a relevant cell type to incorporate into these spherical models would be germinative epithelial cells, important in epithelial-mesenchymal interactions. Germinative epithelial cells do not grow by themselves in culture but only in combination with dermal papilla cells (Reynolds et al. 1993). The entire hair follicle

has also been successfully recapitulated in a culture system by combining four hair follicle cell types in a collagen capsule from a vibrissa follicle, with successful hair formation, indicative that cell culture systems are able resemble the *in vivo* situation (Reynolds and Jahoda 1994).

2.4.2: Inductive capacity of dermal spheres

The dermal component of hair follicles has long been shown to have a role in induction of hair formation and the maintenance of hair growth. Nevertheless, the success of the initial operation procedures carried out with dermal spheres in the amputated follicle assay is encouraging as this is the first example of cultured cells derived from human dermal papilla inducing papilla, end bulb and fibre formation, without incorporation with other cells, or microencapsulation to maintain an aggregative state of the cells. However, a priority experiment now must be to prove the human origin of the dermal papilla component of the follicle, to ensure that regeneration has not occurred. The location of newly formed end bulbs and papilla structures beneath the line of amputation is suggestive that induction rather than regeneration has occurred, although is not a conclusive feature. Nevertheless, this development is exciting as it presents an opportunity to isolate and expand a population of dermal papilla cells, then present them in a way that maintains their *in vivo* characteristics. The inductive capabilities of spheres created from dermal papilla cells, as apposed to interfollicular fibroblasts also distinguishes this unique population of dermal cells from fibroblasts.

Intriguingly, the dermal spheres cell line that was used for the induction experiments did not exhibit versican expression, a proteoglycan usually associated with inductive capability of dermal papilla cells. Versican is believed to be required for normal hair growth as it is absent from the vellus follicles observed in androgenetic alopecia (Soma et al. 2005). However, during mouse pelage follicle development versican is not usually expressed until fibre formation commences, after the initial stages of hair induction (du Cros et al. 1995). The immunofluorescent analysis of the newly formed follicles showed that all the new dermal papillae, believed to be formed from the spheres, expressed versican within them. This is perhaps indicative that the spheres, similar to the original mesenchymal condensation do not have to express versican but

merely have to have the machinery to be able to respond to signalling resulting in the production of versican. However, these experiments were carried out in a system with hair follicles already in it. The question remains to be asked if spheres without versican expression would be capable of inducing de novo follicles, or whether sphere types would exhibit differences in their ability to induce hair growth based on their expression profiles.

The ability of the newly formed follicles to cycle, as demonstrated by the presence of club fibres in two samples demonstrates the ability of the new papillae created from dermal spheres to respond to signals within the host environment that regulate cycle progression. However, in contrast to the fibres formed from induction by the vibrissae papilla which were thick and black, the fibres observed after sphere induction were fine and unpigmented. Whilst the origin of the epidermal component usually dictates appendage formation, it is susceptible to influence from the dermis which influences regional specifications such as fibre type produced (Dhouailly 1977).

Little information is known about the papilla that was propagated to form the cell line used in this study, such as information on donor body site or hair colour. However, if one were to take the assumption that the donor site had pigmented hair, then you would conclude that in culture, the dermal papilla cells have lost their ability to activate melanocytes. In studies using cultured vibrissae dermal papilla cells, a combination of large pigmented and unpigmented vibrissae-like fibres were generated in the amputated follicle assay (Jahoda et al. 1993). This may lead to the conclusion that the sphere has induced a vellus, unpigmented fibre rather than a terminal fibre, reflected by the small size of fibres. Whether a greater number of starting cells in the sphere would induce the formation of a larger fibre remains to be eluded, especially since dermal papilla volume has been shown to influence hair diameter in the whisker (Ibrahim and Wright 1982).

2.4.3: Therapeutic benefits of spheres

2.4.3.1: Fibre versus Follicle Induction

The assay used here, the 'amputated follicle assay' analyses the capacity of dermal papilla cells to induce the formation of a new end bulb and fibre. However, there are other assay systems which evaluate not only the fibre inducing capabilities, but also the follicle induction capabilities of dermal components.
Lichti's group has utilised a model system that establishes the ability of dermal components to continue inducing follicle formation in developing hair buds isolated from newborn and perinatal mice (Lichti et al. 1993; Weinberg et al. 1993). Here, they grafted epidermal cell populations, along with various dermal cell combinations onto the backs of nude mice. Using this system, they have shown that fresh dermal cell preparations from newborn mouse backskin, and from rat vibrissa follicles are able to continue inducing follicle formation and cause subsequent hair growth (Weinberg et al. 1993). However, this inductive capability was lost in cell culture with increasing passage whilst fibroblast 3T3 cells were not able to continue follicle formation implicating the dermal papilla as a crucial component (Weinberg et al. 1993). Moreover, non hair bearing, glabrous dermis, which is not able to initiate follicle formation, is able to continue to induce follicle formation if put in contact with epidermis that has already received the initiating signal for follicle formation (Dhouailly and Sengel 1975).

The method presented by Lichti and Weinburg, 1993, whereby they grafted epidermal cell preparations from newborn mice with dissociated dermal cells onto the back of a nude mouse was later adapted by Stenn's group in the development of the 'patch assay' that required both less time and 10-fold fewer cells than the chamber graft assay (Zheng et al. 2005). Using the patch assay, isolated neonatal dermal cells with epidermal aggregates were injected into the truncal skin of an adult nude mouse. It was found that the dissociated epidermal cells quickly reformed to form a placode-like structure, which later forms the bud and peg of the developing follicle (Zheng et al. 2005)

A perhaps more stringent assay as it analyses follicle neogenesis rather than the capacity to continue induction is the ear wound assay. This assay has been used to demonstrate the inductive capacity of both intact and cultured vibrissae dermal papilla, as dermal specimens implanted into small ear wounds generated follicles containing large vibrissae-like fibres (Jahoda 1992; Jahoda et al. 1993; McElwee et al. 2003). In addition to mouse ear, vibrissae follicle dermal papilla have been shown to induce follicle formation in mouse back skin (Pisansarakit and Moore 1986). A similar experiment in human has shown that the allogeneic transplantation of intact dermal sheath but not dermal papilla can induce new follicle formation in the arm of the recipient, protected from rejection due to its immunotolerant properties (Reynolds et al. 1999). Microencapsulated human dermal papilla cells are also able to induce follicle formation in the ear wound assay (Li et al. 2006), overcoming the common problem of cell migration often observed using cultured human dermal papilla cells.

Again, a more stringent route is to analyse the capacity of implanted dermal components to induce follicle neogenesis in isolated non-hair bearing, glabrous regions of the epidermis. Classic heterotopic recombination experiments have demonstrated that embryonic dermis from both dorsal and snout regions, have the ability to induce follicle formation in glabrous epidermis when recombined together (Kollar 1970; Sengel 1976). More specific, however, is the induction of follicle formation when glabrous footpad is recombined solely with cultured dermal papilla cells from adult pelage follicles, and grafted onto the back of an adult rat in silicone chambers, ruling out local follicular influences (Reynolds and Jahoda 1992). Both cultured and intact rat vibrissa dermal papillae, in addition to embryonic dermal condensations have also been shown to induce follicle formation after grafting with sole epidermis onto the back of a nude mouse (Inamatsu et al. 2006). Both of the grafting assays utilised above require large numbers of cells.

Hoffmann's group demonstrated the ability of both cultured dermal papilla and sheath from the bulb region of mouse vibrissa follicles to induce *de novo* follicle formation when injected directly into footpad (McElwee et al. 2003). Here, there are no external signals from surrounding follicle bearing epidermis that aid follicle morphogenesis. The initiation of follicle growth in footpad by cultured dermal sheath and dermal papilla demonstrates the inductive capabilities of these hair follicle

components. This highlights the capability of both dermal papilla and sheath cells to re-programme and cause differentiation of non-follicular forming epidermis. However, to the best of my knowledge no work has been carried out with human cells in this assay.

More recently, follicle and fibre induction has been documented in cultured rat sole keratinocyte sheets. *In vivo*, these keratinocytes will have received no hair inducing signals. However, when the isolated sole keratinocytes are subcutaneously implanted in combination with rat vibrissae dermal papilla into athymic mice, or syngeneic rats, they are able to respond to dermal papilla signalling to form *de novo* hair follicles (Xing and Kobayashi 2001; Miyashita et al. 2004).

In addition to analysing follicular neogenesis in glabrous skin, researchers have shown the capability of embryonic dermis to cause transdifferentiation of differentiated adult corneal epithelium (Ferraris et al. 1994; Ferraris et al. 2000). This assay analyses the reprogramming capacity of dermal components and is a stringent test of inductive capability. More recently, embryonic dermis recombined with a more simple epithelia, amnion epithelium, was able to induce follicle formation when grafted onto a kidney of a nude mouse (Fliniaux et al. 2004).

Obviously, the dermal spheres described in this thesis were able to induce follicle formation in an amputated follicle, although this assay system is not that stringent. To analyse the inductive capacity of spheres further, experiments to deduce if they are capable of *de novo* follicle induction in glabrous skin should be carried out. Moreover, an interesting and relevant experiment for hair replacement therapies would be to look at the inductive capabilities of the spheres in human tissue that has few follicles, such as breast tissue, with the development of a cell based clinical approach in mind. As this work was in progress, we became aware that other groups were utilising spherical cultures of dermal papilla cells to study follicle induction. Osada *et al*, 2007 cultured mouse vibrissa dermal papilla cells in medium containing Fibroblast growth factor 2 (FGF2), which prolonged the growth capacity of these cells. They then grew spheres containing 10,000 cells in the bottom of 96 well low-binding plates, and implanted these cells along with neonatal epidermal cells using the patch assay (Osada et al. 2007). This group showed that versican expression,

although absent in plated cells was re-expressed upon sphere formation from late passage cells (Osada et al. 2007). This is supportive of the results presented in this thesis. Moreover, spheres implanted with neonatal epidermis showed improved hair follicle inducing ability, even from late passage cells, when compared to separately suspended cells (Osada et al. 2007). Although the patch assay has benefits as it is a simple procedure to carry out, and requires relatively few cells it is not that stringent a test of inductive capacity.

Furthermore, a second group has recently published a paper, in which they utilised a hair follicle bilayer organotypic culture to induce hair follicle formation on the back of a nude mouse, highlighting perhaps the beginning of a trend from 2D to 3D culture models (Wu et al. 2006). The organotypic culture composed of dermal papilla or dermal sheath cells from human scalp follicles, mixed in a collagen gel. Keratinocytes from the bulb matrix in addition to the ORS of the follicle were cultured on top of the collagen rich gels until confluent, after which time they were transplanted onto the back of a nude mouse. Grafts were left for 16 weeks, after which time they had formed typical hair follicle like structures, with concentric layers and occasional hair fibres (Wu et al. 2006).

2.4.3.2: Hair Follicle Transplantation

Although there are various therapeutic strategies for combating hair loss, these are not always effective and often surgery is the only permanent solution. Modern hair transplant surgery to combat androgenetic alopecia involves removing hair containing grafts from the posterior of the scalp, before autologous transplantation onto the frontal scalp in the balding region (Orentreich 1959). However, this has many problems, often associated with the invasiveness of the procedure, the time requirements and limitations of donor tissue, especially in cases of advanced androgenetic alopecia. This has led to the development of techniques, in particular over the last two decades as a method of combating these problems.

Up to and at the beginning of the 1990's transplantation techniques traditionally involved taking a small punch biopsy containing 3-4 follicles from the back of the head, then placing this in the balding region on the frontal scalp (Rassman and Carson

1995). However, this method was replaced by the favoured method of taking a strip of skin containing follicles before micro-dissecting out follicular containing units. This causes less damage to the follicles, although it takes several hours to prepare the follicle units (Limmer 1994). Scarring is also commonly observed with this technique so more recent advances have tried to overcome the problem of scarring with the presentation of the follicular unit extraction technique (Rassman et al. 2002). This technique enables the removal of intact follicular units from the scalp without causing damage to the follicle. Moreover, another line of research has been carried out to demonstrate the viability of hair follicles after preservation in both different solutions, and at different temperatures, with the potential to delay transplantation until sufficient numbers of follicles have been harvested (Kurata et al. 1999; Qian et al. 2005).

Until recently the issue of limitations of tissue supply from donors had not been addressed. In an adaptation of the follicular unit extraction technique Hamologlu's group isolated the upper third, upper half the upper two thirds of the follicle for transplantation, leaving behind the lower portion of the follicle at the donor site (Er et al. 2006). New follicles were induced at both donor and recipient sites, relating to work by Choi's group demonstrating the regeneration of human follicles after horizontal sectioning (Kim et al. 1996). However, regenerated fibres were finer at both donor and recipient sites than prior to surgery. Moreover, numbers of regenerated follicles were lower than observed with the implantation of whole follicular units demonstrating that the issue of donor supply still needs addressing to be able induce large numbers of follicles when there is a limited amount of tissue.

What is unique about the spheres in comparison to dermal papilla is their ß-catenin expression at the junctional locations between cells. This feature allows the presentation of a preformed aggregate that does not dissociate and therefore is similar to the original mesenchymal condensation, able to confer inductive capabilities. The presentation of a preformed aggregate that is inductive could confer many therapeutic benefits. One obvious example is with regards to hair replacement surgery, where a major limitation is the donor reserve, with surgery currently not increasing hair numbers, but rather relocating follicles. The viable expansion of papilla cells, followed by sphere formation during culture would allow the presentation of

numerous aggregates from a single original papilla, thus reducing the length and invasiveness of surgery.

2.4.3.3: Stem cell properties of the dermal papilla: Implications for wound healing

The numerous examples of follicular induction with adult dermal papillae cells emphasises the retention of signalling elements common to the original mesenchymal aggregate that forms the dermal papilla during hair follicle morphogenesis (Reynolds and Jahoda 1991), allowing analogies to be drawn between follicular cycling and morphogenesis. Moreover, the cross-appendage interactions of dermal papillae along with their inductive capabilities highlights the stem cell-like potential of these cells, which in plated cultures have been shown to differentiate into lipid, bone, skeletal and neuronal lineages (Jahoda et al. 2003; Richardson et al. 2005; Rufaut et al. 2006). Moreover, when cultured with Epidermal Growth Factor (EGF) and FGF2 dermal papilla cells generate floating spheres that can differentiate into both neural and mesodermal progeny (Toma et al. 2001; Fernandes et al. 2004).

The stem cell qualities of dermal papilla and sheath implies a potential role for them in wound healing (Jahoda and Reynolds 2001), raising the possibility of skin equivalents to be created capable of forming hair follicles. Current skin equivalents derived from cultured dermal and epidermal cells are used to treat wound sites although the reformed tissue does not contain hair follicles (Auger et al. 1998; Trent and Kirsner 1998). Early work showed that sheep dermal papilla, which induce follicles on the back skin of nude mice, were not capable of inducing follicle formation on cultured skin equivalents raising questions as to the composition of the equivalents (Watson et al. 1994). However, more recent work using rat cells has led to the presentation of a skin equivalent entirely composed of hair follicle cells; DS and ORS, capable of inducing follicle formation when combined with intact dermal papilla at punch biopsy wound sites (Gharzi et al. 2003). However, cultured dermal papilla cells were not able to induce follicle formation when combined with this skin equivalent (Gharzi et al. 2003).

A therapeutic benefit of dermal spheres may be in the development of skin equivalents for wound healing. Previous experiments have documented the ability of intact rat dermal papilla to induce follicle formation in puncture wounds, a property not exhibited by cultured dermal papilla cells (Gharzi et al. 2003). It would be interesting to analyse the ability of aggregated spheres to induce follicle formation in wounds, to determine if they were more similar to a functional intact dermal papilla rather than cultured cells. Moreover, the incorporation of dermal cells into skin grafts to be used in wounding may have alternate benefits such as the ability to reduce scarring (Jahoda and Reynolds 2001), a possibility as papilla regeneration after wounding does not result in the formation of scar tissue (Jahoda and Oliver 1984a).

Currently, the role of hair follicle cells in human skin equivalents can only be inferred from the animal studies, but the basis is there to create a skin equivalent that could lead to significant therapeutic benefit during wound healing. In a manner parallel to dermal papilla and sheath, cells from the bulge region of the follicle have been implicated in epidermal repair after wounding (Levy et al. 2005; Levy et al. 2007) and hence combination of these into wound grafts may confer benefits also.

2.5: Summary and Conclusions

This section of work shows the development and characterisation of a cell based model of the dermal papilla. The model analysed, a self formed sphere of dermal papilla cells bears resemblance to intact dermal papilla by demonstrating reduced aSMA expression, and a decline in mitotic activity from 2D cell cultures to 3D spheres. This spherical model also showed the ability to induce fibre formation, which to the best of my understanding is the first time that cultured human dermal papilla cells have been able to do this when implanted as a unit, without being microencapsulated or combined with other cells. This bears promise for the future of transplantation techniques, as a method of increasing follicle numbers without the requirement of a large amount of follicles prior to transplantation. Moreover, this cell culture model provides us with a good tool to elucidate our understanding of signalling to and from the dermal papilla, as it is more representative of intact dermal papilla than 2D cultured cells. An *in vitro* culture model is indispensable for studying interactions within the hair follicle as cells can be easily manipulated compared to *in vivo*. The development of the 3D spheres, possibly through the incorporation of other hair follicle cell types may become invaluable as a model system of the hair follicle.

Chapter 3: An adhesive and structural analysis of club fibre formation, retention and release

3.1: Introduction

3.1.1: The Vibrissa follicle-a predictable model of hair growth

The vibrissa follicle has long been a popular model with which to analyse hair growth for three reasons. The first, its large size allows easy experimental manipulation. The second, its tightly controlled growth cycle allows the specific selection of follicles at particular stages of their growth cycle. Thirdly, the arrangement of vibrissa follicles on the mystacial pad is in a well organised, constant pattern which further highlights the consistency of this follicle model.

3.1.2: The Hair Cycle in the Vibrissa Follicle

The anagen phase of the vibrissa is similar to that observed in pelage follicles, as previously described in Chapter 1. The anagen stage of vibrissa follicles, can be divided into three distinct phases in line with the six suggested by Chase for pelage follicles (Chase et al. 1951). These are pro-anagen (anagen I-IV), mes-anagen (anagen V) and met-anagen (anagen VI) (Young and Oliver 1976) although in the current thesis they are referred to as early, middle and late anagen. The duration of anagen varies in the different follicles on the mystacial pad, with posterior follicles remaining in anagen for approximately 4-5 weeks in mice, and 6-7 weeks in rats. The anterior columns have shorter anagen durations than the posterior (Ibrahim and Wright 1975). As the growing anagen fibre increases in length, it becomes progressively thicker due to an increase in number of cells in the cortex and medulla, whilst the Huxley's and Henle's layers of the IRS remain constant through the anagen phase (Ibrahim and Wright 1975). This is in contrast to scalp or pelage hair, the cortex and medulla of which change little in diameter during the anagen growth phase. The growing fibre created during anagen grows up alongside the club fibre which is retained from the previous growth cycle (Figure 3.1). In common with pelage club fibres, the vibrissa club has a many pronged root believed to retain the club fibre in place until release (Young and Oliver 1976). However, unlike pelage clubs which are rounded at their tip, vibrissa clubs are distinct as they are asymmetric, with a sharply pointed tip (Jahoda and Oliver 1984b).

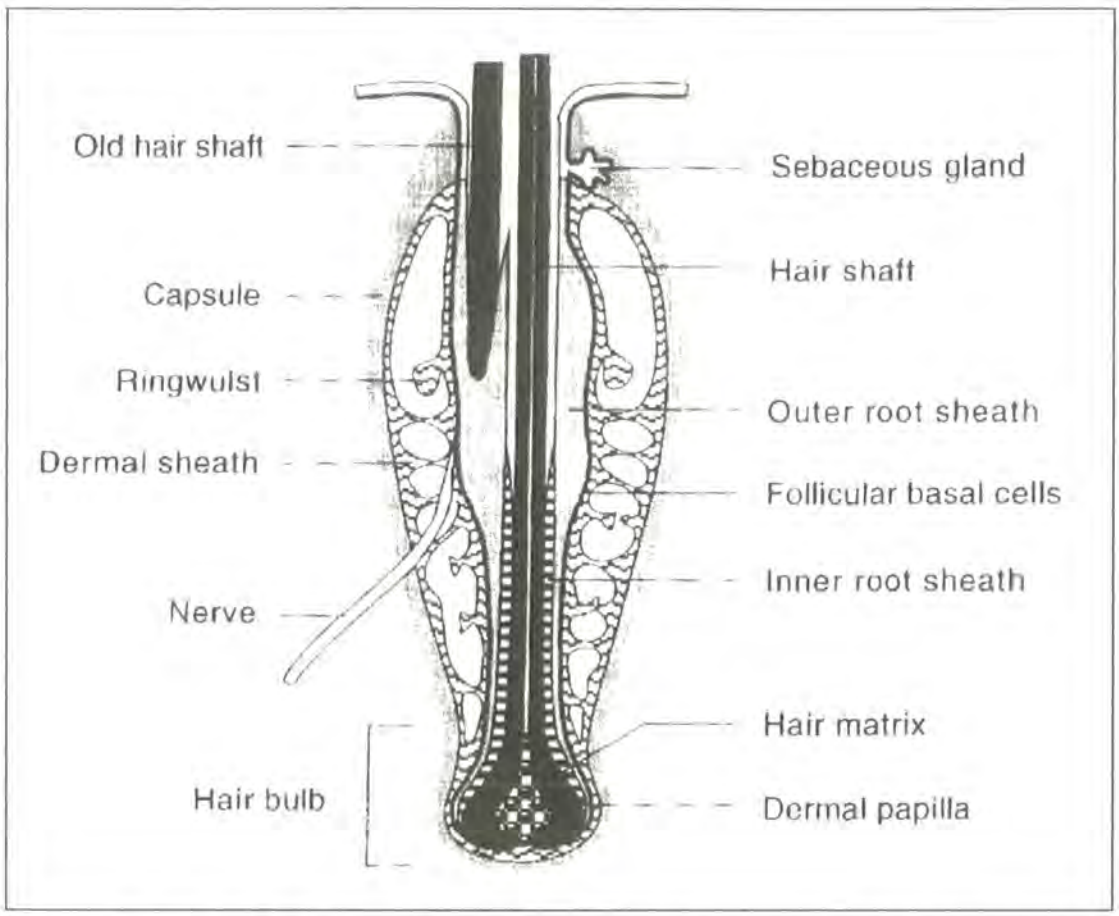

Figure 3. 1: The Rat Vibrissa Follicle (taken from Matsuzaki and Yoshizato, 1998)

Although the anagen phase is similar in vibrissa and pelage follicles, the vibrissa is distinct with regards to the timing and regulation of the catagen and telogen phases. In pelage follicles catagen and telogen can last several weeks compared to vibrissa follicles where these phases are very short, lasting less than three days in total (Ibrahim and Wright 1975). As the vibrissa follicle maintains connections with the surrounding collagen capsule, relatively little upward movement occurs during the catagen to telogen transition as can be seen in Figure 3.2C. This is in comparison to pelage follicles where the dermal papilla regresses upwards into the dermis, where it sits beneath the club fibre. As catagen and telogen make only brief contributions to the vibrissa cycle the new anagen phase is usually initiated before the club fibre, formed during catagen and telogen, has reached its attachment point and is fully mature (Young and Oliver 1976; Jahoda and Oliver 1984b). As the club fibre matures is moves distally up the follicle in an asymmetrical manner so that it finally rests on the side of the nerve entry point for the follicle (Jahoda and Oliver 1984b). The tip of the vibrissa club fibre is pointed, with the oblique side of the tip facing the

direction of the new growing fibre. The flat side of the tip faces the nerve entry point. This is observed in all club fibres, which highlights the predictability and control in this model of follicle cycling.

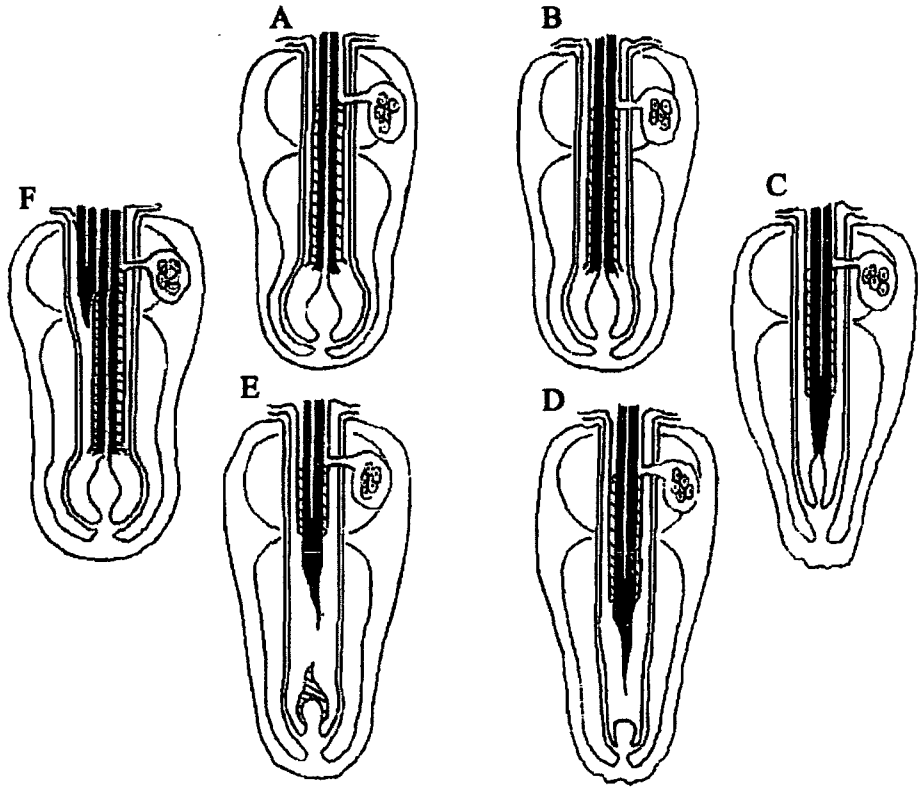

Figure 3. 2: The Growth Cycle of a Vibrissa Follicle in a Rat (taken from Young and Oliver, 1976)

Late anagen (A), just after the club fibre has been released. In catagen (B/C), reorganisation starts to occur around the matrix and the dermal papilla, and the growing fibre is released from its moorings and begins to migrate up the follicle. In addition to catagen, telogen (D) contributes only briefly to the hair cycle and is characterised by a compacted dermal papilla compared to anagen, in addition to a thickened glassy membrane. The initiation of anagen occurs whilst the newly formed club fibre is still migrating upwards (E). The growing fibre grows up alongside the club fibre during anagen (F), and falls out in late anagen when the growing fibre approaches it final and predetermined length.

3.1.3: The Vibrissa follicle-a suitable model for Exogen?

In the vibrissa follicle, as the growing fibre approaches two-thirds or more of its predetermined and final length, the old club fibre is lost (Ibrahim and Wright 1975). As the growing fibre in vibrissa follicles reach the same length during each anagen phase (Dry 1926; Ibrahim and Wright 1975), the timing of club fibre release can be precisely predicted by comparing the relative lengths of the club fibre and the new growing fibre. This makes the vibrissa follicle a useful model with which to analyse changes in the follicle during exogen, as follicles at different stages prior to their release can be specifically selected for studies (Figure 3.3).

Exogen refers not only to the release of the club fibre, but also to the signalling processes that govern it and changes within the follicle prior to club release. When using the vibrissa as a model for exogen, then terminology has to be introduced that reflects the uniqueness of this system (Figure 3.3). Therefore, club fibres in an early anagen follicle will be categorised as 'early exogen' club fibres, meaning that they are club fibres not yet at the point of release. Club fibres in late-anagen follicles, will be termed 'late exogen' club fibres, meaning that they are mature club fibres, ready for release. To distinguish between the process of exogen relating to club fibre maturation and exogen relating to club fibre release, the term teloptosis will be used to refer to club fibre release.

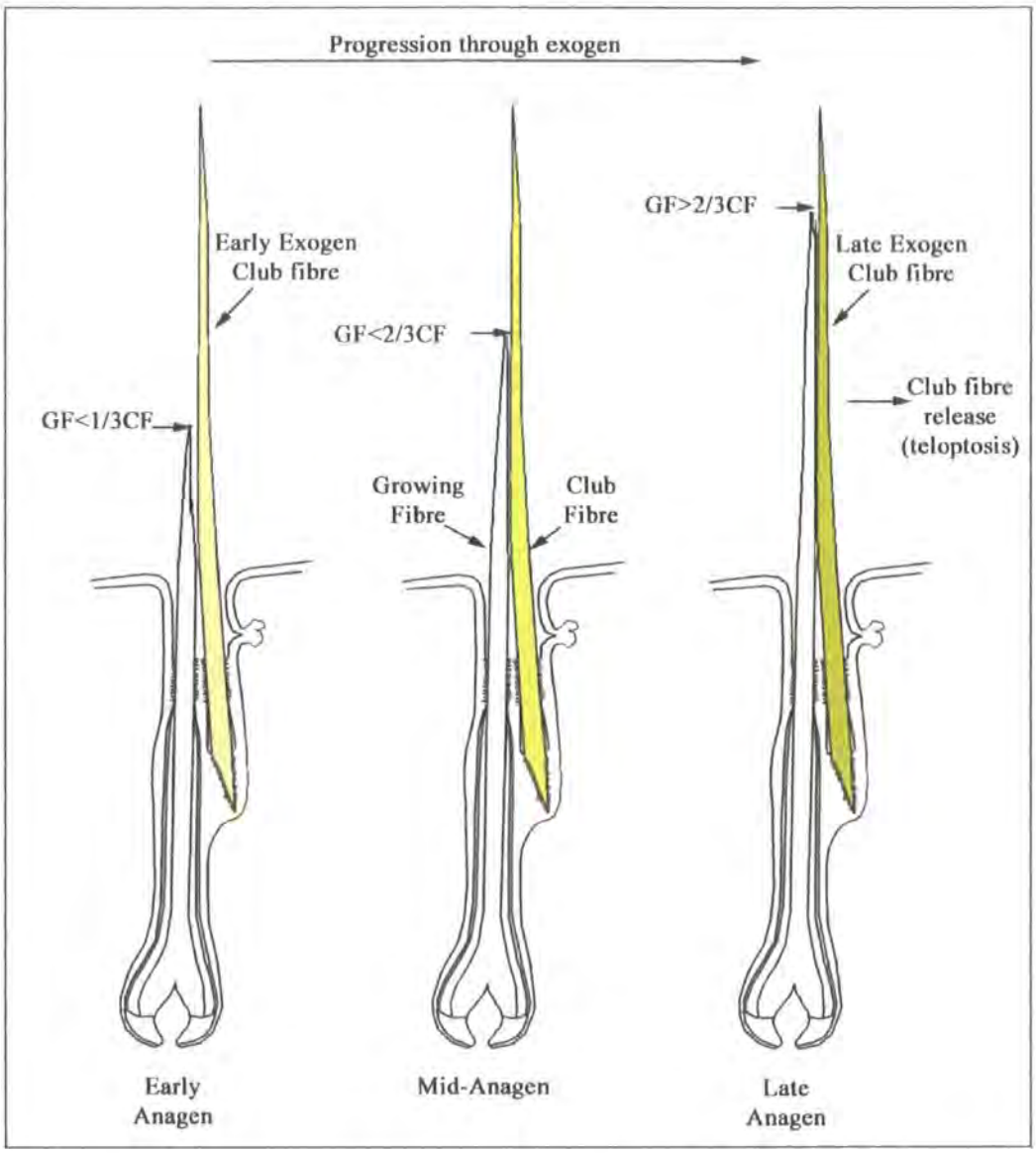

Figure 3. 3: The vibrissa follicle as a model for exogen

In vibrissa follicles the timing of club fibre release is precisely controlled, and the fibre is lost as the growing fibre approaches two-thirds or more of its predetermined and final length. Early anagen follicles contain growing fibres that are less than one-thirds of the length of the club fibre (GF<1/3CF). Club fibres in early anagen follicles are therefore not at the point of release and throughout this thesis will be refered to as early exogen club fibres. Through the progression of exogen, indicated by the increasing intensity of yellow in the club fibre, the growing fibre increases up the length of the club fibre. Once the follicle is in late anagen, the growing fibre is above two thirds of the length of the club (GF>2/3CF), and the club fibre is close to the point of release, or teloptosis. Throughout this thesis, these club fibres will be termed late exogen club fibres.

3.1.4: Factors affecting normal hair growth

As the normal growth characteristics in vibrissa follicles are so consistent from cycle to cycle (Ibrahim and Wright 1975), factors that affect aspects of the growth phase can be accurately analysed. One study has analysed the effects of hormones on the vibrissa hair cycle, as mice of both sexes have vibrissae that grow to the same length in the first two growth cycles, whilst upon reaching sexual maturity at 6 weeks of age male mice grow vibrissae that are 2-3mm longer than their female counterparts (Ibrahim and Wright 1975). This study demonstrated that castration of adult male mice results in a reduction in anagen duration with a corresponding increase in the duration of telogen (Ibrahim and Wright 1983). Castration, resulting in a reduction in testosterone levels reduced the anagen duration of vibrissae so that castrated mice grew vibrissae fibres that were similar in length to their female counterparts. The opposite effect was observed with elevated testosterone levels in immature male mice. In these mice, although growth rates were unaffected the duration of anagen was increased, resulting in longer fibres (Ibrahim and Wright 1983). These experiments demonstrated that vibrissae follicles are responsive to androgens, which are believed to modulate their effects on the hair follicle via the dermal papilla by binding to androgen receptors located here, and altering the release of paracrine factors which influence the growth of keratinocytes (Reviewed in Randall et al. 2000; Randall et al. 2001).

In contrast to a cyclic effect, dietary restrictions affect the growth rate of fibres in vibrissa follicles, which results in the production of shorter fibres (Wright 1965; Ibrahim and Wright 1975). Therefore, although the vibrissa follicle is a predictable model with which to analyse aspects of the hair cycle, under abnormal conditions both growth rates and hair cycling can be altered.

3.1.5: Aims

Within this chapter the first aim was to validate the vibrissa as a suitable model with which to study the process of exogen. Moreover, the question of whether exogen is a gradual or a rapid process was also addressed by comparing fibres at various time points prior to teloptosis.

The second aim within this chapter was to investigate the processes of club fibre formation and retention. The mouse models discussed during Chapter 1 gave an insight into club fibre formation and retention highlighting the structural and adhesive properties of the club fibre within its trichilemma sac as important. Therefore, the vibrissa model was utilised with its predictive exogen stage to investigate club fibre formation and retention based on structural and adhesive changes of the club fibre and the surrounding trichilemma sac. In particular, the Dsg3-/- mouse highlighted adhesive components of cells as important for club fibre retention. Based on this, both early and late exogen club fibres were analysed for changes in desmosomal and adherens junction components.

3.2: Methods

3.2.1: Vibrissae follicle dissection and embedding

Vibrissa follicles from several male and female PVG rats, between 3 and 6 months of age were dissected as described in Chapter 2.2.5.1. They were then placed into MEM and follicles containing early and late exogen club fibres were selected specifically for study. If to be used for antigen detection, follicles were embedded longitudinally in Oct compound (Agar Aids) and stored at -80°C until required. They were orientated with the nerve entry point to the right hand side of the follicle, so that the growing and club fibres would be aligned in the same plane as each other.

3.2.2: Antigen detection

3.2.2.1: Cryostat sectioning

Follicles containing early and late exogen club fibres, embedded in Oct compound, were sectioned into 7μm sections on a Leica 3050S cryostat. The sections were thawed onto Poly-lysine coated microscope slides and left to air dry for 1 hour. Fixation was not required for any of the antigens of interest.

3.2.2.2: Immunofluorescent analysis

After air drying, sections were washed in PBS (3 x 5 minutes) and a 2% solution of BSA in PBS applied, to block non-specific antibody binding. This was incubated with the sections for 30 minutes, during which time the primary antibodies were appropriately diluted (see Table 3.1) in filtered PBS. The blocking solution was removed, and 20μl primary antibody applied to each section. Slides were then covered in a small strip of Parafilm and incubated in a humidified chamber overnight at 4°C.

After removal of unbound primary antibody by washing in PBS (3 x 5 minutes), the appropriate secondary antibody (specific for the host in which the primary antibody was raised), diluted in PBS was applied to sections and left for 1 hour at room temperature, in a dark humidified atmosphere. Unbound secondary antibody was

removed by washing in PBS (3 x 5 minutes). Sections that had been incubated with the anti mouse FITC conjugated secondary antibodies were mounted with coverslips using an anti-photobleaching mounting medium; Vectashield containing PI or DAPI (Vector Laboratories).

At this point, sections incubated with the primary antibodies raised in goat and the biotinylated secondary antibody were incubated with Streptavidin-Cy3 (Jackson Laboratories). Streptavidin-Cy3 was diluted 1/500 in PBS and applied to sections for 30 minutes in a dark humidified atmosphere. Slides were then washed in PBS (3 x 5 minutes) and coverslips mounted in an anti-photobleaching mounting medium; Vectashield (Vector Laboratories).

11-5F fluorescence was visualised and photographed on a BioRad microradiance confocal. β-catenin, Dsg1 and Dsg3 fluorescence was visualised and photographed on a Zeiss Axio Imager.

To evaluate non-specific binding of the primary antibody, monoclonal antibodies were substituted with PBS, whilst polyclonal primary antibodies were substituted with an appropriately diluted isotype control (R&D systems).

Table 3. 1: Primary and Secondary antibodies used in Chapter 3

Antibody	Targeted antigen	Source	Raised in:	Working dilution
11-5F	Desmoplakins I/II	D.Garrod, Manchester	Mouse	1 in 3
Anti β-catenin	β-catenin	Transduction Labs	Mouse	1 in 100
Anti Dsg1	Desmoglein 1	Santa Cruz	Goat	1 in 75
Anti Dsg3	Desmoglein 3	Santa Cruz	Goat	1 in 75
Anti mouse FITC conjugated	Mouse IgG	DAKO	Rabbit	1 in 30
Anti Goat-Biotinylated	Goat IgG	Zymed	Donkey	1 in 300

Table 3. 2: Number of experimental repeats

Antibody	Early exogen repeats	Late exogen repeats
11-5F	5	5
Anti β-catenin	3	4
Anti Dsg1	3	3
Anti Dsg3	3	3

3.2.3: Transmission Electron Microscopy

3.2.3.1: Sample preparation

After follicle dissection, as described in 2.2.5.1, 4 early anagen and 4 late anagen follicles from one PVG rat were placed immediately in Karnovsky fixative for 1 hour at room temperature (Karnovsky 1965). Karnovsky fixative was made fresh and was composed of 2% paraformaldehyde, 2.5% Glutaraldehyde in 0.1M sodium phosphate buffer (Appendix 1). Whilst fixing, follicles were staged into representative early and late exogen samples. Follicles were then post fixed for 1 hour in 1% Osmium Tetroxide (Agar Scientific) buffered in 0.2M Sodium Phosphate buffer, pH 7.4. After post fixing, follicles were dehydrated through a series of ascending grades of ethanol (70%, 95%) with 3 changes, each lasting 15 minutes. They were then submerged in 3 changes, in 100% ethanol, each lasting 30 minutes. Follicles were then immersed in an intermediate solution consisting of a 50:50 mix of 100% alcohol and propylene oxide. Following 3 changes, 10 minutes apart, follicles were placed in propylene oxide, again with 3 changes, 10 minutes apart. Follicles were then placed in a fresh 50:50 araldite resin:propylene oxide mix and left overnight for the resin to infiltrate and the propylene oxide to evaporate. The resin was composed of (in 46.2 grams) 23 grams Araldite CY 212, 22 grams Dodeoenyl succinic anhydride (DDSA) and 1.2 grams Benzyldimethylamine (BDMA) (all from Agar Scientific). Following overnight infiltration the follicles were placed in a fresh resin change for 30 minutes. Their final change was into a rubber mould with fresh araldite, which was then left to polymerise for 48 hours at 60°C.

3.2.3.2: Sectioning and staining of Semithin sections

Semithin sections (0.5μm) of follicles in araldite resin blocks were taken using a glass knife on a Reichert Ultracut S Ultramicrotome. Semithin sections were stained for 1 minute over heat with filtered 1% Toludine Blue (Sigma), before rinsing with distilled water. Slides were blotted dry with filter paper and coverslips then mounted using DPX (Agar Aids).

3.2.3.3: Sectioning and staining of Ultrathin sections

Longitudinal follicle ultrathin sections for TEM were cut using a diamond knife on a Reichert Ultracut S Ultramicrotome. The sections were floated on distilled water, and picked up using formvar coated 200 mesh grids. Once on grids the sections were stained for 10 minutes with 1% Uranyl acetate in 70% alcohol, washed in water, then stained for 10 minutes with Rennolds Lead Citrate.

3.2.3.4: Image Acquisition

Light microscopy of Semithins was taken on a Zeiss Axio Imager.

Photographs of ultrathins were taken on Phillips 400T Transmission electron microscope onto Kodak film. Film was then developed by agitating for 4 minutes in D-19 developer (Kodak). After developing, film was rinsed briefly in cold running water before being fixed for 10 minutes in Unifix (Kodak). After fixation film was rinsed in cold running water for 30 minutes prior to being dried in a 60°C oven for 2 hours. Photos were scanned onto a computer using an Epson Twain 5 Scanner at 600dpi.

3.2.4: Plucked Fibre procedure and analysis

Both growing fibres and club fibres were plucked from the whisker pads of 3 young Whister rats (<5 months) and 3 old rats (>24 months) for analysis. Young rats were obtained from the LSSU at Durham University whilst old rats were obtained from Dr Colin Ingram at Newcastle University. Fibres were plucked using No.4 forceps in the direction of hair growth from Columns A, B and C on the mystacial pad. The club fibre was plucked first, followed by the growing fibre from the same follicle and corresponding fibres were mounted onto labelled slides using adhesive tape. Whilst plucking, the surrounding face pad was held securely with the free hand. A total of 69 club fibres were plucked from the 3 young rats and 202 club fibres from the 9 old rats.

Club fibres were analysed independently of hair cycle stage by two researchers (myself and Dr Gavin Richardson) and categorised into three groups; substantial amounts of cells attached, a few cells attached or clean with no cellular material attached as seen in Table 3.3. The lengths of both the club fibres and the growing fibres were also measured and recorded.

The hair cycle stage was determined by comparing the relative length of the growing fibre and the club fibre. Cycle stages were defined as early, middle and late anagen corresponding to the new growing fibre being less than one third up the length of the club fibre, up to two thirds the length of the club fibre or above two thirds of the length of the club fibre. Cycle stage results were then combined with the results relating to the amount of material attached to the plucked fibre for subsequent analysis.

Table 3. 3: Club fibre groupings based on amount of material attached after plucking

Morphological description of club fibre tip	Representative club fibre
Club fibre has a substantial amount of material attached. Has material on both sides of the club tip.	
Club fibre has a small amount of material attached to the club tip.	
Club fibre is clean from attached material	

3.2.5: Scanning Electron Microscopy

3 early exogen and 3 late exogen club fibres were plucked from a 6 month old female PVG rat and fixed immediately in Karnovsky fixative for 1 hour at room temperature (Karnovsky 1965). Karnovsky fixative was made fresh and composed of 2%

paraformaldehyde, 2.5% Glutaraldehyde in 0.1M sodium phosphate buffer. After fixation the plucked fibres were post fixed in 1% Osmium Tetroxide buffered in 0.2M Sodium Phosphate buffer, pH 7.4. After post fixing, follicles were dehydrated through a series of ascending grades of ethanol (70%, 95%) with 3 changes, each lasting 15 minutes. They were then submerged in 3 changes, in 100% ethanol, each lasting 30 minutes. Fibres were transferred to 100% acetone, and taken through 3 fresh changes, 10 minutes each. After acetone filtration fibres were dried in a critical point dryer for 2 hours before being coated in chromium. Fibres were then mounted onto carbon coated silicone chips with electrical conductive resin, Three Bond 3350C, and kept in a desiccated environment prior to analysis. Images were taken on a Hitachi S5200 Scanning Electron Microscope.

3.3: Results

3.3.1: Immunofluorescence of Cell Adhesion complexes

3.3.1.1: ß-catenin expression in vibrissa follicles

In both early and late exogen club fibres membranous ß-catenin expression was visible throughout the epidermal portion of the follicle. Strong expression was evident in both the basal and suprabasal ORS, increasing in intensity in the companion layer (Figure 3.4A). In the bulb region expression was visible in the germinative matrix along with the presumptive IRS and trichocytes. In addition, all layers of the IRS and hair fibre expressed ß-catenin. With regards to the club fibre, expression was consistent throughout the suprabasal ORS surrounding the fibre. No changes in expression in this region were detectable between follicles containing early and late exogen club fibres (Figure 3.4A/B).

3.3.1.2: Desmoglein expression in vibrissa follicles

Analysis of desmoglein expression surrounding vibrissa club fibres in early exogen showed expression of both Dsg1 and Dsg3 through the suprabasal ORS (Figure 3.5A/B). With relation to the intensity of fluorescence there was no noticeable difference between cells proximal to the club fibre compared with those further away. There was, however, a difference in the staining pattern between these two desmosomal proteins. Dsg1 was only present in the suprabasal ORS, and was absent in the basal layer (Figure 3.5C). However, Dsg3 was present throughout both the suprabasal and basal ORS (Figure 3.5D). No changes in expression were seen with either antibody between follicles containing early and late exogen club fibres.

3.3.1.3: Desmoplakin expression in vibrissa follicles

The II-5F antibody was used to detect desmoplakins I/II throughout anagen vibrissae. Around the club fibre, fluorescence was visible extending throughout the trichilemmal sac, whilst the signal was weakened in the basal layer. In 7 of 10 follicles, desmoplakin expression was more intense in the companion^{CL}, than the remaining suprabasal ORS (Figure 3.6A). This pattern of staining was observed

around both early and late exogen club fibres, with no obvious differences detected around club fibres as they "matured". Staining was present at desmosomal plaques on the cell membrane.

In relation to layers surrounding the growing fibre, desmoplakin was expressed at high levels in the companion layer, but the attenuation of expression in the remaining ORS was noticeable (Figure 3.7A/C). Expression was also present in Huxley's layer and the IRS cuticle, although it was absent from Henle's layer of the IRS, the cortex, cuticle and medulla of the hair fibre. Staining was not observed in the dermal papilla. Further up the length of the growing fibre, desmoplakin increased in the suprabasal ORS corresponding with the onset of keratinisation within Huxley's layer of the IRS. However, expression remained weaker in the basal layer of the ORS (Figure 3.7B)

Figure 3. 4: ß-catenin expression in vibrissa follicles

ß-catenin expression was present in the epidermal compartment of the follicle, with noticeable intensity in the companion layer (arrow). Expression was in the germinative matrix and the presumptive IRS and trichocytes whilst being throughout the ORS. Both early exogen club fibres (A) and late exogen club fibres (B) had ß-catenin expressed in the ORS and companion^{CL} surrounding them. However, there were no visible changes in expression in this region surrounding club fibres between the two exogen populations. The control, (C), with which PBS was substituted for the primary antibody showed no specific staining.

Scale bars: 100 μm
Green: ß-catenin
Blue: DAPI nuclear counterstain

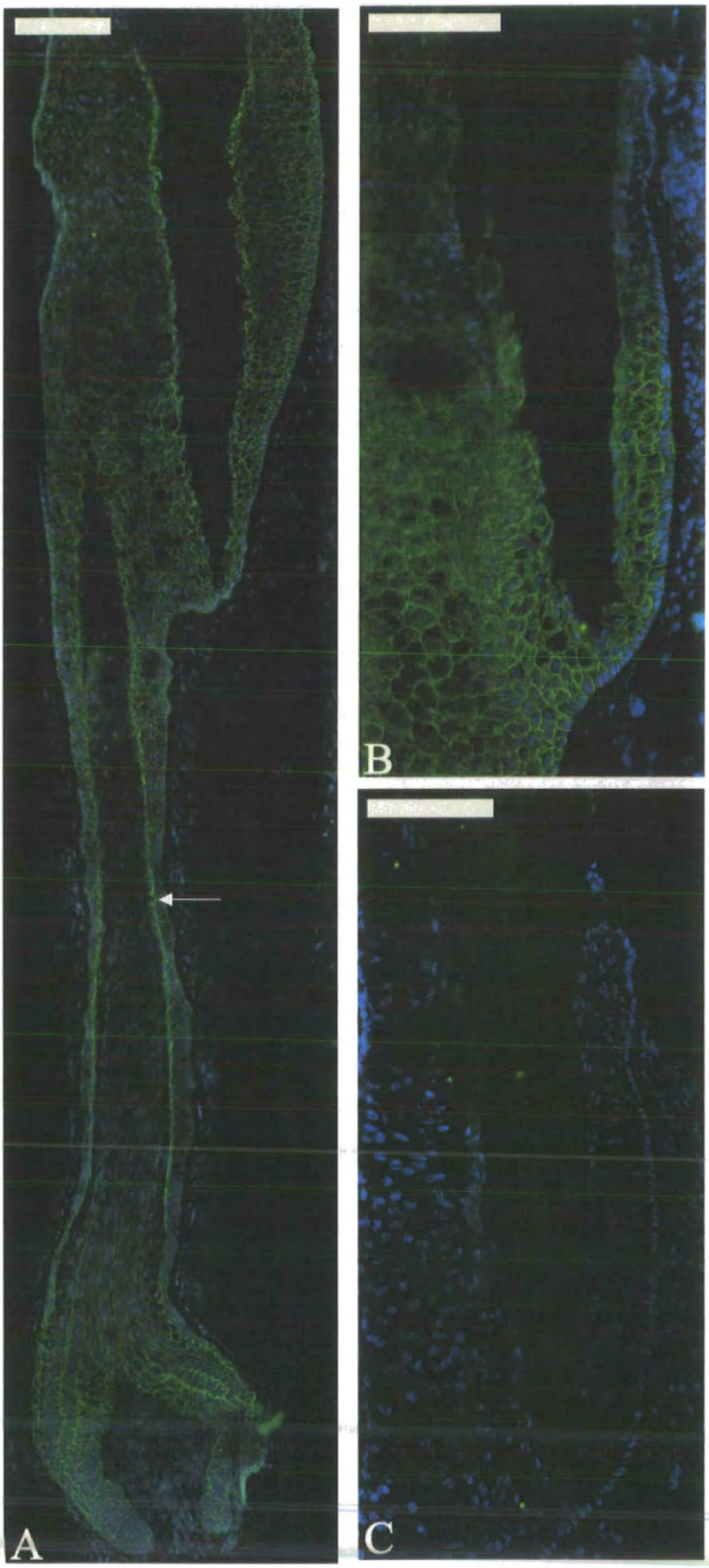
A
B
C

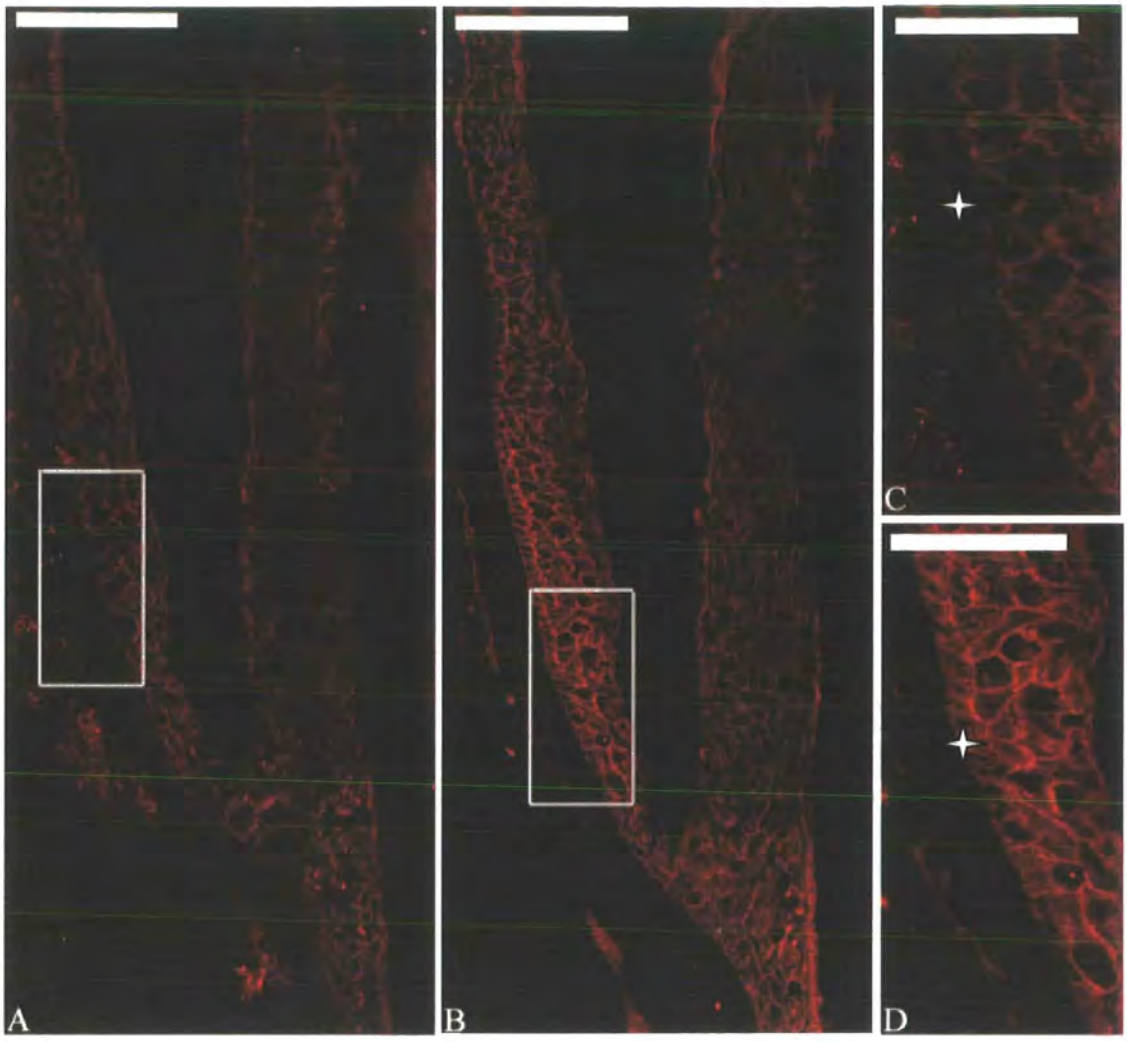

Figure 3. 5: Desmoglein expression surrounding early exogen club fibres in vibrissae follicles

A: Dsg1 expression was relatively weak throughout the suprabasal ORS and appeared absent from the basal layer (see enlargement of boxed area in C). B: Dsg3 expression was more constant between the basal and suprabasal ORS (see enlargement of boxed area in D), being present at cell junctions between these keratinocytes. Stars in C and D demark the basal layer, distinguishing it from the suprabasal keratinocytes.

Scale bars: A/B: 100μm, C/D: 50μm

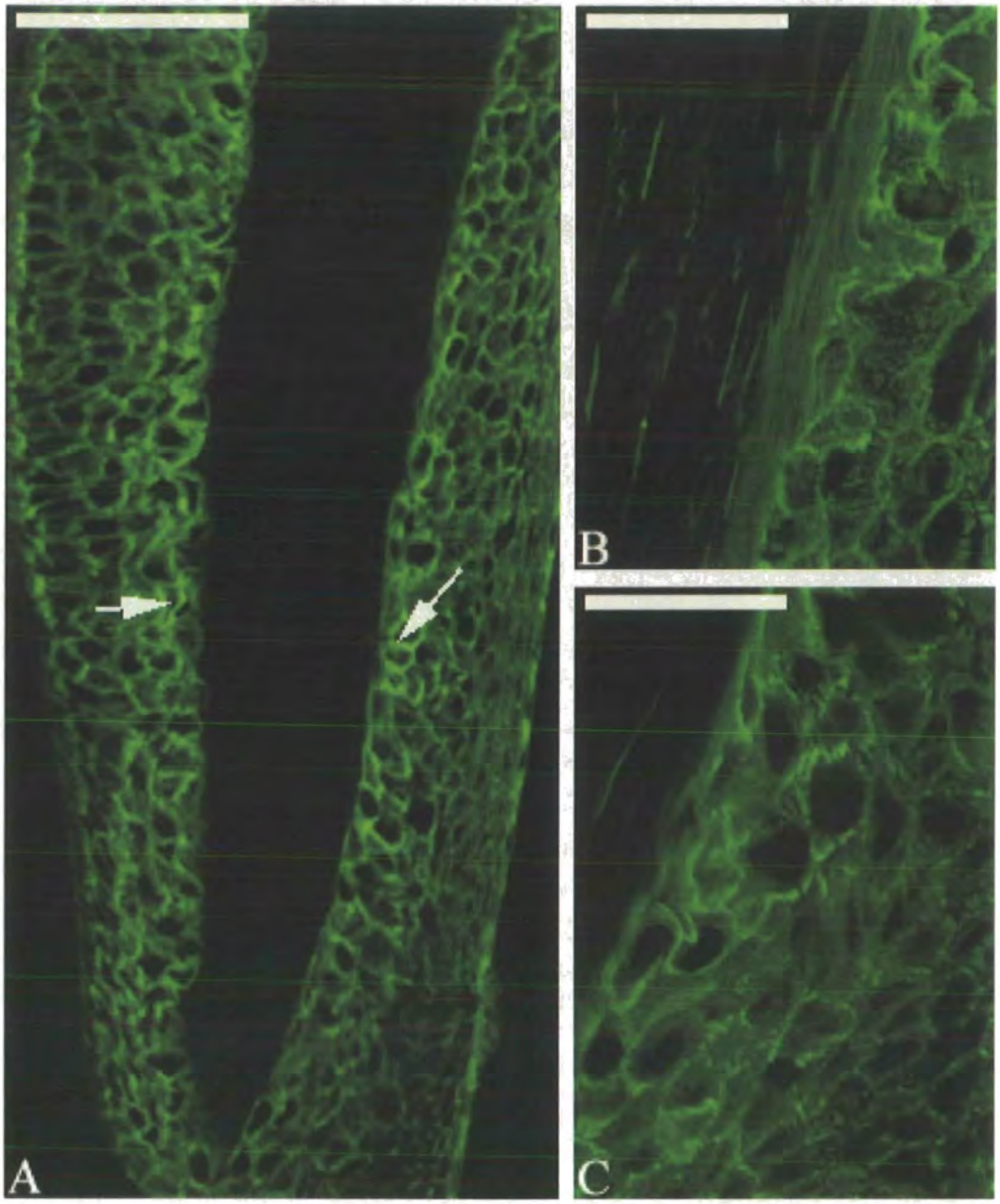

Figure 3. 6: Desmoplakin expression surrounding exogen club fibres in vibrissae follicles

Strong desmoplakin was visible in the companion^{CL} of exogen club fibres (A). This staining pattern was observed surrounding both early and late exogen club fibres. Closer inspection of the companion^{CL} shows staining localised to the cell membrane, representative of desmosomal plaques (B/C).

Green: Desmoplakin,

Scale bars: A: 100μm, B/C: 50μm

Figure 3. 7: Desmoplakin expression in the anagen vibrissa follicle

The anagen vibrissa showed desmoplakin throughout the epidermal portion of the follicle. The area marked by the arrow head is enlarged in B, and shows the level of desmoplakin expression in the ORS above Huxley's layer terminal differentiation compared to below this level (C) (enlargement of area marked by arrow in A) where expression in the ORS is noticeably weaker. The layers of the follicle are well delineated with desmoplakin. The intense staining in the companion layer (5) is evident, especially when compared to the reduced staining in the remaining ORS (6). The area marked by the star in A is enlarged in D, showing the presumptive IRS and hair cuticle stained for desmoplakin. Expression was absent from the dermal papilla (DP).

Green: Desmoplakin
Red: PI nuclear counterstain
Scale Bars: 100μm

1:Hair cuticle
2:IRS cuticle
3: Huxley's layer IRS
4: Henle's layer IRS
5: Companion Layer
6: Suprabasal ORS
7: Basal ORS

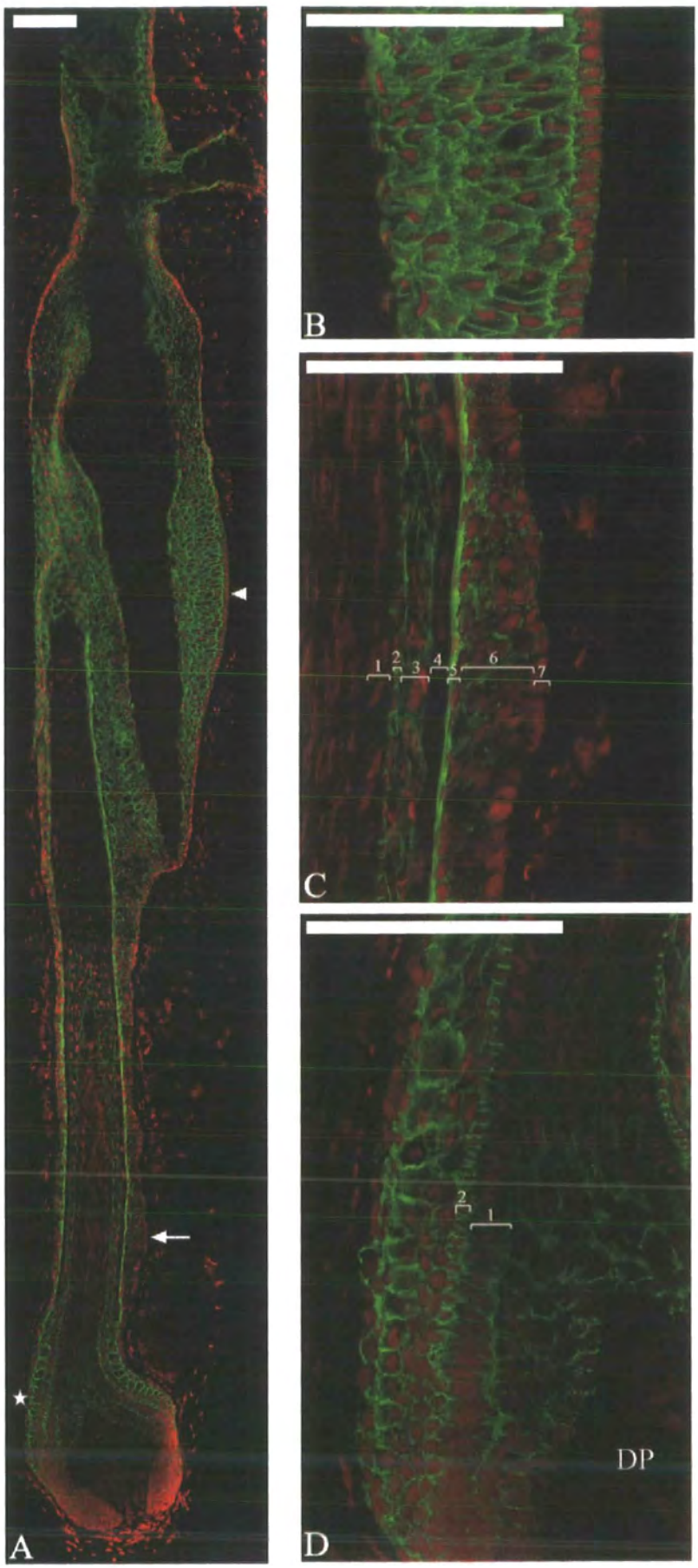
A
B
C
1
2
3
4
5
6
7
D
2
1
DP

3.3.2: Structural analysis

3.3.2.1: Transmission Electron Microscopy of vibrissa club fibres

Light microscopy of toludine blue stained semi thin sections highlighted the electron dense trichilemmal keratin layer that forms the outer surface of the fully formed club fibre (Figure 3.8B). Within this, the pale blue staining detectable was representative of the fibre cuticle.

Longitudinal sections of club fibres embedded in their surrounding ORS were examined on a transmission electron microscope. These showed a non-nucleated electron dense layer that formed the outer layer of the club fibre. Several layers of these electron dense cells were visible around the tip of the vibrissa club fibre making up what is termed trichilemmal keratin, although they were very elongated and flattened making the whole unit rather thin (Figure 3.8C). A double layered plasma membrane was visible between cell layers, serving to highlight a complex interdigitation network between the cells of the trichilemmal keratin.

A large number of complex bristle-like protrusions (Figure 3.9A/B) of the trichilemmal keratin into the surrounding layer of ORS cells were visible, each protrusion with a number of desmosomal complexes affiliated to it. Keratin filaments were seen adjoining these desmosomes, and extending into the cytoplasm of the surrounding cells (Figure 3.9C). Moreover, the cells surrounding the trichilemmal keratin, the companion^{CL}, were also joined to each other through a highly complex network of membrane interdigitations, and massive numbers of desmosomes were visible between the interdigitations between these cells (Figure 3.9D). Keratin filaments were visibly associated with the desmosomal plaques, whilst extensive networks of keratin were also present throughout cells. Both transverse and longitudinal keratin filaments were detected in the cytoplasm along with many free floating ribosomes.

In follicles with early exogen club fibres, laddered membrane coating granules were detectable coating the surface of the trichilemmal keratin cells, with occasional honeycombed granules also seen in the cytoplasm (Figure 3.10A). However, in

contrast, no membrane coating granules of any description were visible in follicles containing late exogen club fibres. The cytoplasm of companion ^{CL} layer cells surrounding early exogen club fibres was relatively clear compared to their late exogen counterparts, which were noticeably more keratinised (Figure 3.10B). Surrounding late exogen club fibres, the condensation of keratin filaments made the cytoplasm appear electron dense. This, along with a loss of cytoplasmic integrity made it difficult to decipher cellular components within these cells (Figure 3.10C).

In the companion^{CL} layer cells few cells with condensed heterochromatin were visible in follicles with early exogen club fibres (Figure 3.10B). This was compared to nuclei in cells surrounding late exogen club fibres, many of which had invaginated cell membranes and condensed chromatin (Figure 3.10C). Occasionally vacuoles were also visible in the cytoplasm, although these were found in cells around both early and late exogen club fibres.

3.3.2.2: Visual analysis of plucked club fibres

A noticeable and obvious correlation between the cycle stage of the follicle and the relative amount of material attached to the plucked club fibre was observed in fibres taken from young rats (Graph 3.1). Early exogen club fibres, plucked from follicles in early anagen had considerable amounts of cellular material attached to them. This was in striking contrast to the plucked late exogen club fibres, which had very little or no cellular material attached at all. Club fibres plucked from follicles in the middle of their hair cycle had some cellular material attached, but generally these were low amounts.

As follicles in matching positions on adjacent mystacial pads are in the same cycle stage, the amounts of material attached to club fibres from matching sites on both the left and right mystacial pad were compared to check consistency in the plucking technique. A 92% correlation was observed between respective results.

Similarly to the young rats, in club fibres plucked from older rats there was an obvious correlation between the amounts of material remaining on the club fibre after plucking and the relative cycle stage of the follicle. However, the data from the

plucked club fibres from old rats indicated that this trend was more gradual in old rats (Graph 3.2), when compared to the data from young rats which indicated distinct and obvious correlations between the amount of material attached to the club fibre and the relative cycle stages. With old rats, several fibres plucked in late anagen follicles, which were theoretically late exogen clubs had substantial amounts of material still attached to them.

3.3.2.3: Scanning Electron Microscopy of plucked club fibres

Club fibres were plucked from vibrissa follicles in early anagen, with the presumption that these fibres would be representative of retained club fibres, termed early exogen clubs. In contrast, club fibres taken from late anagen follicles were presumed to be representative of fibres immediately prior to exogen, termed late exogen clubs. Scanning Electron Microscopy (SEM) was used to analyse differences between these two club fibre types.

Early exogen club fibres were distinct as they were covered in large amounts of cellular material, which caused the tip of the club fibre to have a rounded appearance (Figure 3.11A). The sides of the club fibre also had large numbers of cells attached. In some areas, cells appeared as if they had been peeled back, revealing an underlying layer of hardened flattened cells (Figure 3.11B).

The external surfaces of late exogen club fibres consisted of a number of irregularly shaped flattened cells, presumed to be the trichilemmal keratin layer of the club fibre. These cells were loosely overlaid, giving the fibre a multilayered appearance. This was particularly noticeable at the tip of the fibre which was composed of a number of hardened cells protruding out of the fibre at varying angles resulting in a jagged appearance (Figure 3.12A/C). On closer inspection it was noticeable these cells, although flattened, had an abraded surface, with a number of small raised ridges present in a fingerprint like pattern on the cell surface (Figure 3.12B/C). This was in contrast to cells of the cuticle, higher up the fibres which were flattened with a smooth surface, all lying tightly together on the same plane.

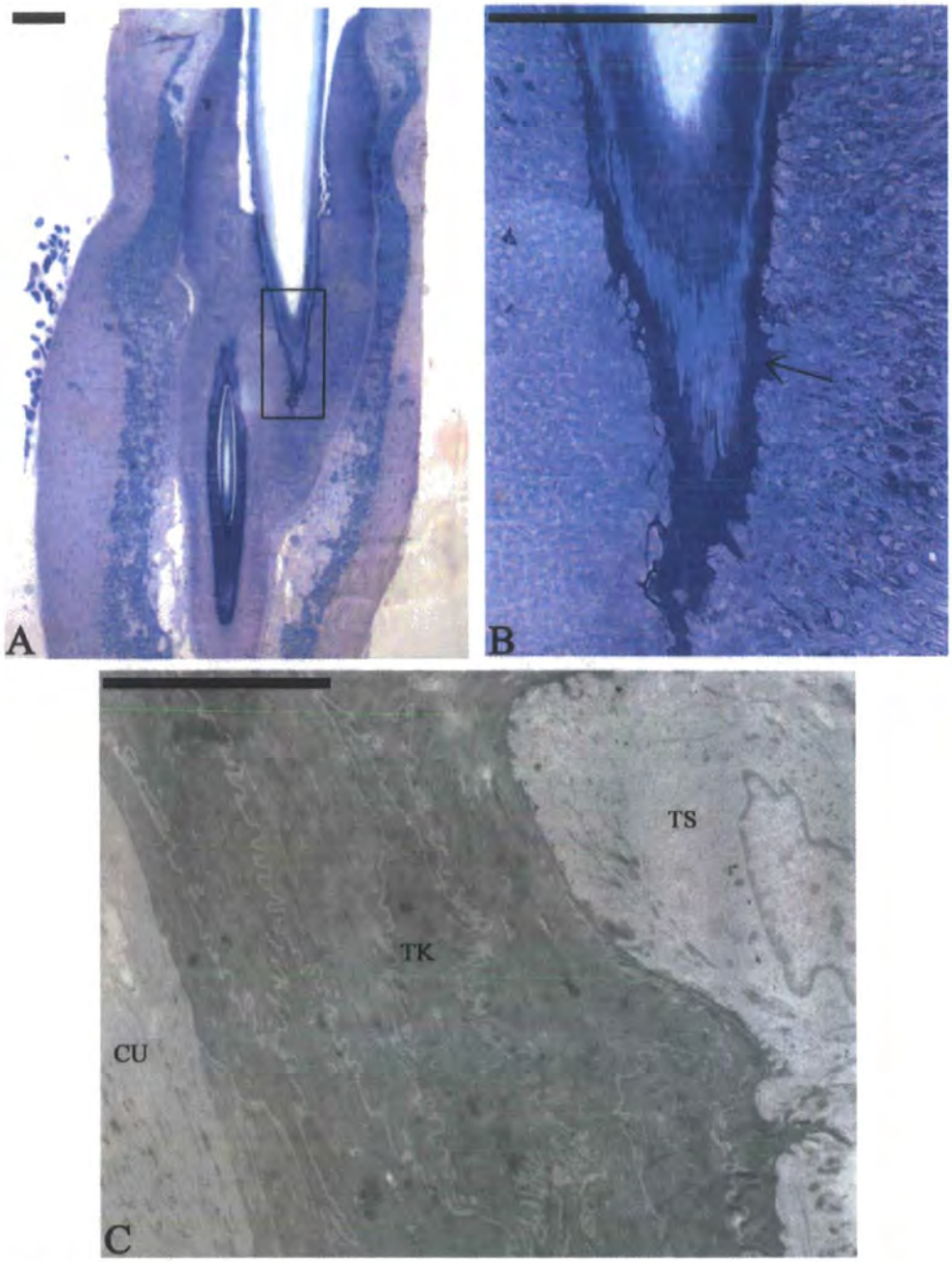

Figure 3. 8: Trichilemmal keratin surrounding vibrissa club fibres

Toluidine blue staining of semithin sections highlighted a dark blue cell layer surrounding the tip of exogen club fibres (A). This dark layer is the trichilemmal keratin of the club fibre, and was characterised by numerous anchoring protrusions (arrow) visible extending from the fibre (B) (boxed area in A). TEM indicated that this layer was several cells thick, whilst all cells were electron dense and non-nucleated (C).

Scale bars A/B: 100μm C: 5μm
CU: Cuticle, TK: Trichilemmal Keratin, TS: Trichilemmal Sac

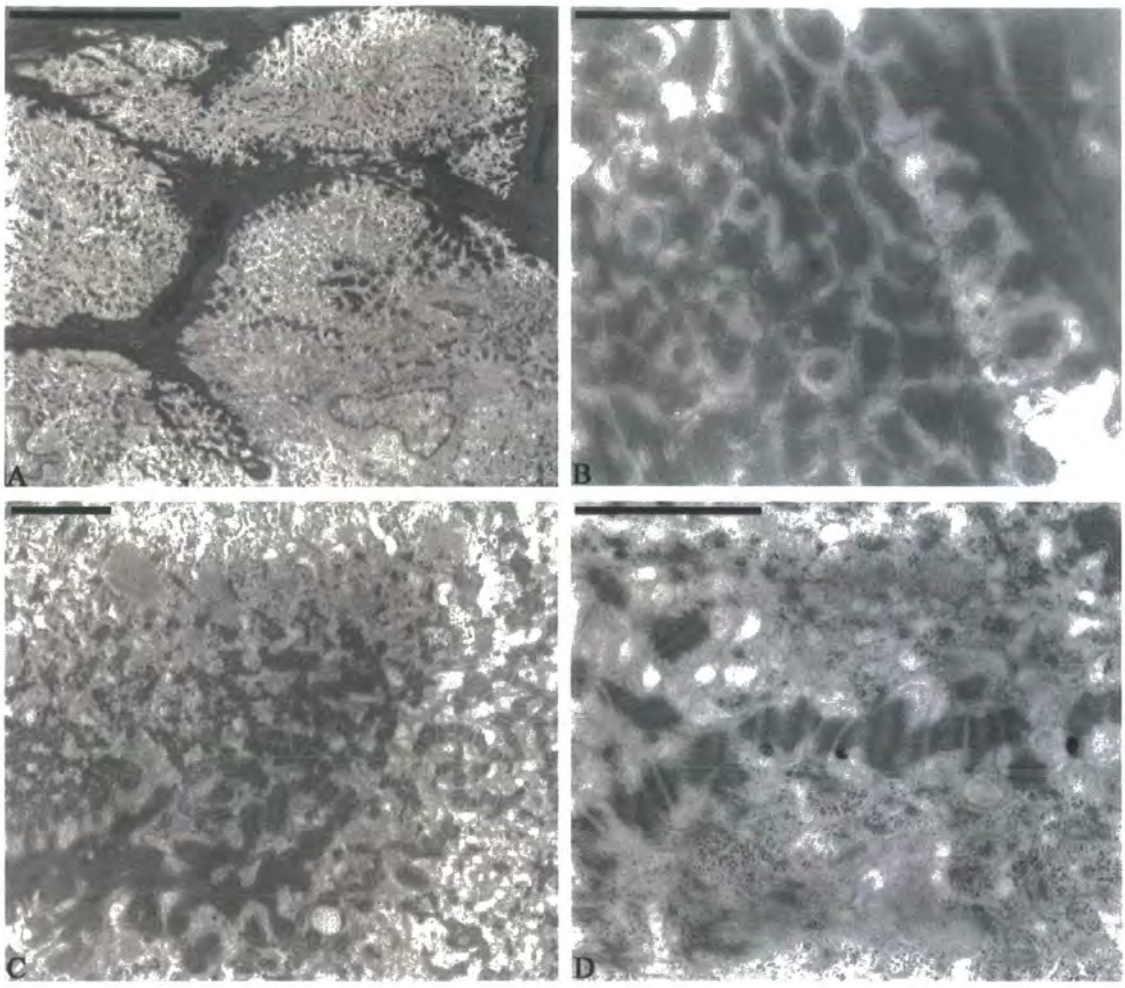

Figure 3. 9: Anchorage of the exogen club fibre

A: Complex finger-like projections of the trichilemmal keratin were observed protruding out into the surrounding ORS (A) at all angles from the club fibre securing the club fibre in place (B). Desmosomal complexes were visible both between the trichilemmal keratin and the surrounding ORS (C) but also between the cells of the ORS (D). Complex interdigitations of cell membranes within the ORS ensured large surface area for desmosomal complexes. Keratin filaments were also observed linking the desmosomes with the cell cytoplasm.

Scale Bars: A:5 μm, B/C/D: 1μm

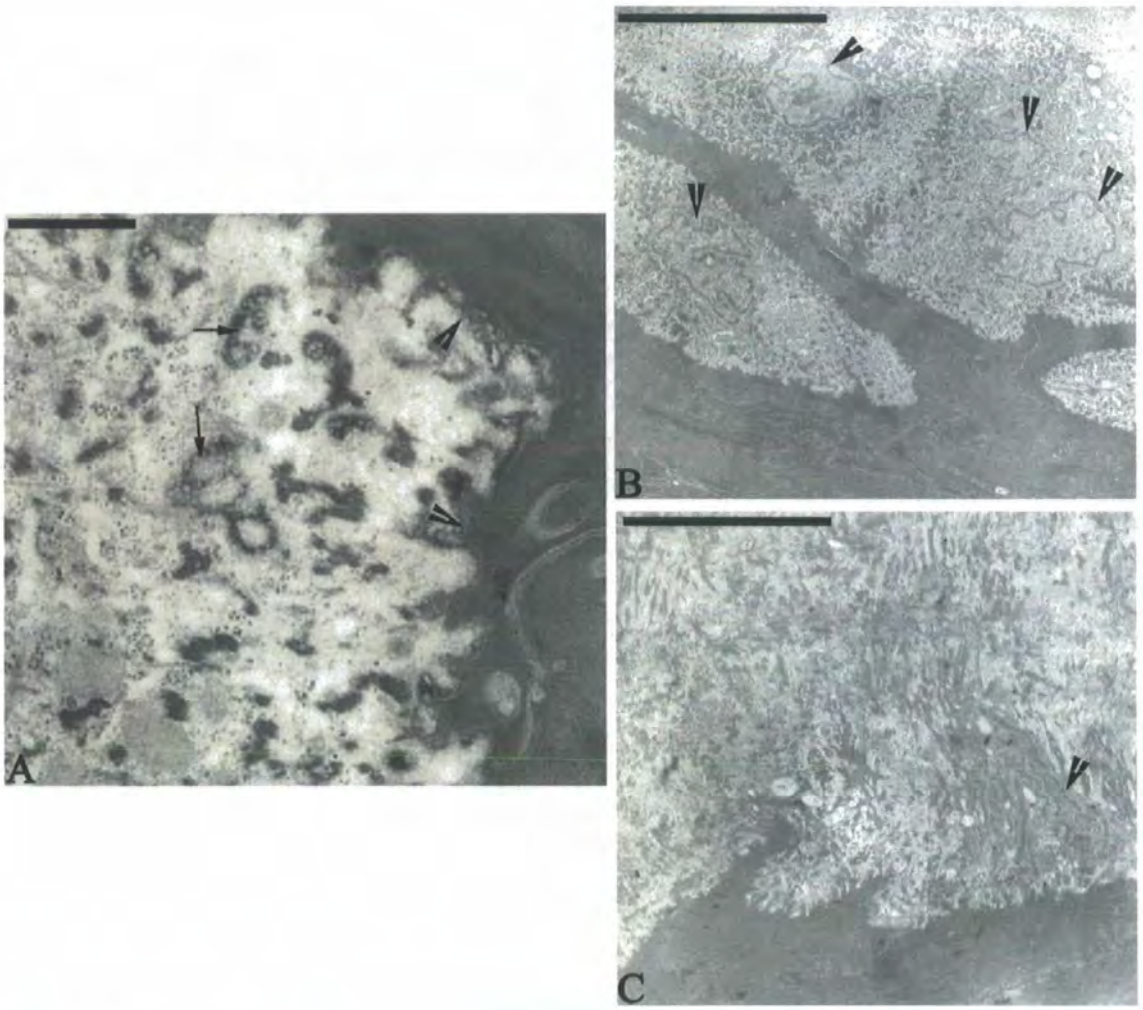

Figure 3. 10: Unique features of early and late exogen club fibres

In follicles with early exogen club fibres, laddered membrane coating granules were detectable coating the surface of the trichilemmal keratin cells (arrow heads), whilst honeycombed granules were also visible in the cytoplasm of the companion^{CL} (arrows) (A). The cytoplasm of companion ^{CL} layer cells surrounding early exogen club fibres also contained healthy nuclei (arrowheads) and was relatively free of keratinised material (B). This was in comparison to the companion ^{CL} of late exogen club fibres where nuclei were difficult to distinguish with invaginated membranes and condensed chromatin (arrowhead). In late exogen, these cells appeared to be keratinised as if they were beginning to undergo cell death (C).

Scale bars: A: 0.1 μm, B/C: 10 μm

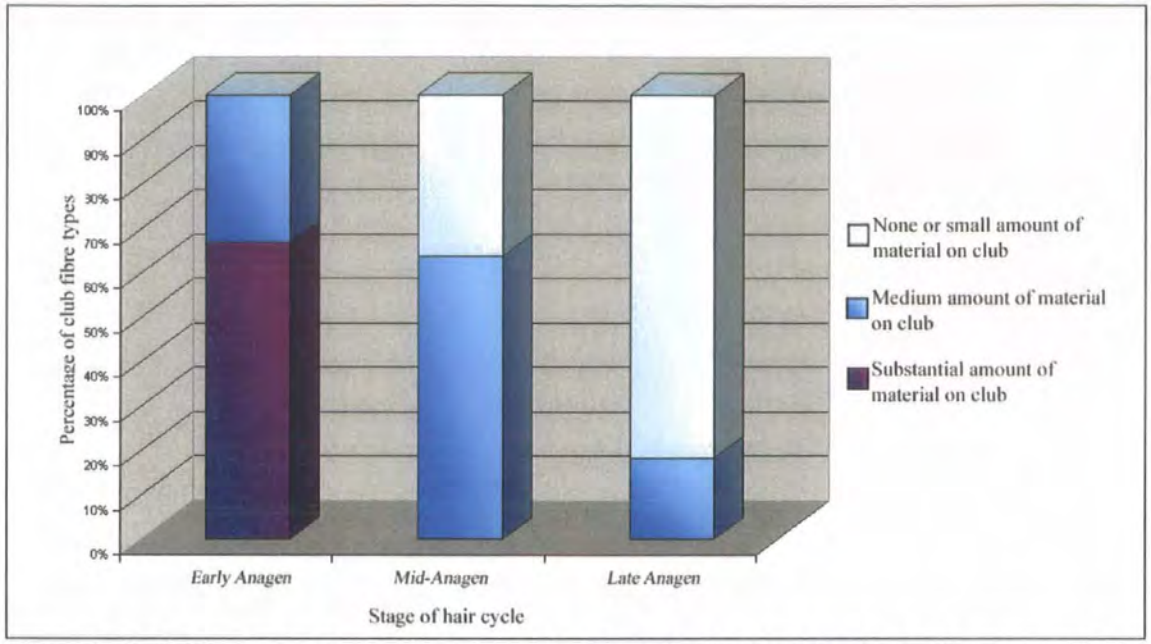

Graph 3. 1: Variation in the amount of material attached to plucked exogen club fibres from vibrissa follicles at different anagen cycle stages in young rats

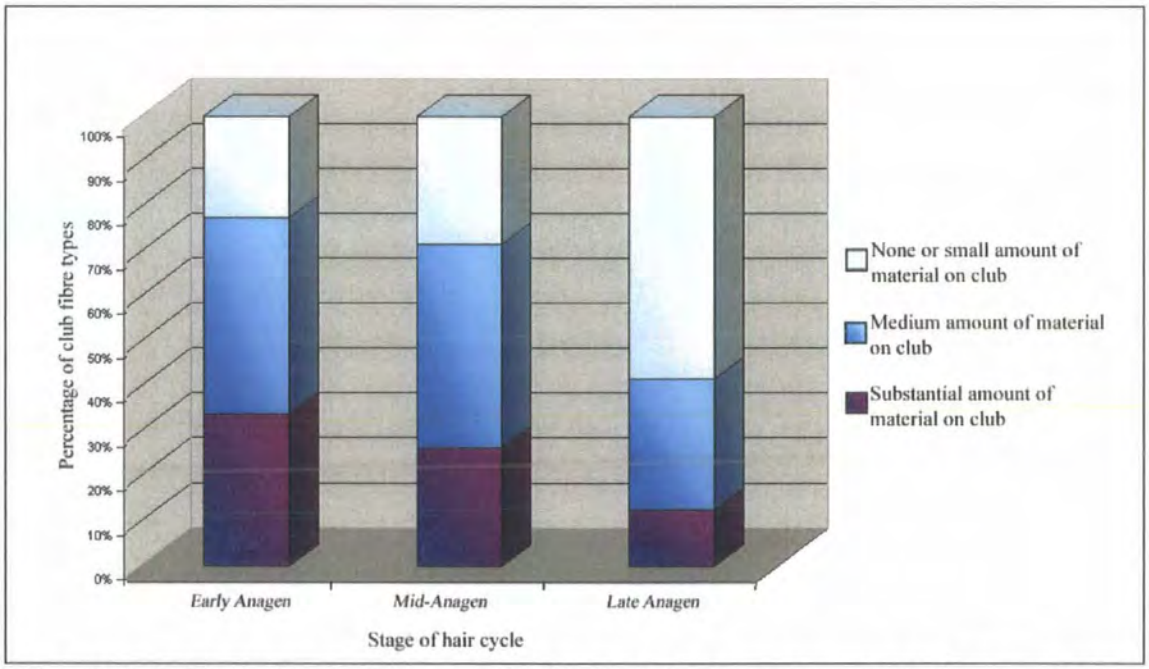

Graph 3. 2: Variation in the amount of material attached to plucked exogen club fibres from vibrissa follicles at different anagen cycle stages in old rats

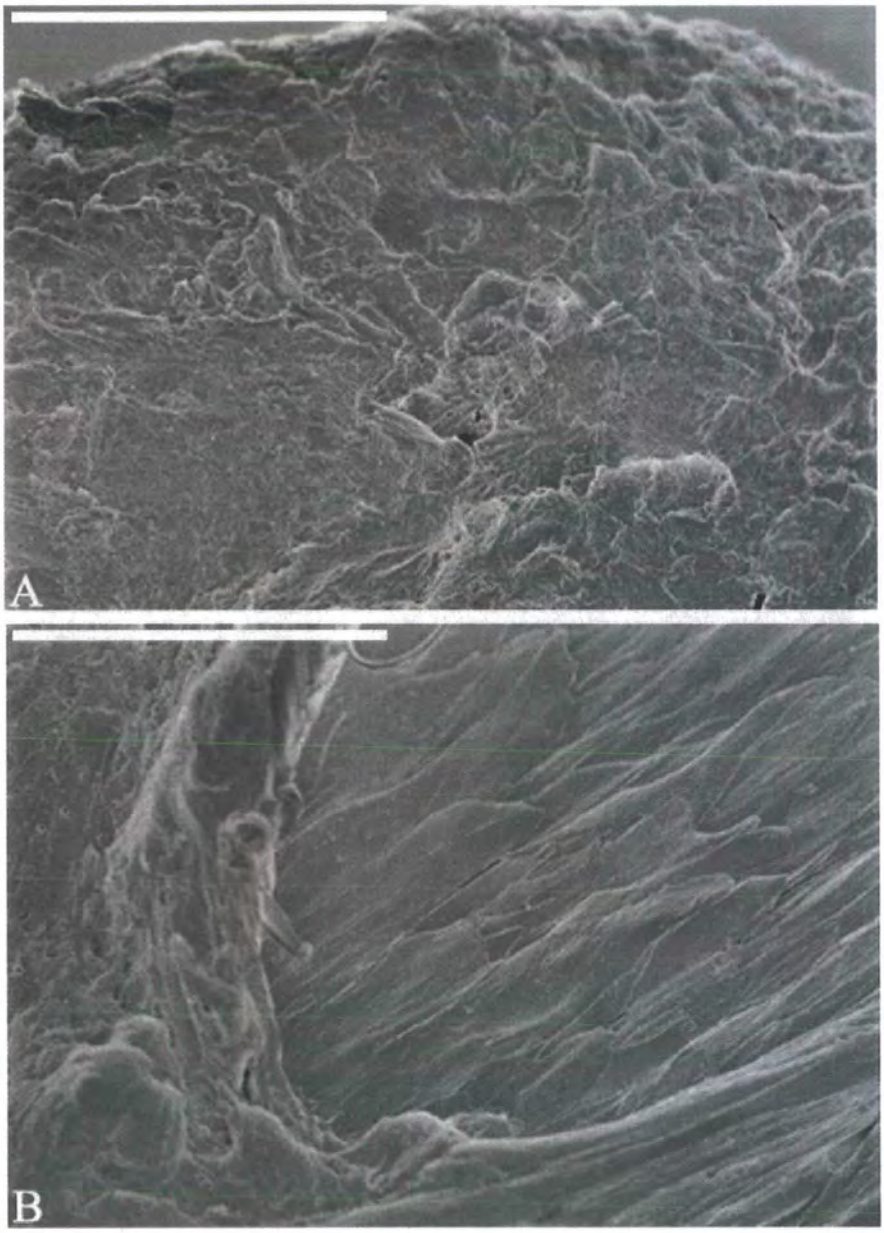

Figure 3. 11: Scanning Electron microscopy of plucked early exogen club fibres
Early exogen club fibres are covered in large amounts of cellular material after plucking causing the club fibre tip and edge to have a rounded appearance (A). In some areas, it appeared that these overlying cells had peeled back to reveal an underlying layer of hardened flattened cells (B).

Scale Bars: 50μm

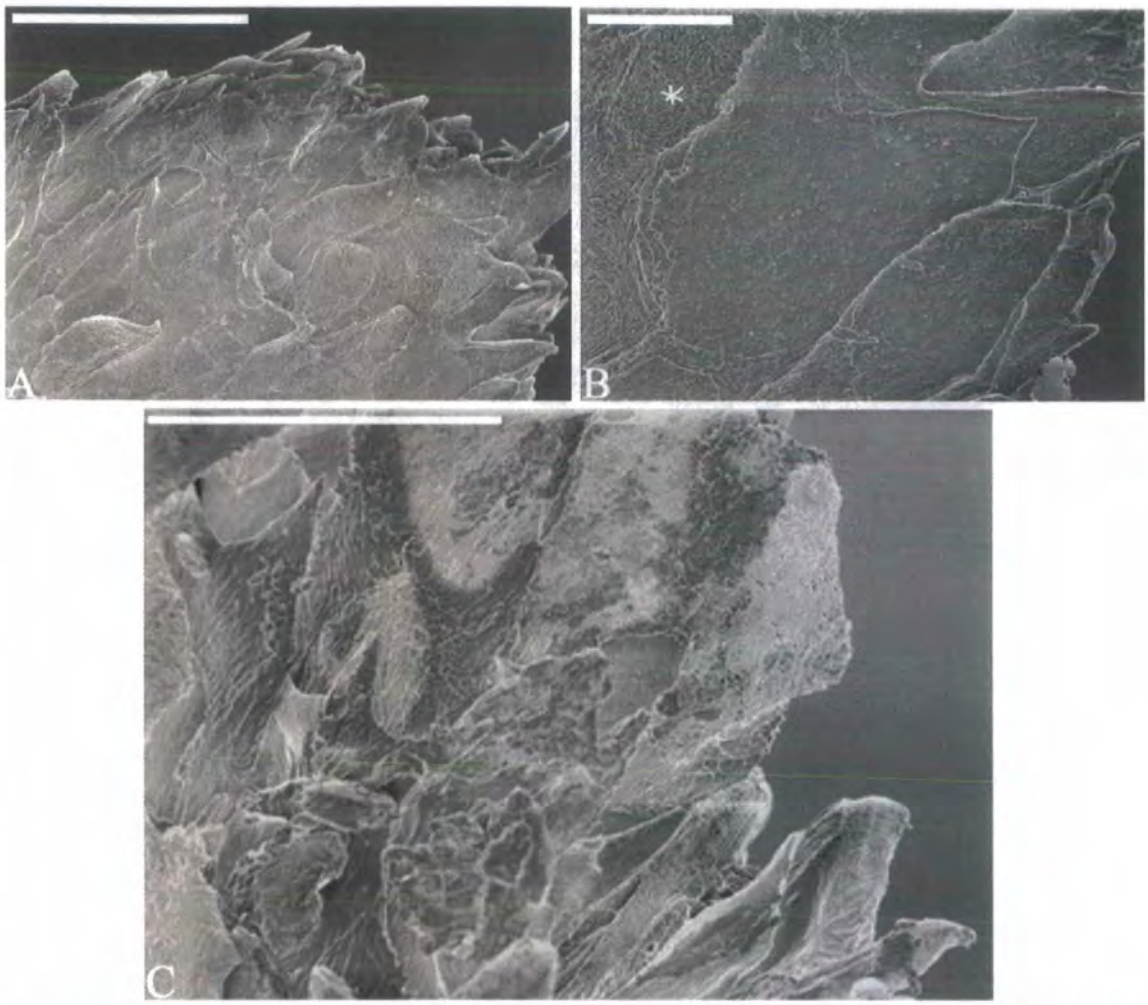

Figure 3. 12: Scanning Electron microscopy of plucked late exogen club fibres
Unlike early exogen club fibres, late exogen club fibres were not covered in cellular material but rather were composed of a number of irregularly shaped flattened cells. These cells were loosely overlaid (A), and on closer appearance appeared to have an abraded surface with a number of small raised ridges, similar to a fingerprint pattern (star) (B). At the tip of the fibre, large numbers of these hardened cells protruded out of the fibre at all angles, resulting in a jagged appearance (C).

Scale Bars: A: 50μm, B: 10μm, C: 20μm

3.4: Analysis and Discussion

3.4.1: Club fibre formation

The trichilemmal keratin layer of the club fibre is electron dense and distinctive due to its large number of anchoring protrusions that jut out at all angles from the fibre itself, holding the club fibre in place in its trichilemma sac. However, the origin of the trichilemmal keratin that surrounds the club fibre is unclear. Early work by Pinkus showed the trichilemmal keratin of the club fibre stained bluish white with Thioflavin T, a histology stain that normally stains keratinised IRS material yellow and hence Pinkus concluded that the electron dense layer surrounding the club fibre is derived from the ORS (Pinkus 1969; Pinkus et al. 1981), with this remaining the dogma ever since. However, SACPIC histology staining of club fibres dyes the trichilemmal keratin border red, in contrast to a yellow cortex (Nutbrown and Randall 1996). SACPIC stains keratinising IRS as red whilst it identifies ORS as blue, indicating that conclusions about the origin of the trichilemmal keratin cannot simply be based on histology staining patterns.

Pinkus indicated that the trichilemmal keratin of the club fibre is derived in the same manner as the trichilemmal keratin of the anagen growing follicle, hence the same name derived from 'trichilemma' meaning ORS. The trichilemmal keratin of the anagen follicle is detected in the isthmus region where the ORS directly abuts onto the hair shaft after sloughing of the IRS. It is formed when the ORS keratinises without forming an intermediate granular layer (Pinkus et al. 1981). However, this sometimes leads to confusion with many researchers extrapolating information about the trichilemmal keratin of the anagen follicle to the electron dense layer that surrounds the club fibre, even though there are unique differences between these two layers. One key example is with Thioflavin T staining, originally used by Pinkus to stain the club fibre trichilemmal keratin bluish white. This does not stain the trichilemmal keratin of the anagen follicle (Honda et al. 1997). Another example is seen with regards to their respective keratin expression pattern. Whereas the trichilemmal keratin of the growing follicle stains specifically for keratin 17, this is not observed in the electron dense layer surrounding the club fibre but instead higher

up the club fibre, above the region of trichilemmal keratinisation (Panteleyev et al. 1997). This suggests differences in either their formation or origin.

3.4.2: The companion layers of the follicle

Although the work by Pinkus has led to the dogma that the trichilemmal keratin of the club fibre is derived from the ORS, some authors do refer to the trichilemmal keratin of the club fibre as an IRS derived structure (Commo and Bernard 1997; Lavker et al. 1998). Moreover, although the main growth of Huxley's and Henle's layers of the IRS are terminated before club fibre formation, morphological studies by Orwin showed a thin double cell layer continuous with these two layers around the base of the club fibre during catagen, whilst the IRS further up the fibre was noticeably thicker (Orwin et al. 1967). This suggests that the IRS precursor cells convert to form the trichilemmal keratin that surrounds the base of the club fibre. Morphologically, one would suppose that if the trichilemmal keratin layer of the club fibre is derived from the IRS, then the cells one layer out would be derived from the companion layer of the anagen fibre. In support of this is the expression of companion layer markers such as K6, plasminogen activator inhibitor 2 (PAI-2), Calretinin, and S100 calcium binding protein A6 (S100A6) in the cell layer that surrounds the club fibre (Lavker et al. 1998; Winter et al. 1998; Ito and Kizawa 2001; Bernot et al. 2002; Poblet et al. 2005; Gu and Coulombe 2007). This leads to the compelling hypothesis that the innermost cell layer that surrounds the club fibre trichilemmal keratin is analogous to the companion layer, and hence the trichilemmal keratin would be IRS derived (Figure 3.13). Mapping of S100A6 through the hair cycle led Ito and Kizawa to propose that companion^{CL} and the companion layer are cycle derived manifestations of each other (Ito and Kizawa 2001). However, no comprehensive labelling studies have been carried out to determine if one is a cycle manifestation of the other of if they are distinct in terms of their origin.

In addition to the large number of desmosomes surrounding the club fibre in the vibrissa, desmoplakin staining indicates that a large number of desmosomes are present in the companion layer of the anagen follicle. This agrees with previous observations showing a large number of desmosomal contacts between Henle's layer and the companion layer, compared to relatively few desmosomal contacts seen

between companion layer and the surrounding ORS. This is believed to aid slippage of the IRS and companion layer up the follicle with the growing fibre (Clemmensen et al. 1991; Langbein et al. 2002; Alibardi 2004; Gu and Coulombe 2007). It is possible, that similar to the slippage plane between the companion layer and the ORS, the plane between the companion^{CL} and the ORS is a breakage plane, when hair is pulled out in a premature situation. The high numbers of desmosomes in the companion^{CL}, and its similarities with the companion layer of the anagen fibre supports this proposal.

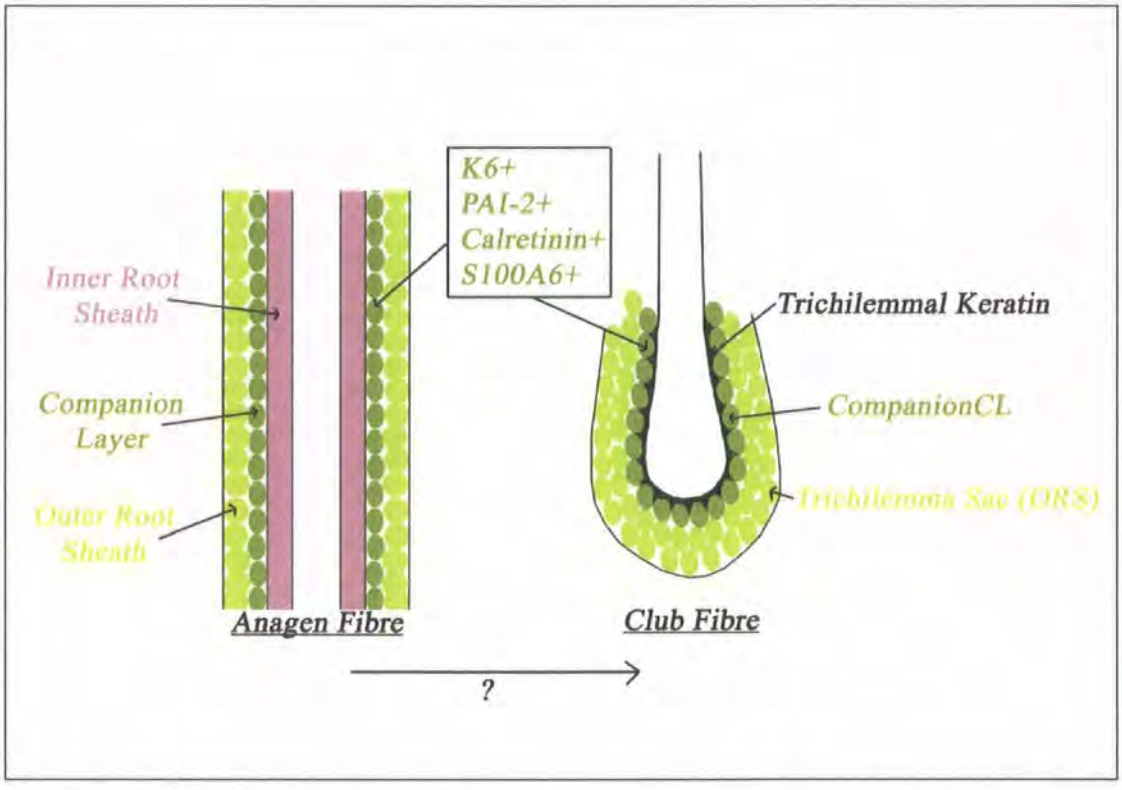

Figure 3. 13: Similarities between the companion layer of the anagen hair and the companion^{CL} of the club fibre

3.4.3: Mechanisms regulating club fibre retention and release

Previously published literature describing the loss of club fibre anchorage due to a targeted disruption of the Dsg3 gene highlights the importance of functional desmosomes in the retention of the club fibre (Koch et al. 1998). With regards to desmoplakin, the most intense expression within the follicle is observed in the companion^{CL} layer immediately surrounding the club fibre in addition to the

companion layer of the growing fibre. In the epidermis, desmoplakin expression is more prominent in the more differentiated suprabasal layers, predominantly the granular layer (Arnemann et al. 1993). However, desmoplakins are constitutive components of desmosomes, with the exception of desmoplakin II in cardiac muscle (Angst et al. 1990). Therefore, this increase is representative of an increase in the number of desmosomes in the more differentiated cell layers of the living epidermis (Klein-Szanto 1977) rather than a change in the differentiation state of the keratinocytes. In the hair follicle therefore, the intense expression of desmoplakin seen in the companion^{CL} is representative of an increase in the number of desmosomes in the companion^{CL} layer compared to the rest of the ORS. This reemphasises the prominence and importance of desmosomal contacts with regards to club fibre retention. This also allows an analogy to be drawn relating the companion^{CL} layer surrounding the club fibre with the granular layer of the epidermis, falling in place with Maurer's comparison of the trichilemmal keratin layer of the club with the stratum corneum of the epidermis (Maurer 1895).

Desmosomes act to provide both cellular rigidity and strength by linking intermediate filaments within cells to provide an integrated filament framework (Kouklis et al. 1994; Smith and Fuchs 1998). This is more evident when integral components of desmosomes such as desmoplakin are mutated, giving rise to intercellular separation, with a resultant pemphigus phenotype of the epidermis observed (Vasioukhin et al. 2001; Alcalai et al. 2003). The presence of high numbers of desmosomes surrounding the club fibre may act to reinforce cellular integrity as a mechanism of maintaining the club fibre. The high number of desmosomes in the companion^{CL} layer suggests that the club fibre is being deliberately retained in its position in the trichilemma sac, as opposed to passively waiting to fall. It is likely that as a result of grooming and other physical forces, the base of the club fibre is under large amounts of mechanical stress, and the desmosomes surrounding the club fibre may act to maintain integrity within the cells here, as a mechanism of retaining the club fibre until an appropriate time for release.

The expression profiles of Dsg1 and Dsg3 surrounding the vibrissae club fibre are similar to the human telogen follicle, where Dsg1 is absent from basal keratinocytes, present in suprabasal keratinocytes only, whilst Dsg3 is present in both the basal and

suprabasal layers (Wu et al. 2003). In vibrissae, Dsg1 expression is equal throughout all suprabasal ORS layers. With an increase in the number of desmosomes detected around the club fibres, it is intriguing as to why levels of Dsg1 or Dsg3 protein do not increase in this region. Within the epidermis, desmoglein expression varies with the differentiation state of keratinocytes. Whilst Dsg3 is associated with either proliferating basal keratinocytes or keratinocytes in the spinous layers, Dsg1 is associated with more differentiated keratinocytes in both the spinous and lower granular layers (Wu et al. 2003). In the vibrissa follicle, the lack of Dsg1 and Dsg3 in all of the desmosomes surrounding the club fibre may indicate that companion^{CL} keratinocytes are more differentiated than the rest of the suprabasal ORS, possibly relating to unique cellular adhesion properties in this layer, with implications for the retention or release of the club fibre.

The increase in desmoplakin expression surrounding the club fibre, correlating with an increase in the number of desmosomes in this region supports the observations made with the TEM. Here, a large number of desmosomes were perceived between the cells of the companion^{CL} layer. The numerous interdigitations between the innermost keratinocytes provide a large surface area for numerous desmosomal contacts, reinforcing the idea that desmosomes are important for club fibre retention. Desmoplakins are the major proteins of the desmosomal plaque complex and are necessary for linking tonofilaments to desmosomes (Kouklis et al. 1994; Smith and Fuchs 1998). The large number of tonofilments associated with desmosomes, seen in the companion^{CL} layer surrounding the club fibre implicates a role for these in both the adhesion of cells to each other and for their structural integrity. What is unusual and seen with both the desmoplakin staining and the TEM is the continued presence of large numbers of desmosomes between the cells of the companion^{CL} layer and bordering the trichilemmal keratin layer of the late exogen club fibres, which one would suppose were close to release. Plucked late exogen club fibres showed an absence of attached cellular material which would suggest a decrease in adhesion between the club fibre and the surrounding trichilemma sac with club fibre maturation.

Moreover, the ladder-like granules seen coating the trichilemmal keratin in early exogen club fibres as indicated by the TEM may act as a source of enzyme activity.

Pinkus observed similar granules in the ORS in the zone of sloughing of the anagen follicle of a dog, showing them to have acid phosphatase activity whilst hypothesising them to be a source of enzymes responsible for IRS degradation (Pinkus et al. 1981). Membrane coating granules are also detected in the epidermis and are a source of proteolytic enzymes required for the degradation of cellular components and junctions during differentiation and desquamation (Haywood 1979; Freinkel and Traczyk 1983). With regards to the club fibre, the release of proteases from the ladder like granules may act to break down the contacts between the trichilemmal keratin and the companion^{CL} layer, enabling teloptosis.

The increase of keratinising cells observed surrounding late exogen club fibres, along with the condensed chromatin and invaginated nuclear membranes observed in these samples indicates that the innermost cells surrounding the club fibre are undergoing a form of cell death. Whether this form of cell death is apoptosis or terminal differentiation is not determined, as both exhibit similar features such as condensed chromatin (Kokileva 1994). Terminal deoxynucleotidyl transferase-mediated dUTP-biotin nick end labelling (TUNEL) staining, which detects cells as they undergo cell death has previously been shown to be present in the companion^{CL} layer of human telogen club fibres (Tanaka et al. 1998). This supports the observations presented here in the vibrissa follicle. In addition to the telogen club, TUNEL staining has also been shown in the companion layer of the human anagen hair follicle, representative of these cells undergoing a specialised form of cell death mediated by keratinisation (Tanaka et al. 1998). Potentially, this is similar to what is occurring in the companion^{CL}. A terminal differentiation mode of cell death would be more plausible as it would create cells with cornified envelopes, able to provide a protective barrier from external influences after teloptosis, for the brief period when a small hole may remain in the skin.

3.4.4: The breakage plane for club fibre release

If proteases break down the contacts between the trichilemmal keratin and the companion^{CL}, it creates this as the breakage plane during club fibre release. The idea that this trichilemmal keratin/companion^{CL} is the breakage plane was supported by the SEM results which showed naked trichilemmal keratin in plucked late exogen

club fibres. If proteolytic enzymes were functional upon release from the membrane coating granules in their observed location then it would indicate that the most important desmosomal contacts for club retention are those directly connecting the trichilemmal keratin and the companion^{CL}. Although the high numbers of desmosomes between cells within the comapnion^{CL} may provide structural support and cellular integrity it is likely that the desmosomes that are most important in club fibre retention are those between the companion^{CL} and the trichilemmal keratin.

If a pelage club fibre is prematurely plucked from the follicle, it is removed with a single layer of cells surrounding it, those from the innermost cell layer of the trichilemma sac (Silver et al. 1969), which for these purposes has been termed companion^{CL}. Furthermore, in the case of the *Dsg3*-/- mouse, club fibres are prematurely lost with the breakage plane between the companion^{CL} and the surrounding keratinocytes (Koch et al. 1998). In the *Dsg3*-/- mouse, anagen fibres are not lost due to observed compensation from Dsg1. However, forced inactivation of *Dsg1* in this mouse results in the loss of the anagen fibre, with the break occurring between the companion layer and the surrounding ORS (Hanakawa et al. 2004). This leads to the proposal that the companion layer, ORS slippage plane is analogous to the boundary between the companion^{CL} cells, and those more distal to the club fibre. Moreover, this would explain why prematurely plucked fibres from pelage follicles have only one cell layer attached (Silver et al. 1969; Ito and Kizawa 2001). Whilst the breakage plane in normal hair loss is between the trichilemmal keratin and the surrounding companion^{CL} layer, the break plane (slippage plane) in premature hair loss is between the companion^{CL} and the surrounding ORS. This slippage/break plane is possibly a protective mechanism that protects from more ORS cells from being lost when hair is forcefully pulled out, or prematurely lost.

3.4.5: Club fibre release-information derived from plucked club fibres

Club fibres from *Dsg3*-/- mice are often observed shed still surrounded by an epithelial envelope (Koch et al. 1998), a feature suggestive that the club fibres have been prematurely shed whilst 'normally' shed club fibres are believed to fall naked

(Kligman 1961). This corresponds with the analysis of the plucked vibrissa club fibres which showed club fibres regarded to be in a mature state, in late exogen were removed without cellular material attached. In contrast, club fibres from early anagen follicles, regarded as early exogen club fibres were removed with cellular material still attached. This highlights the vibrissa follicle as an excellent model in which to study the controls of exogen as club fibres at varying stages of formation and release can be specifically selected for analysis. This also indicates that the nomenclature used to describe the different club fibre types is relevant as they exhibit different retention properties. Moreover, this reinforces the previous suggestion which proposed the break plane for spontaneous shedding to be between the trichilemmal keratin and surrounding cells, whilst the break plane for premature loss was proposed to be between the companion^{CL} layer and the surrounding ORS. The different club fibre morphologies observed after plucking, and reiterated with the SEM, suggests that club fibres are deliberately retained in early exogen, rather than being passively shed in late exogen. If club fibres were being passively shed, then one would expect no differences in the retention properties of the club fibre.

The gradual transition of a decrease in cellular material attached to the club fibre with club fibre maturation suggests that a gradual loosening mechanism from the surrounding epithelial sac is involved in the release of the club fibre, rather than a rapid switch mechanism triggered by a specific signal immediately prior to teloptosis. This has similarities to the mechanism of desquamation, in which a transition of keratinocytes from the basal layer of the epidermis through to the stratum corneum is associated with gradual differentiation changes, the commitment for which occurs in the basal layer of the epidermis (Blanpain et al. 2006). The club fibre may be similar to this, with the duration of retention pre-programmed from the onset of club fibre formation. However, this would not explain the loss of club fibres observed with seasonal moulting, which can be prematurely induced or delayed by manipulating artificial photoperiods (Rougeot et al. 1984), suggesting this programming can be modulated.

It appeared that the tight regulation between the hair cycle and teloptosis apparent in the younger rats was lost with age which further supports the proposal that exogen and teloptosis are events controlled independently from cycle stage. It appears that in

the older rats, either the duration of anagen is decreasing or teloptosis is being delayed, resulting in a loss of coordination that is usually seen between cycle stage and teloptosis in the vibrissa follicle. Perhaps related is the observation that in older rats, the levels of the lysosomal protease Ctsl, a hair cycle regulator, decreases in expression within the vibrissa follicle (Yang et al. 2005). *Ctsl-/-* mice have a perturbed hair cycle, resulting from a premature exit from anagen in addition to premature club fibre loss due to defective anchorage of the trichilemmal keratin to the surrounding ORS (Roth et al. 2000). The decrease in Ctsl along with other changes detected in the aged vibrissae may act to shorten the anagen phase, so that the timing of club fibre release appears delayed. This would be a similar effect to that seen with aging in humans, in which a shortened anagen phase is observed with age related hair loss conditions such as androgenetic alopecia (Courtois et al. 1995; Guarrera and Rebora 2005).

3.4.6: Other observations in the vibrissa follicle

Apart from the observations directly related to the club fibre, some other observations were made when analysing vibrissa follicles with II-5F immunofluorescence. In the suprabasal ORS surrounding the growing fibre of the anagen vibrissa, below the level of the bulge, few desmosomes were present as indicated by low or absent desmoplakin expression. This is suggestive of cell rearrangement or cell migration occurring in this area. This observation relates to work in the mouse vibrissae presented by Barrandon's group who proposed that migration of cells from the bulge region of the follicle down the ORS to the germinative matrix at the base of the follicle occurs continuously throughout anagen, in order to replenish to dividing keratinocytes in the matrix of the bulb region (Oshima et al. 2001). The reduction of desmosomes in this region would aid cell migration within in this area, as compared to the higher numbers seen in the upper follicle, which would act to maintain adhesion and structural integrity between and within cells.

3.5: Summary

In conclusion, TEM and immunofluorescence was utilised to perform analysis of club fibres *in situ*. Whilst the large numbers of desmosomes surrounding the club fibre highlighted their importance in retaining the club fibre within its epithelial sac, the detection of membrane coating granules surrounding the club fibre gave an insight into potential mechanisms of club fibre release. The varying amounts of retained material on plucked club fibres, as shown by SEM and visual analysis gave insight into retention strengths of club fibres in different maturation states. They also allude to a gradual release process of the club fibre, as oppose to an immediate release. Moreover, these visible differences between club fibres verify the vibrissa follicle as a model that would be beneficial in the examination of exogen, as club fibres at specific stages in this process can be selected for analysis. Although this work gives some insight into possible mechanisms of retention and release, we can only speculate upon the families of genes associated with roles in these processes.

Chapter 4: Identification of Novel molecules involved in club fibre retention and release

4.1: Introduction

4.1.1: Synchronised shedding

Hair loss involving the synchronised loss of club fibres from the follicle is termed 'telogen effluvium' (Kligman 1961), the majority of which results from the synchronisation of the follicle transition from anagen to telogen, as noted by a decreased anagen to telogen ratio in patients with telogen effluvium (Whiting 1996a). This can be caused by a variety of factors with an event or trigger such as psychoemotional stress (Arck et al. 2003); childbirth, itself a stressful activity (Lynfield 1960) or a physically traumatic occurrence such as surgery (Kligman 1961; Desai and Roaf 1984). These phenomena cause anagen to terminate which is followed approximately 3 months later by a synchronised exogen, perceived as excess shedding. Premature termination of anagen, seen with drug treatments such as retinoid therapy (Gollnick et al. 1990) also affects club fibre retention. In such cases the club fibre lacks its usual anchoring protrusions, an explanation for which may be that the follicle has undergone a dystrophic catagen stage, due to its premature initiation (Berth-Jones et al. 1990). In contrast, drugs such as minoxidil cause club fibre shedding associated with immediate telogen release and initiation of the anagen phase (Bardelli and Rebora 1989), similar to events observed in animals with a seasonal moult.

In animals with a moult, the majority of follicles are in telogen, and the simultaneous shedding and re-entry into anagen enables animals to grow a new coat. A decrease in day length initiates a change to heavy pelage, whilst an increase in day length will lead to the initiation of sleek coat growth, preceded by the shedding of the old coat. This photoperiodic control of pelage cycles, described in a majority of mammals (Bissonnette 1935; Rougeot et al. 1984; Ryder and Stephenson 1986), is believed to be controlled by the anterior pituitary gland, the location of adrenocorticotropic hormone (ACTH) synthesis. In animals with a moult, high levels of ACTH have also been reported to encourage club fibre loss (al-Khateeb and Johnson 1971) whilst low levels are believed to cause a retention of the club fibre (Johnson 1972). Other groups have commented on ACTH stimulating anagen (Paus et al. 1994) or inducing telogen in mice (Maurer et al. 1997) dependent on the levels of ACTH. Moreover,

human follicles in organ culture demonstrate a typical hypothalamic-pituitary-adrenal (HPA) axis feedback loop when stimulated with corticotropin releasing hormone (CRH) (Ito et al. 2005).

Hormones have long been known to exert control over aspects of the hair cycle, an obvious example of which is seen in the vellus to terminal transition of follicles during puberty (Barth 1987). However, with regards to seasonal shedding, a second pituitary hormone, prolactin, has received much interest. Plasma levels of prolactin are altered with the autumn and spring moults, as demonstrated by variations in plasma levels in response to changing artificial photoperiods in sheep and mink. An increased photoperiod that increases plasma prolactin levels, or endogenously applied prolactin, will induce a moult and a subsequent regrowth similar to a summer coat in mink, sheep and mares (Martinet et al. 1984; Rougeot et al. 1984; Pearson et al. 1996; Thompson et al. 1997; Pearson et al. 1999; Santiago-Moreno et al. 2004). In contrast, a reduced photoperiod that decreases plasma prolactin levels prematurely induces moulting with hair regrowth resembling a winter coat (Martinet et al. 1984; Rose et al. 1985; Martinet et al. 1992; Lincoln and Clarke 1994). These data suggest that a balance is required for correct control. Prolactin modulates transitional phases of the cycle by inducing both catagen and re-entry into anagen. The transition from telogen to anagen also corresponds with fibre shedding and so the effects or prolactin on exogen are not clear cut. Photoperiodic effects are believed to be mediated through melatonin, an encoder of day length that increases with decreasing daylight hours. Melatonin, secreted by the pineal gland, is believed to act on the pituitary gland regulating prolactin levels, as evidenced by the effects of administered melatonin on both plasma prolactin levels and its ability to alter moulting and regrowth cycles in sheep, mink, deer and racoons (Allain and Rougeot 1980; Rose et al. 1984; 1985; Rose et al. 1987; Heydon et al. 1995; Xiao et al. 1995; Rose et al. 1998; Santiago-Moreno et al. 2004). Moreover, drugs such as Bromocriptine that inhibit prolactin secretion and can alter moulting cycles (Duncan and Goldman 1984; Martinet et al. 1984; Rose et al. 1987) are relevant to humans. For example Bromocriptine is used to treat hyperprolactinemia, a condition caused by excess prolactin production, although it can often cause hair shedding as a side effect (Blum and Leiba 1980; Fabre et al. 1993). Hyperprolactinemia is itself a disorder than causes both hirsute and alopecic effects (Schmidt et al. 1989; Schmidt 1994). Perhaps of relevance is that

prolactin and its receptor have recently been detected during the growth cycle of human scalp follicles (Foitzik et al. 2006). In human scalp, a moult is evident during the autumn months (Randall and Ebling 1991), a significant feature as follicles are in anagen durations of several years, and so a number of follicles must synchronously enter telogen for a moult to be noticeable. Interestingly, the relevance of prolactin synthesis in hair follicles that lack a seasonal influence, has also been recognised as the expression of both prolactin and its receptor has been demonstrated during the hair cycle in laboratory mice (Foitzik et al. 2003).

In mouse pelage follicles, both prolactin and the prolactin receptor are hair cycle dependant and have been localised during telogen to the innermost layer of cells surrounding the club fibre (Foitzik et al. 2003). However, although the effect of knocking out the prolactin receptor is to advance onset of the moult in mice, regrowth is also accelerated (Craven et al. 2001). Of interest, perhaps, is that in an induced growth cycle modulated by an increase in prolactin, stratifin mRNA levels decrease during telogen. This maybe relevant because mice with a mutation in stratifin exhibit premature club fibre loss as discussed in Chapter 1.4 (Herron et al. 2005; Li et al. 2005).

Often, when investigating the effects of hormones on hair shedding it is difficult to separate the effects on hair cycle transition with those on exogen itself. However, the seasonal moult is a well anticipated event in most animals and knowing the factors that control this may give an insight into the regulation of exogen. The mere observation that club fibre shedding can be synchronised leads to the proposal that shedding is controlled through signals mediating release, rather than lost passively. However, little is known about the types of signals that may mediate exogen.

4.1.2: Microarray Technology

Gene expression arrays are fast becoming a popular tool to use in biology. They are able to provide a broad overview of the cell, by comparing the expression of thousands of genes at different time points. The biology research community has adopted microarray technology as a powerful way to analyse regulatory pathways and biological processes. For example, developmental changes or tumour progression can

be analysed comparing microarray data at various time points, whilst drug targets can also be monitored over time. Many microarray experiments have confirmed known expression patterns, although this technology, when successful, can also be used to identify new candidate genes in biological processes.

Within the hair follicle, microarray technology has previously been used to identify differences between cell types, thus identifying unique molecular markers of the different hair follicle compartments (Rendl et al. 2005). Much interest has been focsed on the bulge of the follicle, identifying unique markers of this stem cell compartment (Ohyama et al. 2006) whilst other researchers have analysed changes over time through the progression of the hair cycle (Lin et al. 2004). However, as yet this technology has not yet been used to analyse the process of exogen. Microarray technology holds promise for the identification of candidate genes involved in not only club fibre formation and retention, but also signals involved in club fibre release.

4.1.3: Aims

Within this chapter the aim was to identify and validate novel changes associated with club fibre formation, retention and release. The mouse models of exogen in context with relevant literature led to the proposal that exogen was associated with structural, adhesive and proteolytic changes at a cellular level. However, there is no evidence of any initiating signal for exogen. Thus, microarray technology was utilised to detect novel gene changes associated with exogen progression, with the genes in 'structure', 'cell adhesion and ECM', 'proteolysis' and 'signalling' categories selected for further analysis.

4.2: Methods

4.2.1: Animals and tissue isolation

Follicles were dissected from the mystacial pad of 5 month old male PVG rats as described in Chapter 2.2.5.1. They were then classified according to their cycle stage as described previously and grouped by stage in separate dishes of MEM. Follicles were then either frozen in Oct compound for immunohistochemical analysis or microdissected for use in RNA extraction as described in section 4.2.2.

Early exogen club fibres were plucked from male PVG rats using No.4 forceps. Fibres were plucked in the direction of hair growth. Club tips were then cut off using a No.15 scalpel, and placed immediately into 500µl denaturation solution (Ambion) for RNA extraction. 16 fibres from one rat made up one sample, whilst 11 fibres from a second rat made up a second sample.

Back skin was shaved, cut with scissors and then peeled off before being embedded in Oct compound and frozen for tissue analysis. Both backskin and follicles were stored at -80°C until further use.

4.2.2: Follicle Microdissection

Early and late anagen follicles were selected for microdissection. Follicles were cut transversely at the nerve entry point and at the centre of the ringwulst using an RNA free No.15 scalpel blade (Swann Morton) to create three sections (Figure 4.1). The middle pieces were transferred to drops of PBS containing 0.1% DEPC (Sigma) (see Appendix) on the lid of a bacteriological dish (VWR). Each capsule was held steady with a pair of No.5 watchmaker's forceps, and the sharp tip of a needle (26 ½ G x 1 inch, Becton Dickinson) was used to cut open the collagen capsule. The inner sheath was cut from the collagen capsule using the needle, and transferred to denaturation solution (Totally RNA Kit-Ambion). Samples were mixed by shaking, and by drawing the solution up and down a pipette. These microdissected samples were classified as 'early exogen' and 'late exogen', according to the maturation state of their respective club fibres. Nine rats were used to collect material for microarray

analysis with three replicate samples generated for each experiment, each with material from three rats. Each replicate was termed E1, E2 and E3 for early exogen samples whilst late exogen sample replicates were termed L1, L2 and L3. A further nine rats were used to collect material for PCR analysis, again with three replicate samples being created, each containing follicle material from three rats. These replicates were termed EE1-3 and LE1-3 respectively. All replicate samples were placed in microcentrifuge tubes containing 500µl of denaturation solution.

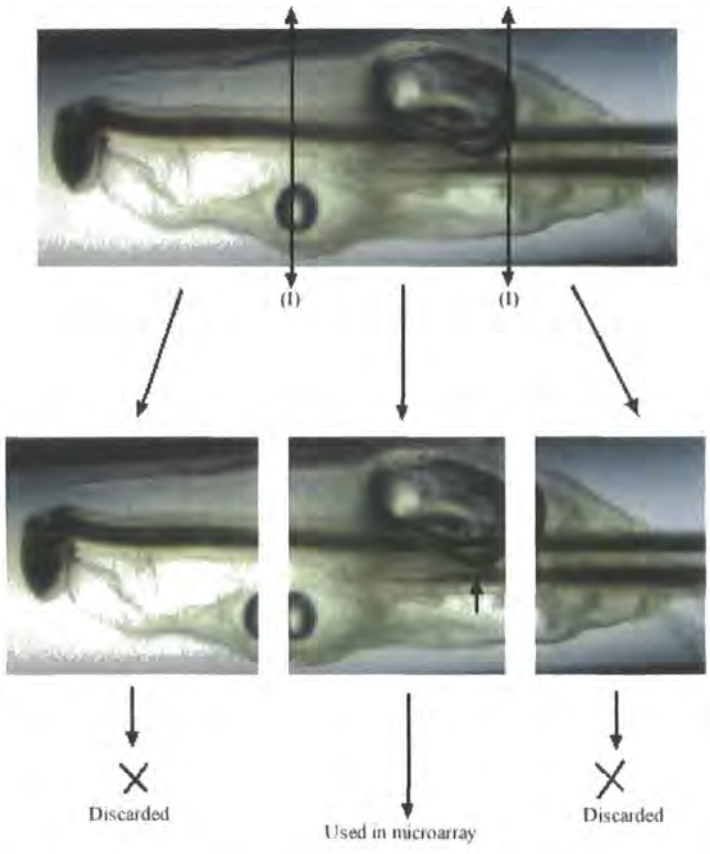

Figure 4. 1: Transverse sectioning of the vibrissa follicle

A vibrissa follicle was cut (I) transversely at the nerve entry point and ringwulst, creating three sections. The centre section, containing the club fibre (arrow) was used further for the microarray analysis. However, the end sections were discarded.

4.2.3: Molecular biology techniques

4.2.3.1: RNA Extraction

All techniques were carried out under RNase free conditions using aerosol resistant filtered pipette tips. All solutions were treated with 0.1% diethylpyrocarbonate (DEPC), an RNase inhibitor, autoclaved, and stored in glass bottles, which had been baked at 140°C for 2 hours. The work space was wiped clean with RNase Zap (Ambion).

RNA was extracted using the ToTALLY RNA™ Kit from Ambion. This is a ready to use kit that adapts the guanidine thiocyanate, acid phenol:chloroform RNA extraction procedure described by Chomczynski and Sacchi (1987).

500µl Phenol Chloroform:Isoamyl alcohol (25:24:1) was added to microcentrifuge tubes containing microdissected follicle samples or early exogen plucked club fibres in 500µl denaturation solution. Microcentrifuge tubes were inverted for 30 seconds, vortexed for 30 seconds then placed on ice for 5 minutes. After this time, they were centrifuged for 10 minutes at 4°C at 11000g. On removal from the centrifuge the phenol chloroform mixture had separated into an aqueous top phase, overlying protein and organic layers. The aqueous phase was transferred to a new microcentrifuge tube using a pipette. Sodium acetate was added at a volume, $1/10^{th}$ of the volume of the aqueous phase. Microcentifuge tubes were then inverted to mix for 10 seconds before addition of 500µl Acid-Phenol:Chloroform (125:24:1). Microcentrifuge tubes were inverted for 30 seconds, vortexed for 30 seconds then placed on ice for 5 minutes. After this time, they were centrifuged for 10 minutes at 4°C at 11000g. After removal from the centrifuge the top aqueous phase was removed and transferred to a fresh microcentrifuge tube. An equal volume of isopropanol was added and samples were inverted to mix before placing at -20°C overnight.

On removal from the -20°C freezer, samples were centrifuged for 15 minutes at 11000g at 4°C. After centrifugation small pellets were visible at the base of the microcentrifuge tubes. The supernatant was removed, leaving the pellet behind. This

was then washed using 300µl 70% EtOH. Microcentrifuge tubes were then centrifuged again for 10 minutes at 3000g at 4°C. Excess EtOH was pipetted off and the sample pellets allowed to air dry at room temperature for 5 minutes. After drying, the pellets were resuspended in 100µl DEPC/EDTA and stored at -80°C until the DNA cleanup stage.

4.2.3.2: DNA cleanup of RNA

Contaminating DNA was removed from RNA samples using the DNA-*free*™ kit from Ambion. To the 100µl volume of RNA in a 1.5ml microcentrifuge tube, 10µl of 10X DNase buffer and 1µl DNase1 were added, and gently mixed by pipetting. Samples were then incubated for thirty-five minutes on a 37°C heating block. After removal from the heat block, 10µl DNase inactivation reagent was added to each sample. Samples were left at room temperature for two minutes, with periodic mixing. After mixing, samples were centrifuged for 2 minutes at 10000g to pellet the DNase inactivation reagent. The supernatant containing RNA free from DNA contamination was then removed and transferred to fresh microcentrifuge tubes.

4.2.3.3: Quantification and assessment of RNA

4.2.3.3.1: Quantification of RNA

The quantity of RNA was determined on a Cecil GeneQuest 2301. 1µl RNA was diluted in 100µl DEPC water and placed in a glass cuvette for readings. Absorbance readings were taken at 260nm and 280nm. Using the Beer-Lambert law, the 260nm reading was used to calculate the amount of RNA. The 260nm/280nm ratio was used to asses RNA purity.

4.2.3.3.2: Assessment of RNA quality

To ensure the quality of extracted RNA, 2ul samples were electrophoresed on a 2.0% gel, containing Ethidium bromide (0.1µg/ml) in 1x Tris Acetate-EDTA (TAE) (See Appendix 1). Before electrophoresis, 2µl of a loading buffer (Appendix 1) was added to each sample tube.

4.2.3.4: Gene Microarray preparation and analysis

A detailed description of the reactions required to prepare biotin labelled cRNA from RNA, for hybridisation onto the Rat230.20 GeneChip is outlined in Figure 4.2. Isolated RNA was only used if its quality appeared good after running it on an electrophoresis gel. Microdissected follicle samples E1, E2, E3, L1, L2 and L3 were prepared as described in Figure 4.2 and in sections 4.2.3.4.2 through to 4.2.3.4.7. However, the RNA extracted from plucked exogen fibres was first amplified as described in section 4.2.3.4.1. Amplified cDNA was then cleaned up, amplified and biotin labelled, fragmented and hybridised using the same procedures as used for non-amplified RNA, as described in sections 4.2.3.4.4 through to 4.2.3.4.7.

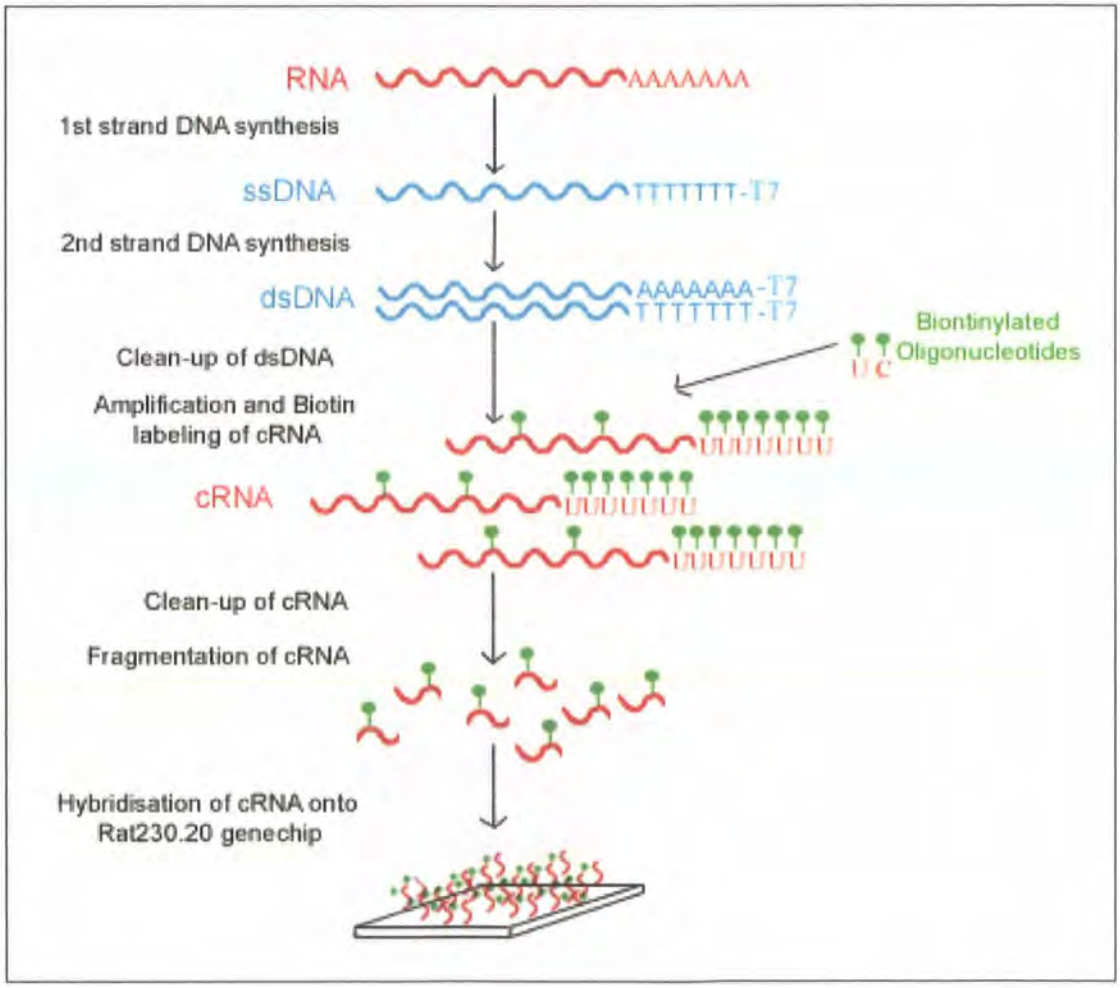

Figure 4. 2: Outline of procedures required for conversion of extracted RNA to cRNA for hybridisation of the the Rat230.20 genechip

4.2.3.4.1: Amplification of RNA extracted from plucked exogen fibres

First and Second Strand Synthesis-First Cycle Amplification

RNA was amplified using the MessageAmp aRNA amplification kit from Ambion. All components were provided. Briefly, 9µl of isolated RNA was placed in a 0.5ml microcentrifuge tube with 1µl T7 Oligo primer and 2µl nuclease free water before incubation for 10 minutes at 70°C on a thermal cycler (Biometra TPersonal). Whilst on the thermal cycler, a master mix cocktail comprising of 2µl 10X 1st Strand Buffer, 1µl Ribonuclease inhibitor, 4µl 5mM dNTP mix and 1µl Reverse Transcriptase per reaction was made. After incubation on the thermal cycler, RNA samples were removed and chilled on ice for 2 minutes. 8µl of master mix cocktail was added to each sample, and pipetted gently to mix. Samples were then placed on a thermal cycler for 2 hours at 42°C during which time first strand cDNA synthesis occurred. Prior to the conclusion of 2 hours on the thermal cycler, a master mix cocktail containing 63µl nuclease free water, 10µl 10X 2nd Strand Buffer, 4µl 5mM dNTP mix, 2µl DNA Polymerase and 1µl RNase H per reaction was made. After 2 hours on the thermal cycler, cDNA samples were removed and 80µl of the master mix added to each sample. Samples were mixed by gentle pipetting and centrifuged briefly. They were then incubated for 2 hours at 16°C. During this time, second strand cDNA synthesis occurred. Double stranded cDNA was removed from the thermal cycler and immediately taken to the cDNA clean up step below.

After second strand cDNA synthesis, cDNA was cleaned following the protocol for cDNA purification in the MessageAmp aRNA amplification kit from Ambion. Briefly, 250µl binding buffer, which precipitated the cDNA, was added to each cDNA sample. The cDNA then transferred to a spin column was then passed through a cDNA filter cartridge by centrifugation at 13000rpm for 1 minute. Flow through was discarded and the cDNA washed by centrifugation with 500µl wash buffer. The cDNA was then eluted using 20µl nuclease free water.

In vitro transcription and clean up of antisense RNA

Whilst the purified cDNA was on ice, a master mix cocktail for in vitro transcription was made. This comprised of 4µl 75mM T7 ATP solution, 4µl 75mM T7 CTP solution, 4µl 75mM T7 GTP solution, 4µl 75mM T7 UTP solution, 4µl T7 10x reaction buffer and 4µl T7 enzyme mix per reaction. All reagents were provided in the MessageAmp aRNA amplification kit. In a 0.5ml microcentrifuge tube, 24µl master mix was added to each sample of eluted cDNA. 14µl mineral oil (Sigma) was placed on top of each reaction to prevent evaporation up the microcentrifuge tube as samples were then left for 14 hours at 37°C on a thermal cycler (Biometra TPersonal). The final product after 14 hours was amplified antisense RNA. Samples were removed from the thermal cycler after 14 hours and contaminating DNA removed from the reaction. After removal of the mineral oil, 2µl DNase 1 was added to each sample. Samples were the placed at 37°C for 30 minutes. After this time, the antisense RNA was cleaned using the aRNA purification module in the MessageAmp aRNA amplification kit. Briefly, 350µl antisense RNA binding buffer was added to each sample, and mixed thoroughly by gentle vortexing. 250µl Ethanol was then added to each sample to precipitate the RNA, and mixed by gentle vortexing. The RNA sample was then passed through a filter cartridge by centrifugation at 13,000 rpm for 1 minute, during which time the antisense RNA bound to the filter. Samples were washed by passing 650µl wash buffer through each filter by centrifugation for 1 minute at 13000rpm. The antisense RNA was then eluted in 100µl preheated elution solution.

First and Second Strand Synthesis-Second Cycle Amplification

The antisense RNA eluted above was used for first strand cDNA synthesis. Together in a 1.5ml microcentrifuge tube 10µl antisense RNA was added together with 2µl Second Round Random Primers, and heated at 70°C for 10 minutes on a heat block. During this 10 minutes, a master mix was made up comprising of 4µl 5x 1st strand buffer, 2µl 0.1M DTT and 1µl 10mM dNTP per reaction. After 10 minutes at 70°C, the antisense RNA was removed from the heat block and chilled briefly on ice. 7µl master mix was added to each sample and incubated for 2 minutes at 42°C. After 2

minutes, 1µl Superscript II was added to each sample, and samples were left for 1 hour at 42°C.

After 1 hour at 42°C, cDNA samples were removed from the heat and 2µl RNase H was added to each sample to remove and remaining RNA. Samples were incubated on a heat block for 30 minutes at 37°C, followed by 5 minutes at 95°C to denature the RNase. Single stranded cDNA samples were then chilled on ice.

To synthesise the second stranded cDNA, 4µl 50µM T7 primer was added to the single stranded cDNA. The reaction was the incubated for 10 minutes at 70°C, during which time a master mix cocktail was made up. The master mix contained 87µl nuclease free water, 30µl 5x 2nd strand buffer, 3µl 10mM dNTP mix and 4µl DNA Polymerase per reaction. After incubation at 70°C, reactions were briefly chilled on ice. 124µl master mix was added to each reaction, which was then incubated at 16°C for 2 hours. After 2 hours, 2µl of T4 DNA polymerase was added to each reaction which was then placed at 16°C for 5 minutes. 10µl 0.5M EDTA was then added to each sample, which was stored at -80°C until required. After this step, second stranded cDNA was cleaned, biotin labelled, fragmented and hybridised as described in sections 4.2.3.4.4 through to 4.2.3.4.7.

4.2.3.4.2: First Strand cDNA Synthesis (without amplification step)

5µg of total isolated RNA was diluted in DEPC treated distilled water to a volume of 10µl before the addition of 2µl T7 Oligo (dT) primer (Affymetrix). RNA was then incubated at 70°C for 10 minutes in a thermal cycler (Biometra TPersonal) to disrupt the secondary structure and hybridise the T7 Oligo (dT) primer. During this time a master mix cocktail was made up comprising of 4µl 5x 1st Strand cDNA buffer (Invitrogen), 2µl 0.1M DTT (Invitrogen) and 1µl 10mM dNTP mix (Invitrogen) per reaction. After removal from the thermal cycler, RNA samples were placed immediately on ice. After cooling, 7µl of cocktail mix was added to each RNA sample, the sample was mixed by gentle pipetting before being incubated for 2 minutes at 42°C on a thermal cycler. After 2 minutes at 42°C 1µl of Superscript II RT (Invitrogen) was added to each RNA sample. Samples were then incubated at

42°C for 1 hour. After 1 hour, the resulting single stranded cDNA samples were removed from the thermal cycler and placed on ice, after which the second strand synthesis step was performed without delay.

4.2.3.4.3: Second Strand Synthesis (without amplification step)

Whilst single stranded cDNA samples were on ice, a cocktail master mix containing 91µl DEPC treated distilled water, 30µl 5x 2nd strand reaction buffer (Invitrogen), 3µl 10mM dNTP mix (Invitrogen), 1µl 10U/µl *E.coli* DNA Ligase (Invitrogen), 4µl 10U/µl *E.coli* DNA Polymerase I (Invitrogen), 1µl 2U/µl *E.coli* RNase H (Invitrogen) per reaction was prepared. 130µl of this cocktail was added to each single stranded cDNA sample before incubation in a thermal cycler (Biometra TPersonal) at 16°C for 2 hours. After 2 hours 2µl T4 DNA Polymerase (Invitrogen) was added to each reaction. Samples were left at 16°C for a further 5 minutes before removal from the thermal cycler. 10µl 0.5M EDTA (Sigma) was added to each double stranded cDNA sample prior to storage at -80°C

4.2.3.4.4: Clean-up of double stranded cDNA

The double stranded cDNA was cleaned using the Gene Chip Sample Cleanup Module (Affymetrix). This module consisted of clean-up spin columns, and wash buffers. The protocol provided by the manufacturer was adhered to throughout. Briefly, cDNA was precipitated with a provided binding buffer, transferred to a spin column membrane through which wash buffer was passed by centrifugation. The cDNA was then resuspended in 14µl of elution buffer, and spun through the spin column membrane by centrifugation.

4.2.3.4.5: Amplification and Biotin Labelling of cRNA

Biotin labelled cRNA was transcribed from the double stranded cDNA using the ENZO *BioArray High Yield* RNA Transcript Labelling kit (Affymetrix).

A cocktail master mix was prepared whilst double stranded cDNA samples thawed after removal from the freezer. This contained 4µl 10x HY Reaction buffer, 4µl 10x

Biotin labelled ribonucleotides, 4μl 10x DTT, μl 10x RNase Inhibitor, and 2μl 20x T7 RNA Polymerase in 14μl RNA free water (all reagents provided in kit) per reaction. 32μl of cocktail mix was added to 8μl double stranded cDNA template in a 0.5ml microcentrifuge tube. Samples were placed on a thermal cycler (Peltier thermal cycler-200, MJ research) for 5 hours at 37°C, with periodic mixing every 45 minutes.

4.2.3.4.6: Clean-up of Biotin labelled cRNA

After 5 hours on the thermal cycler the Biotin labelled cRNA was removed and cleaned using the Gene Chip Sample Cleanup Module. The manufacturers' protocol was followed throughout. Briefly, cRNA was precipitated in cRNA binding buffer and ethanol then placed in a spin column. The column was then washed with cRNA wash buffer, centrifuged, then the cRNA resuspended in 20μl RNase free water, and collected by centrifugation of the column. The cRNA was then quantified using a spectrometer.

4.2.3.4.7: Fragmentation and Hybridisation of Biotin labelled cRNA

To each microcentrifuge tube containing cRNA, 8μl fragmentation buffer was added. This was supplied with the Gene Chip Sample Cleanup Module. Volumes were then made up to 40μl with RNase free water. Samples were then transferred to a thermal cycler (Peltier thermal cycler-200, MJ research) for 3 minutes at 94°C. The fragmented cRNA was then transferred to clean RNA free 1.5ml microcentrifuge tubes for hybridisation onto the genechip. Vladan Miljkovic of the GeneChip array core facility at Columbia University carried out the hybridisation and scanning of the genechip arrays. He hybridised the 6 different samples onto the Rat 230-2.0 genechip (Affymetrix). The Rat 230-2.0 genechip has 11 pairs of oligonucleotide probes to measure the level of transcription of each sequence on the chip.

4.2.3.4.8: Computational Analysis

Data output from the microarray analysis was analysed using two commercially available software packages; GeneSpring GX 7.0 (Agilent Technologies Inc., Palo

Alto, CA, USA) and GeneTraffic™ (Lobion Informatics, La Jolla, CA, USA). Data was normalised against the housekeeping genes, then the median intensity of early exogen samples was set as the baseline, against which late exogen samples were compared. Parametric tests, with the p-cutoff value set to 0.05 were utilised to determine significant differential expression. Probes were then selected if their expression was two fold higher or lower than the baseline to generate lists of differentially expressed gene transcripts between early and late exogen. Hisham Bazzi helped with the computational analysis.

4.3.2.5: Reverse transcriptase polymerase chain reaction

4.3.2.5.1: Reverse Transcription

Reverse transcription was carried out on RNA samples EE1,2,3 and LE1,2,3 after the DNA clean-up step. Initially, 1µl of Oligo(dT)$_{12-18}$ (Invitrogen) and 1µl 10mM dNTP mix (Invitrogen) was added to 1µg of total isolated RNA, which was made with DEPC treated distilled water to a volume of 13µl in an RNA-free 1.5ml microcentrifuge tube. This mix was incubated on a heating block at 65°C for 5 min to disrupt the secondary structure of the RNA. During this time a master mix was prepared containing 4µl 5X first strand buffer (250mM Tris-HCL pH8.3, 375mM KCL, 15 $MgCl_2$), and 2µl 0.1M DDT per reaction. After the initial incubation, RNA was briefly chilled on ice before adding 6µl of the master mix. The tube contents were then incubated at 42°C for 2 minutes to optimise the temperature for the reaction. 1µl of SuperScript™ II Reverse Transcriptase (Invitrogen) was then added to the RNA, and mixed by pipetting. RNA was incubated for 50 minutes at 42°C. Immediately after this first incubation step the sample was incubated at 70°C for 15 minutes to heat inactivate the Reverse Transcriptase enzyme. Resultant cDNA samples were stored at -20°C until required as a template for amplification in PCR.

4.3.2.5.2: Polymerase Chain Reaction

Specific primers for the cDNA sequences of the genes of interest were designed covering an intron-exon boundary, to ensure that no contaminating genomic DNA would affect the results. cDNA sequences were obtained from the NCBI. Since

Oligo$(dT)_{12-18}$ was used in the reverse transcription step rather than random primers, this creates a 3' bias of cDNA. Therefore, primers were designed within 2000 base pairs of the poly-A tail to eliminate this bias.

For each PCR reaction, a master mix cocktail incorporating the primers of interest was made. This buffer, which was prepared on ice comprised of 0.2mM dNTPs (Invitrogen), 1-2mM $MgCl_2$, 0.5μM of both the forward and reverse primers (Sigma), and 1unit Taq polymerase (Invitrogen) in a final volume of 50μl per reaction, made up with sterilised distilled water. 1μg of cDNA was added per reaction, which was mixed gently by pipetting. cDNA controls (no reverse transcription step) were tested with glyceraldehyde 3-phosphate dehydrogenase (GAPDH) primers to ensure that there was no contamination. PCR reactions were then incubated on a Biometra (T Personal) thermal cycler and the following heating cycle programmed.

Step 1: 94°C for 5 minutes

Step 2: 94°C for 30 seconds
Step 3: Annealing temperature for 30 seconds (see Table 4.1)
Step 4: 72°C-10 seconds for every 100 bases of product

Steps 2-4 were repeated 25-35 times

Step 5: 72°C for 5 minutes (final extension)
Step 6: Cool on ice

Whilst the 94°C heat step separates the double stranded DNA, the annealing temperature allows primers to anneal to the separated strands. Optimised annealing temperatures for primer sets are shown in Table 4.1. The intermediate temperature (72°C) allows the Taq polymerase to efficiently elongate the DNA template.

Table 4. 1: RT-PCR Primer details

Primer pairs	Primer Sequence	Annealing temp (°C)	[$MgCl_2$]	**Product Size (base pairs)**
Neuropilin-2 Forward *Neuropilin-2 Reverse*	AGA GTA CCT GGA TCA GCA GTG C TTG CTT TCC TGT CTG GCT TCC C	**58**	1.5mM	**226**
Spondin-1 Forward *Spondin-1 Reverse*	AAT GTC CTA GGA TGC TGG ACG G CCC TGG CCT TCC TTT GGA CTA T	**59**	1.5mM	**404**
Tissue Inhibitor of metalloprotease 3 Forward *Tissue Inhibitor of Metalloprotease 3 Reverse*	CCT TCT GCA ACT CCG ACA TC AGC ATG TCG GTC CAG AGA CA	**56**	1.5mM	**406**
Caveolin-2 Forward *Caveolin-2 Reverse*	GGC TCA TGT AGA GAA ACT TAC AGG ATC TGG TCT GCA ATG GAA TCC C	**56**	1.5mM	**392**
S100 calcium binding protein a4 Forward *S100 calcium binding protein a4 Reverse*	CTT CCA CAA ATA CTC AGG CAA CG TGA AGA AGC CAG AGT AAG GCA C	**56**	1.5mM	**344**
Interleukin-18 Forward *Interleukin-18 Reverse*	CTT GGA ATC AGA CCA CTT TGG C ATT TTG TTG TGT CCT GGC ACA CG	**56**	1.5mM	**350**
S100 calcium binding protein a8 Forward *S100 calcium binding protein a* Reverse*	TGG CAA CTG AAC TGG AGA AGG GTG GCT GTC TTT ATG AGC TGC	**56**	1.5mM	**260**
Tumour Necrosis Factor Super Family Receptor-11b Forward *Tumour Necrosis Factor Super Family Receptor-11b Reverse*	ATC AGG TGC ACG AGC CTT ATC C ACA CTG AAC CAG GCA TGA CAG C	**58**	1.5mM	**363**

Table 4. 1 continued: RT-PCR Primer details

Primer pairs	Primer Sequence	Annealing temp (°C)	[$MgCl_2$]	**Product size (base pairs)**
S100 calcium binding protein 9 Forward *S100 calcium binding protein 9 Reverse*	TCC TGA CAC CCT GAA CAA GG GCA GAT GTT ACA TGG CGA CC	**56**	1.5mM	**282**
Aquaporin 5 Forward *Aquaporin 5 Reverse*	ATG AAC CCA GCC CGA TCT TTC G CT GAT TCC AAA GCG GCT ATG TCC	**58**	1.5mM	**472**
Complement Factor I Forward *Complement Factor I Reverse*	GCA GGT GGC GAT TAA GGA TGG GGC AGG GAC AGA ATT GAT GAG C	**58**	1.5mM	**295**
Proprotein Convertase Kexin/Subtilisn 5 Forward *Proprotein Convertase Kexin/Subtilisn 5 Reverse*	GAG AAC TGT AAG ACG TGC ACT GG GAC TCT TCC GTT GCA TCC TTG C	**59**	1.5mM	**416**
Gap Junction Beta 6 Forward *Gap Junction Beta 6 Reverse*	ATC AAA CGG CAG AAG GTG CGC TGA CCG CTA TCC GAG ATC AGC	**56**	3.0mM	**398**
Kidney Androgen regulator Protein Forward *Kidney Androgen regulator Protein Reverse*	GTG ATC ACT GTC TTC TGT GTG C ATC CAG AAT GGT AGT CAC AGG C	**58**	1.5mM	**380**
Fetuin Beta Forward *Fetuin beta Reverse*	TCT CAG GAC AGC TGT TCA CTC C CAG GTA GAG GAA GGA GAC ATC C	**59**	1.5mM	**384**
Glyceraldehyde 3-phosphate dehydrogenase Forward *Glyceraldehyde 3-phosphate dehydrogenase Reverse*	ATG GCC TAC ATG GCC TCC AAG G AGG CCC CTC CTG TTG TTA TGG G	**58**	1.5mM	**175**

4.3.2.5.3: Detection and analysis of Polymerase chain reaction product

To ensure that each amplified product was of the desired length and that no cross contamination had occurred, 20μl of PCR product was electrophoresed on a 2.0% Agarose gel, containing Ethidium bromide (0.1μg/ml) in 1x TAE buffer (0.8mM Tris, 0.02mM EDTA, pH 7.6). Prior to electrophoresis 4μl of a loading buffer (0.25% bromophenol blue, 40% glycerol) was added to PCR products to visualise the band progression during electrophoresis. A 1kb DNA ladder (Invitrogen) was used to estimate band size. Gel images were recorded on a BioRad Gel Doc System.

4.2.4: Sectioning of follicles and immunofluorescent analysis.

Proteases and their inhibitors were identified a prominent group during the microarray analysis. Previously, serine protease inhibitors have been linked with the club fibre (Lavker et al. 1998; Jensen et al. 2000). However, matrix metalloproteases (MMP's) and their inhibitors have not yet been identified as important during either club fibre formation or retention. For this reason, Tissue Inhibitor of Metalloprotease 3 (TIMP3) was selected for further protein analysis within the hair follicle.

Cellular adhesion is believed to be important during club fibre retention. However, there were very few molecules related to cellular adhesion that were identified with microarray analysis. Therefore, Connexin 30 (Cx30) was selected for further analysis as it was in this limited group. Connexin 43 (Cx43) was also selected although was not identified with the microarray analysis. However, Cx43 is in the same family as Cx30 and has previously been detected in the hair follicle (Iguchi et al. 2003).

Finally Id3 was selected as the fourth protein for further analysis. This was identified by the microarray analysis and has previously been traced through the vibrissa hair cycle (O'Shaughnessy et al. 2004). It therefore seemed relevant to see if Id3 may have a role in club fibre formation or retention in addition to its other roles in the hair follicle.

4.2.4.1: Follicle sectioning

Follicles and back skin which had previously been embedded in Oct compound were brought from the -80°C freezer to the cryostat and allowed to equilibrate to -20°C. Both follicles and backskin were orientated longitudionally and sectioned on a Leica3050S cryostat. 7μm sections were cut with a steel knife, and melted onto poly-lysine coated slides. Slides were allowed to dry at room temperature for 1 hour before further processing.

4.2.4.2: Immuofluorescence labelling

An indirect labelling approach was adopted for all fluorescent analysis in this section of the thesis. Effectively, a primary antibody against the antigen of interest was incubated with sections. A second antibody, conjugated with a flurophore was then introduced that was specific for the first antibody.

After drying onto glass slides, sections being stained with the antibody for the detection of TIMP3 were fixed in Acetone at -20°C for 10 minutes. Slides were then air dried before continuation. None of the other antibodies used in this section required prior fixation and therefore a fixative step was not performed.
After air drying, sections were washed 3 times in PBS, with each wash lasting 3 minutes, to remove excess Oct compound surrounding the tissue sections. Non-specific antibody binding was blocked by incubating the sections in a humidified chamber for 30 minutes with either 2% BSA in PBS, or 5% normal serum raised in the same species of host as the secondary antibody to be used (Sigma). Whilst the block solution was being incubated, primary antibodies against the antigens of interest were prepared at optimised dilutions in PBS (Table 4.2). Slides were tapped to remove the blocking solution, and then 20μl of primary antibody was added to each section. Sections were then covered in small strips of Parafilm and incubated in a humidified chamber for between 12 and 18 hours at 4°C.

Following this incubation, unattached primary antibody was removed with 3 PBS washes, each lasting 3 minutes. Slides were blotted dry with paper tissues (Kimwipes, Kimtech) with care being taken to wipe around sections, leaving them

covered in PBS. Appropriate secondary antibodies (specific for the host in which the primary antibody was raised) were diluted to the optimised dilution in PBS (Table 4.2), and 20μl of diluted antibody applied to each section. Secondary antibodies were covered with Parafilm and left for 1 hour at room temperature in the dark in a humidified chamber. After antibody labelling, unattached secondary antibody was removed with 3 washes in PBS, each lasting 3 minutes. Slides were blotted (around sections) using a paper tissue and coverslips mounted using an anti-photobleaching mounting medium, containing either or the nuclear stains; DAPI or PI (Vector Laboratories). Coverslips were sealed using nail varnish and kept in the fridge until visualisation. They were examined and photographed with either a Biorad microradiance confocal or a Leica Axio Imager

To evaluate non-specific binding, primary antibodies were either substituted with PBS, or with an appropriately diluted isotype control.

Table 4. 2: Primary and Secondary antibody details

Antibody Name	Supplier	Dilution	Host
Anti-TIMP-3	Novacastra	1/50	Mouse
Anti-Connexin 43	Sigma	1/400	Mouse
Anti-Connexin 30	Zymed	1/200	Rabbit
Anti-Id3	Santa Cruz	1/100	Rabbit
Anti-mouse Alexafluor 488	Molecular Probes	1/500	Goat
Anti-rabbit Alexafluor 488	Molecular Probes	1/500	Goat

Table 4. 3: Number of repeats carried out with different primary antibodies on early and late exogen club fibres in early and late anagen vibrissa follicles

Primary Antibody	Early exogen	Late exogen
Anti-TIMP-3	6	6
Anti-Connexin 43	10	9
Anti-Connexin 30	6	5
Anti-Id3	6	5

4.3: Results

4.3.1: Identification of Differentially expressed Genes with gene microarray analysis

Data output from the microarray analysis was analysed using two commercially available software packages; GeneSpring GX 7.0 (Agilent Technologies Inc., Palo Alto, CA, USA) and GeneTraffic™ (Lobion Informatics, La Jolla, CA, USA). Analysis was performed on three replicate sets of early exogen and late exogen samples. After normalisation of the data against housekeeping genes the median intensity of early exogen samples was set as the baseline, against which late exogen samples were compared. Parametric tests, with the p-cutoff value set to 0.05 were utilised to determine significant differential expression. Probes were then selected if their expression was two fold higher or lower than the baseline as demonstrated in Figure 4.3. The GeneSpring software identified One hundred and thirty-eight probes that were differentially expressed between biological samples which can be seen in Appendix 2i (Table 4.4). One hundred and four of these were individual genes, with nine genes repeated. Twenty-five of these are still unknown sequences. K-means clustering performed on the GeneSpring generated list showed correlation between sample replicates as shown in Figure 4.4.

The GeneTraffic software generated a list of two hundred and thirty-two probes, that were differentially expressed between biological samples, which can be see in Appendix 2ii (Table 4.4). Of these, one hundred and seventy-nine were individual genes with twenty-one genes repeated. Thirty-four of these are still unknown sequences. Initially, the two genes lists were analysed and assessed independently to one another. Next, the lists were compared and genes expressed in both gene lists compiled to generate a third and more comprehensive list (see Appendix 2iii). Both software packages gave comparable results with ninety-five probes, representative of 75 genes, expressed on both gene lists (Figure 4.5), with only eleven genes being repeated.

In addition to the microarray analysis of differentially expressed genes, a gene list of transcripts expressed in the tissue surrounding plucked early exogen club fibres was

generated. This list comprised of several thousand genes. Therefore, in order to extract useful data from this list, it was compared with the differentially expressed gene list. Of the seventy-five genes expressed on both the GeneSpring and GeneTraffic gene lists, fifty-nine of these were expressed in the tissue surrounding plucked early exogen club fibres.

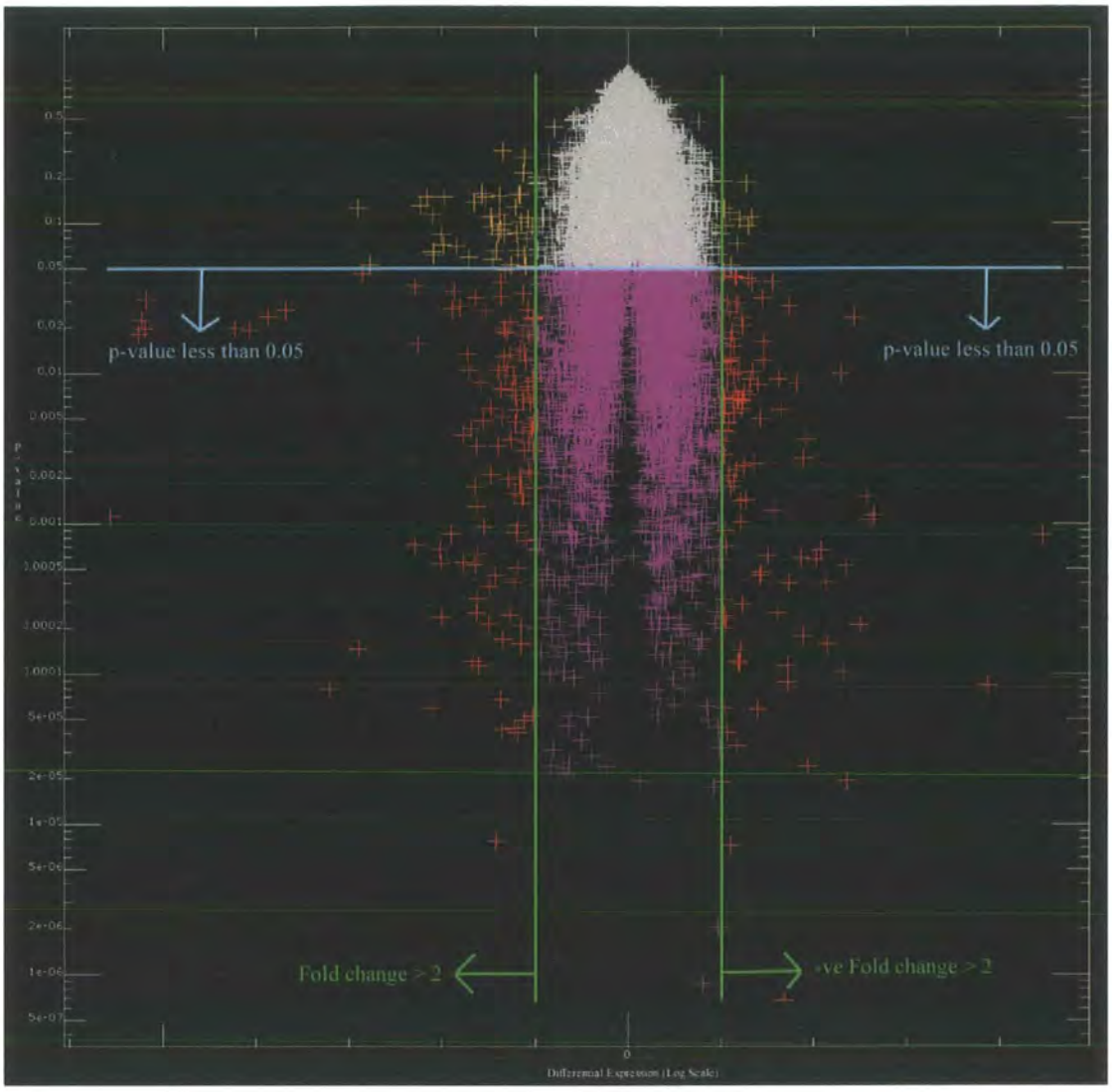

Figure 4. 3: Differential expression versus p-value of gene transcripts

The log values of fold changes are seen on the x-axis. The purple and white crosses within the green lines represent probesets that changed less than 2-fold in expression between early and late exogen populations. The orange crosses represent probe sets that were differentially expressed, but their change was not considered significant. The blue line is the cut-off p-value. A p-value of less than 0.05 is considered significant in a parametric test. Therefore, red crosses represent probesets that are change more than 2-fold in expression between early and late exogen, and are of significance, at a level not likely to have occurred by chance.

Figure 4. 4: K-means clustering of GeneSpring data.

The K-means clustering demonstrates that gene transcripts show similar intensities across sample replicates within early exogen and late exogen populations. The first 3 columns represent gene expression within early exogen samples, which are regarded as the baseline for gene expression. Genes in late exogen samples are either upregulated in comparison to early exogen or down regulated in comparison to their early exogen counterparts. The scale bar represents the level of gene expression ranging from zero to 5-fold of the gene expression at the baseline, which is regarded as 1. Downregulation of a gene is indicated by a change from yellow to blue whilst upregulation is indicated by a change to red. The change in colour of a gene is representative of a fold change, as indicated on the expression scale bar.

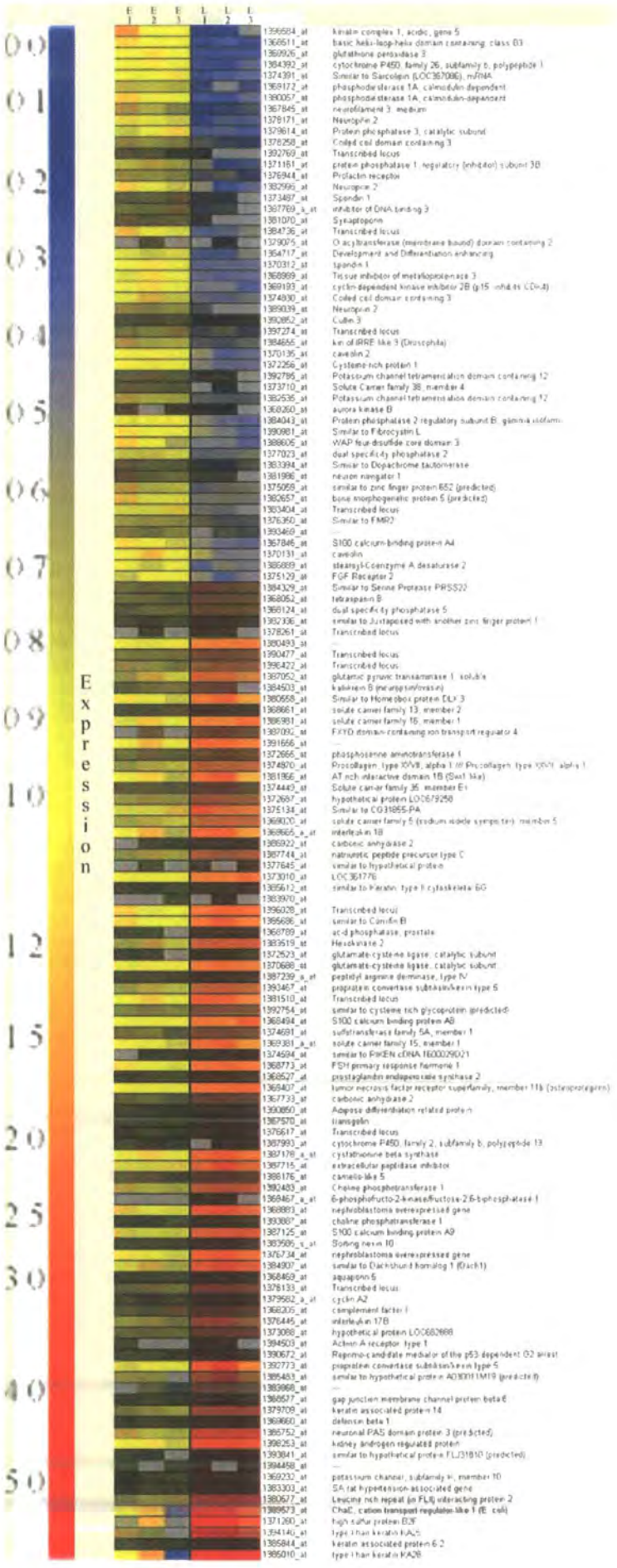
E 1
E 2
E 3
L 1
L 2
L 3
Expression
1366584_at keratin complex 1, acidic, gene 5
1368511_at basic helix-loop-helix domain containing, class B3
1368926_at glutathione peroxidase 3
1384392_at cytochrome P450, family 26, subfamily b, polypeptide 1
1374391_at Similar to Sarcolipin (LOC367086), mRNA
1369172_at phosphodiesterase 1A, calmodulin-dependent
1380057_at phosphodiesterase 1A, calmodulin-dependent
1367845_at neurofilament 3, medium
1378171_at Neuropilin 2
1379614_at Protein phosphatase 3, catalytic subunit
1378258_at Coiled coil domain containing 3
1392769_at Transcribed locus
1371161_at protein phosphatase 1, regulatory (inhibitor) subunit 3B
1376944_at Prolactin receptor
1382999_at Neuropilin 2
1373487_at Spondin 1
1367769_a_at inhibitor of DNA binding 3
1381070_at Synaptoporin
1384736_at Transcribed locus
1379075_at O-acyltransferase (membrane bound) domain containing 2
1364717_at Development and Differentiation enhancing
1370312_at spondin 1
1368969_at Tissue inhibitor of metalloproteinase 3
1369193_at cyclin-dependent kinase inhibitor 2B (p15, inhibits CDK4)
1374930_at Coiled coil domain containing 3
1389039_at Neuropilin 2
1392852_at Cullin 3
1397274_at Transcribed locus
1384665_at kin of IRRE like 3 (Drosophila)
1370135_at caveolin 2
1372256_at Cysteine-rich protein 1
1392795_at Potassium channel tetramerisation domain containing 12
1373710_at Solute Carrier family 38, member 4
1382535_at Potassium channel tetramerisation domain containing 12
1368260_at aurora kinase B
1384043_at Protein phosphatase 2 regulatory subunit B, gamma isoform
1390981_at Similar to Fibrocystin L
1388605_at WAP four-disulfide core domain 3
1377023_at dual specificity phosphatase 2
1383394_at Similar to Dopachrome tautomerase
1381986_at neuron navigator 1
1375055_at similar to zinc finger protein 652 (predicted)
1382657_at bone morphogenetic protein 5 (predicted)
1383404_at Transcribed locus
1376350_at Similar to FMR2
1393469_at ---
1367846_at S100 calcium-binding protein A4
1370131_at caveolin
1385889_at stearoyl-Coenzyme A desaturase 2
1375129_at FGF Receptor 2
1384329_at Similar to Serine Protease PRSS23
1368052_at tetraspanin 8
1368124_at dual specificity phosphatase 5
1382706_at similar to Juxtaposed with another zinc finger protein 1
1378261_at Transcribed locus
1380493_at ---
1390477_at Transcribed locus
1396422_at Transcribed locus
1387052_at glutamic-pyruvic transaminase 1, soluble
1384503_at kallikrein 8 (neuropsin/ovasin)
1380558_at Similar to Homeobox protein DLX-3
1368661_at solute carrier family 13, member 2
1386981_at solute carrier family 16, member 1
1387092_at FXYD domain-containing ion transport regulator 4
1391666_at ---
1372665_at phosphoserine aminotransferase 1
1374870_at Procollagen, type XXVII, alpha 1 /// Procollagen, type XXVII, alpha 1
1381966_at AT rich interactive domain 1B (Swi1 like)
1374443_at Solute carrier family 35, member E1
1372697_at hypothetical protein LOC679258
1375134_at Similar to CG31855-PA
1369020_at solute carrier family 5 (sodium iodide symporter), member 5
1368665_a_at interleukin 18
1386922_at carbonic anhydrase 2
1387744_at natriuretic peptide precursor type C
1377645_at similar to hypothetical protein
1373010_at LOC361776
1385612_at similar to Paralin, type II cytoskeletal 60
1383970_at ---
1396028_at Transcribed locus
1366686_at similar to Camillin B1
1368789_at acid phosphatase, prostate
1383519_at Hexokinase 2
1372523_at glutamate-cysteine ligase, catalytic subunit
1370688_at glutamate-cysteine ligase, catalytic subunit
1387239_a_at peptidyl arginine deiminase, type IV
1393467_at proprotein convertase subtilisin/kexin type 5
1381510_at Transcribed locus
1392754_at similar to cysteine rich glycoprotein (predicted)
1368494_at S100 calcium binding protein A8
1374681_at sulfotransferase family 5A, member 1
1369381_a_at solute carrier family 15, member 1
1374594_at similar to FinEN cDNA fl60002f021
1368773_at FSH primary response hormone 1
1368527_at prostaglandin endoperoxide synthase 2
1369437_at tumor necrosis factor receptor superfamily, member 11b (osteoprotegerin)
1367733_at carbonic anhydrase 2
1390850_at Adipose differentiation related protein
1367570_at transgelin
1376617_at Transcribed locus
1387993_at cytochrome P450, family 2, subfamily b, polypeptide 13
1387178_a_at cystathionine beta synthase
1387715_at extracellular peptidase inhibitor
1368176_at camello-like 5
1392483_at Choline phosphotransferase 1
1369467_a_at 6-phosphofructo-2-kinase/fructose-2,6-biphosphatase 1
1368883_at nephroblastoma overexpressed gene
1393887_at choline phosphotransferase 1
1387125_at S100 calcium binding protein A9
1383585_s_at Sorting nexin 10
1376734_at nephroblastoma overexpressed gene
1384907_at similar to Dachshund homolog 1 (Dach1)
1368469_at aquaporin 5
1378133_at Transcribed locus
1379582_a_at cyclin A2
1368205_at complement factor I
1376445_at interleukin 17B
1373088_at hypothetical protein LOC682688
1394503_at Activin A receptor, type 1
1390672_at Regnase-1 and-like mediator of the p53-dependent G2-arrest
1392773_at proprotein convertase subtilisin/kexin type 5
1385483_at similar to hypothetical protein A030011M19 (predicted)
1383968_at ---
1368527_at gap junction membrane channel protein beta 6
1379709_at keratin associated protein 14
1369660_at defensin beta 1
1386752_at neuronal PAS domain protein 3 (predicted)
1398253_at kidney androgen regulated protein
1393841_at similar to hypothetical protein FLJ31810 (predicted)
1394458_at ---
1369232_at potassium channel, subfamily K, member 10
1383303_at SA rat hypertension-associated gene
1380577_at Leucine rich repeat (in FLII) interacting protein 2
1389573_at ChaC, cation transport regulator-like 1 (E. coli)
1371260_at high sulfur protein B3F
1394140_at type I hair keratin KA25
1385844_at keratin associated protein 6-2
1385010_at type I hair keratin KA26

Total probesets on microarray: 31,000

		Early Exogen	Late Exogen	Total
GeneSpring Software	Probesets	50	88	138
	Known Genes	39	65	104
	Repeats	6	3	9
	Unknown	5	20	25

		Early Exogen	Late Exogen	Total
GeneTraffic Software	Probesets	110	123	232
	Known Genes	81	97	179
	Repeats	11	10	21
	Unknown	18	16	34

		Early Exogen	Late Exogen	Total
GeneSpring GeneTraffic Overlap	Probesets	35	60	95
	Known Genes	27	48	75
	Repeats	6	5	11
	Unknown	2	7	9

Table 4. 4: Differentially expressed genes between early and late exogen populations, as identified by different software analysis

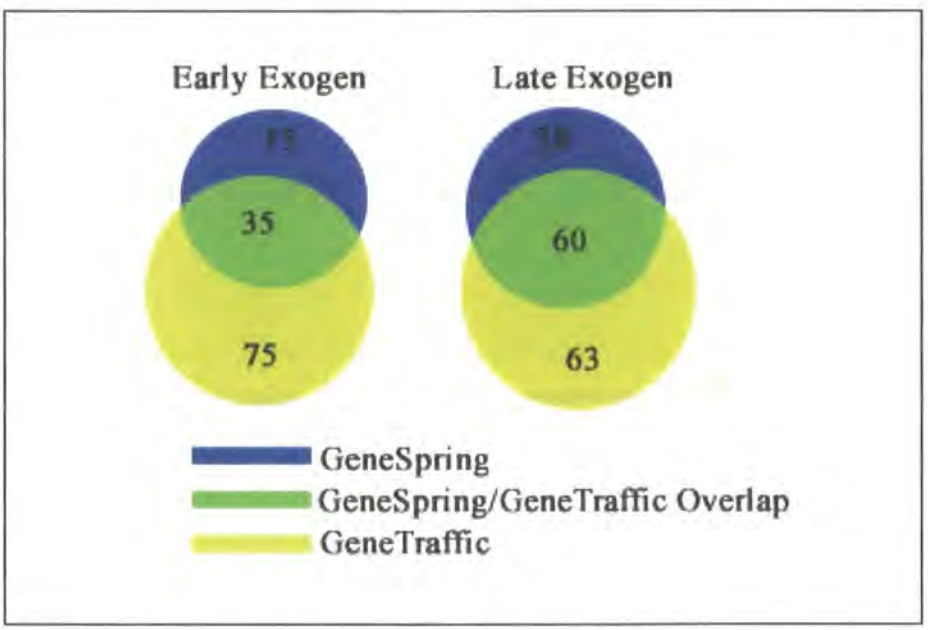

Figure 4. 5: Venn diagrams showing overlap between probe sets identified with different microarray analysis software.

4.3.2: Reverse transcriptase polymerase chain reaction

4.3.2.1: RT-PCR validation of Microarray approach

In order to validate the microarray analysis as a method of identifying accurate gene expression changes, semi quantitative reverse transcriptase-PCR analysis was performed on a set of RNA samples used in the original microarray hybridisation.

After reverse transcription, fifteen primer sets were used to analyse gene expression in the early exogen and late exogen cDNA samples, E1 and L1. One of these was GAPDH, a housekeeping gene, chosen because the microarray computer analysis normalised samples against the housekeeping genes. The remaining fourteen genes were all highlighted as being differentially expressed more than two fold between samples. As fold changes between samples were relatively low it was difficult to quantify fold changes. Rather, PCR results were analysed according to the direction of fold change, rather than the quantity of the change (Figure 4.6). Analysis indicated that thirteen out of the fourteen chosen genes had fold changes in the directions indicated by the original software analysis. Four of these genes were higher in E1 samples, whilst nine were higher in L1 samples. Only one gene, a protease inhibitor Fetuin Beta, presumed to be up in L1 after the original microarray analysis was not as expected, being higher in the E1 sample in the PCR analysis.

4.3.2.2: RT-PCR verification of differential expression

After validation of the microarray method, three new replicates sets of RNA were generated, each composed of an EE and a LE sample. After reverse transcription, PCR analysis was carried out to see if the results generated with the microarray analysis were replicable.

Analysis was run in triplicate with the three new sample sets. Thirteen primer sets were used in total to analyse gene expression, one being the housekeeping gene GAPDH. Five of the genes analysed were higher in early exogen samples used for the microarray analysis, a result replicated with the new sample sets. Moreover, the remaining seven genes analysed were all higher in late exogen samples used for the

microarray analysis, which the PCR analysis confirmed was the case in the new replicate sets (Figure 4.7).

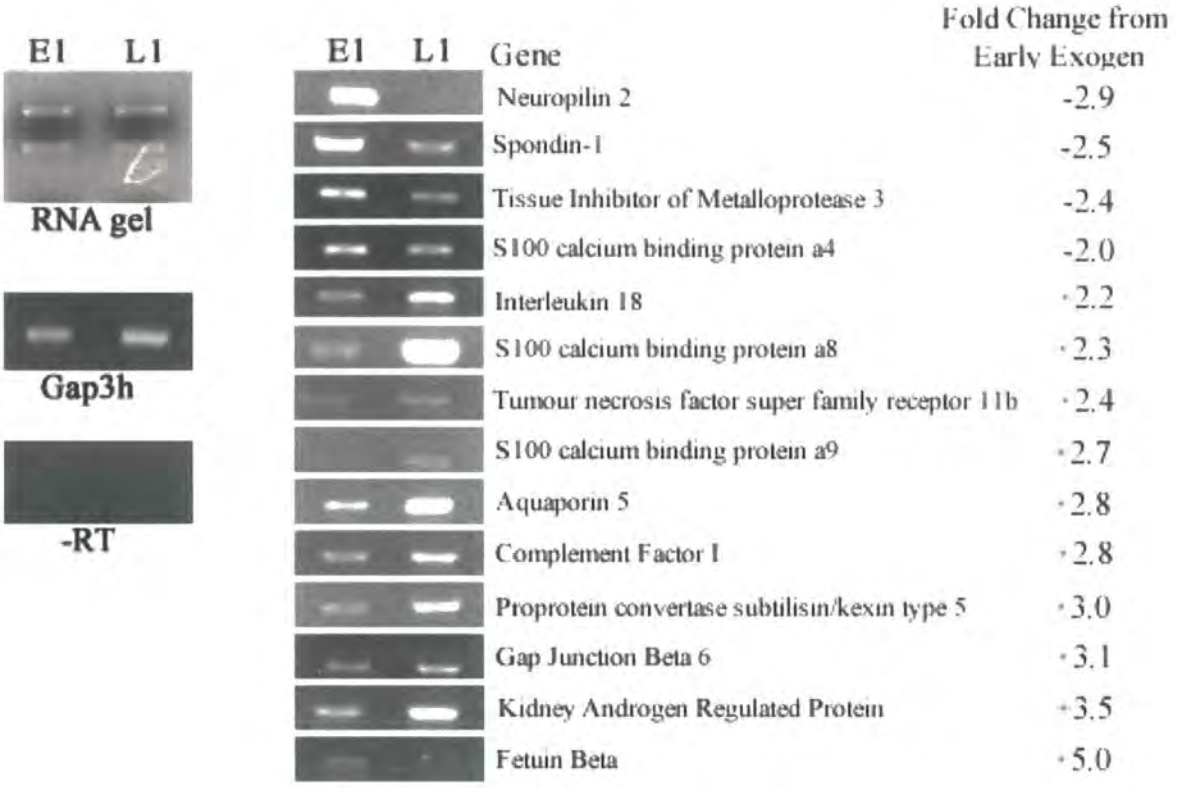

Figure 4. 6: RT-PCR analysis of gene transcripts in E1 and L1 sample sets, identified as differentially expressed between early and late exogen.

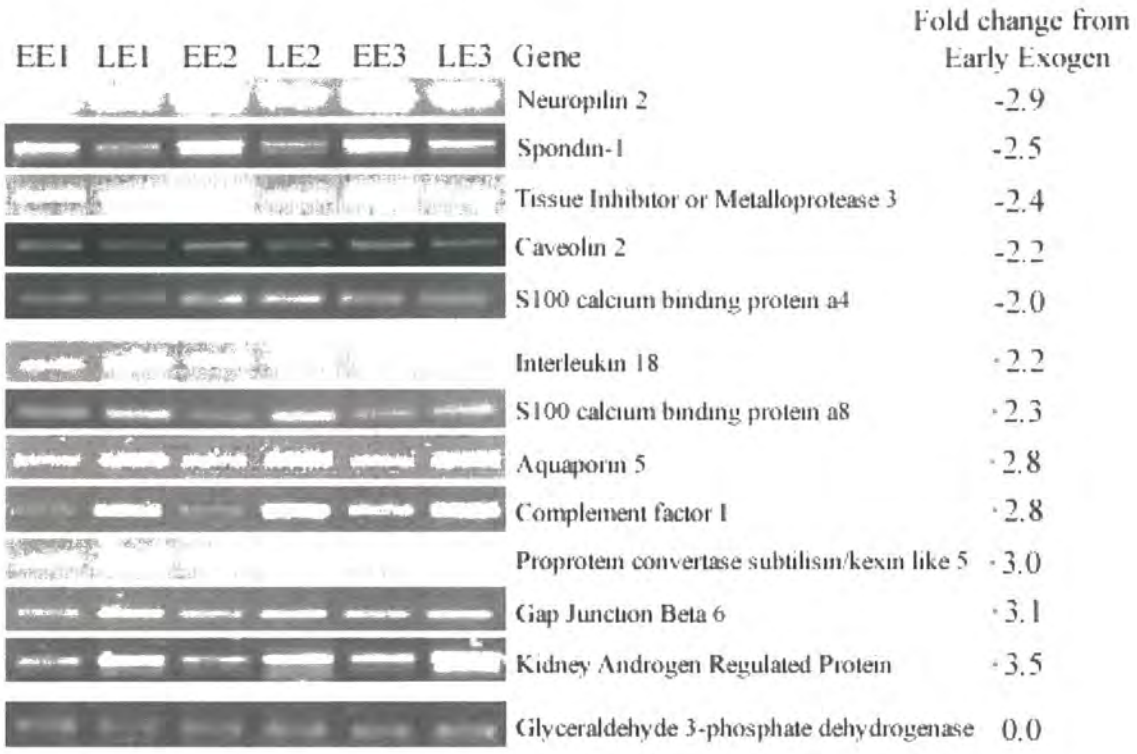

Figure 4. 7: RT-PCR analysis of gene transcripts identified as differentially expressed between early and late exogen using new replicates.

4.3.3: Group analysis of microarray

The list of ninety-five probes identified with both the GeneSpring and GeneTraffic software contained seventy-five known genes. After PCR analysis to validate the directions of fold change, genes were categorised based on their biological processes. No outstanding differences between sample populations were observed with any genes. However, by grouping the different genes into relevant biological categories, interesting patterns began to emerge that highlighted particular biological processes as relevant during exogen.

Genes encoding proteins that were: a) structural constituents of a cell; b) involved in cell adhesion and the extracellular matrix (ECM); c) involved in signalling or d) involved in proteolysis, were put into their respective categories. In addition to these four prior selected categories, natural groupings of cell cycle genes; other enzymes; transcription related genes and; transporter related genes emerged. Genes that did not fall into any of the above categories were labelled as 'other' whilst nine transcripts remained 'unknown'. The proteolysis category was separated into proteases and protease inhibitors whilst the signalling category was separated into signal transduction and signals. Moreover, the cell cycle category was separated into cell cycle promotion and cell cycle arrest. The numbers of genes in respective categories is represented graphically in Figure 4.8.

The category with the most interesting changes in gene expression was that of genes involved in "proteolysis". Five proteases were upregulated in late exogen samples compared to none being expressed in early exogen. Moreover, in addition to this distinct change, two protease inhibitors were more highly expressed in early exogen compared to just one in late exogen. The extent of this change in protease and protease inhibitor expression through the progression of exogen can be seen clearly in Figure 4.9. Whilst one of the proteases in late exogen, Similar to Cysteine-rich glycoprotein, exhibited metalloprotease activity, there was only one inhibitor of metalloproteases, *TIMP3*. The remaining four proteases and two protease inhibitors were all serine proteases.

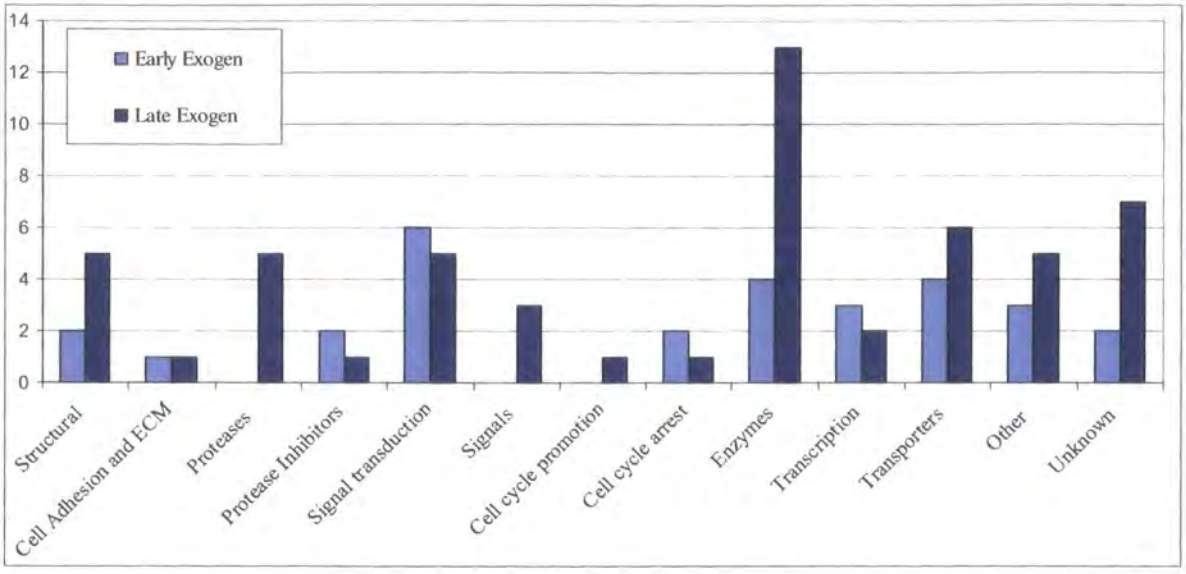

Figure 4. 8: Molecular Signature of Early and Late Exogen populations

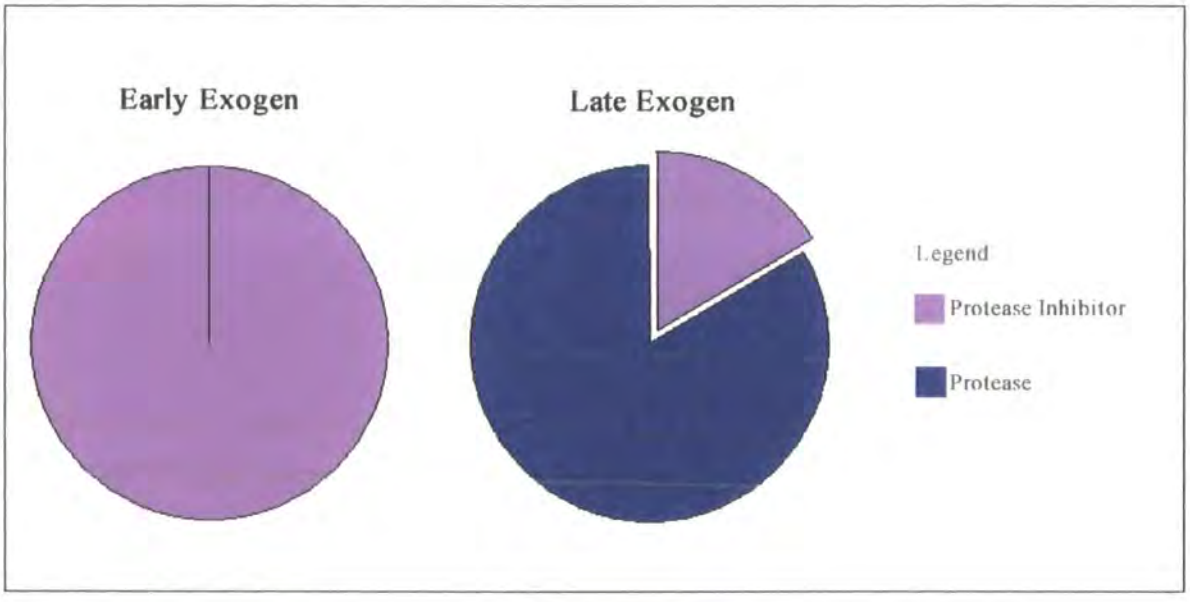

Figure 4. 9: Differential expression of Proteases and Protease Inhibitors in early and late exogen populations

A second category, which perhaps was expected to be more comprehensive after reading the literature, was the "cell adhesion and ECM" category. Only two genes fell into this; Spondin 1 (*Spon1*) and Gap Junction channel protein Beta 6 (*Gjb6*). Whilst *Spon1* was 2.5 fold higher in early exogen samples than late exogen, *Gjb6* was 3.1 fold higher in late exogen samples when compared to early exogen. *Spon1* encodes a protein that is present in the extracellular matrix whilst *Gjb6* is a structural component of gap junctions.

A third category was the "Structural" category, where seven genes were assigned to. Of these seven, two were higher in early exogen compared to late exogen, whilst the remaining five were upregulated in late exogen compared to early exogen. In particular, expression of Similar to Cornifin B, a component of the cornified envelope was higher in late exogen samples compared to early exogen. This was in addition to two Type I hair keratins, whilst none of these are more highly expressed in early exogen samples.

The fourth category to be prior selected was the "signalling" category. Genes involved in signalling were categorised with eleven genes being associated with "signal transduction", six of these up in early exogen and the remaining five up in late exogen. Two dual specificity phosphatases, 2 and 5 (*Dusp2, Dusp5*), were present in the signal transduction category, both thought to be involved in epidermal differentiation (Radoja et al. 2006). Moreover, one gene expressed higher in early exogen, Phosphodiesterase 1A, calmodulin dependent (*Pde1a*) is calcium dependent whilst a second, Protein phosphatase 3, catalytic subunit (*Ppp3cb*) encodes a calcineurin subunit. The expression of calcium dependent genes in addition to differentiation markers alludes to a possible calcium dependent signalling pathway controlling differentiation in the cells surrounding the club fibre with the progression of exogen. The "signalling" category was also composed of "signals", of which three were identified, all being upregulated in late exogen samples compared to early exogen. Two of these-Interleukin 18 (*IL18*) and Interleukin 17B (*IL17B*) encode cytokines whilst the remaining gene, Natriuretic peptide precursor type C (*Nppc*), encodes a neuropeptide.

A category which emerged independently from the others was the cell cycle category. This comprised of four genes in total, one which mediates cell cycle promotion whilst three that mediate cell cycle arrest. Of these four, three genes were also expressed in the tissue surrounding plucked club fibres. A second list that emerged independently from the assigned lists decided upon after literature research was the enzyme category. This included enzymes other than proteases, and was the largest category in the group analysis, as can be seen in Figure 4.8. This category of enzymes was formed primarily from enzymes involved in cell metabolism, with only one enzyme Cyp26b1 being involved in another process, this being retinoic acid catabolism. Two of the enzymes on the gene list had been prior localised to the hair follicle; tyrosinase-related protein-2 (*Trp2*) (Ohyama et al. 2006) and prostaglandin-endoperoxide synthase 2 (*Ptgs2*) (Muller-Decker et al. 2003).

The three remaining categories were transcription, transportation and other. In the transcription category five genes were present with three higher in early exogen than late exogen, and the remaining two genes higher in late exogen than early. All five of these genes were expressed in the plucked gene list, whilst one, *Id3*, had been previously detected in the vibrissa hair follicle (O'Shaughnessy et al. 2004).

The transporters category encompassed genes encoding proteins involved predominantly in ion and water transport. Other transporters present were responsible for the transport of amino acids and other small molecules. The final category was 'other', comprising of genes that did not fit into the other eight categories although a number of these genes appeared to be relevant as they encode calcium dependent or calcium binding proteins.

4.3.4: Localisation of TIMP3 expression with immunofluorescence

4.3.4.1: TIMP3 expression in vibrissa follicles

In the adult anagen vibrissae, TIMP3 staining was visible at the suprabulbar end of the follicle. Around the club fibre TIMP3 was expressed in cells in close proximity to the fibre, whilst the attenuation of this expression in cells distal from the fibre was particularly notable. At the club tip expression of TIMP3 was visible in the 3-4 cell layers adjacent to the fibre whilst in contrast; at the upper end of the club fibre expression appeared to be restricted to 1-2 cell layers as seen in Figure 4.10A and 4.10B. Expression was only seen in the ORS cells surrounding the club fibre, not in the electron dense trichilemmal keratin layer of the club fibre that protrudes out into the surrounding ORS. Club fibres from both early and late anagen samples were analysed for changes in expression and although a 2.4 fold decrease in gene expression from early to late exogen was detected with the microarray analysis, no obvious change in protein expression was observed surrounding early and late exogen club fibres using immunofluorescence. Expression of TIMP3 protein was also present in the trichilemma sac remaining after club fibre release, when clear holes were visible showing the previous location of the fibre. However, expression here was weaker than the expression seen surrounding anchored club fibres, with only a few cells showing perinuclear and granular TIMP3 expression (Figure 4.10C)

The localisation of TIMP3 within ORS cells surrounding the club fibre varied somewhat between cells. There was a combination of weaker granular staining of TIMP3 in the ECM compared with a much stronger, more perinuclear pattern of staining visible in cells adjacent to the fibre. These two staining patterns are shown in Figure 4.11B.

In addition to the cells surrounding the club fibre, TIMP3 was also expressed in a restricted population of ORS cells, but this only appeared at and above the level of onset of terminal differentiation in Huxley's layer of the IRS (Figure 4.12B). From this level upwards expression appeared in the companion layer, the innermost layer of the ORS, gradually spreading outwards into the surrounding ORS in a V-shape further up the follicle. This TIMP3 marking of the more differentiated cells of the

ORS was detectable with a granular staining pattern only, in contrast to a combination of granular and perinuclear staining that was visible around the club fibre. Weak expression was also seen in the IRS layers of the follicle, in Huxley's layer as it underwent terminal differentiation (Figure 4.12C) whilst expression in the cuticle of the IRS appeared with the onset of terminal differentiation within this layer, disappearing again afterwards (Figure 4.12D). Of the three IRS layer, Henle's layer differentiates first at the bulbar end of the follicle. Within this layer, TIMP3 expression was seen in the cells prior to their differentiation. However, expression of TIMP3 was not visible after cellular differentiation within Henle's layer (Figure 4.12E).

4.3.4.2: TIMP3 expression in non-vibrissae systems-Rat Back Skin

In rat back skin TIMP3 protein was strongly expressed at nuclear peripheries, in one or two suprabasal cell layers immediately adjacent to the telogen club fibre. The staining in these layers was particularly noticeable when compared to the weaker granular staining seen in the remaining ORS (Figure 4.13 A-C).

Figure 4. 10: TIMP3 expression around the vibrissa club fibre

A) In vibrissa follicles with club fibres in early exogen, TIMP3 staining is visible in three to four layers of ORS cells with close proximity to the club fibre, with the attenuation of expression in cells more distal from the fibre being particularly noticeable. A greater number of cells at the club fibre tip (arrowhead) show TIMP3 expression compared to cells further up the club fibre (arrow) where little expression is visible. Two patterns of staining are visible, one is granular, whilst the other, a perinuclear stain, is more prominent. The control (D) replacing the TIMP3 antibody with mouse IgG showed no specific staining.

B) Vibrissa follicles with late exogen club fibres show a similar TIMP3 expression pattern to that seen surrounding early exogen club fibres. In both cases greater staining is seen surrounding the tip of the club fibre, with a combination of granular and perinuclear staining in the cells. Expression is not visible in the electron dense trichilemmal keratin layer that forms the club fibre outer edge. The control (E) replacing the TIMP3 antibody with mouse IgG showed no specific staining.

C) In vibrissa follicles in late anagen/early catagen after release of the club fibre, it is possible to see the hole left by the lost fibre. Here TIMP3 expression is diminished compared to the expression visible surrounding anchored club fibres. Perinuclear expression and weak granular expression is visible in a few select cells surrounding the fibre. The control (F) replacing the TIMP3 antibody with mouse IgG showed no specific staining.

Green: TIMP3
Red: PI nuclear counterstain
Scale bars: 100μm

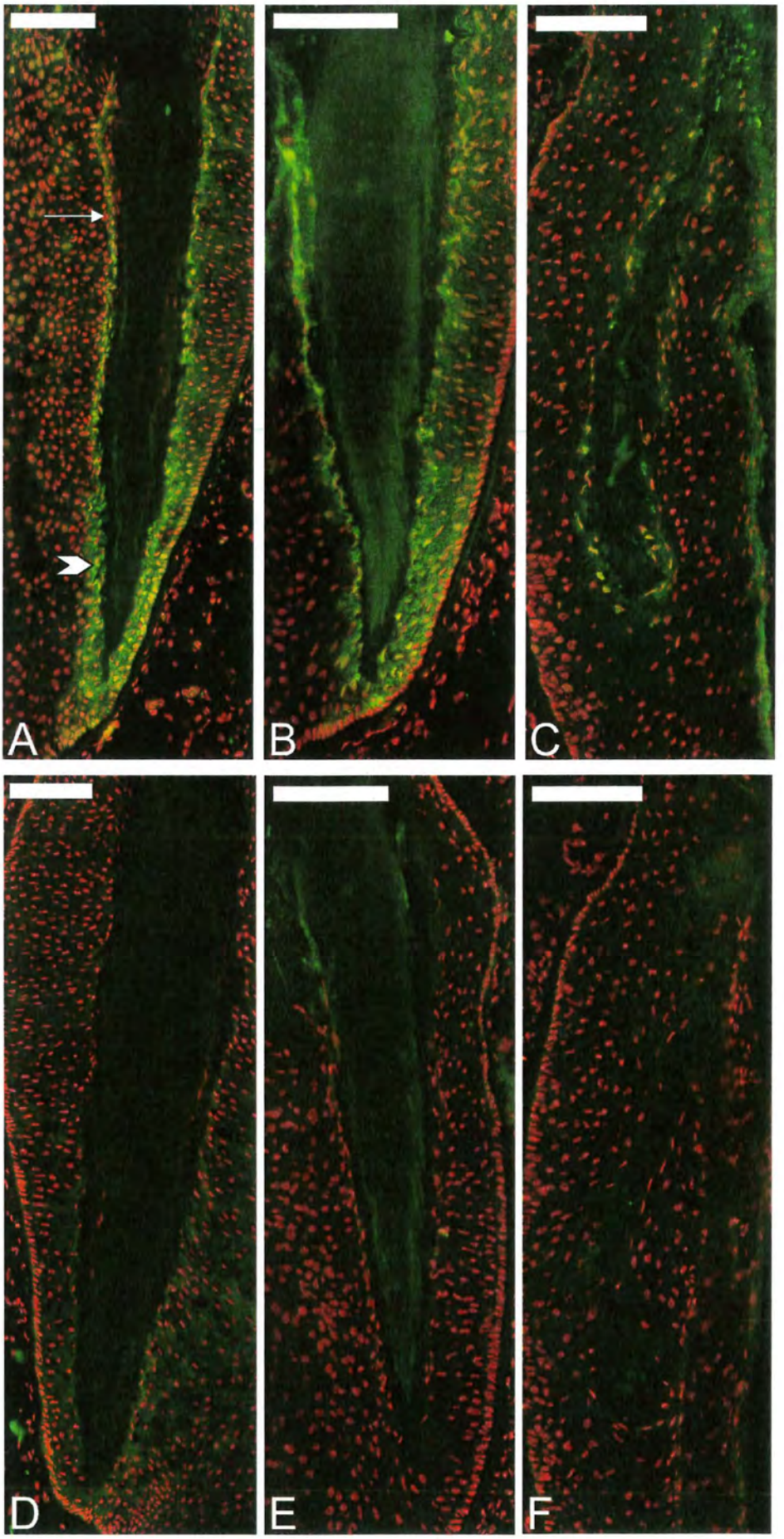
A
B
C
D
E
F

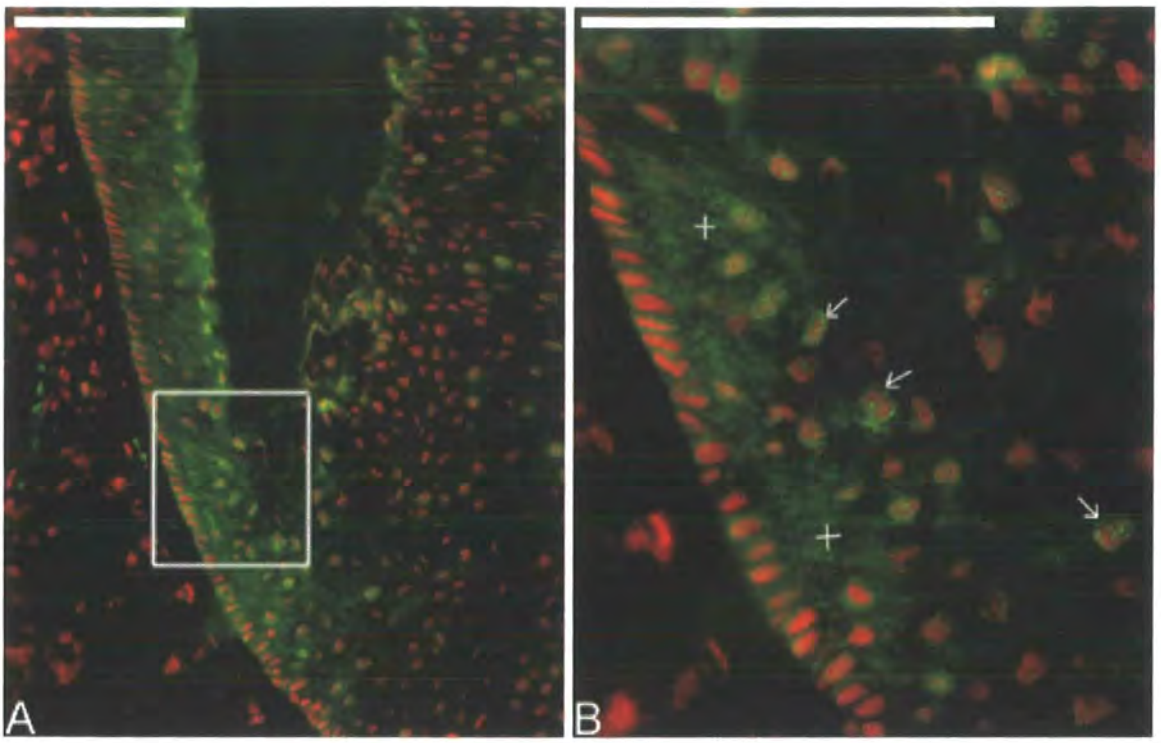

Figure 4. 11: Granular and Perinuclear staining surrounding exogen club fibres

Two patterns of staining are visible surrounding vibrissa club fibres. B, the enlargement of the boxed area in A shows that the first, a granular staining pattern (crosses) is visible throughout the ORS whilst the second, a perinuclear staining pattern (arrows) is visible in the three to four layers surrounding the club fibre.

Green: TIMP 3

Red: PI nuclear counterstain

Scale bars: 100μm

Figure 4. 12: TIMP3 expression in an anagen vibrissa follicle

In the anagen vibrissa follicle (A) TIMP3 expression surrounding the growing fibre is in the IRS and ORS as the different cell layers undergo terminal differentiation. Expression is also in the innermost cell layers of the ORS surrounding the club fibre. With reference to the growing fibre, expression in the ORS (star, area enlarged in B) begins after complete keratinisation of the IRS has occurred, occurring first in the companion layer of the ORS as it undergoes terminal differentiation, then spreading out in the surrounding ORS as it differentiates so that expression appears in a V-shape as you move up the follicle. In Huxley's layer of the IRS (cross, area enlarged in C) expression is visible with the onset of terminal differentiation, disappearing after complete keratinisation of this layer. A similar profile is seen in the cuticle of the IRS, with the appearance of TIMP3 expression coinciding with the onset of differentiation within this layer (arrow head, area enlarged in D). In the region where Henle's layer of the IRS undergoes terminal differentiation (arrow, area enlarged in E), TIMP3 expression is seen in cells prior to complete keratinisation occurs. Expression within all lineages of the IRS and ORS surrounding the anagen growing fibre is granular.

Green: TIMP3
Red: PI nuclear counterstain
Scale Bars: 100μm

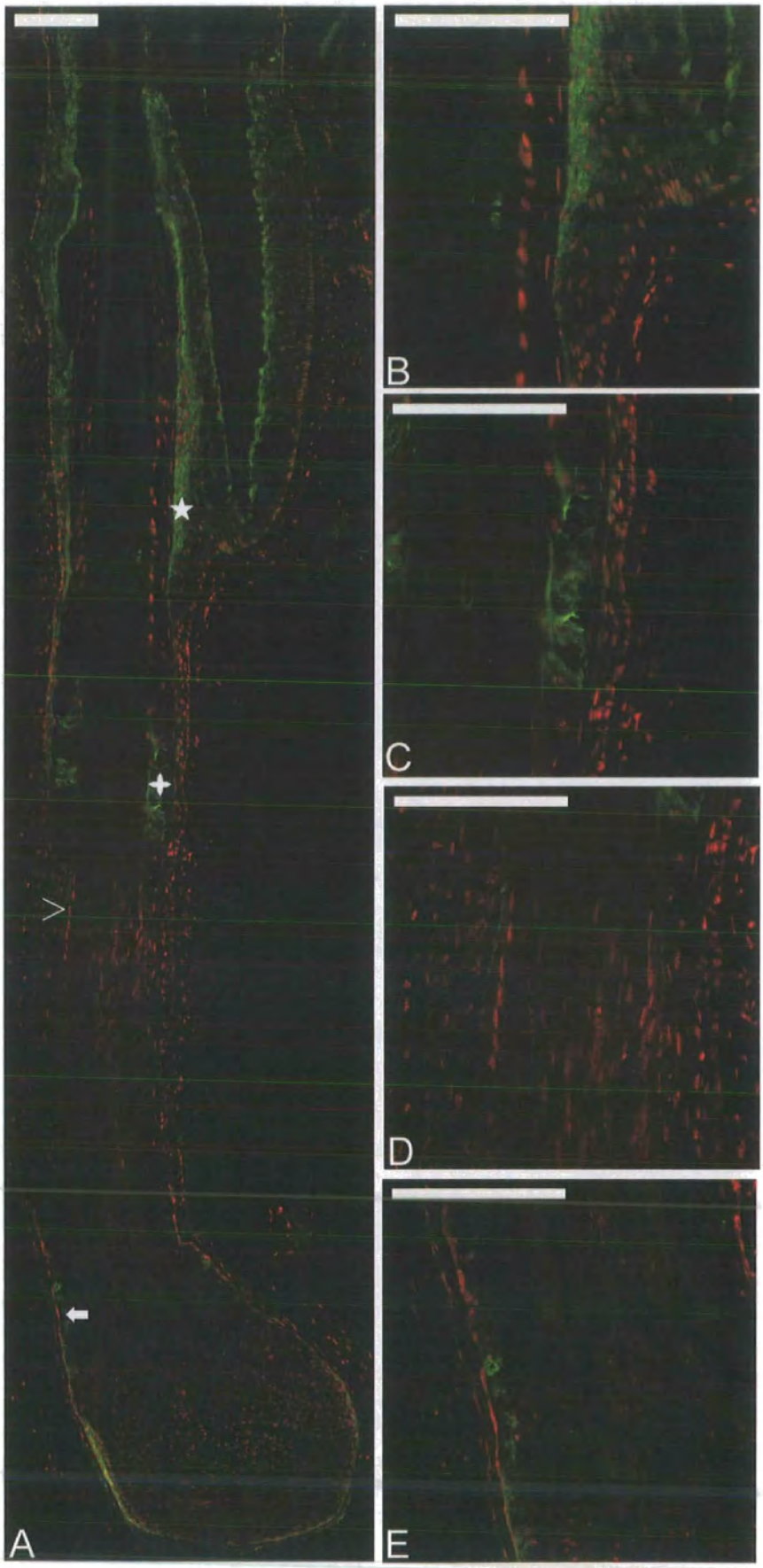
A
B
C
D
E

Figure 4. 13: TIMP3 expression surrounding club fibres in rat back skin

A) Strong TIMP3 expression is detected in the innermost layer of the ORS that surround the telogen club fibre in rat back skin. The sharp contrast in the expression levels between the innermost cell layer and those more distal are noticeable. TIMP3 expression is absent from the dermal papilla, and the secondary hair germ of the telogen follicle.

B, C) Perinuclear TIMP3 staining is intense in the cells immediately adjacent to the club fibre whilst weaker granular staining can be seen in the surrounding ORS, further out from the club fibre.

C) The negative control, with TIMP3 primary replaced with an equal concentration of mouse IgG shows no specific staining.

Green: TIMP3
Red: PI nuclear counterstain
Scale Bars: 100μm

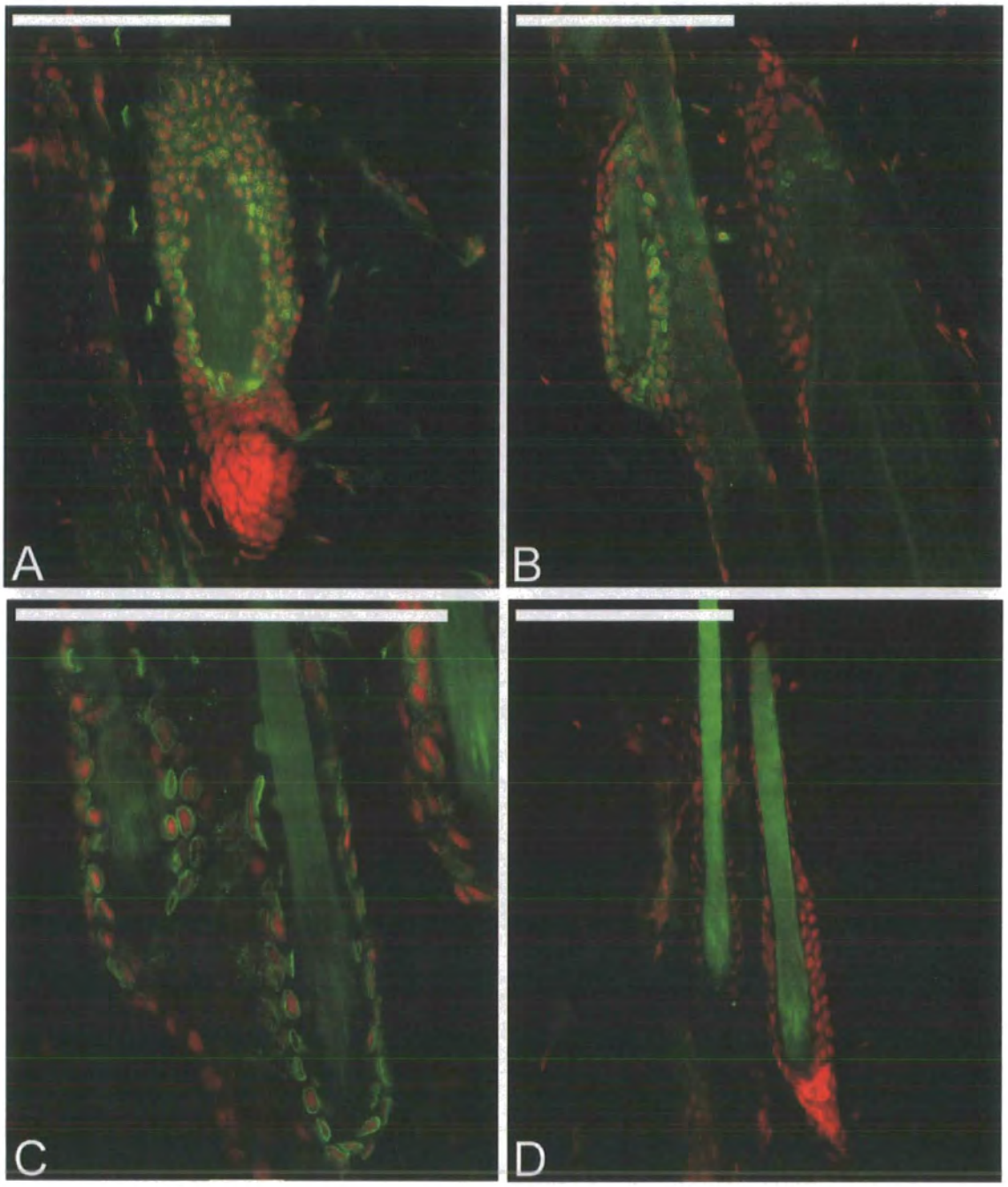
A
B
C
D

4.3.5: Localisation of connexin expression with immunofluorescence

4.3.5.1: Connexin expression surrounding vibrissa club fibres

A member of the gap junction family Cx43, encoded by *Gja1* was analysed with immunofluorescence, although microarray analysis had not picked up changes in expression of this gene between early and late exogen. However, *Gja1* gene expression was present in RNA extracted from plucked club fibres indicating that it was present around the club fibre, and so protein expression of the encoded connexin was analysed. A second connexin analysed was Cx30. The microarray analysis using Genespring and Genetraffic showed that there was a 3.45 fold increase in expression of *Gjb6*, the gene encoding gap junction protein Cx30, around late exogen club fibres compared with the same locality from early exogen club fibres. In order to correlate the presence of *Gjb6* mRNA with the expression of the corresponding protein, immunofluorescence was performed to analyse the expression of Cx30 throughout the follicle, in particular the area around the club fibre.

Immunoreactivity of Cx43 was seen at the upper end of the follicle in membrane associated plaques from the basal layer throughout the suprabasal ORS surrounding the club fibre. During telogen, at the start of club fibre formation, Cx43 expression was most intense in the cells at the tip of the club fibre (Figure 4.14A). As the fibre moved up the follicle immunoreactivity was concentrated to cell layers most proximal to the developing club fibre. The difference in intensity between these innermost cells and those distal to the club was more evident and striking at this earlier stage in club formation than the difference seen surrounding the club fibres in early anagen follicles (Figure 4.14 A-E). In six of the ten samples with early exogen club fibres the most intense staining was seen in the companion^{CL} surrounding the club fibre (Figure 4.14D), where staining diminishing in intensity more distal from the club fibre. In the remaining 4 samples with early exogen club fibres expression levels appeared equal throughout the entire ORS. In contrast, in all samples with late exogen club fibres, expression did not vary throughout the ORS.

This expression pattern of Cx43 was in sharp contrast to that of Cx30, which although present in the ORS was notably absent from the cells immediately surrounding the

club fibre (Figure 4.15). The location of Cx30 in the ORS of the follicle was also in contrast to that of Cx43, and was not typical of normal connexin distribution in cells as it was present in the cytoplasm in a fine granular pattern, and was not observed at the cell membrane.

4.3.5.2: Connexin expression around club fibres in non-vibrissae systems-Rat Back Skin

Strong Cx43 immunoreactivity surrounding telogen fibres in rat back skin was detectable in one or two cell layers of the ORS immediately adjacent to the telogen club fibre. Basal keratinocytes had either weak, sparse punctuate staining, or it was absent altogether (Figure 4.16 A-B). Weak expression was visible in the papilla of telogen follicle, and in the companion layer of adjacent growing fibres. The Cx30 staining pattern was inversely correlated to that of Cx43, with staining noticeably absent from the first one or two cell layers adjacent to the club but present in the cytoplasm of cells distal from the fibre (Figure 4.16 C-D). Cx30 antigen was also absent in the dermal papilla of telogen follicles. The negative controls, where the primary antibodies were replaced with rabbit IgG showed no specific reactivity (Figure 4.16 E-F)

4.3.5.3: Connexin expression surrounding anagen growing fibres in vibrissa follicles

Cx43 was expressed in various different lineages of the adult anagen vibrissae (Figure 4.17A). Starting from the more differentiated lineages of the follicle expression was absent in the medulla but present as a punctuate stain at the cell membrane of cells in the cortex of the hair fibre. Expression here was intense compared to the weak expression of Cx43 detectable in the presumptive fibre cuticle disappearing completely in the cuticle itself. Weak expression was visible in the IRS cuticle and in Huxley's layer although expression disappeared in this layer coinciding with keratinisation. A similar phenomenon was observed in Henle's layer where expression observed disappeared with keratinisation. Adjacent to Henle's layer, the companion layer of the ORS contained strong expression of Cx43. Expression was

also visible throughout the rest of the ORS through to the basal layer, although at a reduced intensity compared to the companion layer,.

For Cx30 (Figure 4.17B), compared with the strong staining throughout the ORS, weaker immunoreactivity was present in the cuticle of the IRS, disappearing at the level of keratinisation. Immunoreactivity was absent from all layers of the hair fibre and Henle's layer whilst Huxley's layer of the IRS showed weak expression.

4.3.5.4: Connexin expression in the bulb of the vibrissae follicle

During late telogen/early anagen initiation Cx43 was absent from basal cell membranes at both the inner and outer dermal-epidermal junctions (Figure 4.18A). This was compared to anagen follicle bulbs, where Cx43 expression in the epidermal part of the bulb intensified on the basal surface of epidermal cells from the widest part of the dermal papilla down to the neck of the papilla. Moreover, in anagen follicle bulbs, sparsely distributed yet strong Cx43 staining was visible in the dermal papilla and dermal sheath, whereas in the epidermal part of the bulb strong Cx43 staining was evident throughout the matrix and differentiating lineages of the bulb region of an anagen follicle (Figure 4.18 C/E).

Conversely, in late telogen/early anagen Cx30 expression was prominent in the outer root sheath directly adjacent to the thickened glassy membrane observed in telogen follicles (Figure 4.18B). This was in contrast to the absence of Cx30 surrounding the dermal papilla in telogen, except for the very tip of the new apex, where weak expression in the epidermal portion was visible. Very strong reactivity for Cx30 was also seen at the basal tip of the epidermis, both of these expression profiles being unique to the telogen/anagen initiation stage of the cycle. In contrast, in anagen a few cells of the ORS where it merges proximally into the bulb were positive for Cx30 although expression was notably weak compared to the intense stain seen in telogen/anagen initiation. Also, in the early anagen follicle a few select germinative cells at the base of the follicle were positive for Cx30 (Figure 4.18D), expression which had decreased by late anagen. (Figure 4.18F). During anagen Cx30 expression was absent from the dermal papilla but present in a single layer of epidermal cells at the papilla-epidermal junction, the presumptive medulla, extending

over the apical tip of the papilla down to the critical line of Auber (Auber 1952), below which expression was absent. Moreover, expression was absent at the outer basement membrane junction, where during telogen it had been intense.

In contrast to the cytoplasmic expression of Cx30 observed in cells of the ORS, in the inner lineages of the follicle expression was punctate, and present at the cell membrane.

Figure 4. 14: Connexin 43 expression decreases with club fibre maturation in the vibrissae

A late catagen/early telogen follicle shows strong Cx43 expression (green) as the tip of the club fibre becomes detached and begins migrating up the follicle (A). Follicles in the very early stages of anagen that have club fibres still moving up the follicle show strong connexin expression both at the tip, but also in the cell layers of the ORS located next to the club fibre higher up (B, C). Once the club fibre has reached its permanent position the asymmetry of the club is more visible. In D the left side of the club fibre (arrow) is slanted and positioned next the new growing fibre as it emerges whilst the straight edge (arrowhead) on the right of the fibre is positioned closer to the basement membrane. Once in a permanent position Cx43 expression is strong on both edges of the club fibre in the companion^{CL}, although weaker in intensity when compared to the very early exogen club fibres (D). The intensity of Cx43 staining in fibres is lost gradually as the club fibre matures, evident in the follicles containing late exogen club fibres, which will be lost with the onset of the new catagen phase (E).

Green: Cx43
Red: PI nuclear stain (A, C)
Blue: Dapi nuclear stain (B, D, E)
Scale Bars: 100μm

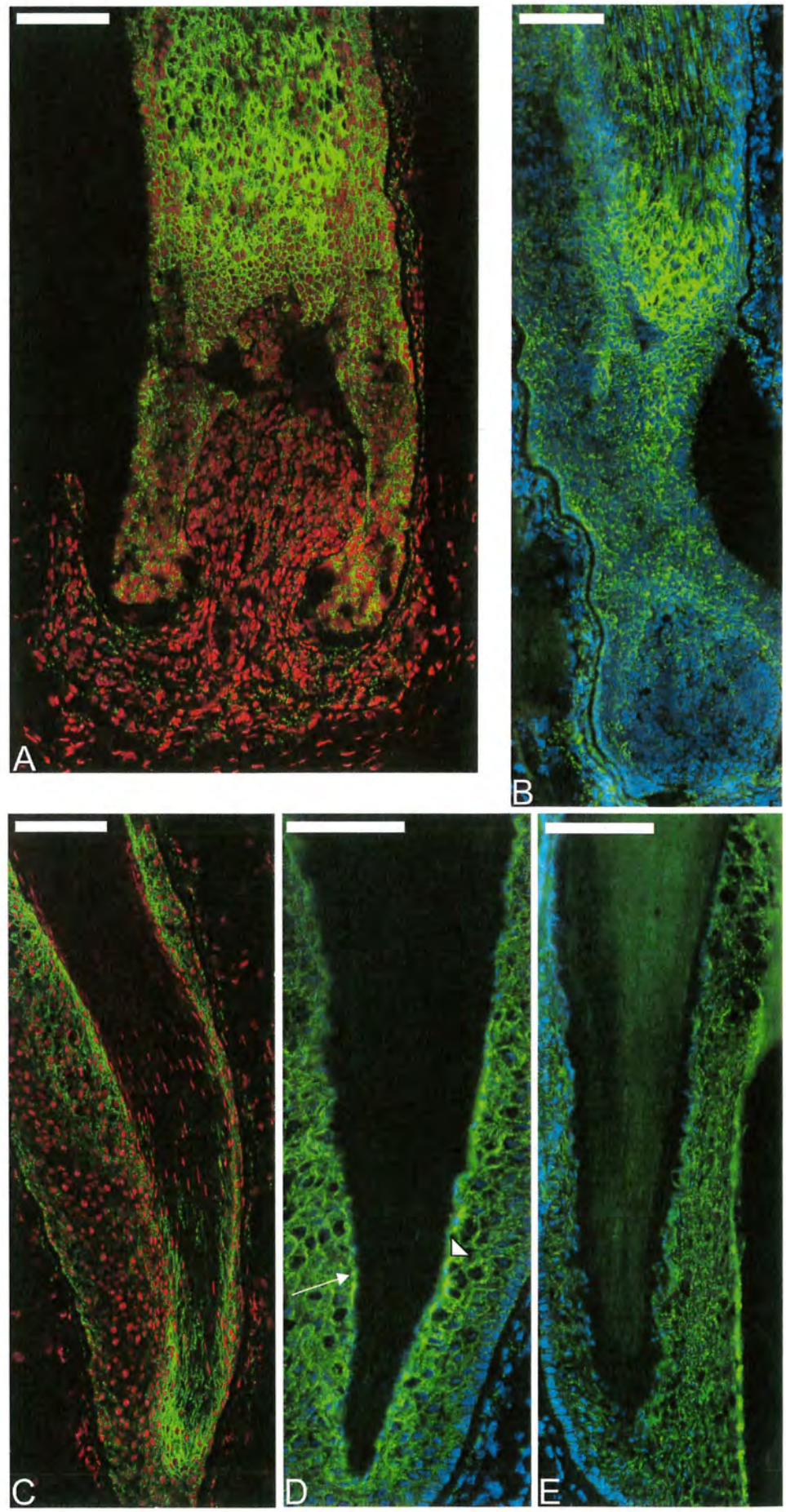
A
B
C
D
E

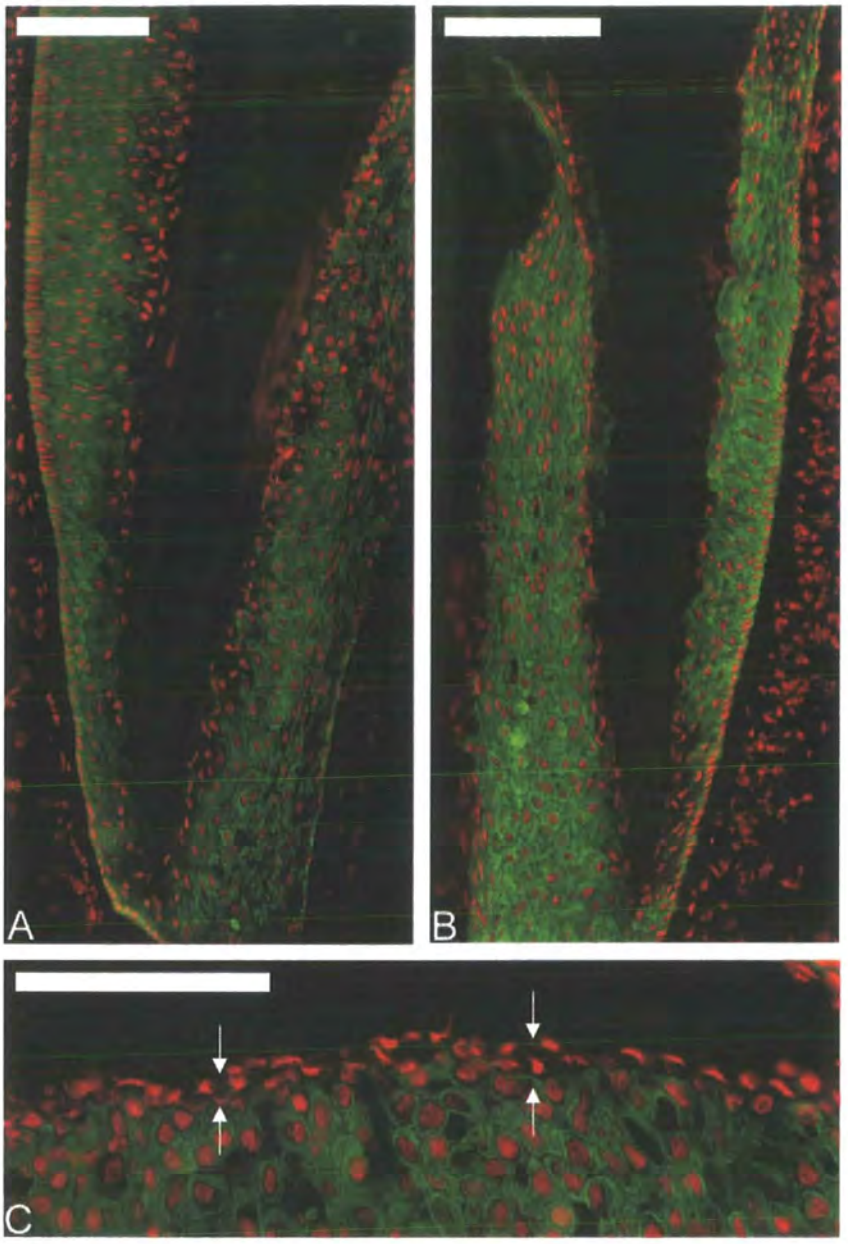

Figure 4. 15: Connexin 30 is absent from the Companion^{CL}

Cx30 expression surrounding early (A) and late exogen club fibres (B) exhibit similar expression patterns. Cytoplasmic expression of Cx30 is seen in both the suprabasal and basal ORS. However, in the companion^{CL} (between arrows), Cx30 is absent (C).

Green: Cx30

Red: PI nuclear stain

Scale Bars: 100μm

Figure 4. 16: Connexin expression in Rat Back Skin

Faint Cx43 antigen (green) is detected in the papilla from telogen follicles (A). Weak expression is seen at cell membranes in the ORS compared to intense expression seen in the companion^{CL} (A, B). The companion layer of anagen fibres is also intensely stained with Cx43 (B). In contrast to Cx43, Cx30 (green) expression is absent from the telogen dermal papilla (C). Expression in the ORS is cytoplasmic with an absence of antigen in the companion^{CL} (D), inversely correlated to the expression pattern of Cx43. A control using Rabbit IgG to replace the primary antibody showed no specific staining in either the papilla (E) or the ORS surrounding the club fibre (F).

Green: Cx43 (A, B), Cx30 (C, D)
Red: PI Nuclear Stain
Scale bars: 100μm

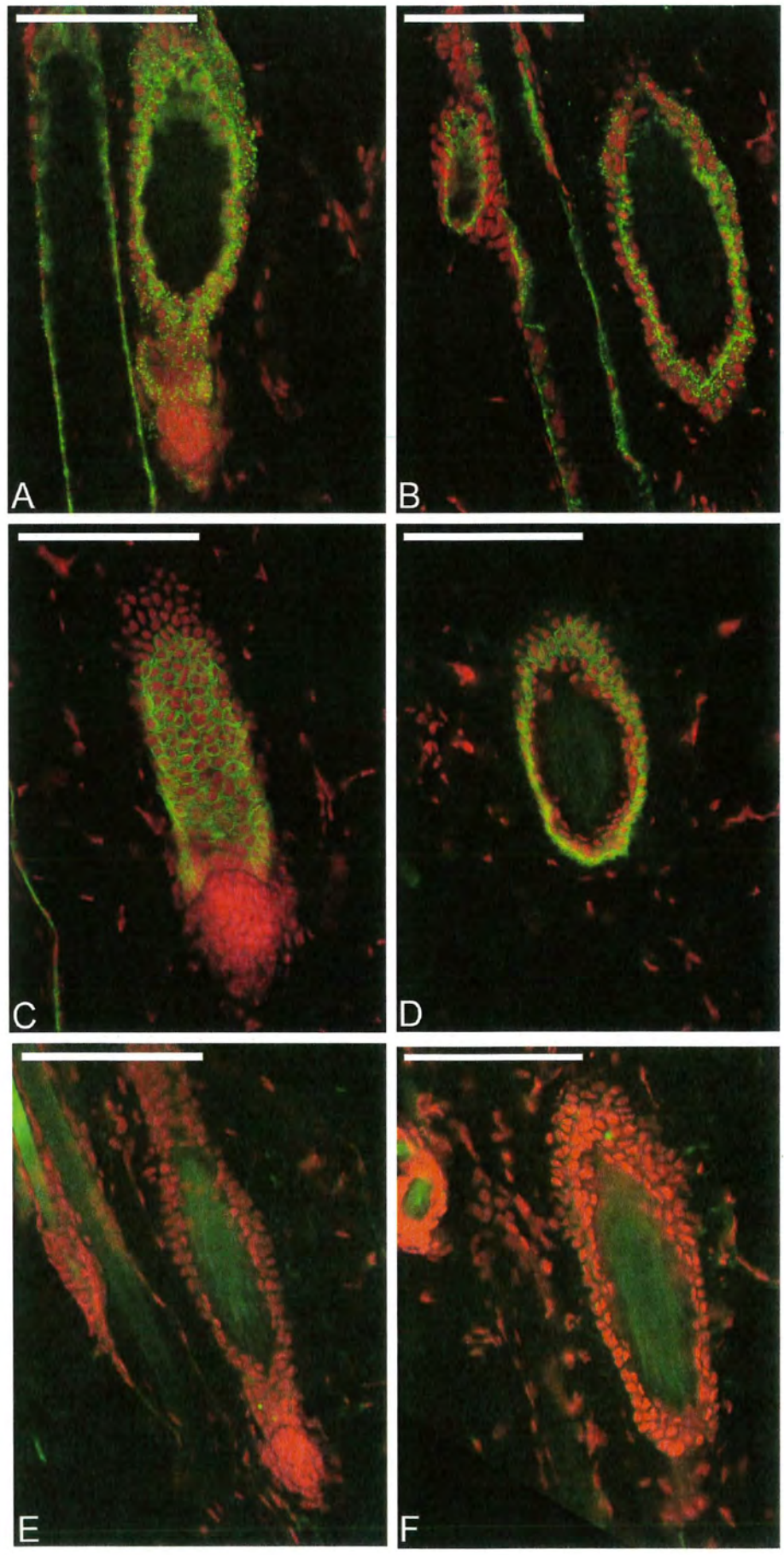
A
B
C
D
E
F

Figure 4. 17: Connexin expression in the anagen vibrissa follicle

(A) Cx43 expression (green) in the vibrissa follicle is punctate and located at the cell membrane throughout. Expression is visible in the hair cortex, the cuticle and Huxley's layers of the IRS, up to the level of keratinisation for this layer. In the ORS expression is strongest in the companion layer, decreasing in intensity through to the basal layer of the follicle. Expression in the dermal sheath of the follicle aids to highlight the thick basement membrane zone of the follicle, which is negative for Cx43.

(B) Cx30 expression (green) is predominantly in the ORS of the vibrissa, where it is localised in the cytoplasm. In the bulbar region of the follicle the antigen is present in the presumptive medulla, and in a few cells of the germinative matrix at very base of the bulb. The staining in the bulbar region is membranous suggestive of different roles of Cx30 within the follicle.

(C) A negative control (Primary replaced with rabbit IgG) shows no staining in any regions of the follicle

Green: Cx43 (A), Cx30 (B)
Red: PI nuclear stain
Scale bars: 200μm

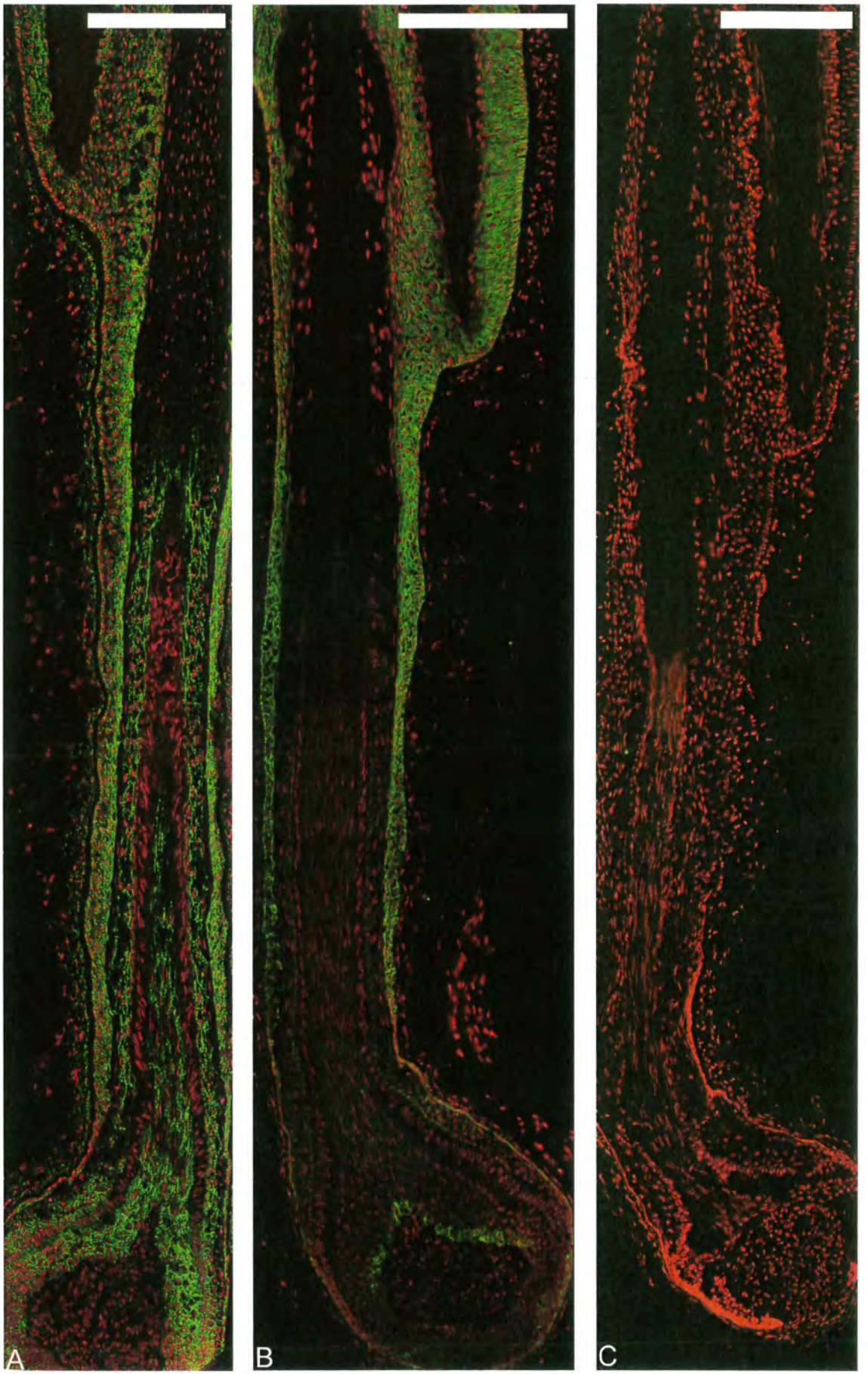
A
B
C

Figure 4. 18: Connexin expression in the bulb of the vibrissa follicle

Cx43 expression during late telogen/early anagen is located at cell membranes, and observed in the majority of the epidermal portion of the bulb, although is absent from the basal membrane of basal cells where they contact both the inner and outer basement membranes (A). In contrast, strong expression in the basal membrane (arrow) is observed at the widest regions of the dermal papilla, down to the papilla neck, in both early anagen (C) and late anagen (E) samples.

Cx30 expression (green) is intense in the ORS directly next to the thickened glassy membrane during telogen/early anagen (B). Increased expression during this cycle stage is also prominent at the very basal tip of the epidermis contrasting with diminished expression on the epidermal side of the apical tip of the papilla when compared to anagen. In early anagen samples, Cx30 is present in a few select cells of the germinative matrix and ORS where it merges into the bulb, whilst also being present in the presumptive medulla of the follicle (D). In the late anagen bulb Cx30 expression has diminished in the germinative matrix, although expression remains in the presumptive medulla (F). Cx30 is not present in the dermal papilla during any cycle stage (B, D, F) in contrast to Cx43 which is present in the dermal papilla (A, C, E).

Green: Cx43 (A, C, E), Cx30 (B, D, F)
Red: PI nuclear Stain
Scale Bars: 100μm

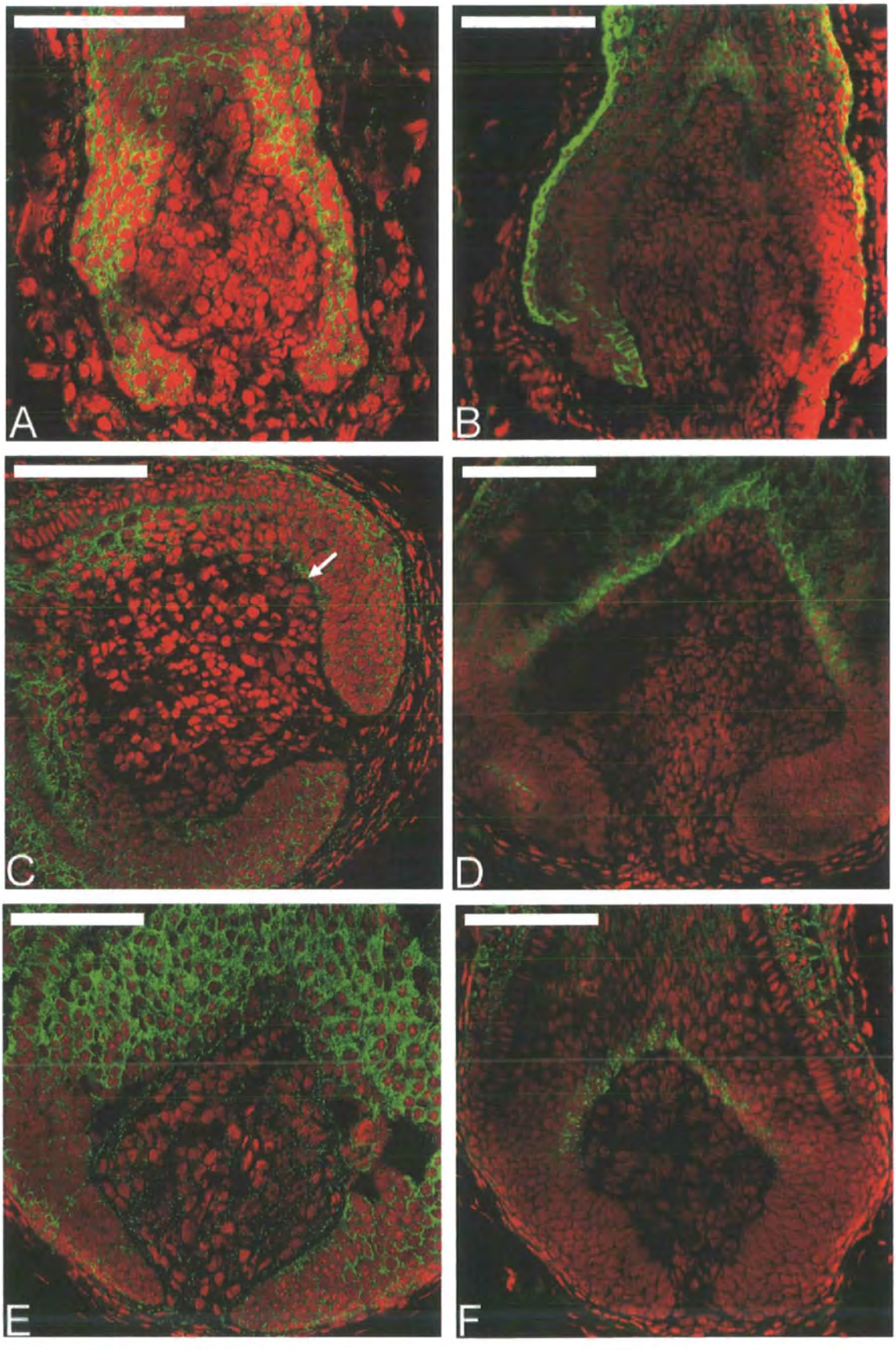
A
B
C
D
E
F

4.3.6: Id3 expression in the adult Vibrissa follicle

The microarray analysis compared the region surrounding both early and late exogen club fibres. The results from this indicated that Id3 gene expression was 2.5 fold higher in the cells that surround the early exogen club fibre when compared to the same locality in late exogen. Analysis using immunofluorescence showed relatively little difference in the suprabasal keratinocytes surrounding early and late exogen club fibres. However, a striking difference between early and late anagen follicles was detectable in the area just below the bulge region of the vibrissae. In this zone of the ORS, which extended down to where Huxley's layer of the IRS differentiates, the subcellular location of Id3 was cytoplasmic rather than nuclear. This incidence was only visible in early anagen follicles (Figure 4.19A), as compared to late anagen follicles (Figure 4.19D) where no cytoplasmic staining was observed, only nuclear. This cytoplasmic staining of this group of ORS cells, in early anagen follicles was noticeably brighter than in the surrounding ORS cells.

Further, in early anagen follicles, a few singular cells of the ORS alongside the growing hair were positive for Id3 whilst in the majority of keratinocytes Id3 was absent (Figure 4.20A). At the neck of the bulb region there was a significant increase in the number of bright Id3 positive cells localised in the ORS. At this point, where the ORS becomes just one cell layer thick and merges into the bottom of the proliferating matrix a thin trail of Id3 positive cells was observed (Figure 4.21A). Compared to these observations, in late anagen follicles the majority of cells of the ORS surrounding the growing fibre were positive for Id3 (Figure 4.20B). The neck of the bulb was also brightly immunoreactive for Id3, although there were none or very few positive cells in the ORS at the base of the bulb (Figure 4.21B).

Catagen follicles were similar to late anagen follicles in that strong Id3 expression (Figure 4.17C) was seen all down the ORS on both sides of the follicle. The ORS at the neck of the bulb was also positive for Id3. However, the germinative cells that remain at the base of the follicle in catagen (Reynolds and Jahoda 1991) did not show any Id3 protein expression (Figure 4.18C).

Figure 4. 19: Id3 expression surrounding club fibres in the vibrissa follicle

(A) Id3 expression (green) surrounding the early exogen club fibre is visible in cell nuclei throughout the ORS and in the basal layer of the follicle. Arrows in panel A indicate a region in the suprabasal ORS between the lower end of the club tip and the early anagen growing fibre where Id3 expression is prominent in the cell cytoplasm as appose to the nuclei. (D) In the ORS surrounding late club fibres Id3 expression is visible in cell nuclei of both suprabasal and basal ORS cells. There is no visible cytoplasmic staining in the suprabasal ORS region between the club fibre and growing fibres. A and B are equivalent panels, as are D and E, but only panels B and E show the PI nuclear counterstain (red). Representative controls with PBS replacing the primary antibody show no non-specific staining in the ORS surrounding both early exogen (C) and late exogen (F) club fibres.

Green: Id3
Red: PI nuclear counterstain
Scale bars: 200μm

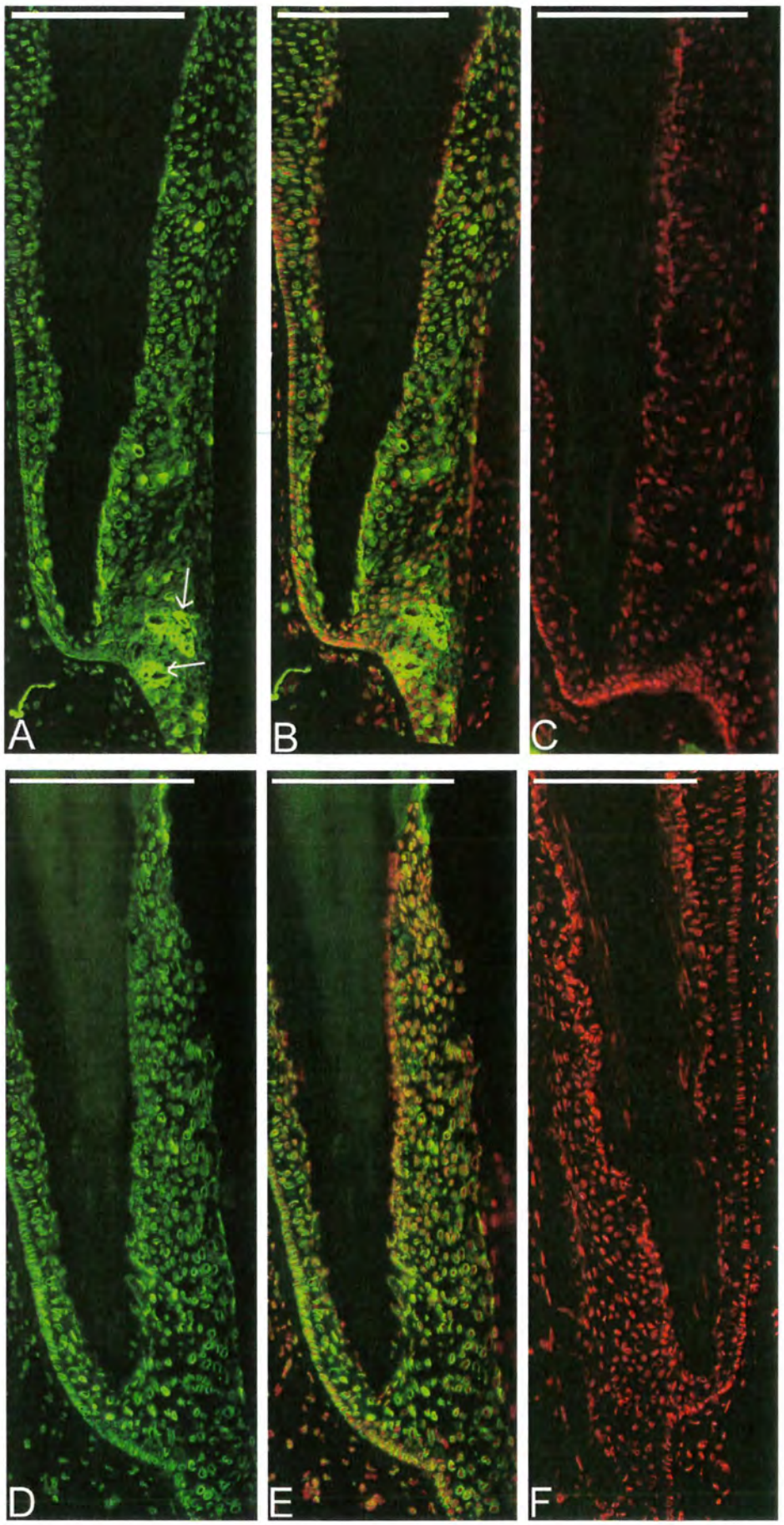
A
B
C
D
E
F

Figure 4. 20: Id3 expression in anagen and catagen vibrissa follicles

(A) Expression of Id3 (green) in the early anagen vibrissa is predominantly in the ORS of the upper follicle. Expression is attenuated in the ORS moving down the follicle at the level of Huxley's layer differentiation. Just before the loss of the signal, cytoplasmic expression of Id3 is visible in the cells surrounding the growing fibre. In the lower ORS, a few singular cells (arrows) are positive for Id3, increasing in density in the ORS at the neck of the bulb region (arrowheads).

(B) In the late anagen follicle Id3 is expressed throughout the ORS in both the upper and lower halves of the follicle. The neck of the bulb region is also positive for Id3 although expression does not extend into the lowermost part of the bulb.

(C) In the catagen follicle Id3 expression is found in the ORS extending alongside the fibre. Expression is strong so the loss of expression in the bulb region is particularly notable.

Green: Id3
Red: PI nuclear counterstain
Scale bars: 200μm

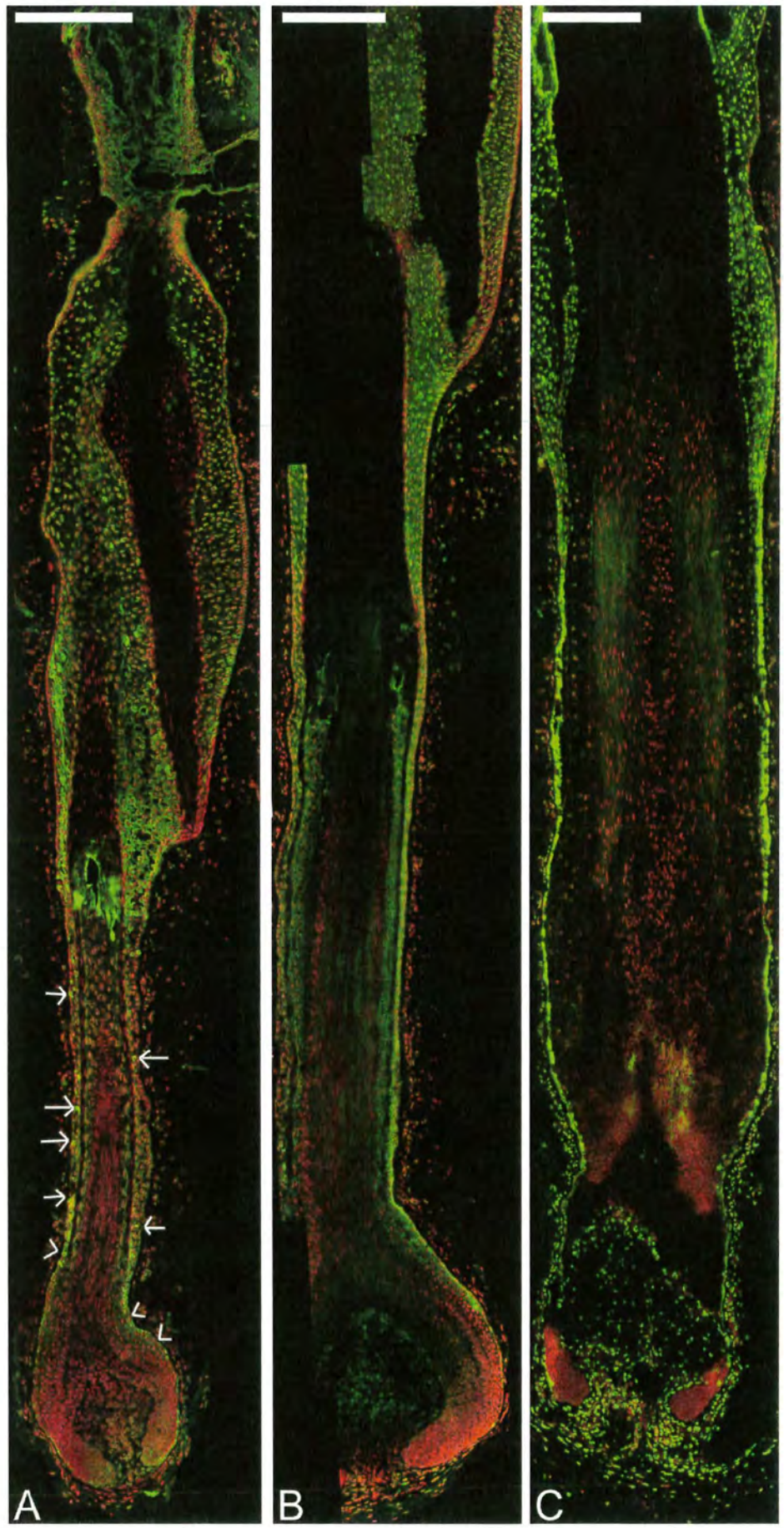
A
B
C

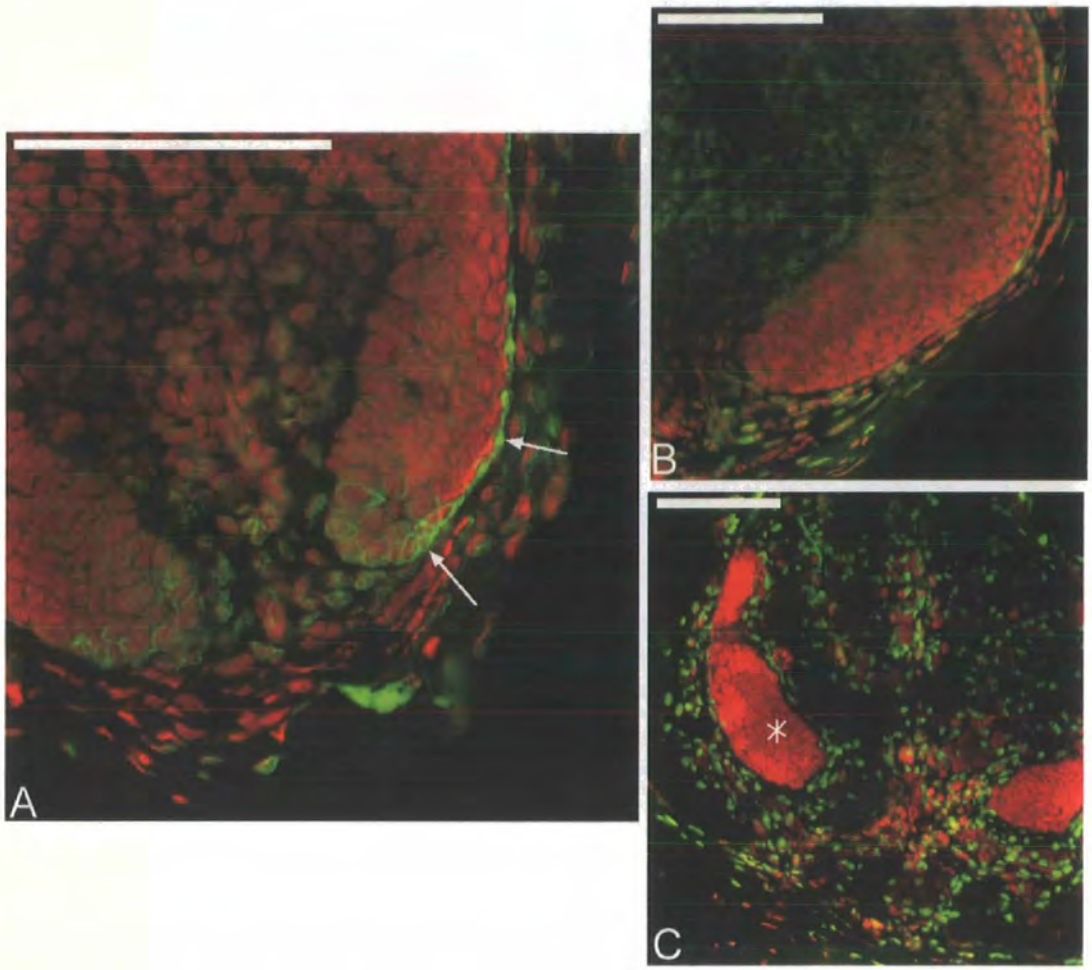

Figure 4. 21: Id3 in the bulb of the vibrissa follicle

In the early anagen bulb (A) Id3 expression extends round in the ORS and is present in cells at the basal tip of the epidermis (arrows). In late anagen (B) this Id3 expression has disappeared at the base of the bulb. During catagen (C) the remaining germinative matrix is visible (star). Id3 expression is absent here.

Green: Id3

Red: PI nuclear counterstain

Scale bars: 100μm

4.4: Conclusions and Analysis

4.4.1: Microarray analysis as an informative tool

A microarray approach is often adopted to identify key gene changes, enabling researchers to focus on particular genes in their research. In this microarray experiment no gene transcripts were identified that showed a substantial fold change between sample populations. However, although the fold changes presented between populations here were relatively small, they were replicable, validating them as accurate transcript changes.

A number of transcripts of genes previously reported present in pelage or scalp hair follicles, and more specifically in the selected region of the follicle were identified as differentially expressed in the microarray. These include Prolactin Receptor (Prlr), expressed specifically in the companion^{CL} in mouse pelage follicles (Foitzik et al. 2003). Moreover, Gjb6 (Essenfelder et al. 2005), and Id3 (O'Shaughnessy et al. 2004), both expressed in the ORS of human and mouse pelage respectively, were identified as differentially expressed. For the analysis not only were club fibres selected, but also the majority of the vibrissa follicle above the nerve entry point and below the ringwulst. This is a large area compared to the small region around the club fibre that we were interested in. This large sample population is reflected by the upregulation of the *S100 calcium binding protein a9* (*S100a9)* transcript in late exogen, as the protein encoded by this gene is expressed in the medulla of the hair fibre (Schmidt et al. 2001). Moreover, the expression of the gene encoding the high sulphur protein B2F was also increased in late exogen samples, whilst this protein has previously been located in the cortex of the hair fibre (Mitsui et al. 1998). The gene transcript for *Trp-2*, also called dopachrome tautomerase, was identified as more highly expressed in early exogen samples compared to late exogen. This gene has recently been identified in the bulge region of human hair follicles (Ohyama et al. 2006) although here was also expressed in the plucked fibre gene list. The enzyme *Ptgs2*, involved in prostaglandin biosynthesis was also identified as differentially expressed, being 2.4 fold higher in late exogen than early exogen, although was not expressed in the tissue surrounding plucked early exogen club fibres. This has also been previously located in the basal layer of the ORS of mouse pelage anagen hair

follicles, decreasing through catagen and telogen (Muller-Decker et al. 2003). It is thought that stimulation of prostaglandin biosynthesis prolongs the anagen phase of human scalp follicles (Michelet et al. 1997), especially as a transgenic mouse expressing overexpressing *Ptgs2* exhibits a shortened anagen phase and associated alopecia (Muller-Decker et al. 2003).

The gene *Crip1* was also identified on the microarray as up in early exogen populations 2.2 fold over late exogen. This has previously been reported in the ORS of the ferret hair follicle, where gene expression decreased in late anagen compared to all other stages (Gordon et al. 2004).

As a large cell based area was selected for microarray analysis, many gene changes may be related to other changes in the follicle, such as those in the bulge region, or the cortex of the hair fibre. The small fold changes observed with the microarray analysis may be explained by this as larger changes in the region of the club fibre may have been diluted out amongst the broader cell population. An alternative approach would have been to directly compare plucked club fibres at different stages, although the limited amount of material from these would have required amplification, and possibly distortion of results. This is particularly relevant for late exogen club fibres to which little, if any, material is attached. However, as early exogen club fibres have cellular material attached, these were selected, their gene expression amplified, and a gene profile generated of them. Although the resulting list was several thousand genes long, the procedure was useful. Plucked club fibre profiling enabled cross referencing with the differentially expressed gene lists. This allowed genes in the vicinity of the club fibre to be selected, with the assumption made that they would be more relevant for studying the club fibre.

As no individual genes were identified with very high fold changes between early and late exogen populations, gene transcripts were grouped into respective categories to try and extract more information from the data. This method was successful, identifying categories which could be relevant for extracting information about club fibre formation, retention and release. In particular, a key group identified that showed variation between early and late exogen samples was the protease/protease inhibitor grouping. This highlights a potential role for proteases in club fibre release.

Although groups were initially selected based on information generated from literature searches, a number of transcripts did not fit into these assigned categories. In line with the remaining gene transcripts, categories that distinguished between genes involved in transcription, transportation, those with enzyme activity or involved in regulation of the cell cycle were assigned. Grouping of the data clustered together previously unassociated genes. Although only small fold changes were observed with the microarray analysis, presentation of data in a group format helped to identify key processes, such as proteolytic degradation, that may be occurring in the cells surrounding the club fibre.

4.4.2: A role for proteases in club fibre retention and release

Microarray analysis comparing early exogen and late exogen vibrissa club fibres identified a number of proteases and protease inhibitors that varied in gene expression during club fibre maturation. These could be grouped into Serine Proteases and their inhibitors, or matrix metalloproteases (MMP's) and their inhibitors. Therefore, this analysis identified these two protease groups as potential targets for further investigation into club fibre retention and loss. Protease inhibitors were present in the early stages of club maturation whilst an increase in protease expression correlated inversely with a decrease in protease inhibitors seen with the maturation of the club fibre, highlighting a role for proteases in mediating club fibre release. The relatively small changes in protease and inhibitor levels observed in the microarray results, rather than a larger change in one gene indicates that a collective process is involved in the proteolytic release of the club fibre.

Although not falling into the serine protease or MMP category, the cysteine protease, Ctsl has previously been implicated in club fibre formation highlighting the importance of proteases and their inhibitors in both hair cycling and club formation. Mice deficient for *Ctsl* have a club fibre mooring defect due to poorly formed trichilemmal keratin layers and desmosomal contacts that are unable to secure the club fibre (Tobin et al. 2002). This deficiency has also been detected as the molecular defect underlying the *furless* phenotype (Roth et al. 2000) and these authors proposed that the loss of this lysosomal protease disturbs normal telogen development, as a consequence of a delayed catagen phase. Lack of *Ctsl* also causes

hyperproliferation and thickening of the epidermis since cathepsins usually maintain a balance between proliferation and terminal differentiation of epidermal keratinocytes (Roth et al. 2000).

Of proteases identified with the microarray analysis kallikrein 8 (Klk8), a serine protease associated with terminal differentiation and epidermal desquamation (Kuwae et al. 2002; Kishibe et al. 2006), has previously been detected in the vibrissa follicle localised to Huxley's layer of the IRS and hair cortex (Inoue et al. 1998). Contrasting work from another group who used in-situ hybridisation to detect *KLK8* in human scalp tissue showed no mRNA expression in the hair follicle although many other family members were expressed (Komatsu et al. 2003). In particular, these authors found Kallikrein 5 (*KLK5*) and Kallikrein 7 (*KLK7*), respectively known as Stratum Corneum Tryptic Enzyme (SCTE) and Stratum Corneum Chymotryptic Enzyme (SCCE), in the human hair follicle. Both *SCTE* and *SCCE* were found localised throughout the IRS during anagen (Sondell et al. 1994; Ekholm and Egelrud 1998; Ekholm et al. 2000), whilst *SCCE* was also present in the companion layer of the follicle (Ekholm and Egelrud 1998; Ekholm et al. 2000). In the epidermis SCTE is expressed in the stratum corneum (Ekholm et al. 2000) whilst SCCE expression is detected in both the stratum corneum and the granular layer (Lundström and Egelrud 1991; Sondell et al. 1994) with proposed roles regulating epidermal desquamation (Egelrud 2000; Brattsand et al. 2005). Expression of SCCE during telogen has not been documented, although given the close similarities between the companion layer and the single cell layer surrounding the club fibre (discussed in Chapter 3.4.2) it is tempting to speculate that SCCE may be present around the club fibre, with a role in desmosomal cleavage controlling club fibre release. This idea is especially interesting since SCCE is responsible for the *in vitro* degradation of the desmosomal component Dsg1 (Caubet et al. 2004), detected in the suprabasal ORS surrounding both vibrissa and scalp (Wu et al. 2003) club fibres. In 2002 Egelrud's group produced a transgenic mouse expressing human *SCCE* which exhibited increased epidermal thickness with hyperkeratosis, hair loss surrounding the eyes, and thinning of pelage hair with increasing age of the mice (Hansson et al. 2002).

The serine protease inhibitor, PAI-2, present in the granular layer of the epidermis has also been detected in one to two cell layers of keratinocytes around the telogen

club fibre in both mice and humans (Lavker et al. 1998; Jensen et al. 2000). The presence of PAI-2 around the club fibre has led to speculation that the last step before club release is proteolytic (Lavker et al. 1998; Milner et al. 2002) which accords with the results generated in the microarray analysis in this thesis implicating serine proteases and their inhibitors as possible mediators of club retention and release. The role of PAI-2 is not fully understood although in addition to its presence in the hair follicle and upper layers of the epidermis, PAI-2 has also been detected in the matrix and nail bed of the nail (Lavker et al. 1998). All three of these sites contain cell types prior to them undergoing terminal differentiation (Lavker et al. 1998). One proposal is that PAI-2 has a cyto-protective role in the hair follicle, preventing apoptosis of the cells, and degradation of cellular components such as desmosomes that are important in retaining the club fibre (Lavker et al. 1998). Another theory is that PAI-2 has a role at the club fibre attachment site inhibiting terminal differentiation, and maintaining some structural flexibility between the trichilemmal keratin and ORS, thus preventing brittleness which would prevent the club fibre becoming detached during grooming (Lavker et al. 1998). This is in parallel to the role of PAI-2 in the epidermis where expression of the protease inhibitor in more differentiated keratinocytes is thought to protect them from premature maturation by inhibiting expression of involucrin in the cornified envelope (Lian and Yang 2004).

Serine proteases regulate various physiological processes within the body through a variety of functions such as tissue remodelling and protein processing and digestion. In the skin their role is a predominantly required to initiate signalling and proteolytic cascades required for the degradation of intercellular adhesive components such as desmosomes during epidermal differentiation and desquamation (Brattsand et al. 2005). A balance of serine proteases is required for proper epidermal function as both overexpression or improper functioning of proteases can lead to a number of disorders associated with altered barrier function (Ny and Egelrud 2004; Leyvraz et al. 2005), or hyperkeratosis and epidermal thickening (Hansson et al. 2002). In contrast to serine proteases, MMP's are primarily located in the ECM where they assist in protein degradation and tissue remodelling. TIMPs, of which 4 have so far been characterised (Docherty et al. 1985; Apte et al. 1994; Greene et al. 1996; Hammani et al. 1996), play a key role in maintaining the balance between degradation and deposition of the ECM, by inhibiting MMP's (Gomez et al. 1997).

The presence of serine proteases in the skin and hair follicle has previously been investigated. With intercellular adhesive components believed to be of fundamental importance for club fibre retention, an obvious assumption is that serine proteases may assist in the degradation of these, enabling club fibre release. However, relatively little is known about the remodelling of the ECM and its role during club fibre retention and loss, and this area merits further discussion.

TIMP1 gene expression has previously been detected in the IRS of mouse pelage follicles during anagen (Kawabe et al. 1991) whilst *TIMP3* mRNA has been located in the ORS of human scalp follicles during anagen (Airola et al. 1998). The identification of the metalloproteinase inhibitor TIMP3, surrounding club fibres is novel. This, the second protease inhibitor to be detected in the companion^{CL} layer further supports the hypothesis that the last step before club release is proteolytic. TIMP3, like other members of its family can inhibit several MMP proteins (Apte et al. 1995). However, separate from its MMP inhibitory activity TIMP3 has properties making it unique amongst the TIMP family. One example is that it is capable of inhibiting the TNFa converting enzyme (TACE), also known as ADAM-17 (Amour et al. 1998), thereby controlling the cleavage and release of the active Tumour necrosis factor alpha (TNFa) cytokine at the cell surface. Within the hair follicle TACE is detected in the more differentiated suprabasal ORS keratinocytes that surround the growing fibre (Kawaguchi et al. 2004) although no data has been published on TACE expression surrounding club fibres. However, mice lacking TACE have curly vibrissae and perturbed hair coats, with a dense but disorganised distribution (Peschon et al. 1998) highlighting a role for TACE protein processing within the hair follicle. In addition to TACE, TIMP3 can also inhibit ADAM12S, ADAM19,(Loechel et al. 2000), and along with TIMP1, ADAM10 (Amour et al. 2000), a second member of the family with TNFa convertase function (Lunn et al. 1997; Rosendahl et al. 1997). The ADAM family is a group of cell surface bound proteins with protease and cell adhesion properties which contain both a disintegrin and a metalloprotease domain (ADAM) enabling them the participate in cell-cell and cell matrix interactions (Wolfsberg et al. 1995). TIMP3 is also capable of inhibiting the aggrecan degrading enzymes ADAMTS-4 and ADAMTS-5 (Kashiwagi et al. 2001) perhaps of significance with regards to club fibre formation and loss since *ADAMTS-like 5* mRNA was upregulated in the GeneTraffic generated genelist 2.0

fold in late exogen club fibres samples compared to early exogen, correlating with the decrease in *TIMP3* mRNA expression seen in this stage of club fibre maturation.

In addition to those mentioned above, another unique property of TIMP3 is that it is capable of modulating cell death, both through initiation (Baker et al. 1998; Bond et al. 2000; Fata et al. 2001; Bond et al. 2002; Edwards 2004) and inhibition (Fata et al. 2001; Leco et al. 2001; Mylona et al. 2006) of apoptosis whilst the other TIMP proteins can only inhibit this process. It is thought TIMP3 is able to initiate and modulate apoptosis though the inhibition of TNFa induced apoptosis (Smith et al. 1997; Drynda et al. 2005) whilst signalling via a Fas death domain (FADD) to promote a caspase mediated cell death pathway (Bond et al. 2002). Whilst in various other organs of the body caspase mediated signalling induces classical apoptosis, in the epidermis a caspase mediated pathway regulates the process of terminal differentiation in keratinocytes as they progress upwards through the layers of the epidermis (Weil et al. 1999; Allombert-Blaise et al. 2003; Chaturvedi et al. 2006). Perhaps indicative of a function of TIMP3 in regulating terminal differentiation is its expression in the companion layer, which only appears at the level of keratinisation in Huxley's layer, the region of the companion layer where keratinisation and terminal differentiation occur as indicated by the presence of TUNEL positive cells (Soma et al. 1998). In the light of TIMP3 expression surrounding the club fibre observed here, and taking into account the presence of TUNEL positive cells surrounding club fibres (Tanaka et al. 1998), and the apoptotic nuclei detected by ECM as discussed in Chapter 3.4.3, it is tempting to speculate a role for TIMP3 in mediating terminal differentiation of the companion^{CL} prior to club fibre release. The idea that TIMP3 has a role during terminal differentiation is further supported by the observed pattern seen within the IRS of the vibrissa, where TIMP3 levels increased during terminal differentiation but declined again afterwards.

The observed expression profile of TIMP3 in the cells of both the vibrissa and pelage follicles was a combination of granular or perinuclear. Granular expression is expected and is indicative of the role of TIMP3 as either an MMP or a TACE inhibitor, where its likely role is to prevent degradation of the ECM or to mediate terminal differentiation as discussed above. Previously thought to be exclusively located in the ECM (Gomez et al. 1997), expression outside of this region is less

common although TIMP3 has been observed in the cytoplasm of tumour cells and is believed to inhibit tumour growth (Tunuguntla et al. 2003; Curran et al. 2004; Darnton et al. 2005; Mylona et al. 2006). TIMP3, which is specifically expressed in the G1 phase of the cell cycle (Leco et al. 1994; Wick et al. 1994; Wick et al. 1995) has been shown to hold cells in the G1 phase of the cell cycle as a result of transforming growth factor (TGF) activation (Wick et al. 1994). The perinuclear expression of TIMP3 specific to the companion^{CL} layer, but not to the companion layer, is indicative of a variation in processes occurring as these cells terminally differentiate. Perinuclear localisation of TIMP3 surrounding the club fibre may be related to the function TIMP3 induced G1 arrest. If this were occurring it could help to regulate the progression of terminal differentiation, by maintaining cells in a viable state for longer so that they remain actively interdigitated and secured to the trichilemmal keratin projections through desmosomal contacts-thus holding in the club fibre. Moreover, the higher number of genes encoding proteins involved in cell cycle arrest compared with genes encoding cell cycle progression, as highlighted in the group analysis, leads to the proposal that the companion^{CL} undergoes terminal differentiation as a mechanistic process prior to the release of the club fibre.

Unlike many other proteases detected in the hair follicle, some groups have reported TIMP3 to be absent from interfollicular epidermis (Airola et al. 1998; Vaalamo et al. 1999). However, more recent work has shown TIMP3 expression confined to a few select cells in the basal layer, but still absent from suprabasal layers (Zebrowska et al. 2005; Narbutt et al. 2006). The expression within the follicle is unusual since the companion^{CL} is more differentiated then the remaining ORS as indicated by desmoglein expression (Wu et al. 2003), and therefore it is unexpected to see basal layer markers in this region. However, previous studies have not discussed the specificity of TIMP3 within the basal layer of the epidermis (Zebrowska et al. 2005; Narbutt et al. 2006), and a possible explanation is that expression is appearing in a subpopulation of basal cells as they commit to terminal differentiation, thereby arresting the cell cycle as a mechanistic first step in this process. Supporting this hypothesis is the 6-fold down regulation of *Timp3* mRNA seen in the epidermis of mice who have a psoriasis-like skin disease, induced by an epidermal deletion of JunB, a gene mapped to the psoriasis susceptibility region PSORS6 (Zenz et al. 2005). Psoriasis, in which both TACE and TNFa are upregulated (Kawaguchi et al.

2005), is usually characterised by hyperproliferation of basal cell layers. This is in combination with a delayed onset of terminal differentiation as indicated by the absence of early differentiation markers Keratin 1 and Keratin 10 which are usually present in a subpopulation of basal cells as they commit to terminally differentiate (Bernard et al. 1992). In the epidermis, the commitment to terminal differentiation occurs in the basal layer and is associated initially with cell cycle withdrawal and the upregulation of specific markers (Albers et al. 1987; Watt 1989). By contrast, within the ORS, mitotic figures are observed in both the basal and suprabasal ORS, bar the companion layer (Ito 1989), showing that ORS cells do not necessarily commit to terminal differentiation on exiting the basal layer. Hence, the expression of TIMP3 in the companion^{CL} surrounding the club fibre and in the upper levels of the companion layer may indicate a change in the commitment state of these cells, distinguishing them from the surrounding ORS.

4.4.3: Connexins in the hair follicle

Typically connexins are the structural components of gap junctions. Six connexins form a connexon which spans the cell membrane. When connexons from neighbouring cells dock together this results in the formation of a gap junction (Goodenough 1975), an intercellular communication channel that allows cellular response and signalling by providing a transfer route for ions, nucleotides and other small molecules such as second messengers. Along with these activities, it has been hypothesised that connexin and gap junction signalling has roles in the control of proliferation, differentiation, migration and developmental signalling (reviewed in Richard 2000). The functions attributed to gap junctions and connexins were previously mainly inferred from correlative data since there was a lack of experimental evidence supporting these theories. However, more recently, the importance of signalling via connexins has been illustrated by emerging work describing the prevalence of ectodermal disorders associated with mutations in members of the connexin family, providing direct support for a link between gap junctional communication and tissue homeostasis (reviewed in Kelsell et al. 2001). The generation of connexin knockout mice has also provided experimental evidence supporting connexins in these roles (Reaume et al. 1995; Gong et al. 1999; Teubner et al. 2003).

A number of connexin mutations have been linked to inherited skin disorders, perhaps not unexpectedly since many connexin family members are detected, and have important roles in the epidermis (Guo et al. 1992; Butterweck et al. 1994; Goliger and Paul 1994; Risek et al. 1994; Salomon et al. 1994; Tada and Hashimoto 1997; Di et al. 2001). Of specific interest here is the connexin gene *Gjb6*, where point mutations in the coding region of the gene have given rise to hidrotic ectodermal dysplasia (Lamartine et al. 2000a; Lamartine et al. 2000b; Smith et al. 2002; Zhang et al. 2003; Essenfelder et al. 2004) also known as Clouston syndrome. Mutations in *Gjb6* give rise to distinctive phenotypes such as diffuse palmoplanter keratoderma, or thickening of palm skin as well as nail dystrophies and alopecia as additional characteristic phenotypes (Ando et al. 1988). This link between connexin mutations and hyperproliferative epidermal disorders supports a distinct role for gap junction proteins in regulating both proliferation and differentiation of the epidermis. This control most likely extends to the hair follicle where various connexins have been detected in both the adult follicle and during follicle development (Choudhry et al. 1997; Iguchi et al. 2003; Matic and Simon 2003; Arita et al. 2004; Essenfelder et al. 2005).

4.4.3.1: Differentiation of the Companion^{CL} - evidence from Cx43 expression

The first connexin analysed here was Cx43, encoded by *Gja1*. To date, twenty eight mutations in this gene have been documented, which underlie the condition Oculodentodigital dysplasia (Paznekas et al. 2003). This condition is mainly associated with developmental abnormalities of the face, eyes, limbs and teeth (Richardson et al. 2004) although in a few incidences hair abnormalities such as sparse hair or curly hair have been documented (Kjaer et al. 2004; Kelly et al. 2006). Although Cx43 is the most abundant connexin in the body (reviewed in Laird 2006), the phenotypes associated with its mutations are not as severe as one might expect. This is due to a degree of redundancy between connexins, as observed between connexins in the epidermis (Kretz et al. 2004). Mice lacking the C-terminal domain of Cx43 have prematurely terminally differentiating keratinocytes, leading to the production of large squames which are shed from the skin. The underlying epidermis in these mice is also thinner due to the accelerated differentiation of cell layers

resulting in epidermal barrier defects (Maass et al. 2004). In these animals, the truncated Cx43 still forms gap junctions, but these lack the essential functions of Cx43. This is in contrast to mice where Cx43 is absent, where compensation by other connexins is observed (Kretz et al. 2004; Maass et al. 2004).

Differences in the epidermal expression of Cx43 have been highlighted between rodent and human skin. In rodent back skin, expression is localised to the basal and, most intensely, the spinous layer (Butterweck et al. 1994; Goliger and Paul 1994). By contrast in human skin, Cx43 is expressed in the granular layer as well as the spinous layer with only weak basal layer expression (Guo et al. 1992; Salomon et al. 1994). Although expression is visible in the basal layer, slow cycling stem cells located here do not express Cx43 (Matic et al. 2002). This is also the case for stem cells in the bulge of the vibrissa hair follicle (Matic and Simon 2003), although the presence of gap junctions in the bulge has been detected with electron microscopy (Arita et al. 2004). The varying expression of Cx43 in back skin correlates with the degree of differentiation of the epidermis, also reported in an organotypic rat skin culture composed of basal, suprabasal and cornified layers (Maher et al. 2005). Using these cultures, Laird's group showed that Cx26 and Cx43 are regulated during epidermal differentiation whilst depicting the life cycle of connexins through keratinocyte differentiation to programmed cell death (Maher et al. 2005).

In the vibrissa follicle Cx43 is expressed throughout the ORS. However, the highest levels of expression were detected in the more differentiated cells of the ORS, that is in the companion layer of the anagen fibre, and the companion^{CL}. The reduction in expression of Cx43 in the companion^{CL} with exogen progression reflects a change in the differentiation state of these cells prior to club fibre loss. Based on this observation I propose that cell signalling, mediated through gap junction channels containing Cx43 is likely to control the differentiation process in the companion^{CL}, maintaining the cells in a pre-terminally differentiated state. Whether terminal differentiation of keratinocytes is a prerequisite for club fibre loss, or whether a signal for club fibre release which results in the breakdown of cell contacts is independent of the differentiation state remains unknown.

An interesting correlation between retinoids and connexins has been presented by Bertram's group, who showed that retinoid treated human skin has an increase in Cx43 protein in the granular layer of the epidermis which is believed to be of mechanistic significance (Guo et al. 1992). Previously, this group had shown that retinoid action on cell proliferation correlated with an increase in gap junctional communication and Cx43 expression in the mouse 10T1/2 cell line (Mehta et al. 1989). Both these findings are of significance since retinoids are known to be regulators of epithelial proliferation and differentiation, having positive effects on cell growth whilst inhibiting terminal differentiation (Fuchs and Green 1981; Kopan et al. 1987; Kopan and Fuchs 1989). By exhibiting control over Cx43 at the transcriptional level, retinoids are hypothesised to inhibit keratinocyte differentiation through gap junctional communication (Vine et al. 2005). In the context of the hair follicle retinoid therapy affects hair cycling by causing premature exit from anagen, combined with alopecia due to defective telogen anchorage (Berth-Jones and Hutchinson 1995). Retinoid treatment of hair follicle organ cultures causes catagen regression, premature club hair formation and is believed to be mediated through TGFß, a key inducer of catagen (Foitzik et al. 2005). TGFß, which also causes club fibre formation and anagen termination in organ culture (Soma et al. 1998; Foitzik et al. 2000) has been implicated as a key modulator of Cx43 expression (Chiba et al. 1994; Hirschi et al. 2003; Kabir et al. 2005) and is a possible signal transmitter between retinoids and Cx43 . The differentiation of ORS cells during club fibre development, modulated through gap junctional signalling is perhaps a downstream effect of TGFß signalling.

4.4.3.2: Cell death in the companion^{CL} - evidence from Cx30 expression

The second connexin investigated here, Cx30, has close sequence homology with Connexin 26 (Cx26) both in rodents (Dahl et al. 1996) and humans (Grifa et al. 1999), explaining why germline mutations in either, underlie disorders with similar phenotypes. Often, disorders are associated with alterations in ectodermal epithelium, both giving rise to typical phenotypes such as palmoplanter keratoderma (Jan et al. 2004).

The expression pattern of Cx30 in the ORS of both rat vibrissa and mouse pelage follicles was unusual as expression was present in the cytoplasm, and not at the cell membrane unlike the other compartments of the follicle. These results presented here are in distinct contrast to previous expression studies in the human follicle which showed localisation of Cx30 at the cell membrane of ORS keratinocytes (Essenfelder et al. 2005). Both the Cx30 antibody used in this thesis and the Cx30 antibody used by Essenfelder *et al* originate from the same source. In addition, this antibody has previously been shown to specifically label Cx30 (Nagy et al. 1999; Rash et al. 2001), and hence this variation in cellular localisation between human scalp and rat vibrissa follicles is surprising. The varying cellular location of Cx30 between species and in different compartments of the vibrissa may be indicative of Cx30 having more than one role within the hair follicle, possibly mediated through the splicing of the Cx30 gene, of which four of the potential six variants have been detected in hair follicle keratinocytes (Essenfelder et al. 2005). Localisation of connexins in the cytoplasm has been documented in other studies which have suggested connexins have functions independent of gap junctional communication, such as growth inhibition (Krutovskikh et al. 2000; Qin et al. 2002; Dang et al. 2003; Qin et al. 2003).

In keratinocytes transfected with mutant forms of Cx30, with the harboured mutations resembling the dominant mutations seen in Cx30 from patients with Hidrotic Ectodermal Dysplasia Cx30, expression of Cx30 is localised in the cytoplasm (Common et al. 2002). This cytoplasmic localisation is attributed to impaired protein trafficking from the cytoplasm to the cell membrane (Common et al. 2002). A prominent feature in the epidermis of patients with Hidrotic Ectodermal Dysplasia is the number of desmosomal discs that are still present in the stratum corneum (Ando et al. 1988). This suggests that apoptosis required for proper desquamation and desmosomal degradation is not occurring. The cytoplasmic expression of Cx26, a close homolog of Cx30, has been reported to co-localise with anti-apoptotic markers, suggesting a putative role for cytoplasmic connexins in the prevention of apoptosis (Kanczuga-Koda et al. 2005). This would explain the observations seen in Hidrotic Ectodermal Dysplasia caused by a lack of apoptosis. Linking this with the hair follicle, the presence of apoptotic cells, thought to be mediating a specialised process of keratinisation, are observed in the cells of the companion layer and in the companion^{CL} (Tanaka et al. 1998). This provides an explanation for the absence of

Cx30 in the companion^{CL} cells next to the club. The presence of Cx30 in the remaining ORS may therefore be indicative of its protective role in preventing cell death as demonstrated in Figure 4.22. The observations described here regarding the expression of Cx30, or rather its absence as seen in the suprabasal keratinocytes surrounding both pelage and vibrissa club fibres highlights the differences between the cells immediately adjacent to the club fibre as compared to the rest of the ORS.

Furthermore, the analysis of plucked club fibres showed that no *Gjb6* expression (Cx30) was present in the cells that remained attached to early exogen club fibres when pulled out prematurely. This observation supports the proposal in Chapter 3.4.4 that suggests the breakage plane in premature club fibre loss, perhaps due to excessive grooming or hair tugs during fighting, is between the companion^{CL} and the remaining ORS. This is perhaps a protective mechanism to that would prevent the loss of a large number of ORS cells during premature or trauma induced hair loss.

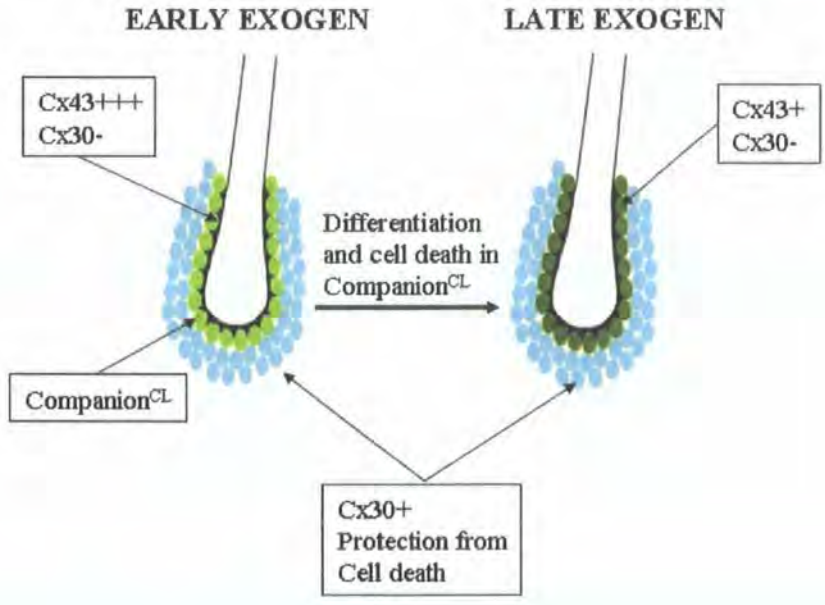

Figure 4. 22: Connexin expression surrounding exogen club fibres
Cx43 expression in the hair follicle decreases in the companion^{CL} with the progression from early to late exogen, inversely correlated with increase of differentiation within this layer. In contrast, Cx30 is not expressed in the companion^{CL} but is present in the surrounding trichilemma sac where we propose that it acts to protect these cells from a terminal differentiation mode of cell death.

4.4.4: Analogies between skin differentiation and desquamation and club formation and shedding-evidence from microarray

Within the groupings that I chose to represent different activities, a number of gene transcripts are linked that have a common involvement in terminal differentiation and cornification. For example, the gene transcript of the cornified envelope protein, *Sprr1b*, was upregulated in late exogen samples. This is in addition to the differential expression of genes encoding the retinoic acid degrading enzyme Cyp26b1, and the protease Klk8, both involved in regulating terminal differentiation.

In 1895, Maurer first identified what we now know as the trichilemmal keratin layer of the club fibre, initially describing it as the stratum corneum layer of the hair follicle (Maurer 1895). The trichilemmal keratin may act in a similar way to the stratum corneum, and provide a slough-able barrier between the hair and the proximal follicle. To maintain a consistent thickness of the stratum corneum, and its integrity as a barrier, there is a delicate balance between the rate of proliferation of corneocytes and the rate of desquamation (Ya-Xian et al. 1999; Egelrud 2000). This dynamic turnover is not, however, a feature of club hair 'desquamation' as shedding is a unique event, whereas stratum corneum desquamates continuously as the epidermis is renewed. However, the key processes that regulate differentiation and desquamation of the epidermis may be mirrored in club fibre maturation and release. In 1984, Vandevelde and Allaerts demonstrated that there was an increasing thiol-disulphide conversion in the epithelial sac surrounding the club fibre trichilemmal keratin, coinciding with the onset of the succeeding hair generation and proposed this as a contributory factor in the loosening of the old club fibre from its epithelial sac (Vandevelde and Allaerts 1984). They likened this process to cornification as a similar thiol-disulphide conversion is associated with epithelial keratinisation prior to desquamation (Broekaert et al. 1982). Of interest on the microarray data is the enzyme *Gpx3* that was higher surrounding early exogen club fibres when compared to late exogen club fibres. This enzyme oxidises the thiol group on glutathione to produce glutathione disulphide. Moreover, in late exogen the enzyme *Gclc* is upregulated, a rate limiting enzyme in glutathione synthesis. The interplay between these two enzymes may be key in altering the thiol-disulphide ratio of the companion^{CL}. This may be what gives

rise to the observed differentiation within this layer, as seen with the changing Cx43 expression.

Although corneocytes are 'dead' in the sense they are non-nucleated, and in this way are similar to the trichilemmal keratin layer of the club fibre, proteolysis of intercellular adhesive structures is a key process in the desquamation process, facilitating the reduction of cell cohesion to the point when the corneocyte is easily dislodged (Bisset et al. 1987; Egelrud et al. 1988; Lundström and Egelrud 1988; 1989; Chapman and Walsh 1990). A similar proteolytic mechanism has been proposed for club fibre cleavage from its surrounding epithelial sac, as chymotryptic and trysin activity has been detected in spontaneously shed club fibres (Milner et al. 2002). Spontaneously shed club fibres are also distinct in that they lack cytological detailing such as prominent nuclei and an abundant cytoplasm which is seen in the cells surrounding club fibres that are prematurely plucked. This suggests that cells surrounding spontaneously shed club fibres have undergone proteolytic degradation leading to the cleavage of the fibre from its surrounding trichilemma sac (Milner et al. 2002). Moreover PAI-2, which is detected in the granular layer of the epidermis and has a role regulating epidermal differentiation (Dano et al. 1985; Lyons-Giordano et al. 1994), is detected in a single layer of keratinocytes that borders the trichilemmal keratin layer of the club fibre in both mice and humans (Lavker et al. 1998; Jensen et al. 2000). This is consistent with Maurer's analogy of the trichilemmal keratin as the stratum corneum, as the cell layer adjacent to the trichilemmal is similar to the granular layer of the epidermis.

Supporting a possible link between desquamation and club shedding are clinical observations of altered hair shedding in cases of severe dandruff and seborrheic dermatitis, disorders exhibiting altered epidermal desquamation. Pierard-Franchimont *et al* (2006) found a positive correlation with the number of club fibres in plucked trichogram counts, and the severity of dandruff. This may be due to a shift in the anagen:telogen ratio towards an increased number of telogen follicles, or alternatively may be indicative of an increase in the length of time a club is retained prior to shedding suggesting a delayed exogen with dandruff, with the cycle of the follicle unaffected. Antidandruff treatments have also been proposed to increase the proportion of follicles in anagen as measured by plucked trichograms (Pierard-

Franchimont et al. 2002). However, care must be taken interpreting such results because a treatment induced loss of club fibres could drive up the calculated anagen:telogen ratio as latent follicles are not taken into account using a plucked trichogram method of density measurement, and could contribute to an increased percentage of anagen.

Few factors involved in differentiation have been described in the club hair trichilemmal keratin or the trichilemma sac. However, some molecular entities found in this study support the idea of similarities between epidermal differentiation and the regulation of differentiation in club formation and retention. These include *IL18* and *Prlr*, both identified in the microarray analysis as higher in late exogen, and in the tissue surrounding plucked fibres. Both IL18 and Prlr are upregulated after the onset of calcium induced terminal differentiation in epidermal keratinocytes (Poumay et al. 1999; Kong and Li 2002). Moreover, in addition to Prlr which was detected in this study, Carcinoembryonic antigen (CEA), Calretinin and S100A6 are detected specifically in the companion^{CL} (Honda et al. 1997; Ito and Kizawa 2001; Foitzik et al. 2003; Poblet et al. 2005). Whilst Prlr is upregulated after the onset of terminal differentiation, CEA has a proposed cell adhesion role during epidermal differentiation and in the nail bed (Egawa et al. 1996; Egawa et al. 2000). These observations support a plausible link between differentiation of the skin and around the club fibre. Moreover, both S100A6 and Calretinin are members of the calcium binding S100 family, located on the epidermal differentiation gene complex (SchaÈfer et al. 1995) with likely roles regulating calcium dependent terminal differentiation. A main difference however, between the innermost cell layer surrounding the club fibre and the epidermis is the lack of a calcium gradient to drive differentiation. In the epidermis, a calcium gradient is observed through from the basal layer of the epidermis up to the stratum granulosm (Menon et al. 1985; Elias et al. 2002). As the companion^{CL} is a single layer of cells, a calcium gradient cannot exist between cells. Nevertheless, modulation of intracellular calcium levels may enable regulation of calcium dependent enzymes such as transglutaminase, with a functional role in the cross linking of the cornified envelope during terminal differentiation (Kalinin et al. 2002). Perhaps the numbers of calcium dependent signal transducers identified by the microarray analysis as differentially expressed are of significance. Moreover, the expression of transglutaminase 3 in late exogen, as

identified on the GeneTraffic gene list (Appendix 2ii) may also be of significance during this process.

4.4.5: Signal mediated release of the club fibre

Although there is evidence of differentiation of the companion^{CL} associated with the progression through exogen there is still little evidence per se of a distinct signal that initiates club fibre release. Of the three signals identified through microarray technology, two were cytokines whilst one was a neuropeptide, Natriuretic Peptide Precurser C (*Nppc*). However, no hair abnormalities have been reported in Nppc knockout mice (Chusho et al. 2001).

IL18, which is expressed in the granular and cornified layers of mouse epidermis, increases with calcium induced differentiation in keratinocytes (Kong and Li 2002). Moreover, this IL18 increase can be inhibited by blocking the calcium induced keratinocyte differentiation with a protein kinase C (PKC) inhibitor (Kong and Li 2002). This is perhaps relevant as the calcium gradient observed in the epidermis that regulates the transition from the basal to the cornified layers is coordinated in part through a PKC signalling cascade (Dlugosz and Yuspa 1993; 1994; Denning et al. 1995; Rutberg et al. 1996; Denning et al. 2000).

Within the hair follicle, the presence of both *Pde1a*, and *Ppp3cb*, as identified in this study, alludes to a possible calcium dependent signalling cascade in the companion^{CL} as Ppp3cb encodes a calcineurin subunit, whilst Pde1a is calmodulin dependent (Wang et al. 1996). However, whilst in the epidermis Notch-1 is thought to be a critical signal in basal keratinocyte commitment to differentiation (Rangarajan et al. 2001; Blanpain et al. 2006), the microarray approach adopted here did not identify a critical signal that regulates differentiation of the companion^{CL} prior to club fibre release.

4.4.6: Other observations:

4.4.6.1: Anagen initiation and wound repair-linking with connexins

Connexin proteins, in particular Cx26, Cx30, Cx30.1 and Cx43 have been shown to have distinct expression patterns during epithelial wound healing in both rodents (Goliger and Paul 1995; Coutinho et al. 2003; Kretz et al. 2003) and humans (Brandner et al. 2004). Typically it seems that the initial response after injury is to down-regulate the expression of all connexins at the wound site, followed shortly by a dramatic increase in the expression of Cx26 and Cx30 at the leading edge of the wound. Becker's group showed an inverse correlation between Cx26, Cx30 and proliferation in the cells adjacent to the wound suggesting a possible negative role of these proteins in proliferation (Coutinho et al. 2003). In contrast to Cx26 and Cx30, the expression of Cx43 remains low during initial wound healing until epithelialisation of the wound is completed, after which a dramatic increase is observed in the differentiating cells of the epidermis. This implies that the down-regulation of Cx43 is a prerequisite for the migration of keratinocytes to the wound edge (Coutinho et al. 2003). This hypothesis is supported by other results showing the continued presence of Cx43 at non-healing wound sites (Brandner et al. 2004). Related results have emerged from Ott's lab, where a mouse with a conditional *Cx43* gene knockout targeted to the epidermis was used to examine the effect of a loss of Cx43 following wounding (Kretz et al. 2003). In this mouse, the rate of wound closure was accelerated by a day compared to the wildtype, an observation concurrent with results presented by Becker's lab who used a topically applied anti-sense oligodeoxyribonucleotide to reduce the protein expression of Cx43, thereby accelerating wound closure in mouse skin (Qiu et al. 2003). The anti-sense oligodeoxyribonucleotide approach has also been shown to accelerate healing in burn wounds, by reducing the spread of death signals from injured cells to the surrounding tissue, thereby reducing wound thickness and scar tissue (Coutinho et al. 2005). These findings are concurrent with the perceived role of gap junctions and suggest that gap junctional communication plays a key role during wound healing.

In addition to the role of connexins, during wound closure there is most likely an involvement from a stem cell population, required to regenerate the epidermis. Stem

cells have been identified migrating from a stem cell niche in the hair follicle, the bulge, into the epidermis in response to wounding (Taylor et al. 2000) whilst the dermal sheath has also been hypothesised to have a role in dermal wound healing (Jahoda and Reynolds 2001). Moreover, expression studies have shown that Cx26, Cx30 and Cx43 are downregulated in the ORS and IRS of hair follicles with close proximity to wound sites as an initial response to wounding, possibly due to de-differentiation of keratinocytes as they migrate to the wound (Coutinho et al. 2003).

The mechanics underlying wound healing are very similar to those involved in anagen progression during the hair follicle cycle, as directed migration of keratinocytes is required for both. Increasingly, hair follicle regeneration is becoming a popular model with which to study wound healing (Coulombe 2003) as evidence emerges that the two processes, regeneration and wound repair, are more closely related than previously thought. An example of this is seen with keratinocyte specific Stat3 disrupted mice, which have normal hair follicle development but after the first growth cycle show a disrupted onset of the second anagen phase. Additionally, these mice exhibit severely impaired wound healing, both of these disruptions being due to the loss of Stat-3 mediated keratinocyte migration from the bulge region of the follicle (Sano et al. 1999; Sano et al. 2001).

Basement membrane remodelling is a prominent feature during both anagen initiation in the hair cycle and wound healing. In particular in the hair follicle, studies in the rat vibrissa (Young and Oliver 1976; Young 1980; Jahoda et al. 1992b) have indicated that the most dynamic changes occur during late telogen and the initiation of anagen when the outer dermal-epidermal junction, termed the glassy membrane, thickens significantly whilst displaying a double layered structure into which dermal sheath cells protrude (Jahoda et al. 1992b). This change correlates with an increase in fibronectin expression when compared to late anagen and catagen follicles (Jahoda et al. 1992b). Changes in the outer basement membrane are in contrast to those seen at the base of the papilla-epidermal junction where sparse fibronectin levels are observed (Jahoda et al. 1992b). The changes in fibronectin expression during basement membrane remodelling were the most apparent in the follicle, whilst Laminin and collagen IV expression remained continuous over the whole basement membrane zone during this process. Ultrastructurally, thickening at the base of the

inner papilla-epidermal membrane is observed during late telogen and the initiation of anagen whilst at the tip of the papilla the basal lamina remains just one cell layer thick (Jahoda et al. 1992b).

The dynamic changes of the lower vibrissa follicle during the telogen to anagen transition have parallels with the present observations concerning connexin expression in the vibrissa follicle bulb, which provoke discussions as to the role of gap junctional communication at the initiation of anagen. One interesting observation is the increase in Cx30 expression in keratinocytes adjacent to the glassy membrane during the initiation of anagen, highlighting a similarity between these cells and those at the leading migratory edge during wound healing. The complementary loss of Cx43 at the basal edges of these cells further supports the comparison of this layer of cells with the leading edge during wound repair.

The transition of expression of Cx30 from the outer epidermal surface to the inner epidermal surface in the telogen to anagen transition correlates with the changing profile of fibronectin in the underlying basement membrane (Jahoda et al. 1992b) possibly linking fibronectin with a role in the control of gap junction formation and signalling in the bulb of the follicle. The variable components of the underlying extracellular matrix in keratinocyte cultures has been shown to influence gap junction formation and intercellular communication, with an underlying fibronectin substrate influencing signalling the least when compared to laminin and collagen substrates (Lampe et al. 1998). The same phenomenon may be present in the follicle, with the formation of gap junctions being influenced by the changing extracellular matrix profile in the basement membrane. With regards to the dermal-epidermal interaction at the inner basement membrane interface, it is unlikely that gap junctional signalling acts directly to transmit signals from the papilla to the surrounding epithelium, regardless of the Cx43 expression in the dermal papilla. Dye transfer assays performed during hair follicle development showed no gap junction communication between these two compartments (Choudhry et al. 1997). However, the components of the basement membrane may act as an intermediate between these two compartments, modulating gap junctional signalling through its changing expression profile in the initiation of anagen. Elements of the extracellular matrix may have a yet unrecognised role during anagen initiation, acting to induce gap junctional

formation and signalling required for follicle growth. The expression of Cx30 at the cell membrane on the epidermal side of the new papilla apex, and in a few select germinative cells presents a possible function for Cx30 mediated gap junctional signalling during follicle growth.

4.4.6.2: A possible role for Id3 in stem cell trafficking

The hair follicle harbours a stem cell population, the bulge, (Cotsarelis et al. 1990) that can undergo two distinct pathways of migration/commitment either upwards towards the epidermis in response to wounding or downwards to form various lineages of the hair follicle in response to mesenchymal-epithelial interactions at the initiation of anagen (Taylor et al. 2000). In 2001, Barrandon's group presented a traffic light hypothesis of stem cell migration within the mouse vibrissa follicle. They proposed that in this specialised follicle, stem cells or multipotent progenitor cells migrate from the bulge down to the bulb throughout the period of anagen to replenish the rapidly proliferating keratinocytes of the bulb region (Oshima et al. 2001). Their hypothesis, outlined in Figure 4.23 indicated that in late anagen through to catagen and telogen, migration is halted at the level of the hair bulb and the incoming cells from above begin to pile up in the ORS alongside the growing fibre. Movement resumes again at the beginning of the new anagen cycle. The migration pattern within the specialised mouse vibrissa is similar to what you would expect to see in the human scalp hair follicle, which has a long anagen period and requires continuous migration of stem cells from the bulge to replenish the matrix and maintain the follicle in anagen (Lyle et al. 1998). However, in mouse pelage follicles which have a short anagen duration, migration from the bulge is not required during anagen, just a movement from the bulge region at anagen onset (Hanakawa et al. 2004).

Expression of the transcriptional regulator Id3 has previously been associated pre-migratory and migratory neural crest stem cells, and has a role preventing premature differentiation of neural crest cells, and loss of the neural crest progenitor pools (Kee and Bronner-Fraser 2005; Light et al. 2005). More recent work has indicated that the pluripotent stem cells in the bulge region of the vibrissa follicle, are neural crest derived (Sieber-Blum and Grim 2004). Taking this information together with the pattern of Id3 staining in vibrissae as described in this thesis it is tempting to

speculate that the Id3 positive cells seen in the lower ORS during anagen have their origin in the bulge of the follicle. It is plausible that these Id3 positive cells of the ORS are neural crest derived, and are migrating from the bulge to the germinative matrix. The increase in positive cells in late anagen and catagen vibrissa is consistent with this notion, as the patterning of Id3 correlates with stem cell location in the traffic light hypothesis of migration.

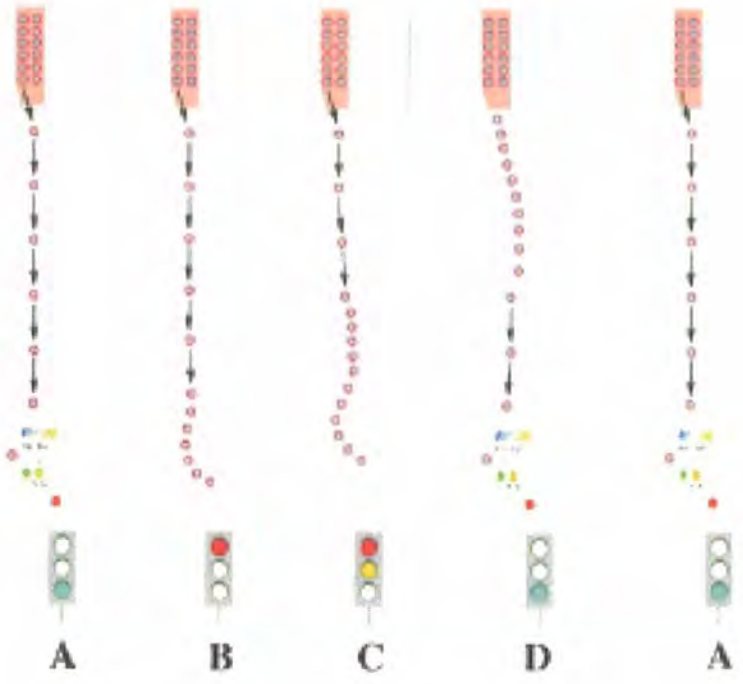

Figure 4. 23: Traffic light hypothesis of Stem cell migration in the Vibrissae (taken from Oshima *et al* (2001)

Panel A: During anagen, stem cells continuosly migrate from the bulge down to the hair bulb. When whisker growth stops, during late anagen and catagen (Panel B) these stem cells start to build up higher and higher in the follicle (Panel C). On the iniation of anagen again (Panel D) stem cells start moving from the bottom of this pile of stem cells. Once back in anagen, the build up of stem cells begins to migrate again, and spread out down towards the bulb (Panel A)

In the area of ORS beneath the bulge during early anagen, a cluster of Id3 positive cells was also visible, although Id3 had a cytoplasmic location. Usually, Id3 is detected in the nucleus where its functional role is as a dominant negative inhibitor of basic helix loop helix (bHLH) transcription factors, thereby playing a pivotal role in the control of cell growth, differentiation and cell lineage commitment. Cytoplasmic localisation of Id3 may be a method by which post-translational regulation of the protein can be exhibited although the presence of Id3 in the cytoplasm may regulated through various pathways. Norton and his co-workers (Deed et al. 1996) showed that in the absence of bHLH transcription factors, which contain a nuclear localisation signal, Id3 was localised to the cytoplasm. In the presence of these factors, they showed Id3 to be chaperoned to the nucleus. Contrasting work by Samanta and Kessler found that Id's can sequester bHLH proteins in the cytoplasm thus promoting cell differentiation (Samanta and Kessler 2004). Yokota's group have also presented work showing active nuclear export of Id proteins, which inhibits the suppressive behaviour of Id's on bHLH factors (Kurooka and Yokota 2005; Makita et al. 2006). This various work shows the variety of dynamic ways in which Id proteins can be regulated, and these different ways are likely to have an impact on the regulation of transcription within the nucleus.

In the bulge region of the hair follicle two distinct populations of cells have been identified (Blanpain et al. 2004), both of which are growth inhibited although regulated by separate transcription programs. The first population consists of stem cells in the basal layer of the ORS, whilst the second population is derived from the original bulge population, and is formed during the first postnatal hair cycle. Both populations form the stem cell niche although the suprabasal bulge cells and are distinct in that they have lost their basal lamina contacts, and have potentially undergone early hair follicle commitment. However, they retain all the stem cell characteristics of bulge cells such as self renewal and multipotency (Blanpain et al. 2004). The location of the suprabasal bulge cells correlates with the cytoplasmic expression of Id3 protein. Expression of Id3 mRNA within the bulge region is part of the molecular signature of this stem cell niche within the hair follicle (Blanpain et al. 2004; Morris et al. 2004; Tumbar et al. 2004) so Id3 protein is not unexpected here. The cytoplasmic location of Id3 within the suprabasal bulge cells may be a unique means by which the cell is controlling the negative regulation of transcription that

underlies cell fate determination. Potentially, cytoplasmic localisation of Id3 may allow early commitment of the cell towards a hair follicle lineage prior to migration down the follicle.

Although the hair germ is a biologically and morphologically distinct unit from the bulge (Ito et al. 2002), the former has been shown to be derived from the lowermost portion of the latter in late catagen in mouse pelage follicles (Ito et al. 2004). The cells of the secondary hair germ are not irreversibly committed and are able to revert back to bulge stem cells in response to wounding (Ito et al. 2004). Originally stem cells within the hair germ were believe to originate from the lower part of the follicle (Chase et al. 1951) although lineage analysis on bulge cells from mouse pelage follicles has indicated that they are able to form all epidermal lineages of the hair follicle (Morris et al. 2004), thus validating the presence of bulge cells in the hair germ. With anagen initiation, the secondary hair germ is thought to form the germinative matrix surrounding the dermal papilla. Although a secondary hair germ has not been identified in the vibrissa follicle, it does have a germinative matrix, with clonagenic potential. The germinative cells seen at the base of the bulb in the vibrissa follicle are thought to be derived from the bulge region. There are thought to be three types of epithelial cells comprising this germinative region (Osada and Kobayashi 2001) the first of which, type 1, are slow cycling cells located at the base of the bulb regarded as stem cells or young transit amplifying cells as they have both the ability to self renew or form type 2 cells. Type 2 cells, found in the basal layer of cells around the dermal papilla proliferate more than type 1 cells, and are able to form type 3 cells which are matrix cells destined to terminally differentiate into the various lineages of the follicle (Osada and Kobayashi 2001). The location of Id3 cells in early anagen vibrissae corresponds with the localisation of Type 1 cells at the base of the matrix. It appears that Id3 is lost from the stem cells or their close progenitors enabling transcription, and differentiation into multiple lineages of the hair follicle. Three cell types were detected in the germinative region of the bulb throughout the vibrissa cycle except for the late anagen/catagen stage when only type 3 cells were detectable (Osada and Kobayashi 2001). If Id3 only marks type 1 cells, this would explain the loss of Id3 in the base of the hair bulb in the late anagen and catagen samples, corresponding to the loss of stem cells or their progenitors from the germinative compartment.

4.5: Summary

In summary, microarray technology was utilised to try and identify novel genes associated with the proposed cycle stage 'exogen'. Group analysis of the software generated genelists yielded some interesting results. The most consistant and convincing changes seen between early and late exogen club fibres were in their protease and protease inhibitor expression, suggestive of a proteolytic mediated club fibre release (Figure 4.24). Moreover, the decrease in Cx43 expression surrounding club fibres as they prepare for release is suggestive of companion^{CL} specific differentiation (Figure 4.24). Before final release there is evidence that cell death occurs in the companion^{CL}, distinguishing this layer from the surrounding trichilemma sac.

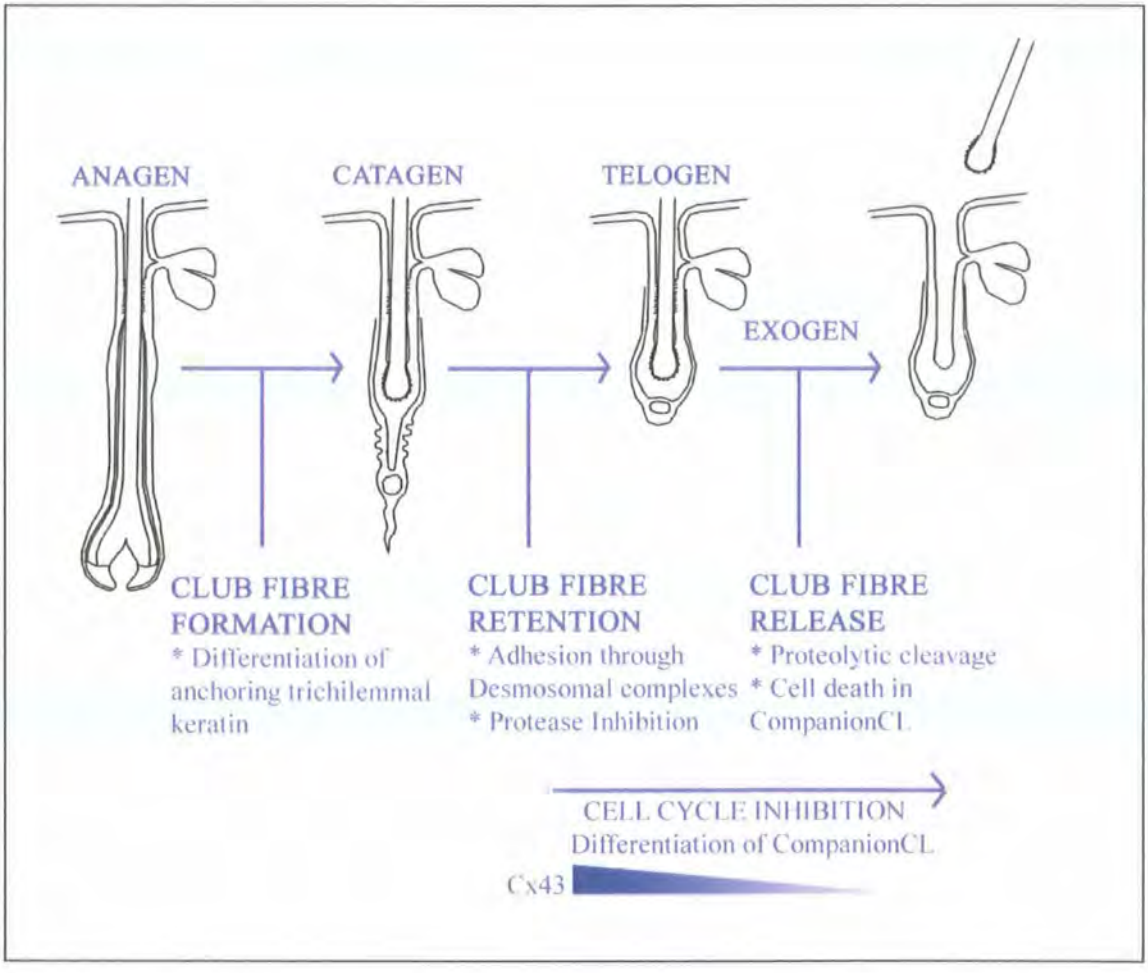

Figure 4. 24: Mechanisms of club fibre formation, retention and release

Aside from a possible hormonal signal, there is little evidence from this vibrissa follicle model of the initiating signal for club fibre release. The mode of club fibre release has many parallels with differentiation and desquamation within the epidermis, and valuable information may be learnt from drawing on this system.

The work in this chapter focused on identifying and validating changes surrounding the club fibre as it prepares for release. However, of importance now is to functionally validate these observed changes as important for club fibre retention and release.

Chapter 5: General Discussion

5.1: Introduction

It is common for animals to grow new hairs before the old club falls out to ensure that they are never naked or without key sensory apparatus such as the whisker. In the majority of cases, premature hair loss in animals would be disastrous as the hair fibre not only provides camouflage but protects against heat loss and heat gain (Stenn and Paus 2001). However, in certain breeds of domestic sheep the wool fibre is shed prior to the formation of a new growing fibre, leaving the follicle empty (Auber and Burns 1947). A similar finding to this has been observed in human scalp hair where a period of latency is observed where a telogen follicle exists without a club hair prior to initiation of anagen (Courtois et al. 1995). This latency period, termed 'kenogen', refers to the state of a follicle without any fibre, and increases with age and balding status in both men and women (Courtois et al. 1994; 1995; Guarrera and Rebora 2005). In particular, in women, an increase in the duration of kenogen has been positively correlated with an increase in the vellus hairs to terminal hair ratio, characteristic of female pattern hair loss (Guarrera and Rebora 2005). Female androgenetic alopecia, or female pattern hair loss, controversially referred to as the female equivalent of male pattern balding (Ludwig 1977) is the most common type of hair loss in women. It can cause psychological stress and reduced body image, and has a more deleterious psychological effect on women that in men (Cash et al. 1993). Although termed female androgenetic alopecia there is little evidence to suggest that increased androgen levels are involved in mediating hair loss (Birch et al. 2006). Moreover, the pattern of hair loss is different from male pattern baldness, being characterised by a diffuse thinning rather than total balding in the frontal and crown regions of the scalp. This is also thought to be associated with in increase in terminal to vellus transitions (Birch et al. 2001; Norwood 2001; Paik et al. 2001). Follicular miniaturisation, the conversion of a vellus to a terminal follicle was traditionally believed to be a slow continuous process, occurring over many cycles. However, Jahoda, 1998, suggested that it may occur as series of step changes between growth cycles, an idea adapted by Whiting who suggested that miniaturisation occurred over one hair growth cycle (Whiting 2001). However, more recent work has led to a three-step mechanism for miniaturisation being proposed whereby follicles firstly exhibit a shortened anagen phase, followed by a reduction in hair thickness, which gradually turns to a vellus follicle (Hoffmann and Van Neste 2005; Van Neste 2006). Studies

in the UK, the USA, Japan and Korea have indicated an increased prevalence of female pattern hair loss associated with ageing (Birch et al. 2001; Norwood 2001; Paik et al. 2001; Tajima et al. 2007).

Another cause of hair thinning is chronic telogen effluvium (CTE), which is to do with the loss of the club fibre rather than the terminal follicle. Chronic, as opposed to acute CTE can last for a number of years and is characterised by diffuse thinning over the entire scalp, excessive daily hair shedding increasing in incidence in middle aged women between 30 and 60 (Whiting 1996b). CTE may represent some synchronisation of follicles in the cycle, but also a reduction in the length of anagen which will lead to increased telogen.

5.1.1: Current research targets in the hair follicle

In searching for therapeutic methods to combat age associated hair loss, potential investigative routes are to detect agents that prolong the growth phase anagen, or to eliminate kenogen by re-initiating anagen from telogen follicles. Another strategy would be to reverse the terminal to vellus transition of the follicle. Currently on the market, the hair loss drug Minoxidil is thought to target all of these areas, although is only successful in a small cohort of people (Whiting 1992; Jacobs et al. 1993). The mechanism of Minoxidil within the follicle is not well understood although hypotheses generally propose it to work as a potassium channel opener, relating to its role outside of the follicle. Arase's group proposed that that Minoxidil increases Adenosine levels through the activation of the potassium channel component SUR2B, resulting in the stimulation of an Adenosine receptor mediated signalling pathway which induces cell growth factors such as Vascular Endothelial Growth Factor (VEGF) in the dermal papilla (Li et al. 2001). Although the effects of Minoxidil on VEGF stimulation in cultured dermal papilla cells have been documented (Lachgar et al. 1998) there is limited evidence on Minoxidil having any effect on potassium channels either in the dermal papilla or the outer root sheath, with most reports showing no effects of Minoxidil on ion gradients within the follicle (Nakaya et al. 1994; Hamaoka et al. 1997). Another suggestion as to the mechanism of Minoxidil is that it increases blood flow to the follicle through increased vascularisation, supported by its effect on VEGF levels (Lachgar et al. 1998). However, work

presented demonstrating the prolongation of follicle growth in organ culture by Minoxidil shows that it is capable of exerting growth effects on the follicle that are unrelated to vascularisation (Buhl et al. 1989; Kiesewetter et al. 1991). Although the mechanism of action of Minoxidil within the follicle is not well known the presentation of novel potassium channel openers that prolong deer follicle growth in vivo is a development within this field (Davies et al. 2005). Moreover, Adenosine is now being employed as a therapeutic agent to prolong hair growth, having been incorporated into the hair loss treatment 'Adenogen' by the cosmetic company Shiseido.

Finasteride is another drug currently available although it is not recommended for pre-menopausal women and does not work on female scalp hair loss. This is because Finasteride works by inhibiting the enzyme 5-alpha reductase (Sudduth and Koronkowski 1993). This enzyme is fundamental in the conversion of testosterone to dihydrotestosterone, a key driving factor in male pattern baldness (Randall 1994). Therefore, Finasteride is only effective as a treatment for male pattern baldness, or for hirsute post-menopausal women (Fruzzetti et al. 1994; Moghetti et al. 1994; Kaufman and Dawber 1999; McClellan and Markham 1999).

Another popular research route is in the identification of natural plant products which have hair growth promoting abilities by inhibiting the apoptotic, catagen inducing effects of TGFß. Currently, extracts from the 'tea of heaven' plant and Procyanindin B-3, a component of barley have been identified (Kamimura and Takahashi 2002; Tsuji et al. 2003), as being important with regard to the development of therapeutic treatments.

5.1.2: Does exogen represent a useful therapeutic target?

In the wool industry, chemical de-fleecing agents have been sought for many years, especially those which do not perturb subsequent wool growth (Reis 1975; Reis et al. 1975a; Reis et al. 1975b; Reis et al. 1999; Luo et al. 2000). Moreover in man, the benefit would be to improve hair density on the scalp by retaining club hairs under conditions where a higher proportion of hair follicles are in telogen, analogous to the pelt of many animals. However, the permanent retention of club hairs would not be

desirable; it remains to be calculated to what extent the prolonged retention of a small but significant proportion of club hairs would have on the overall hair density. The modelling work of Halloy may provide the basis for estimating such parameters (Halloy et al. 2000; 2002) although as of yet exogen has not been incorporated as a cycle stage into computerised studies. The incorporation of cycle stages kenogen and exogen into modelling studies may prove useful when calculating the changes required for a desired effect.

Benefits for hair loss disorders in man would be seen with the prolonging of the duration of anagen or, to approach it from a different angle, the inhibition of catagen. Another effective strategy would be to reduce the duration of kenogen phase, either by delaying exogen or the initiation of anagen. Delaying exogen may provide immediate therapeutic relief, possibly relevant for somebody suffering from chronic telogen effluvium. However, as with all treatments, the underlying causes of hair loss should be deciphered when deciding upon treatment strategies; for example cases of hair loss associated with increased follicular miniaturisation could be better targeted by driving the follicle back from a vellus to a terminal state.

5.2: Implications of current work

Both anagen initiation, in addition to club fibre retention and loss are two areas of the hair follicle cycle that when disrupted can result in hair loss, and therefore serve as potential target areas for the prevention of hair loss. In this thesis I have described two investigative routes, analysing these two aspects of the hair follicle and its cycle, with the development of therapeutic strategies in mind.

In my first results chapter I investigated a new three dimensional model of dermal papilla cell culture and analysed its potential as a representative model of the dermal papilla. In addition to this, I demonstrated the hair fibre inducing capabilities of this model. These results could have a profound impact in the development of technologies beneficial for anagen and fibre induction. Not only is this exciting in the development of transplantation techniques, but this model may serve to further our understanding of the dermal papilla, and interactions between cells in response to anagen initiation.

Secondly, I have described work using the vibrissa follicle model for studying club fibre formation, retention and release. In Chapter 3 I analysed the structural aspects of the club fibre, focusing on formation and retention. I also validated the vibrissa model as extremely useful for the investigation of exogen, and showed exogen to be a progressive gradual process rather than a sudden event. The formation of the club fibre raises interesting questions relating to its origin. My own observations of the similarities between the companion layer and the companion^{CL} led me to scrutinise the literature in this area. This threw up the possibility that the companion^{CL} is derived from the companion layer, and hence the trichilemmal keratin is derived from the IRS. This challenges an established dogma that says that the trichilemmal keratin is derived from the ORS.

In Chapter 4 I gathered information on the processes involved in club fibre retention and release, although I did not identify a key initiating signal for exogen. However, in considering the results, important points emerging relating to the concept of club fibre release. The presence of desmosomes as well as many enzymes and enzyme inhibitors in the region of the club fibre sac imply that proteolysis is the most likely

final event in release of the naked club fibre and that this is proceeded by differentiation of the companion^{CL} in preparation for release. An increasing body of literature, supported by my observations would suggest that exogen is an actively controlled event, with distinctive features associated with club fibre maturation as it prepares for release.

5.3: Possible Future Directions

There are several aspects of this study which merit further investigation.

- In continuation of the dermal sphere work, a next obvious step would be to analyse the inductive capacity of human dermal spheres when transplanted into human tissue prior to grafting onto the back of a mouse.

- Analysis of dermal spheres in combination with other cells, such as GE cells may provide a better model with which to work with. Different cell combinations and their effects on the inductive capabilities of the dermal spheres is one route which could be explored further.

- With regards to the work relating to the club fibre it would be interesting to resolve the issue of the origin of the companion^{CL} and the trichilemmal keratin. Studies which track individual cells (perhaps after initiation of catagen) within an organ culture system could be carried out to determine this.

- The presence of proteases and their inhibitors surrounding the club fibre makes it compelling to suggest that proteases and cell death mediate release of the club fibre. However, to carry out functional studies which show mechanistic effect of proteases on the process of exogen would be the next important step to take.

- The protease/protease inhibitor studies should be continued in the human hair follicle to identify target proteases for potential therapeutic intervention.

- Of interest within this study were the similarities of differentiation within the companion^{CL}, when compared with differentiation within the epidermis. It would be interesting to take ORS cells *in vitro*, and to track changes in them as they differentiate, in addition to utilising these cells to further analyse potential signalling cascades in the cells that surround the club fibre.

- Working with transgenic or mutant mice was not possible with this study, due to conditions associated with my funding. However, analysis of these mice in more detail may elude further information about the processes of exogen. In this context the creation of a transgenic mouse, perhaps with a gene of interest driven by a K6 promoter, targeting it to the companion layers of the follicle would be an interesting route to follow.

References

Airola, K., M. Ahonen, N. Johansson, P. Heikkila, J. Kere, V.M. Kahari and U.K. Saarialho-Kere (1998). "Human TIMP-3 is expressed during fetal development, hair growth cycle, and cancer progression." J Histochem Cytochem **46**(4): 437-47.

Albers, K.M., F. Greif, R.W. Setzer and L.B. Taichman (1987). "Cell-cycle withdrawal in cultured keratinocytes." Differentiation **34**(3): 236-40.

Alcalai, R., S. Metzger, S. Rosenheck, V. Meiner and T. Chajek-Shaul (2003). "A Recessive Mutation in Desmoplakin Causes Arrhythmogenic Right Ventricular Dysplasia, Skin Disorder, and Woolly Hair." J Am Coll Cardiol **42**(2).

Alibardi, L. (2004). "Fine structure of marsupial hairs, with emphasis on trichohyalin and the structure of the inner root sheath." J Morphol **261**(3): 390-402.

al-Khateeb, A. and E. Johnson (1971). "Seasonal changes of pelage in the vole (Microtus agrestis). 3. The role of the endocrine system." Gen Comp Endocrinol **16**(2): 236-40.

Allain, D. and J. Rougeot (1980). "Induction of autumn moult in mink (Mustela vison Peale and Beauvois) with melatonin." Reprod Nutr Dev **20**(1A): 197-201.

Allombert-Blaise, C., S. Tamiji, L. Mortier, H. Fauvel, M. Tual, E. Delaporte, F. Piette, E.M. DeLassale, P. Formstecher, P. Marchetti and R. Polakowska (2003). "Terminal differentiation of human epidermal keratinocytes involves mitochondria- and caspase-dependent cell death pathway." Cell Death Differ **10**(7): 850-2.

Alonso, L. and E. Fuchs (2006). "The hair cycle." J Cell Sci **119**(Pt 3): 391-3.

Amour, A., C.G. Knight, A. Webster, P.M. Slocombe, P.E. Stephens, V. Knauper, A.J. Docherty and G. Murphy (2000). "The in vitro activity of ADAM-10 is inhibited by TIMP-1 and TIMP-3." FEBS Lett **473**(3): 275-9.

Amour, A., P.M. Slocombe, A. Webster, M. Butler, C.G. Knight, B.J. Smith, P.E. Stephens, C. Shelley, M. Hutton, V. Knauper, A.J. Docherty and G. Murphy (1998). "TNF-alpha converting enzyme (TACE) is inhibited by TIMP-3." FEBS Lett **435**(1): 39-44.

Ando, Y., T. Tanaka, Y. Horiguchi, K. Ikai and H. Tomono (1988). "Hidrotic ectodermal dysplasia: a clinical and ultrastructural observation." Dermatologica **176**(4): 205-11.

Angst, B.D., L.A. Nilles and K.J. Green (1990). "Desmoplakin II expression is not restricted to stratified epithelia." J Cell Sci **97 (Pt 2)**: 247-57.

Apte, S.S., M.G. Mattei and B.R. Olsen (1994). "Cloning of the cDNA encoding human tissue inhibitor of metalloproteinases-3 (TIMP-3) and mapping of the TIMP3 gene to chromosome 22." Genomics **19**(1): 86-90.

Apte, S.S., B.R. Olsen and G. Murphy (1995). "The gene structure of tissue inhibitor of metalloproteinases (TIMP)-3 and its inhibitory activities define the distinct TIMP gene family." J Biol Chem **270**(24): 14313-8.

Arck, P.C., B. Handjiski, E.M. Peters, A.S. Peter, E. Hagen, A. Fischer, B.F. Klapp and R. Paus (2003). "Stress inhibits hair growth in mice by induction of premature catagen development and deleterious perifollicular inflammatory events via neuropeptide substance P-dependent pathways." Am J Pathol **162**(3): 803-14.

Arita, K., M. Akiyama, Y. Tsuji, J.R. McMillan, R.A. Eady and H. Shimizu (2004). "Gap junction development in the human fetal hair follicle and bulge region." Br J Dermatol **150**(3): 429-34.

Arnemann, J., K.H. Sullivan, A.I. Magee, I.A. King and R.S. Buxton (1993). "Stratification-related expression of isoforms of the desmosomal cadherins in human epidermis." J Cell Sci **104 (Pt 3)**: 741-50.

Auber, L. (1952). "The anatomy of follicle producing wool-fibers with special reference to keratinization." Trans Roy Soc Ed **62**: 191-254.

Auber, L. and M. Burns (1947). "Replacement of Fibres in Sheep." Nature **160**(4076): 836-836.

Auger, F.A., M. Rouabhia, F. Goulet, F. Berthod, V. Moulin and L. Germain (1998). "Tissue-engineered human skin substitutes developed from collagen-populated hydrated gels: clinical and fundamental applications." Med Biol Eng Comput **36**(6): 801-12.

Baker, A.H., A.B. Zaltsman, S.J. George and A.C. Newby (1998). "Divergent effects of tissue inhibitor of metalloproteinase-1, -2, or -3 overexpression on rat vascular smooth muscle cell invasion, proliferation, and death in vitro. TIMP-3 promotes apoptosis." J Clin Invest **101**(6): 1478-87.

Bamford, J.T. (1987). "A falling out following minoxidil: telogen effluvium." J Am Acad Dermatol **16**(1 Pt 1): 144-6.

Bardelli, A. and A. Rebora (1989). "Telogen effluvium and minoxidil." J Am Acad Dermatol **21**(3 Pt 1): 572-3.

Barth, J.H. (1987). "Normal hair growth in children." Pediatr Dermatol **4**(3): 173-184.

Bayer-Garner, I.B., R.D. Sanderson and B.R. Smoller (2002). "Syndecan-1 is strongly expressed in the anagen hair follicle outer root sheath and in the dermal papilla but expression diminishes with involution of the hair follicle." Am J Dermatopathol **24**(6): 484-9.

Bernard, F., T. Magnaldo and M. Darmon (1992). "Delayed onset of epidermal differentiation in psoriasis." J Invest Dermatol **98**(6): 902-10.

Bernot, K.M., P.A. Coulombe and K.M. McGowan (2002). "Keratin 16 expression defines a subset of epithelial cells during skin morphogenesis and the hair cycle." J Invest Dermatol **119**(5): 1137-49.

Berth-Jones, J. and P.E. Hutchinson (1995). "Novel cycle changes in scalp hair are caused by etretinate therapy." Br J Dermatol **132**(3): 367-75.

Berth-Jones, J., D. Shuttleworth and P.E. Hutchinson (1990). "A study of etretinate alopecia." Br J Dermatol **122**(6): 751-5.

Birch, M.P., H. Lashen, S. Agarwal and A.G. Messenger (2006). "Female pattern hair loss, sebum excretion and the end-organ response to androgens." Br J Dermatol **154**: 85-89.

Birch, M.P., J.F. Messenger and A.G. Messenger (2001). "Hair density, hair diameter and the prevalence of female pattern hair loss." Br J Dermatol **144**: 297-304.

Bisset, D.L., J.F. McBride and L.F. Patrick (1987). "Role of protein and calcium in stratum corneum cell cohesion." Arch Dermatol Res **279**: 184-189.

Bissonnette, T.H. (1935). "Relations of hair cycles in ferrets to changes in the anterior hypophysis and to light cycles." Anat Rec **63**: 159-168.

Blanpain, C. and E. Fuchs (2006). "Epidermal Stem Cells of the Skin." Annu Rev Cell Dev Biol **22**: 339-373.

Blanpain, C., W.E. Lowry, A. Geoghegan, L. Polak and E. Fuchs (2004). "Self-renewal, multipotency, and the existence of two cell populations within an epithelial stem cell niche." Cell **118**(5): 635-48.

Blanpain, C., W.E. Lowry, H.A. Pasolli and E. Fuchs (2006). "Canonical notch signaling functions as a commitment switch in the epidermal lineage." Genes Dev **20**(21): 3022-35.

Blum, I. and S. Leiba (1980). "Increased hair loss as a side effect of bromocriptine treatment." N Engl J Med **303**(24): 1418.

Blume, U., J. Ferracin, M. Verschoore, J.M. Czernielewski and H. Schaefer (1991). "Physiology of the vellus hair follicle: hair growth and sebum excretion." Br J Dermatol **124**(1): 21-8.

Bond, M., G. Murphy, M.R. Bennett, A. Amour, V. Knauper, A.C. Newby and A.H. Baker (2000). "Localization of the death domain of tissue inhibitor of metalloproteinase-3 to the N terminus. Metalloproteinase inhibition is associated with proapoptotic activity." J Biol Chem **275**(52): 41358-63.

Bond, M., G. Murphy, M.R. Bennett, A.C. Newby and A.H. Baker (2002). "Tissue inhibitor of metalloproteinase-3 induces a Fas-associated death domain-dependent type II apoptotic pathway." J Biol Chem **277**(16): 13787-95.

Botchkarev, V.A. and J. Kishimoto (2003). "Molecular control of epithelial-mesenchymal interactions during hair follicle cycling." J Investig Dermatol Symp Proc **8**(1): 46-55.

Brandner, J.M., P. Houdek, B. Husing, C. Kaiser and I. Moll (2004). "Connexins 26, 30, and 43: differences among spontaneous, chronic, and accelerated human wound healing." J Invest Dermatol **122**(5): 1310-20.

Bratka-Robia, C.B., G. Mitteregger, A. Aichinger, M. Egerbacher, M. Helmreich and E. Bamberg (2002). "Primary cell culture and morphological charaterization of canine dermal papilla cells and dermal fibroblasts." Vet Dermatol **13**: 1-6.

Brattsand, M., K. Stefansson, C. Lundh, Y. Haasum and T. Egelrud (2005). "A Proteolytic Cascade of Kallikreins in the Stratum Corneum." J Invest Dermatol **124**: 198-203.

Broekaert, D., K. Cooreman, P. Coucke, S. Nsabumukunzi, P. Reyniers, P. Kluyskens and E. Gillis (1982). "A quantitative histochemical study of sulphydryl and disulphide content during normal epidermal keratinization." Histochem J **14**(4): 573-84.

Buhl, A.E., D.J. Waldon, T.T. Kawabe and J.M. Holland (1989). "Minoxidil stimulates mouse vibrissae follicles in organ culture." J Invest Dermatol **92**(3): 315-20.

Butterweck, A., C. Elfgang, K. Willecke and O. Traub (1994). "Differential expression of the gap junction proteins connexin45, -43, -40, -31, and -26 in mouse skin." Eur J Cell Biol **65**(1): 152-63.

Cao, T., P. Racz, K.M. Szauter, G. Groma, G.Y. Nakamatsu, B. Fogelgren, E. Pankotai, Q. He and K. Csiszer (2007). "Mutation in *Mpzl3*, a Gene Encoding a Predicted the Adhesion Protein, in the Rough Coat (rc) Mice with Severe Skin and Hair Abnormalities." J Invest Dermatol **127**: 1375-1386.

Cash, T.F. (1992). "The psychological effects of androgenetic alopecia in men." J Am Acad Dermatol **26**(6): 926-31.

Cash, T.F. (1999). "The psychosocial consequences of androgenetic alopecia: a review of the research literature." Br J Dermatol **141**(3): 398-405.

Cash, T.F., V.H. Price and R.C. Savin (1993). "Psychological effects of androgenetic alopecia on women: comparisons with balding men and with female control subjects." J Am Acad Dermatol **29**(4): 568-75.

Caubet, C., N. Jonca, M. Brattsand, M. Guerrin, D. Bernard, R. Schmidt, T. Egelrud, M. Simon and G. Serre (2004). "Degradation of corneodesmosome proteins by two serine proteases of the kallikrein family, SCTE/KLK5/hK5 and SCCE/KLK7/hK7." J Invest Dermatol **122**(5): 1235–1244.

Chapman, D.M. (1992). "The anchoring strengths of various chest hair root types." Clin Exp Dermatol **17**(6): 421-3.

Chapman, S.J. and A. Walsh (1990). "Desmosomes, corneosomes and desquamation. An ultrastructural study of adult pig epidermis." Arch Dermatol Res **282**: 304-310.

Chase, H.B. (1954). "Growth of the hair." Physiol Rev **34**(1): 113-26.

Chase, H.B., R. Rauch and V.W. Smith (1951). "Critical stages of hair development and pigmentation in the mouse." Physiol Zool **24**(1): 1-8.

Chaturvedi, V., L.A. Sitailo, B. Bodner, M.F. Denning and B.J. Nickoloff (2006). "Defining the caspase-containing apoptotic machinery contributing to cornification in human epidermal equivalents." Exp Dermatol **15**(1): 14-22.

Chiba, H., N. Sawada, M. Oyamada, T. Kojima, K. Iba, S. Ishii and M. Mori (1994). "Hormonal regulation of connexin 43 expression and gap junctional communication in human osteoblastic cells." Cell Struct Funct **19**(3): 173-7.

Chomczynski, P. and N. Sacchi (1987). "Single-step method of RNA isolation by acid guanidinium thiocyanate-phenol-chloroform extraction." Anal Biochem **162**: 156-159.

Choudhry, R., J.D. Pitts and M.B. Hodgins (1997). "Changing patterns of gap junctional intercellular communication and connexin distribution in mouse epidermis and hair follicles during embryonic development." Dev Dyn **210**(4): 417-30.

Chui, H.C., C.H. Chang, J. Chen and S.H. Jee (1996). "Human hair follicle dermal papilla cell, dermal sheath cell and interstitial dermal fibroblast characteristics." J Formos Med Assoc **95**(667-674).

Chung, T.A., J.B. Lee, H.S. Jang, K.S. Kwon and C.K. Oh (1998). "A clinical, microbiological, and histopathologic study of trichostasis spinulosa." J Dermatol **25**(11): 697-702.

Chusho, H., N. Tamura, Y. Ogawa, A. Yasoda, M. Suda, T. Miyazawa, K. Nakamura, K. Nakao, T. Kurihara, Y. Komatsu, H. Itoh, K. Tanaka, Y. Saito and M. Katsuki (2001). "Dwarfism and early death in mice lacking C-type natriuretic peptide." Proc Natl Acad Sci U S A **98**(7): 4016-21.

Clemmensen, O.J., B. Hainau and B. Hansted (1991). "The ultrastructure of the transition zone between specialized cells ("Flugelzellen") of Huxley's layer of

the inner root sheath and cells of the outer root sheath of the human hair follicle." Am J Dermatopathol **13**(3): 264-70.

Commo, S. and B.A. Bernard (1997). "Immunohistochemical analysis of tissue remodeling during the anagen-catagen transition of human hair follicle." Br J Dermatol **137**: 31-38.

Commo, S., O. Gaillard and B.A. Bernard (2000). "The human hair follicle contains two distinct K19 positive compartments in the outer root sheath: a unifying hypothesis for stem cell reservoir?" Differentiation **66**(4-5): 157-64.

Common, J.E., D. Becker, W.L. Di, I.M. Leigh, E.A. O'Toole and D.P. Kelsell (2002). "Functional studies of human skin disease- and deafness-associated connexin 30 mutations." Biochem Biophys Res Commun **298**(5): 651-6.

Cotsarelis, G., T.T. Sun and R.M. Lavker (1990). "Label-retaining cells reside in the bulge area of pilosebaceous unit: implications for follicular stem cells, hair cycle, and skin carcinogenesis." Cell **61**(7): 1329-37.

Couchman, J.R. (1993). "Hair follicle proteoglycans." J Invest Dermatol **101**(1 Suppl): 60S-64S.

Couchman, J.R., J.L. King and K.J. McCarthy (1990). "Distribution of two basement membrane proteoglycans through hair follicle development and the hair growth cycle in the rat." J Invest Dermatol **94**(1): 65-70.

Coulombe, P.A. (2003). "Wound epithelialization: accelerating the pace of discovery." J Invest Dermatol **121**(2): 219-30.

Courtois, M., G. Loussouarn, C. Hourseau and J.F. Grollier (1994). "Hair cycle and alopecia." Skin Pharmacol **7**(1-2): 84-9.

Courtois, M., G. Loussouarn, C. Hourseau and J.F. Grollier (1995). "Ageing and hair cycles." Br J Dermatol **132**(1): 86-93.

Coutinho, P., C. Qiu, S. Frank, K. Tamber and D. Becker (2003). "Dynamic changes in connexin expression correlate with key events in the wound healing process." Cell Biol Int **27**(7): 525-41.

Coutinho, P., C. Qiu, S. Frank, C.M. Wang, T. Brown, C.R. Green and D.L. Becker (2005). "Limiting burn extension by transient inhibition of Connexin43 expression at the site of injury." Br J Plast Surg **58**(5): 658-67.

Craven, A.J., C.J. Ormandy, F.G. Robertson, R.J. Wilkins, P.A. Kelly, A.J. Nixon and A.J. Pearson (2001). "Prolactin signaling influences the timing mechanism of the hair follicle: analysis of hair growth cycles in prolactin receptor knockout mice." Endocrinology **142**(6): 2533-9.

Curran, S., S.R. Dundas, J. Buxton, M.F. Leeman, R. Ramsay and G.I. Murray (2004). "Matrix metalloproteinase/tissue inhibitors of matrix metalloproteinase phenotype identifies poor prognosis colorectal cancers." Clin Cancer Res **10**(24): 8229-34.

Dahl, E., D. Manthey, Y. Chen, H.J. Schwarz, Y.S. Chang, P.A. Lalley, B.J. Nicholson and K. Willecke (1996). "Molecular cloning and functional expression of mouse connexin-30,a gap junction gene highly expressed in adult brain and skin." J Biol Chem **271**(30): 17903-10.

Danforth, C.H. (1925). "Hair in its relation to questions of homology and phylogeny." Am J Anat **86**: 342-356.

Dang, X., B.W. Doble and E. Kardami (2003). "The carboxy-tail of connexin-43 localizes to the nucleus and inhibits cell growth." Mol Cell Biochem **242**(1-2): 35-8.

Dano, K., P.A. Andreason, J. Grondahl-Hansen, P. Kristensen, L.S. Nielsen and L. Skriver (1985). "Plasminogen activators, tissue degredation and cancer." Adv Cancer Res **44**: 139-266.

Darnton, S.J., L.J. Hardie, R.S. Muc, C.P. Wild and A.G. Casson (2005). "Tissue inhibitor of metalloproteinase-3 (TIMP-3) gene is methylated in the development of esophageal adenocarcinoma: loss of expression correlates with poor prognosis." Int J Cancer **115**(3): 351-8.

Davies, G.C., M.J. Thornton, T.J. Jenner, Y.J. Chen, J.B. Hansen, R.D. Carr and V.A. Randall (2005). "Novel and established potassium channel openers stimulate hair growth in vitro: implications for their modes of action in hair follicles." J Invest Dermatol **124**(4): 686-94.

Deed, R.W., S. Armitage and J.D. Norton (1996). "Nuclear localization and regulation of Id protein through an E protein-mediated chaperone mechanism." J Biol Chem **271**(39): 23603-6.

Denning, M.F., A.A. Dlugosz, C. Cheng, P.J. Dempsey, R.J. Coffey, Jr., D.W. Threadgill, T. Magnuson and S.H. Yuspa (2000). "Cross-talk between epidermal growth factor receptor and protein kinase C during calcium-induced differentiation of keratinocytes." Exp Dermatol **9**(3): 192-9.

Denning, M.F., A.A. Dlugosz, E.K. Williams, Z. Szallasi, P.M. Blumberg and S.H. Yuspa (1995). "Specific protein kinase C isozymes mediate the induction of keratinocyte differentiation markers by calcium." Cell Growth Differ **6**(2): 149-57.

Derweet, J., A. King and M.L. Geerts (1982). "Morphological changes in the proximal area of the rat's hair follicle during early catagen." Arch Dermatol Res **272**: 79-92.

Desai, S.P. and E.R. Roaf (1984). "Telogen effluvium after anesthesia and surgery." Anesth Analg **63**(1): 83-4.

Dhouailly, D. (1977). "Regional specification of cutaneous appendages in mammals." Dev Genes Evol **181**(1): 3-10.

Dhouailly, D. and P. Sengel (1972). "[Morphogenesis of feather and hair, studied by means of heterospecific associations of dermis and epidermis between chicken and mice]." C R Acad Sci Hebd Seances Acad Sci D **275**(3): 479-82.

Dhouailly, D. and P. Sengel (1973). "[Morphogenic interactions between reptilian epidermis and birds or mammalian dermis]." C R Acad Sci Hebd Seances Acad Sci D **277**(13): 1221-4.

Dhouailly, D. and P. Sengel (1975). "[Feather- and hair-forming properties of dermal cells of glabrous skin from bird and mammals]." C R Acad Sci Hebd Seances Acad Sci D **281**(14): 1007-10.

Di, W.L., E.L. Rugg, I.M. Leigh and D.P. Kelsell (2001). "Multiple epidermal connexins are expressed in different keratinocyte subpopulations including connexin 31." J Invest Dermatol **117**(4): 958-64.

Dlugosz, A.A. and S.H. Yuspa (1993). "Coordinate changes in gene expression which mark the spinous to granular cell transition in epidermis are regulated by protein kinase C." J Cell Biol **120**(1): 217-25.

Dlugosz, A.A. and S.H. Yuspa (1994). "Protein kinase C regulates keratinocyte transglutaminase (TGK) gene expression in cultured primary mouse epidermal keratinocytes induced to terminally differentiate by calcium." J Invest Dermatol **102**(4): 409-14.

Docherty, A.J., A. Lyons, B.J. Smith, E.M. Wright, P.E. Stephens, T.J. Harris, G. Murphy and J.J. Reynolds (1985). "Sequence of human tissue inhibitor of metalloproteinases and its identity to erythroid-potentiating activity." Nature **318**(6041): 66-9.

Donetti, E., E. Boschini, A. Cerini, S. Selleri, C. Rumio and I. Barajon (2004). "Desmocollin 1 expression and desmosomal remodeling during terminal differentiation of human anagen hair follicle: an electron microscopic study." Exp Dermatol **13**(5): 289-97.

Dry, F. (1926). "The Coat of a Mouse (*Mus Musculus*)." J Genet **16**: 281-340.

Drynda, A., P.H. Quax, M. Neumann, W.H. van der Laan, G. Pap, S. Drynda, I. Meinecke, J. Kekow, W. Neumann, T.W. Huizinga, M. Naumann, W. Konig and T. Pap (2005). "Gene transfer of tissue inhibitor of metalloproteinases-3 reverses the inhibitory effects of TNF-alpha on Fas-induced apoptosis in rheumatoid arthritis synovial fibroblasts." J Immunol **174**(10): 6524-31.

du Cros, D.L., R.G. LeBaron and J.R. Couchman (1995). "Association of versican with dermal matrices and its potential role in hair follicle development and cycling." J Invest Dermatol **105**(3): 426-31.

Duncan, M.J. and B.D. Goldman (1984). "Hormonal regulation of the annual pelage color cycle in the Djungarian hamster, Phodopus sungorus. II. Role of prolactin." J Exp Zool **230**(1): 97-103.

Ebling, F.J. and E. Johnson (1964). "The Action of Hormones on Spontaneous Hair Growth Cycles in the Rat." J Endocrinol **29**: 193-201.

Edwards, D.R. (2004). "TIMP-3 and endocrine therapy of breast cancer: an apoptosis connection emerges." J Pathol **202**(4): 391-4.

Egawa, K., Y. Honda, M. Kuroki, Y. Inaba and T. Ono (1996). "Carcinoembryonic antigen and related antigens expressed on keratinocytes in inflammatory dermatoses." Br J Dermatol **134**(3): 451-9.

Egawa, K., M. Kuroki, Y. Inoue and T. Ono (2000). "Nail bed keratinocytes express an antigen of the carcinoembryonic antigen family." Br J Dermatol **143**(1): 79-83.

Egelrud, T. (2000). "Desquamation in the stratum corneum." Acta Derm Venereol Suppl (Stockh) **208**: 44-45.

Egelrud, T., P.-. Hofer and A. Lundström (1988). "Proteolytic degredation of desmosomes in plantar stratum corneum leads to cell dissociation in vitro." Acta Derm Venereol (Stockh) **68**: 93-97.

Ekholm, E., M. Brattsand and T. Egelrud (2000). "Stratum corneum tryptic enzyme in normal epidermis: A missing link in the desquamation process?" J Invest Dermatol **114**: 56-63.

Ekholm, E. and T. Egelrud (1998). "The expression of stratum corneum chymotryptic enzyme in human anagen hair follicles: Further evidence for its involvement in desquamation-like processes." Br J Dermatol **139**: 585-590.

Elias, P.M., S.K. Ahn, B.E. Brown, D. Crumrine and K.R. Feingold (2002). "Origin of the Epidermal Calcium Gradient: Regulation by Barrier Status and Role of Active vs Passive Mechanisms." **119**(6): 1269-1274.

Elliott, K., T.J. Stephenson and A.G. Messenger (1999). "Differences in hair follicle dermal papilla volume are due to extracellular matrix volume and cell number: implications for the control of hair follicle size and androgen responses." J Invest Dermatol **113**(6): 873-7.

Er, E., M. Kulahci and E. Hamiloglu (2006). "In vivo follicular unit multiplication: is it possible to harvest an unlimited donor supply?" Dermatol Surg **32**(11): 1322-6; discussion 1325-6.

Essenfelder, G.M., R. Bruzzone, J. Lamartine, A. Charollais, C. Blanchet-Bardon, M.T. Barbe, P. Meda and G. Waksman (2004). "Connexin30 mutations responsible for hidrotic ectodermal dysplasia cause abnormal hemichannel activity." Hum Mol Genet **13**(16): 1703-14.

Essenfelder, G.M., G. Larderet, G. Waksman and J. Lamartine (2005). "Gene structure and promoter analysis of the human GJB6 gene encoding connexin 30." Gene **350**(1): 33-40.

Fabre, N., J.L. Montastruc and O. Rascol (1993). "Alopecia: an adverse effect of bromocriptine." Clin Neuropharmacol **16**(3): 266-8.

Fata, J.E., K.J. Leco, E.B. Voura, H.Y. Yu, P. Waterhouse, G. Murphy, R.A. Moorehead and R. Khokha (2001). "Accelerated apoptosis in the Timp-3-deficient mammary gland." J Clin Invest **108**(6): 831-41.

Fernandes, K.J., I.A. McKenzie, P. Mill, K.M. Smith, M. Akhavan, F. Barnabe-Heider, J. Biernaskie, A. Junek, N.R. Kobayashi, J.G. Toma, D.R. Kaplan, P.A. Labosky, V. Rafuse, C.C. Hui and F.D. Miller (2004). "A dermal niche for multipotent adult skin-derived precursor cells." Nat Cell Biol **6**(11): 1082-93.

Ferraris, C., C. Chaloin-Dufau and D. Dhouailly (1994). "Transdifferentiation of embryonic and postnatal rabbit corneal epithelial cells." Differentiation **57**(2): 89-96.

Ferraris, C., G. Chevalier, B. Favier, C.A. Jahoda and D. Dhouailly (2000). "Adult corneal epithelium basal cells possess the capacity to activate epidermal, pilosebaceous and sweat gland genetic programs in response to embryonic dermal stimuli." Development **127**(24): 5487-95.

Fliniaux, I., J.P. Viallet, D. Dhouailly and C.A. Jahoda (2004). "Transformation of amnion epithelium into skin and hair follicles." Differentiation **72**(9-10): 558-65.

Foitzik, K., K. Krause, F. Conrad, M. Nakamura, W. Funk and R. Paus (2006). "Human scalp hair follicles are both a target and a source of prolactin, which serves as an autocrine and/or paracrine promoter of apoptosis-driven hair follicle regression." Am J Pathol **168**(3): 748-56.

Foitzik, K., K. Krause, A.J. Nixon, C.A. Ford, U. Ohnemus, A.J. Pearson and R. Paus (2003). "Prolactin and its receptor are expressed in murine hair follicle epithelium, show hair cycle-dependent expression, and induce catagen." Am J Pathol **162**(5): 1611-21.

Foitzik, K., G. Lindner, S. Mueller-Roever, M. Maurer, N. Botchkareva, V. Botchkarev, B. Handjiski, M. Metz, T. Hibino, T. Soma, G.P. Dotto and R. Paus (2000). "Control of murine hair follicle regression (catagen) by TGF-beta1 in vivo." Faseb J **14**(5): 752-60.

Foitzik, K., T. Spexard, M. Nakamura, U. Halsner and R. Paus (2005). "Towards dissecting the pathogenesis of retinoid-induced hair loss: all-trans retinoic acid induces premature hair follicle regression (catagen) by upregulation of transforming growth factor-beta2 in the dermal papilla." J Invest Dermatol **124**(6): 1119-26.

Freinkel, R.K. and T.N. Traczyk (1983). "Acid hydrolases of the epidermis: Subcellular localization and relationship to cornification." J Invest Dermatol **80**: 441-446.

Fruzzetti, F., D. de Lorenzo, D. Parrini and C. Ricci (1994). "Effects of finasteride, a 5 alpha-reductase inhibitor, on circulating androgens and gonadotropin secretion in hirsute women." J Clin Endocrinol Metab **79**(3): 831-5.

Fuchs, E. and H. Green (1981). "Regulation of terminal differentiation of cultured human keratinocytes by vitamin A." Cell **25**(3): 617-25.

Gharzi, A., A.J. Reynolds and C.A. Jahoda (2003). "Plasticity of hair follicle dermal cells in wound healing and induction." Exp Dermatol **12**(2): 126-36.

Goliger, J.A. and D.L. Paul (1994). "Expression of gap junction proteins Cx26, Cx31.1, Cx37, and Cx43 in developing and mature rat epidermis." Dev Dyn **200**(1): 1-13.

Goliger, J.A. and D.L. Paul (1995). "Wounding alters epidermal connexin expression and gap junction-mediated intercellular communication." Mol Biol Cell **6**(11): 1491-501.

Gollnick, H., U. Blume and C.E. Orfanos (1990). "[Adverse drug reactions on hair]." Z Hautkr **65**(12): 1128-34.

Gomez, D.E., D.F. Alonso, H. Yoshiji and U.P. Thorgeirsson (1997). "Tissue inhibitors of metalloproteinases: structure, regulation and biological functions." Eur J Cell Biol **74**(2): 111-22.

Gong, X., K. Agopian, N.M. Kumar and N.B. Gilula (1999). "Genetic factors influence cataract formation in alpha 3 connexin knockout mice." Dev Genet **24**(1-2): 27-32.

Goodenough, D.A. (1975). "The structure of cell membranes involved in intercellular communication." Am J Clin Pathol **63**(5): 636-45.

Gordon, S.W., M.S. Elston, Z. Yu, A.J. Nixon, A.J. Craven, A.J. Pearson and J.V. Conaglen (2004). Cysteine-rich intestinal proteins are differentially expressed in hair follicles. 4th Intercontinental meeting of Hair Research Societies, Berlin, Blackwell Publishing.

Green, E.L. (1954). "The Genetics of a New Hair Deficiency, Furless - in the House Mouse." Journal of Heredity **45**(3): 115-118.

Greene, J., M. Wang, Y.E. Liu, L.A. Raymond, C. Rosen and Y.E. Shi (1996). "Molecular cloning and characterization of human tissue inhibitor of metalloproteinase 4." J Biol Chem **271**(48): 30375-80.

Grifa, A., C.A. Wagner, L. D'Ambrosio, S. Melchionda, F. Bernardi, N. Lopez-Bigas, R. Rabionet, M. Arbones, M.D. Monica, X. Estivill, L. Zelante, F. Lang and P. Gasparini (1999). "Mutations in GJB6 cause nonsyndromic autosomal dominant deafness at DFNA3 locus." Nat Genet **23**(1): 16-8.

Gu, L.H. and P.A. Coulombe (2007). "Keratin Expression Provides Novel Insight into the Morphogenesis and Function of the Companion Layer in Hair Follicles." J Invest Dermatol(127): 1061-1073.

Guarrera, M. and A. Rebora (2005). "Kenogen in female androgenetic alopecia. A longitudinal study." Dermatology **210**(1): 18-20.

Guo, H., P. Acevedo, F.D. Parsa and J.S. Bertram (1992). "Gap-junctional protein connexin 43 is expressed in dermis and epidermis of human skin: differential modulation by retinoids." J Invest Dermatol **99**(4): 460-7.

Hadshiew, I.M., K. Foitzik, P.C. Arck and R. Paus (2004). "Burden of hair loss: stress and the underestimated psychosocial impact of telogen effluvium and androgenetic alopecia." J Invest Dermatol **123**(3): 455-7.

Halloy, J., B.A. Bernard, G. Loussouarn and A. Goldbeter (2000). "Modeling the dynamics of human hair cycles by follicular automaton." Proc Natl Acad Sci U S A **97**(15): 8328-8333.

Halloy, J., B.A. Bernard, G. Loussouarn and A. Goldbeter (2002). "The follicular automaton model: effect of stochasticity and of synchronization of hair cycles." J Theor Biol **214**(3): 469-479.

Hamaoka, H., K. Minakuchi, H. Miyoshi, S. Arase, C.H. Chen and Y. Nakaya (1997). "Effect of K+ channel openers on K+ channel in cultured human dermal papilla cells." J Med Invest **44**(1-2): 73-7.

Hammani, K., A. Blakis, D. Morsette, A.M. Bowcock, C. Schmutte, P. Henriet and Y.A. DeClerck (1996). "Structure and characterization of the human tissue inhibitor of metalloproteinases-2 gene." J Biol Chem **271**(41): 25498-505.

Hanakawa, Y., H. Li, C. Lin, J.R. Stanley and G. Cotsarelis (2004). "Desmogleins 1 and 3 in the companion layer anchor mouse anagen hair to the follicle." J Invest Dermatol **123**(5): 817-22.

Hanakawa, Y., N. Matsuyoshi and J.R. Stanley (2002). "Expression of desmoglein 1 compensates for genetic loss of desmoglein 3 in keratinocyte adhesion." J Invest Dermatol **119**(1): 27-31.

Hansson, L., A. Backman, A. Ny, M. Edlund, E. Ekholm, B. Ekstrand Hammarstrom, J. Tornell, P. Wallbrandt, H. Wennbo and T. Egelrud (2002). "Epidermal overexpression of stratum corneum chymotryptic enzyme in mice: a model for chronic itchy dermatitis." J Invest Dermatol **118**(3): 444-9.

Hardy, M.H. (1992). "The secret life of the hair follicle." Trends Genet **8**(2): 55-61.

Harris, S. and C. Jahoda (2001). "A correlation between versican and neurofilament expression patterns during the development and adult cycling of rat vibrissa follicles." Mech Dev **101**(1-2): 227-231.

Harrison, S. and R. Sinclair (2002). "Telogen effluvium." Clin Exp Dermatol **27**(5): 389-5.

Hashimoto, T., T. Kazama, M. Ito, K. Urano, Y. Katakai, N. Yamaguchi and Y. Ueyama (2001). "Histologic study of the regeneration process of human hair

follicles grafted onto SCID mice after bulb amputation." J Investig Dermatol Symp Proc **6**(1): 38-42.

Havlickova, B., T. Biro, A. Mescalchin, P. Arenberger and R. Paus (2004). "Towards optimization of an organotypic assay system that imitates human hair follicle-like epithelial-mesenchymal interactions." Br J Dermatol **151**(4): 753-65.

Hayashi, K., T. Cao, H. Passmore, C. Jourdan-Le Saux, B. Fogelgren, S. Khan, I. Hornstra, Y. Kim, M. Hayashi and K. Csiszar (2004). "Progressive hair loss and myocardial degeneration in rough coat mice: reduced lysyl oxidase-like (LOXL) in the skin and heart." J Invest Dermatol **123**(5): 864-71.

Haywood, A.F. (1979). "Membrane coating granules." Int Rev Cytol **59**: 97-127.

Headington, J.T. (1993). "Telogen effluvium. New concepts and review." Arch Dermatol **129**(3): 356-63.

Herron, B.J., R.A. Liddell, A. Parker, S. Grant, J. Kinne, J.K. Fisher and L.D. Siracusa (2005). "A mutation in stratifin is responsible for the repeated epilation (*Er*) phenotype in mice." Nat Genet **37**(11): 1210-1212.

Heydon, M.J., J.A. Milne, B.R. Brinklow and A.S. Loudon (1995). "Manipulating melatonin in red deer (Cervus elaphus): differences in the response to food restriction and lactation on the timing of the breeding season and prolactin-dependent pelage changes." J Exp Zool **273**(1): 12-20.

Higgins, S., P. Young, J. Brody and G. Cunha (1989). "Induction of functional cytodifferentiation in the epithelium of tissue recombinants. I. Homotypic seminal vesicle recombinants." Development **106**(2): 219-234.

Hirschi, K.K., J.M. Burt, K.D. Hirschi and C. Dai (2003). "Gap junction communication mediates transforming growth factor-beta activation and endothelial-induced mural cell differentiation." Circ Res **93**(5): 429-37.

Hoffmann, R. and D. Van Neste (2005). "Recent findings with computerized methods for scalp hair growth measurements." J Investig Dermatol Symp Proc **10**(3): 285-8.

Honda, Y., K. Egawa, M. Kuroki and T. Ono (1997). "Hair cycle-dependent expression of a nonspecific cross reacting antigen (NCA)-50/90-like molecule on follicular keratinocytes." Arch Dermatol Res **289**(8): 457-65.

Horne, K.A. and C.A. Jahoda (1992). "Restoration of hair growth by surgical implantation of follicular dermal sheath." Development **116**(3): 563-71.

Horne, K.A., C.A. Jahoda and R.F. Oliver (1986). "Whisker growth induced by implantation of cultured vibrissa dermal papilla cells in the adult rat." J Embryol Exp Morphol **97**: 111-24.

Hunt, N. and S. McHale (2005). "The psychological impact of alopecia." Bmj **331**(7522): 951-3.

Ibrahim, L. and E.A. Wright (1975). "The growth of rats and mice vibrissae under normal and some abnormal conditions." J Embryol Exp Morphol **33**(4): 831-44.

Ibrahim, L. and E.A. Wright (1982). "A quantitative study of hair growth using mouse and rat vibrissal follicles. I. Dermal papilla volume determines hair volume." J Embryol Exp Morphol **72**: 209-24.

Ibrahim, L. and E.A. Wright (1983). "Effect of castration and testosterone propionate on mouse vibrissae." Br J Dermatol **108**: 321-326.

Iguchi, M., M. Hara, H. Manome, H. Kobayasi, H. Tagami and S. Aiba (2003). "Communication network in the follicular papilla and connective tissue sheath through gap junctions in human hair follicles." Exp Dermatol **12**(3): 283-8.

Inamatsu, M., T. Matsuzaki, H. Iwanari and K. Yoshizato (1998). "Establishment of rat dermal papilla cell lines that sustain the potency to induce hair follicles from afollicular skin." J Invest Dermatol **111**(5): 767-75.

Inamatsu, M., T. Tochio, A. Makabe, T. Endo, S. Oomizu, E. Kobayashi and K. Yoshizato (2006). "Embryonic dermal condensation and adult dermal papilla induce hair follicles in adult glabrous epidermis through different mechanisms." Dev Growth Differ **48**(2): 73-86.

Inoue, N., K. Kuwae, A. Ishida-Yamamoto, H. Iizuka, M. Shibata, S. Yoshida, K. Kato and S. Shiosaka (1998). "Expression of neuropsin in the keratinizing epithelial tissue-immunohistochemical analysis of wild-type and nude mice." J Invest Dermatol **110**(6): 923-31.

Ito, M. (1986). "The innermost cell layer of the outer root sheath in anagen hair follicle: light and electron microscopic study." Arch Dermatol Res **279**(2): 112-9.

Ito, M. (1988). "Electron microscopic study on cell differentiation in anagen hair follicles in mice." J Invest Dermatol **90**(1): 65-72.

Ito, M. (1989). "Biologic roles of the innermost cell layer of the outer root sheath in human anagen hair follicle: further electron microscopic study." Arch Dermatol Res **281**(4): 254-9.

Ito, M. and K. Kizawa (2001). "Expression of calcium-binding S100 proteins A4 and A6 in regions of the epithelial sac associated with the onset of hair follicle regeneration." J Invest Dermatol **116**(6): 956-63.

Ito, M., K. Kizawa, K. Hamada and G. Cotsarelis (2004). "Hair follicle stem cells in the lower bulge form the secondary germ, a biochemically distinct but functionally equivalent progenitor cell population, at the termination of catagen." Differentiation **72**(9-10): 548-57.

Ito, M., K. Kizawa, M. Toyoda and M. Morohashi (2002). "Label-retaining cells in the bulge region are directed to cell death after plucking, followed by healing from the surviving hair germ." J Invest Dermatol **119**(6): 1310-6.

Ito, N., T. Ito, A. Kromminga, A. Bettermann, M. Takigawa, F. Kees, R.H. Straub and R. Paus (2005). "Human hair follicles display a functional equivalent of the hypothalamic-pituitary-adrenal axis and synthesize cortisol." Faseb J **19**(10): 1332-4.

Jacobs, J.P., C.A. Szpunar and M.L. Warner (1993). "Use of topical minoxidil therapy for androgenetic alopecia in women." Int J Dermatol **32**: 758-762.

Jahoda, C. and R.F. Oliver (1981). "The growth of vibrissa dermal papilla cells in vitro." Br J Dermatol **105**(6): 623-7.

Jahoda, C.A. (1992). "Induction of follicle formation and hair growth by vibrissa dermal papillae implanted into rat ear wounds: vibrissa-type fibres are specified." Development **115**(4): 1103-9.

Jahoda, C.A. (1998). "Cellular and developmental aspects of androgenetic alopecia." Exp Dermatol **7**(5): 235-48.

Jahoda, C.A. (2003). "Cell movement in the hair follicle dermis - more than a two-way street?" J Invest Dermatol **121**(6): ix-xi.

Jahoda, C.A., K.A. Horne, A. Mauger, S. Bard and P. Sengel (1992a). "Cellular and extracellular involvement in the regeneration of the rat lower vibrissa follicle." Development **114**(4): 887-97.

Jahoda, C.A., K.A. Horne and R.F. Oliver (1984). "Induction of hair growth by implantation of cultured dermal papilla cells." Nature **311**(5986): 560-2.

Jahoda, C.A., A. Mauger, S. Bard and P. Sengel (1992b). "Changes in fibronectin, laminin and type IV collagen distribution relate to basement membrane restructuring during the rat vibrissa follicle hair growth cycle." J Anat **181 (Pt 1)**: 47-60.

Jahoda, C.A. and R.F. Oliver (1984a). "Histological studies of the effects of wounding vibrissa follicles in the hooded rat." J Embryol Exp Morphol **83**: 95-108.

Jahoda, C.A. and R.F. Oliver (1984b). "Observations on the relationship between nerve supply and hair positioning in the rat vibrissa follicle." J Anat **139 (Pt 2)**: 333-9.

Jahoda, C.A. and R.F. Oliver (1984c). "Vibrissa dermal papilla cell aggregative behaviour in vivo and in vitro." J Embryol Exp Morphol **79**: 211-24.

Jahoda, C.A., R.F. Oliver, A.J. Reynolds, J.C. Forrester, J.W. Gillespie, P.B. Cserhalmi-Friedman, A.M. Christiano and K.A. Horne (2001). "Trans-species hair growth induction by human hair follicle dermal papillae." Exp Dermatol **10**(4): 229-37.

Jahoda, C.A., R.F. Oliver, A.J. Reynolds, J.C. Forrester and K.A. Horne (1996). "Human hair follicle regeneration following amputation and grafting into the nude mouse." J Invest Dermatol **107**(6): 804-7.

Jahoda, C.A. and A.J. Reynolds (2001). "Hair follicle dermal sheath cells: unsung participants in wound healing." Lancet **358**(9291): 1445-8.

Jahoda, C.A., A.J. Reynolds, C. Chaponnier, J.C. Forester and G. Gabbiani (1991). "Smooth muscle alpha-actin is a marker for hair follicle dermis in vivo and in vitro." J Cell Sci **99 (Pt 3)**: 627-36.

Jahoda, C.A., A.J. Reynolds and R.F. Oliver (1993). "Induction of hair growth in ear wounds by cultured dermal papilla cells." J Invest Dermatol **101**(4): 584-90.

Jahoda, C.A., J. Whitehouse, A.J. Reynolds and N. Hole (2003). "Hair follicle dermal cells differentiate into adipogenic and osteogenic lineages." Exp Dermatol **12**(6): 849-59.

Jan, A.Y., S. Amin, P. Ratajczak, G. Richard and V.P. Sybert (2004). "Genetic heterogeneity of KID syndrome: identification of a Cx30 gene (GJB6) mutation in a patient with KID syndrome and congenital atrichia." J Invest Dermatol **122**(5): 1108-13.

Jensen, P.J., T. Yang, D.W. Yu, M.S. Baker, B. Risse, T.T. Sun and R.M. Lavker (2000). "Serpins in the human hair follicle." J Invest Dermatol **114**(5): 917-22.

Johnson, E. (1972). "Moulting Cycles." Mammalian Rev **1**: 198-208.

Kabir, N., K. Chaturvedi, L.S. Liu and D.K. Sarkar (2005). "Transforming growth factor-beta3 increases gap-junctional communication among folliculostellate cells to release basic fibroblast growth factor." Endocrinology **146**(9): 4054-60.

Kalinin, A.E., A.V. Kajava and P.M. Steinert (2002). "Epithelial barrier function: Assembly and structural features of the cornified cell envelope." Bioessays **24**: 789–800.

Kamimura, A. and T. Takahashi (2002). "Procyanidin B-3, isolated from barley and identified as a hair-growth stimulant, has the potential to counteract inhibitory regulation by TGF-beta1." Exp Dermatol **11**(6): 532-41.

Kanczuga-Koda, L., S. Sulkowski, M. Koda, E. Skrzydlewska and M. Sulkowska (2005). "Connexin 26 correlates with Bcl-xL and Bax proteins expression in colorectal cancer." World J Gastroenterol **11**(10): 1544-8.

Karnovsky, M.J. (1965). "A formaldehyde-gluteraldehyde fixative of high osmolarity for use in electron microscopy." J Cell Biol **27**: 137-138A.

Kashiwagi, M., M. Tortorella, H. Nagase and K. Brew (2001). "TIMP-3 is a potent inhibitor of aggrecanase 1 (ADAM-TS4) and aggrecanase 2 (ADAM-TS5)." J Biol Chem **276**(16): 12501-4.

Kaufman, K.D. and R.P.R. Dawber (1999). "Finasteride, a Type 2 5alpha-reductase inhibitor, in the treatment of men with androgenetic alopecia." Expert Opin Investig Drugs **8**(4): 403-415.

Kawabe, T.T., T.J. Rea, A.M. Flenniken, B.R. Williams, V.E. Groppi and A.E. Buhl (1991). "Localization of TIMP in cycling mouse hair." Development **111**(4): 877-9.

Kawaguchi, M., Y. Mitsuhashi and S. Kondo (2004). "Localization of tumour necrosis factor-alpha converting enzyme in normal human skin." Clin Exp Dermatol **29**(2): 185-7.

Kawaguchi, M., Y. Mitsuhashi and S. Kondo (2005). "Overexpression of tumour necrosis factor-alpha-converting enzyme in psoriasis." Br J Dermatol **152**(5): 915-9.

Kee, Y. and M. Bronner-Fraser (2005). "To proliferate or to die: role of Id3 in cell cycle progression and survival of neural crest progenitors." Genes Dev **19**(6): 744-55.

Kelly, S.C., P. Ratajczak, M. Keller, S.M. Purcell, T. Griffin and G. Richard (2006). "A novel GJA 1 mutation in oculo-dento-digital dysplasia with curly hair and hyperkeratosis." Eur J Dermatol **16**(3): 241-5.

Kelsell, D.P., W.L. Di and M.J. Houseman (2001). "Connexin mutations in skin disease and hearing loss." Am J Hum Genet **68**(3): 559-68.

Kiesewetter, F., P. Langer and H. Schell (1991). "Minoxidil stimulates mouse vibrissae follicles in organ culture." J Invest Dermatol **96**(2): 295-6.

Kim, J.C. and Y.C. Choi (1995). "Regrowth of grafted human scalp hair after removal of the bulb." Dermatol Surg **21**(4): 312-3.

Kim, J.C., M.K. Kim and Y.C. Choi (1996). Regeneration of the human scalp hair follicle after horizontal sectioning: implications for pluripotent stem cells and melanocyte reservoir. Hair Research for the Next Millennium. D. Van Neste and V.A. Randall. Amsterdam, Elsevier: 135-139.

Kim, S.R., S.Y. Cha, M.K. Kim, J.C. Kim and Y.K. Sung (2006). "Induction of versican by ascorbic acid 2-phosphate in dermal papilla cells." J Dermatol Sci **43**(1): 60-2.

Kishibe, M., Y. Bando, R. Terayama, K. Namikawa, H. Takahashi, Y. Hashimoto, A. Ishida-Yamamoto, Y.P. Jiang, B. Mitrovic, D. Perez, H. Iizuka and S. Yoshida

(2006). "Kallikrein 8 is involved in skin desquamation in cooperation with other kallikreins." J Biol Chem.

Kishimoto, J., R. Ehama, L. Wu, S. Jiang, N. Jiang and R.E. Burgeson (1999). "Selective activation of the versican promoter by epithelial- mesenchymal interactions during hair follicle development." Proc Natl Acad Sci U S A **96**(13): 7336-41.

Kjaer, K.W., L. Hansen, H. Eiberg, P. Leicht, J.M. Opitz and N. Tommerup (2004). "Novel Connexin 43 (GJA1) mutation causes oculo-dento-digital dysplasia with curly hair." Am J Med Genet A **127**(2): 152-7.

Klein-Szanto, A.J. (1977). "Stereologic baseline data of normal human epidermis." J Invest Dermatol **68**(2): 73-8.

Kligman, A.M. (1959). "The human hair cycle." J Invest Dermatol **33**: 307-16.

Kligman, A.M. (1961). "Pathologic dynamics of human hair loss. I. Telogen effuvium." Arch Dermatol **83**: 175-98.

Koch, P.J., M.G. Mahoney, G. Cotsarelis, K. Rothenberger, R.M. Lavker and J.R. Stanley (1998). "Desmoglein 3 anchors telogen hair in the follicle." J Cell Sci **111 (Pt 17)**: 2529-37.

Koch, P.J., M.G. Mahoney, H. Ishikawa, L. Pulkkinen, J. Uitto, L. Shultz, G.F. Murphy, D. Whitaker-Menezes and J.R. Stanley (1997). "Targeted disruption of the pemphigus vulgaris antigen (desmoglein 3) gene in mice causes loss of keratinocyte cell adhesion with a phenotype similar to pemphigus vulgaris." J Cell Biol **137**: 1091-1102.

Kokileva, L. (1994). "Multi-step chromatin degradation in apoptosis: DNA breakdown in apoptosis." Int Arch Allergy Immunol **105**: 339–343.

Kollar, E.J. (1970). "The induction of hair follicles by embryonic dermal papillae." J Invest Dermatol **55**(6): 374-8.

Komatsu, N., M. Takata, N. Otsuki, T. Toyama, R. Ohka, K. Takehara and K. Saijoh (2003). "Expression and Localization of Tissue Kallikrein mRNAs in Human Epidermis and Appendages." J Invest Dermatol **121**(3): 542-549.

Kong, J. and Y.C. Li (2002). "Upregulation of interleukin-18 expression in mouse primary keratinocytes induced to differentiate by calcium." Arch Dermatol Res **294**(8): 370-6.

Kopan, R. and E. Fuchs (1989). "The use of retinoic acid to probe the relation between hyperproliferation-associated keratins and cell proliferation in normal and malignant epidermal cells." J Cell Biol **109**(1): 295-307.

Kopan, R., G. Traska and E. Fuchs (1987). "Retinoids as important regulators of terminal differentiation: examining keratin expression in individual epidermal cells at various stages of keratinization." J Cell Biol **105**(1): 427-40.

Kouklis, P.D., E. Hutton and E. Fuchs (1994). "Making a connection: direct binding between keratin intermediate filaments and desmosomal proteins." J Cell Biol **127**(4): 1049-60.

Kretz, M., C. Euwens, S. Hombach, D. Eckardt, B. Teubner, O. Traub, K. Willecke and T. Ott (2003). "Altered connexin expression and wound healing in the epidermis of connexin-deficient mice." J Cell Sci **116**(Pt 16): 3443-52.

Kretz, M., K. Maass and K. Willecke (2004). "Expression and function of connexins in the epidermis, analyzed with transgenic mouse mutants." Eur J Cell Biol **83**(11-12): 647-54.

Krutovskikh, V.A., S.M. Troyanovsky, C. Piccoli, H. Tsuda, M. Asamoto and H. Yamasaki (2000). "Differential effect of subcellular localization of communication impairing gap junction protein connexin43 on tumor cell growth in vivo." Oncogene **19**(4): 505-13.

Kurata, S., T. Ezaki, S. Itami, H. Terashi and S. Takayusu (1999). "Viability of isolated single hair follicles preserved at 4 degrees C." Dermatol Surg **25**(1): 26-9.

Kurooka, H. and Y. Yokota (2005). "Nucleo-cytoplasmic shuttling of Id2, a negative regulator of basic helix-loop-helix transcription factors." J Biol Chem **280**(6): 4313-20.

Kuwae, K., K. Matsumoto-Miyai, S. Yoshida, T. Sadayama, K. Yoshikawa, K. Hosokawa and S. Shiosaka (2002). "Epidermal expression of serine protease,

neuropsin (KLK8) in normal and pathological skin samples." Mol Pathol **55**(4): 235-41.

Lachgar, S., M. Charveron, Y. Gall and J.L. Bonafe (1998). "Minoxidil upregulates the expression of vascular endothelial growth factor in human hair dermal papilla cells." Br J Dermatol **138**(3): 407-11.

Laird, D.W. (2006). "Life cycle of connexins in health and disease." Biochem J **394**(Pt 3): 527-43.

Lamartine, J., G. Munhoz Essenfelder, Z. Kibar, I. Lanneluc, E. Callouet, D. Laoudj, G. Lemaitre, C. Hand, S.J. Hayflick, J. Zonana, S. Antonarakis, U. Radhakrishna, D.P. Kelsell, A.L. Christianson, A. Pitaval, V. Der Kaloustian, C. Fraser, C. Blanchet-Bardon, G.A. Rouleau and G. Waksman (2000a). "Mutations in GJB6 cause hidrotic ectodermal dysplasia." Nat Genet **26**(2): 142-4.

Lamartine, J., A. Pitaval, P. Soularue, I. Lanneluc, G. Lemaitre, Z. Kibar, G.A. Rouleau and G. Waksman (2000b). "A 1.5-Mb physical map of the hidrotic ectodermal dysplasia (Clouston syndrome) gene region on human chromosome 13q11." Genomics **67**(2): 232-6.

Lampe, P.D., B.P. Nguyen, S. Gil, M. Usui, J. Olerud, Y. Takada and W.G. Carter (1998). "Cellular interaction of integrin alpha3beta1 with laminin 5 promotes gap junctional communication." J Cell Biol **143**(6): 1735-47.

Langbein, L., M.A. Rogers, S. Praetzel, N. Aoki, H. Winter and J. Schweizer (2002). "A novel epithelial keratin, hK6irs1, is expressed differentially in all layers of the inner root sheath, including specialized huxley cells (Flugelzellen) of the human hair follicle." J Invest Dermatol **118**(5): 789-99.

Lavker, R.M., B. Risse, H. Brown, D. Ginsburg, J. Pearson, M.S. Baker and P.J. Jensen (1998). "Localization of plasminogen activator inhibitor type 2 (PAI-2) in hair and nail: implications for terminal differentiation." J Invest Dermatol **110**(6): 917-22.

Leco, K.J., R. Khokha, N. Pavloff, S.P. Hawkes and D.R. Edwards (1994). "Tissue inhibitor of metalloproteinases-3 (TIMP-3) is an extracellular matrix-associated

protein with a distinctive pattern of expression in mouse cells and tissues." J Biol Chem **269**(12): 9352-60.

Leco, K.J., P. Waterhouse, O.H. Sanchez, K.L. Gowing, A.R. Poole, A. Wakeham, T.W. Mak and R. Khokha (2001). "Spontaneous air space enlargement in the lungs of mice lacking tissue inhibitor of metalloproteinases-3 (TIMP-3)." J Clin Invest **108**(6): 817-29.

Legue, E. and J.F. Nicolas (2005). "Hair follicle renewal: organisation of stem cells in the matrix and the role of stereotyped lineages and behaviours." Development **132**: 4143-4154.

Levy, V., C. Lindon, B.D. Harfe and B.A. Morgan (2005). "Distinct stem cell populations regenerate the follicle and interfollicular epidermis." Dev Cell **9**(6): 855-61.

Levy, V., C. Lindon, Y. Zheng, B.D. Harfe and B.A. Morgan (2007). "Epidermal stem cells arise from the hair follicle after wounding." Faseb J.

Leyvraz, C., R.P. Charles, I. Rubera, M. Guitard, S. Rotman, B. Breiden, K. Sandhoff and E. Hummler (2005). "The epidermal barrier function is dependent on the serine protease CAP1/Prss8." J Cell Biol **170**(3): 487-96.

Li, M., A. Marubayashi, Y. Nakaya, K. Fukui and S. Arase (2001). "Minoxidil-induced hair growth is mediated by adenosine in cultured dermal papilla cells: possible involvement of sulfonylurea receptor 2B as a target of minoxidil." J Invest Dermatol **117**(6): 1594-600.

Li, Q., Q. Lu, G. Estepa and I.M. Verma (2005). "Identification of 14-3-3 ó mutation causing cutaneous abnormality in repeated-epilation mutant mouse." Proc Natl Acad Sci U S A **102**(44): 15977-15982.

Li, Y., C.M. Lin, X.N. Cai, G.Q. Li and K. Huang (2006). "[Induction of hair follicle regeneration in mice ear by microencapsulated human hair dermal papilla cells]." Zhonghua Zheng Xing Wai Ke Za Zhi **22**(2): 88-91.

Lian, X. and T. Yang (2004). "Plasminogen activator inhibitor 2: expression and role in differentiation of epidermal keratinocyte." Biol Cell **96**(2): 109-16.

Lichti, U., W.C. Weinberg, L.V. Goodman, S. Ledbetter, T. Dooley, D. Morgan and S.H. Yuspa (1993). "*In Vivo* Regulation of Murine Hair Growth: Insights from

grafting defined cell populations onto nude mice." J Invest Dermatol **101**: 124S-129S.

Light, W., A.E. Vernon, A. Lasorella, A. Iavarone and C. LaBonne (2005). "Xenopus Id3 is required downstream of Myc for the formation of multipotent neural crest progenitor cells." Development **132**(8): 1831-41.

Lillie, F.R. and H. Wang (1941). "Physiology and development of the feather. V: Experimental morphogenesis." Physiol Zool **14**: 103-133.

Lillie, F.R. and H. Wang (1944). "Physiology and development of the feather. VII: An experimental study of induction." Physiol Zool **17**: 1-31.

Limat, A. and F.K. Noser (1986). "Serial cultivation of single keratinocytes from the outer root sheath of human scalp hair follicles." J Invest Dermatol **87**(4): 485-8.

Limmer, B.L. (1994). "Elliptical donor stereoscopically assisted micrografting as an approach to further refinement in hair transplantation." J Dermatol Surg Oncol **20**(12): 789-93.

Lin, K.K., D. Chudova, G.W. Hatfield, P. Smyth and B. Andersen (2004). "Identification of hair cycle-associated genes from time-course gene expression profile data by using replicate variance." Proc Natl Acad Sci U S A **101**(45): 15955-60.

Lincoln, G.A. and I.J. Clarke (1994). "Photoperiodically-induced cycles in the secretion of prolactin in hypothalamo-pituitary disconnected rams: evidence for translation of the melatonin signal in the pituitary gland." J Neuroendocrinol **6**(3): 251-60.

Lindner, G., V.A. Botchkarev, N.V. Botchkareva, G. Ling, C. van der Veen and R. Paus (1997). "Analysis of apoptosis during hair follicle regression (catagen)." Am J Pathol **151**(6): 1601-17.

Loechel, F., J.W. Fox, G. Murphy, R. Albrechtsen and U.M. Wewer (2000). "ADAM 12-S cleaves IGFBP-3 and IGFBP-5 and is inhibited by TIMP-3." Biochem Biophys Res Commun **278**(3): 511-5.

Ludwig, E. (1977). "Classification of the types of androgenetic alopecia (common baldness) occurring in the female sex." Br J Dermatol **97**(3): 247-54.

Lundström, A. and T. Egelrud (1988). "Cell shedding from human plantar skin in vitro: evidence of its dependence on endogenous proteolysis." J Invest Dermatol **91**(340-343).

Lundström, A. and T. Egelrud (1989). "Evidence that cell shedding from plantar skin in vitro involves endogenous proteolysis of the desmosomal protein desmoglein I." J Invest Dermatol **94**: 216-220.

Lundström, A. and T. Egelrud (1991). "Stratum corneum chymotryptic enzyme: a proteinase which may be generally present in the stratum corneum and with a possible involvement in desquamation." Acta Derm Venereol **71**: 471-474.

Lunn, C.A., X. Fan, B. Dalie, K. Miller, P.J. Zavodny, S.K. Narula and D. Lundell (1997). "Purification of ADAM 10 from bovine spleen as a TNFalpha convertase." FEBS Lett **400**(3): 333-5.

Luo, J., A.J. Litherland, T. Sahlu, R. Puchala, M. Lachica and A.L. Goetsch (2000). "Effects of mimosine on fiber shedding, follicle activity, and fiber regrowth in Spanish goats." J Anim Sci **78**(6): 1551-5.

Lyle, S., M. Christofidou-Solomidou, Y. Liu, D.E. Elder, S. Albelda and G. Cotsarelis (1998). "The C8/144B monoclonal antibody recognizes cytokeratin 15 and defines the location of human hair follicle stem cells." J Cell Sci **111 (Pt 21)**: 3179-88.

Lyle, S., M. Christofidou-Solomidou, Y. Liu, D.E. Elder, S. Albelda and G. Cotsarelis (1999). "Human hair follicle bulge cells are biochemically distinct and possess an epithelial stem cell phenotype." J Investig Dermatol Symp Proc **4**(3): 296-301.

Lynfield, Y.L. (1960). "Effect of pregnancy on the human hair cycle." J Invest Dermatol **35**: 323-7.

Lyons-Giordano, B., D. Loskutoff, C.S. Chen, G. Lazarus, M. Keeton and P.J. Jensen (1994). "Expression of plasminogen activator inhibitor type 2 in normal and psoriatic epidermis." Histochemistry **101**: 105-112.

Ma, L., J. Liu, T. Wu, M. Plikus, T.X. Jiang, Q. Bi, Y.H. Liu, S. Muller-Rover, H. Peters, J.P. Sundberg, R. Maxson, R.L. Maas and C.M. Chuong (2003). "'Cyclic

alopecia' in Msx2 mutants: defects in hair cycling and hair shaft differentiation." Development **130**(2): 379-89.

Maass, K., A. Ghanem, J.S. Kim, M. Saathoff, S. Urschel, G. Kirfel, R. Grummer, M. Kretz, T. Lewalter, K. Tiemann, E. Winterhager, V. Herzog and K. Willecke (2004). "Defective epidermal barrier in neonatal mice lacking the C-terminal region of connexin43." Mol Biol Cell **15**(10): 4597-608.

Magerl, M., S. Kauser, R. Paus and D.J. Tobin (2002). "Simple and rapid method to isolate and culture follicular papillae from human scalp hair follicles." Exp Dermatol **11**(4): 381-5.

Maher, A.C., T. Thomas, J.L. Riley, G. Veitch, Q. Shao and D.W. Laird (2005). "Rat epidermal keratinocytes as an organotypic model for examining the role of Cx43 and Cx26 in skin differentiation." Cell Commun Adhes **12**(5-6): 219-30.

Makita, J., H. Kurooka, K. Mori, Y. Akagi and Y. Yokota (2006). "Identification of the nuclear export signal in the helix-loop-helix inhibitor Id1." FEBS Lett **580**(7): 1812-6.

Martinet, L., D. Allain and C. Weiner (1984). "Role of prolactin in the photoperiodic control of moulting in the mink (Mustela vison)." J Endocrinol **103**(1): 9-15.

Martinet, L., M. Mondain-Monval and R. Monnerie (1992). "Endogenous circannual rhythms and photorefractoriness of testis activity, moult and prolactin concentrations in mink (Mustela vison)." J Reprod Fertil **95**(2): 325-38.

Matic, M., W.H. Evans, P.R. Brink and M. Simon (2002). "Epidermal stem cells do not communicate through gap junctions." J Invest Dermatol **118**(1): 110-6.

Matic, M. and M. Simon (2003). "Label-retaining cells (presumptive stem cells) of mice vibrissae do not express gap junction protein connexin 43." J Investig Dermatol Symp Proc **8**(1): 91-5.

Matsuzaki, T. and K. Yoshizato (1998). "Role of hair papilla cells on induction and regeneration processes of hair follicles." Wound Repair Regen **6**(6): 524-30.

Maurer, F. (1895). Die epidermis und ihre Abkömmlinge. Leipzig, Wilhelm Engelmann.

Maurer, M., E. Fischer, B. Handijski, E. von Stebut, B. Algermissen, A. Bavandi and R. Paus (1997). "Activated skin mast cells are involved in muring hair follicle regression (catagen)." Lab Invest **77**: 319-332.

McClellan, K.J. and A. Markham (1999). "Finasteride: a review of its use in male pattern hair loss." Drugs **57**(1): 111-26.

McElwee, K.J., S. Kissling, E. Wenzel, A. Huth and R. Hoffmann (2003). "Cultured peribulbar dermal sheath cells can induce hair follicle development and contribute to the dermal sheath and dermal papilla." J Invest Dermatol **121**(6): 1267-75.

Mehta, P.P., J.S. Bertram and W.R. Loewenstein (1989). "The actions of retinoids on cellular growth correlate with their actions on gap junctional communication." J Cell Biol **108**(3): 1053-65.

Menon, G.K., S. Grayson and P.M. Elias (1985). "Ionic calcium reservoirs in mammalian epidermis: ultrastructural localization by ion-capture cytochemistry." J Invest Dermatol **84**: 508-512.

Messenger, A.G. (1984). "The culture of dermal papilla cells from human hair follicles." Br J Dermatol **110**(6): 685-9.

Messenger, A.G., H.J. Senior and S.S. Bleehen (1986). "The in vitro properties of dermal papilla cell lines established from human hair follicles." Br J Dermatol **114**(4): 425-30.

Michelet, J.F., S. Commo, N. Billoni, Y.F. Mahe and B.A. Bernard (1997). "Activation of cytoprotective prostaglandin synthase-1 by minoxidil as a possible explanation for its hair growth-stimulating effect." J Invest Dermatol(108): 205–209.

Milner, Y., J. Sudnik, M. Filippi, M. Kizoulis, M. Kashgarian and K. Stenn (2002). "Exogen, shedding phase of the hair growth cycle: characterization of a mouse model." J Invest Dermatol **119**(3): 639-44.

Mitsui, S., A. Ohuchi, T. Adachi-Yamada, M. Hotta, R. Tsuboi and H. Ogawa (1998). "Structure and hair follicle-specific expression of genes encoding the rat high sulfur protein B2 family." Gene **208**(2): 123-129.

Miyashita, H., Y. Hakamata, E. Kobayashi and K. Kobayashi (2004). "Characterization of hair follicles induced in implanted, cultured rat keratinocyte sheets." Exp Dermatol **13**: 491-498.

Moghetti, P., R. Castello, C.M. Magnani, F. Tosi, C. Negri, D. Armanini, G. Bellotti and M. Muggeo (1994). "Clinical and hormonal effects of the 5 alpha-reductase inhibitor finasteride in idiopathic hirsutism." J Clin Endocrinol Metab **79**(4): 1115-21.

Morris, R.J., Y. Liu, L. Marles, Z. Yang, C. Trempus, S. Li, J.S. Lin, J.A. Sawicki and G. Cotsarelis (2004). "Capturing and profiling adult hair follicle stem cells." Nat Biotechnol **22**(4): 411-7.

Muller-Decker, K., C. Leder, M. Neumann, G. Neufang, C. Bayerl, J. Schweizer, F. Marks and G. Furstenberger (2003). "Expression of cyclooxygenase isozymes during morphogenesis and cycling of pelage hair follicles in mouse skin: precocious onset of the first catagen phase and alopecia upon cyclooxygenase-2 overexpression." J Invest Dermatol **121**(4): 661-8.

Muller-Rover, S., B. Handjiski, C. van der Veen, S. Eichmuller, K. Foitzik, I.A. McKay, K.S. Stenn and R. Paus (2001). "A comprehensive guide for the accurate classification of murine hair follicles in distinct hair cycle stages." J Invest Dermatol **117**(1): 3-15.

Mylona, E., C. Magkou, I. Giannopoulou, G. Agrogiannis, S. Markaki, A. Keramopoulos and L. Nakopoulou (2006). "Expression of tissue inhibitor of matrix metalloproteinases (TIMP)-3 protein in invasive breast carcinoma: Relation to tumor phenotype and clinical outcome." Breast Cancer Res **8**(5): R57.

Nagy, J.I., D. Patel, P.A. Ochalski and G.L. Stelmack (1999). "Connexin30 in rodent, cat and human brain: selective expression in gray matter astrocytes, co-localization with connexin43 at gap junctions and late developmental appearance." Neuroscience **88**(2): 447-68.

Nakaya, Y., H. Hamaoka, S. Kato and S. Arase (1994). "Effect of minoxidil sulfate and pinacidil on single potassium channel current in cultured human outer root sheath cells and dermal papilla cells." J Dermatol Sci **7 Suppl**: S104-8.

Nanba, D., Y. Nakanishi and Y. Hieda (2003). "Establishment of cadherin-based intercellular junctions in the dermal papilla of the developing hair follicle." Anat Rec A Discov Mol Cell Evol Biol **270**(2): 97-102.

Narbutt, J., E. Waszczykowska, J. Lukamowicz, A. Sysa-Jedrzejowska, J. Kobos and A. Zebrowska (2006). "Disturbances of the expression of metalloproteinases and their tissue inhibitors cause destruction of the basement membrane in pemphigoid." Pol J Pathol **57**(2): 71-6.

Norwood, O.T. (2001). "Incidence of female pattern androgenetic alopecia." Dermatol Surg **27**: 53-54.

Noser, F.K. and A. Limat (1987). "Organotypic culture of outer root sheath cells from human hair follicles using a new culture device." In Vitro Cell Dev Biol **23**(8): 541-5.

Nutbrown, M. and V.A. Randall (1996). Recognition of cellular differentiation in the human hair follilce at the light microscope level using SACPIC staining. Hair research for the next millenium. D. Van Neste and V.A. Randall. Amsterdam, Elsevier: 161-166.

Ny, A. and T. Egelrud (2004). "Epidermal hyperproliferation and decreased skin barrier function in mice overexpressing stratum corneum chymotryptic enzyme." Acta Derm Venereol **84**(1): 18-22.

Ohyama, M., A. Terunuma, C.L. Tock, M.F. Radonovich, C.A. Pise-Masison, S.B. Hopping, J.N. Brady, M.C. Udey and J.C. Vogel (2006). "Characterization and isolation of stem cell-enriched human hair follicle bulge cells." J Clin Invest **116**(1): 249-60.

Okuyama, R., B.C. Nguyen, C. Talora, E. Ogawa, A. Tommasi di Vignano, M. Lioumi, G. Chiorino, H. Tagami, M. Woo and G.P. Dotto (2004). "High commitment of embryonic keratinocytes to terminal differentiation through a Notch1-caspase 3 regulatory mechanism." Dev Cell **6**(4): 551-62.

Oliver, R.F. (1966a). "Histological Studies of Whisker Regeneration in Hooded Rat." Journal of Embryology and Experimental Morphology **16**: 231-&.

Oliver, R.F. (1966b). "Regeneration of dermal papillae in rat vibrissae." J Invest Dermatol **47**(5): 496-7.

Oliver, R.F. (1966c). "Whisker Growth after Removal of Dermal Papilla and Lengths of Follicle in Hooded Rat." Journal of Embryology and Experimental Morphology **15**: 331-&.

Oliver, R.F. (1967). "The experimental induction of whisker growth in the hooded rat by implantation of dermal papillae." J Embryol Exp Morphol **18**(1): 43-51.

Oliver, R.F. (1969). Regeneration of the dermal papilla and its influence on whisker growth. Advances in Biology of Skin. W. Montagna and R.L. Dobson. Oxford, Pergamon Press. **9**.

Olsen, E., H.H. Rasmussen and J.E. Celis (1995). "Identification of proteins that are abnormally regulated in differentiated cultured human keratinocytes." Electrophoresis **16**(12): 2241-8.

Orentreich, N. (1959). "Autografts in alopecias and other selected dermatological conditions." Ann N Y Acad Sci **83**: 463-79.

Orwin, D.F. (1971). "Cell differentiation in the lower outer sheath of the Romney wool follicle: a companion cell layer." Aust J Biol Sci **24**(5): 989-99.

Orwin, D.F., H.B. Chase and A.F. Silver (1967). "Catagen in the hairless house mouse." Am J Anat **121**(3): 489-507.

Osada, A., T. Iwabuchi, J. Kishimoto, T. Hamazaki and H. Okochi (2007). "Long-Term Culture of Mouse Vibrissal Dermal Papilla Cells and De Novo Hair Follicle Induction." Tissue Eng **13**(5): 975-982.

Osada, A. and K. Kobayashi (2001). "Characterization of vibrissa germinative cells: transition of cell types." Exp Dermatol **10**(6): 430-7.

O'Shaughnessy, R.F., A.M. Christiano and C.A. Jahoda (2004). "The role of BMP signalling in the control of ID3 expression in the hair follicle." Exp Dermatol **13**(10): 621-9.

Oshima, H., A. Rochat, C. Kedzia, K. Kobayashi and Y. Barrandon (2001). "Morphogenesis and renewal of hair follicles from adult multipotent stem cells." Cell **104**(2): 233-45.

Paik, J.H., J.B. Yoon, W.Y. Sim, B.S. Kim and N.I. Kim (2001). "The prevalence and types of androgenetic alopecia in Korean men and women." Br J Dermatol **145**(1): 95-9.

Panteleyev, A.A., N.V. Botchkareva, J.P. Sundberg, A.M. Christiano and R. Paus (1999). "The role of the hairless (hr) gene in the regulation of hair follicle catagen transformation." Am J Pathol **155**(1): 159-71.

Panteleyev, A.A., C.A. Jahoda and A.M. Christiano (2001). "Hair follicle predetermination." J Cell Sci **114**(Pt 19): 3419-31.

Panteleyev, A.A., R. Paus and A.M. Christiano (2000). "Patterns of hairless (hr) gene expression in mouse hair follicle morphogenesis and cycling." Am J Pathol **157**(4): 1071-9.

Panteleyev, A.A., R. Paus, R. Wanner, W. Nurnberg, S. Eichmuller, R. Thiel, J. Zhang, B.M. Henz and T. Rosenbach (1997). "Keratin 17 gene expression during the murine hair cycle." J Invest Dermatol **108**(3): 324-9.

Panteleyev, A.A., C. van der Veen, T. Rosenbach, S. Muller-Rover, V.E. Sokolov and R. Paus (1998). "Towards defining the pathogenesis of the hairless phenotype." J Invest Dermatol **110**(6): 902-7.

Parakkal, P.F. (1970). "Morphogenesis of the hair follicle during catagen." Z Zellforsch Mikrosk Anat **107**(2): 174-86.

Paus, R., M. Maurer, A. Slominski and B.M. Czarnetzki (1994). "Mast cell involvement in murine hair growth." Dev Biol **163**: 230-240.

Paus, R., S. Muller-Rover and V.A. Botchkarev (1999). "Chronobiology of the hair follicle: hunting the " hair cycle clock"." J Investig Dermatol Symp Proc **4**(3): 338-45.

Paznekas, W.A., S.A. Boyadjiev, R.E. Shapiro, O. Daniels, B. Wollnik, C.E. Keegan, J.W. Innis, M.B. Dinulos, C. Christian, M.C. Hannibal and E.W. Jabs (2003). "Connexin 43 (GJA1) mutations cause the pleiotropic phenotype of oculodentodigital dysplasia." Am J Hum Genet **72**(2): 408-18.

Pearson, A.J., M.G. Ashby, J.E. Wildermoth, A.J. Craven and A.J. Nixon (1999). "Effect of exogenous prolactin on the hair growth cycle." Exp Dermatol **8**: 358-360.

Pearson, A.J., A.L. Parry, M.G. Ashby, V.J. Choy, J.E. Wildermoth and A.J. Craven (1996). "Inhibitory effect of increased photoperiod on wool follicle growth." J Endocrinol **148**(1): 157-66.

Pena, J.C., A. Kelekar, E.V. Fuchs and C.B. Thompson (1999). "Manipulation of outer root sheath cell survival perturbs the hair-growth cycle." Embo J **18**(13): 3596-603.

Peschon, J.J., J.L. Slack, P. Reddy, K.L. Stocking, S.W. Sunnarborg, D.C. Lee, W.E. Russell, B.J. Castner, R.S. Johnson, J.N. Fitzner, R.W. Boyce, N. Nelson, C.J. Kozlosky, M.F. Wolfson, C.T. Rauch, D.P. Cerretti, R.J. Paxton, C.J. March and R.A. Black (1998). "An essential role for ectodomain shedding in mammalian development." Science **282**(5392): 1281-4.

Philpott, M.P., G.E. Westgate and T. Kealey (1991). "An in vitro model for the study of human hair growth." Ann N Y Acad Sci **642**: 148-64; discussion 164-6.

Pierard-Franchimont, C., V. Goffin, F. Henry, I. Uhoda, C. Braham and G.E. Pierard (2002). "Nudging hair shedding by antidandruff shampoos. A comparison of 1% ketoconazole, 1% piroctone olamine and 1% zinc pyrithione formulations." Int J Cosmet Sci **24**(5): 249-256.

Pierard-Franchimont, C. and G.E. Pierard (2001). "Teloptosis, a turning point in hair shedding biorhythms." Dermatology **203**(2): 115-7.

Pierard-Franchimont, C., E. Xhauflaire-Uhoda, G. Loussouarn, D. Saint Leger and G.E. Pierard (2006). "Dandruff-associated smouldering alopecia: a chronobiological assessment over 5 years." Clin Exp Dermatol **31**(1): 23-6.

Pinkus, H. (1969). ""Sebaceous cysts" are trichilemmal cysts." Arch Dermatol **99**(5): 544-55.

Pinkus, H., T. Iwasaki and Y. Mishima (1981). "Outer root sheath keratinization in anagen and catagen of the mammalian hair follicle. A seventh distinct type of keratinization in the hair follicle: trichilemmal keratinization." J Anat **133**(Pt 1): 19-35.

Pisansarakit, P. and G.P.M. Moore (1986). "Induction of hair follicles in mouse skin by rat vibrissae dermal papillae." J Embryol Exp Morphol **94**: 113-119.

Poblet, E., F. Jimenez, C. de Cabo, A. Prieto-Martin and R. Sanchez-Prieto (2005). "The calcium-binding protein calretinin is a marker of the companion cell layer of the human hair follicle." Br J Dermatol **152**(6): 1316-20.

Potter, G.B., G.M. Beaudoin, 3rd, C.L. DeRenzo, J.M. Zarach, S.H. Chen and C.C. Thompson (2001). "The hairless gene mutated in congenital hair loss disorders encodes a novel nuclear receptor corepressor." Genes Dev **15**(20): 2687-701.

Poumay, Y., G. Jolivet, M.R. Pittelkow, F. Herphelin, I.Y. De Potter, V. Mitev and L. Houdebine (1999). "Human epidermal keratinocytes upregulate expression of the Prolactin Receptor after the onset of terminal differentiation, but do not respond to Prolactin." Archives of Biochemisty and Biophysics **364**(2): 247-253.

Powell, B.C., G.R. Cam, M.J. Fietz and G.E. Rogers (1986). "Clustered arrangement of keratin intermediate filament genes." Proc Natl Acad Sci U S A **83**(14): 5048-52.

Powell, B.C. and G.E. Rogers (1990). "Cyclic hair-loss and regrowth in transgenic mice overexpressing an intermediate filament gene." Embo J **9**(5): 1485-93.

Price, M.L. and W.A. Griffiths (1985). "Normal body hair--a review." Clin Exp Dermatol **10**(2): 87-97.

Qian, J., W. Li, G. Zhang, L. Yan and W. Sun (2005). "How Long Can Hair Follicle Units Be Preserved at 0 and 4°C for Delayed Transplant?" Dermatol Surg **31**: 1-23.

Qin, H., Q. Shao, H. Curtis, J. Galipeau, D.J. Belliveau, T. Wang, M.A. Alaoui-Jamali and D.W. Laird (2002). "Retroviral delivery of connexin genes to human breast tumor cells inhibits in vivo tumor growth by a mechanism that is independent of significant gap junctional intercellular communication." J Biol Chem **277**(32): 29132-8.

Qin, H., Q. Shao, S.A. Igdoura, M.A. Alaoui-Jamali and D.W. Laird (2003). "Lysosomal and proteasomal degradation play distinct roles in the life cycle of Cx43 in gap junctional intercellular communication-deficient and -competent breast tumor cells." J Biol Chem **278**(32): 30005-14.

Qiu, C., P. Coutinho, S. Frank, S. Franke, L.Y. Law, P. Martin, C.R. Green and D.L. Becker (2003). "Targeting connexin43 expression accelerates the rate of wound repair." Curr Biol **13**(19): 1697-703.

Radoja, N., A. Gazel, T. Banno, S. Yano and M. Blumenberg (2006). "Transcriptional profiling of epidermal differentiation." Physiol Genomics **27**(1): 65-78.

Randall, V.A. (1994). "Role of 5 alpha-reductase in health and disease." Baillieres Clin Endocrinol Metab **8**(2): 405-31.

Randall, V.A. and F.J. Ebling (1991). "Seasonal changes in human hair growth." Br J Dermatol **124**(2): 146-51.

Randall, V.A., N.A. Hibberts, M.J. Thornton, K. Hamada, A.E. Merrick, S. Kato, T.J. Jenner, I. De Oliveira and A.G. Messenger (2000). "The hair follicle: a paradoxical androgen target organ." Horm Res **54**(5-6): 243-50.

Randall, V.A., N.A. Hibberts, M.J. Thornton, A.E. Merrick, K. Hamada, S. Kato, T.J. Jenner, I. de Oliveira and A.G. Messenger (2001). "Do androgens influence hair growth by altering the paracrine factors secreted by dermal papilla cells?" Eur J Dermatol **11**(4): 315-20.

Rangarajan, A., C. Talora, R. Okuyama, M. Nicolas, C. Mammucari, H. Oh, J.C. Aster, S. Krishna, D. Metzger, P. Chambon, L. Miele, M. Aguet, F. Radtke and G.P. Dotto (2001). "Notch signaling is a direct determinant of keratinocyte growth arrest and entry into differentiation." Embo J **20**(13): 3427-36.

Rash, J.E., T. Yasumura, F.E. Dudek and J.I. Nagy (2001). "Cell-specific expression of connexins and evidence of restricted gap junctional coupling between glial cells and between neurons." J Neurosci **21**(6): 1983-2000.

Rassman, W.R., R.M. Bernstein, R. McClellan, R. Jones, E. Worton and H. Uyttendaele (2002). "Follicular unit extraction: minimally invasive surgery for hair transplantation." Dermatol Surg **28**(8): 720-8.

Rassman, W.R. and S. Carson (1995). "Micrografting in extensive quantities. The ideal hair restoration procedure." Dermatol Surg **21**(4): 306-11.

Reynolds, A.J., C. Lawrence, P.B. Cserhalmi-Friedman, A.M. Christiano and C.A. Jahoda (1999). "Trans-gender induction of hair follicles." Nature **402**(6757): 33-4.

Reynolds, A.J., C.M. Lawrence and C.A. Jahoda (1993). "Human hair follicle germinative epidermal cell culture." J Invest Dermatol **101**(4): 634-8.

Richard, G. (2000). "Connexins: a connection with the skin." Exp Dermatol **9**(2): 77-96.

Richardson, G.D., E.C. Arnott, C.J. Whitehouse, C.M. Lawrence, A.J. Reynolds, N. Hole and C.A. Jahoda (2005). "Plasticity of rodent and human hair follicle dermal cells: implications for cell therapy and tissue engineering." J Investig Dermatol Symp Proc **10**(3): 180-3.

Richardson, R., D. Donnai, F. Meire and M.J. Dixon (2004). "Expression of Gja1 correlates with the phenotype observed in oculodentodigital syndrome/type III syndactyly." J Med Genet **41**(1): 60-7.

Risek, B., F.G. Klier and N.B. Gilula (1994). "Developmental regulation and structural organization of connexins in epidermal gap junctions." Dev Biol **164**(1): 183-96.

Robinson, M., A.J. Reynolds, A. Gharzi and C.A. Jahoda (2001). "In vivo induction of hair growth by dermal cells isolated from hair follicles after extended organ culture." J Invest Dermatol **117**(3): 596-604.

Rochat, A., K. Kobayashi and Y. Barrandon (1994). "Location of stem cells of human hair follicles by clonal analysis." Cell **76**(6): 1063-73.

Rook, A. (1965). "Endocrine Influences on Hair Growth." Br Med J **1**(5435): 609-14.

Rook, A. and R.P.R. Dawber (1982). Diseases of the Hair and Scalp. The comparative physiology, embryology and physiology of human hair. R.P.R. Dawber. Oxford, UK, Blackwell Publishing: 1-17.

Rose, J., M. Kennedy, B. Johnston and W. Foster (1998). "Serum prolactin and dehydroepiandrosterone concentrations during the summer and winter hair growth cycles of mink (Mustela vison)." Comp Biochem Physiol A Mol Integr Physiol **121**(3): 263-71.

Rose, J., J. Oldfield and F. Stormshak (1987). "Apparent role of melatonin and prolactin in initiating winter fur growth in mink." Gen Comp Endocrinol **65**(2): 212-5.

Rose, J., F. Stormshak, J. Oldfield and J. Adair (1984). "Induction of winter fur growth in mink (Mustela vison) with melatonin." J Anim Sci **58**(1): 57-61.

Rose, J., F. Stormshak, J. Oldfield and J. Adair (1985). "The effects of photoperiod and melatonin on serum prolactin levels of mink during the autumn molt." J Pineal Res **2**(1): 13-9.

Rosendahl, M.S., S.C. Ko, D.L. Long, M.T. Brewer, B. Rosenzweig, E. Hedl, L. Anderson, S.M. Pyle, J. Moreland, M.A. Meyers, T. Kohno, D. Lyons and H.S. Lichenstein (1997). "Identification and characterization of a pro-tumor necrosis factor-alpha-processing enzyme from the ADAM family of zinc metalloproteases." J Biol Chem **272**(39): 24588-93.

Roth, S.I. (1965). The cytology of the murine resting (telogen) hair follicle. Biology of the skin and hair growth. A.G. Lyne and B.F. Short. Sydney, Angus and Robertson: 233-250.

Roth, W., J. Deussing, V.A. Botchkarev, M. Pauly-Evers, P. Saftig, A. Hafner, P. Schmidt, W. Schmahl, J. Scherer, I. Anton-Lamprecht, K. Von Figura, R. Paus and C. Peters (2000). "Cathepsin L deficiency as molecular defect of furless: hyperproliferation of keratinocytes and pertubation of hair follicle cycling." Faseb J **14**(13): 2075-86.

Rothnagel, J.A., M.A. Longley, R.A. Holder, D.S. Bundman, T. Seki, J.R. Bickenbach and D.R. Roop (1994). "Genetic disorders of keratin: are scarring alopecias a sub-set?" J Dermatol Sci **7 Suppl**: S164-9.

Rothnagel, J.A. and D.R. Roop (1995). "Hair follicle companion layer: reacquainting an old friend." J Invest Dermatol **104**(5 Suppl): 42S-43S.

Rougeot, J., D. Allain and L. Martinet (1984). "Photoperiodic and hormonal control of seasonal coat changes in mammals with special reference to sheep and mink." Acta Zoologica Fennica **171**: 13-18.

Rufaut, N.W., N.T. Goldthorpe, J.E. Wildermoth and O.A. Wallace (2006). "Myogenic differentiation of dermal papilla cells from bovine skin." J Cell Physiol **209**(3): 959-66.

Rufaut, N.W., A.J. Pearson, A.J. Nixon, T.T. Wheeler and R.J. Wilkins (1999). "Identification of differentially expressed genes during a wool follicle growth cycle induced by prolactin." J Invest Dermatol **113**(6): 865-72.

Rutberg, S.E., M.L. Kolpak, J.A. Gourley, G. Tan, J.P. Henry and D. Shander (2006). "Differences in expression of specific biomarkers distinguish human beard from scalp dermal papilla cells." J Invest Dermatol **126**: 2583-2595.

Rutberg, S.E., E. Saez, A. Glick, A.A. Dlugosz, B.M. Spiegelman and S.H. Yuspa (1996). "Differentiation of mouse keratinocytes is accompanied by PKC-dependent changes in AP-1 proteins." Oncogene **13**(1): 167-76.

Ryder, M.L. (1965). "Wool fibre shedding and seasonal variation in wool growth." Proc R Soc Med **58**(10): 806-8.

Ryder, M.L. and S.K. Stephenson (1986). Seasonal changes in the fleece and their hormonal control. Wool Growth. London, Academic: 593-625.

Saitoh, M., M. Uzuka and M. Sakamoto (1970). "Human hair cycle." J Invest Dermatol **54**(1): 65-81.

Salomon, D., E. Masgrau, S. Vischer, S. Ullrich, E. Dupont, P. Sappino, J.H. Saurat and P. Meda (1994). "Topography of mammalian connexins in human skin." J Invest Dermatol **103**(2): 240-7.

Samanta, J. and J.A. Kessler (2004). "Interactions between ID and OLIG proteins mediate the inhibitory effects of BMP4 on oligodendroglial differentiation." Development **131**(17): 4131-42.

Sano, S., S. Itami, K. Takeda, M. Tarutani, Y. Yamaguchi, H. Miura, K. Yoshikawa, S. Akira and J. Takeda (1999). "Keratinocyte-specific ablation of Stat3 exhibits impaired skin remodeling, but does not affect skin morphogenesis." Embo J **18**(17): 4657-68.

Sano, S., J. Takeda, K. Yoshikawa and S. Itami (2001). "Tissue regeneration: hair follicle as a model." J Investig Dermatol Symp Proc **6**(1): 43-8.

Santiago-Moreno, J., A. Lopez-Sebastian, A. del Campo, A. Gonzalez-Bulnes, R. Picazo and A. Gomez-Brunet (2004). "Effect of constant-release melatonin implants and prolonged exposure to a long day photoperiod on prolactin secretion and hair growth in mouflon (Ovis gmelini musimon)." Domest Anim Endocrinol **26**(4): 303-14.

Satokata, I., L. Ma, H. Ohshima, M. Bei, I. Woo, K. Nishizawa, T. Maeda, Y. Takano, M. Uchiyama, S. Heaney, H. Peters, Z. Tang, R. Maxson and R. Maas (2000). "Msx2 deficiency in mice causes pleiotropic defects in bone growth and ectodermal organ formation." Nat Genet **24**(4): 391-5.

SchaÈfer, B.W., R. Wicki, D. Engelkamp, M.G. Mattei and C.W. Heizmann (1995). "Isolation of a YAC clone covering a cluster of nine S100 genes on human chromosome 1q21: rationale for a new nomenclature of the S100 calcium-binding protein family." Genomics **25**: 638-643.

Schmidt, J.B. (1994). "Hormonal basis of male and female androgenic alopecia: clinical relevance." Skin Pharmacol **7**(1-2): 61-6.

Schmidt, J.B., B. Schurz, J. Huber and J. Spona (1989). "[Hypothyroidism and hyperprolactinemia as a possible cause of androgenetic alopecia in the female]." Z Hautkr **64**(1): 9-12.

Schmidt, M., R. Gillitzer, A. Toksoy, E.B. Brocker, U.R. Rapp, R. Paus, J. Roth, S. Ludwig and M. Goebeler (2001). "Selective expression of calcium-binding proteins S100a8 and S100a9 at distinct sites of hair follicles." J Invest Dermatol **117**(3): 748-50.

Schmidt, S. (2003). "Female alopecia: the mediating effect of attachment patterns on changes in subjective health indicators." Br J Dermatol **148**(6): 1205-11.

Schweizer, J., P.E. Bowden, P.A. Coulombe, L. Langbein, E.B. Lane, T.M. Magin, L. Maltais, M.B. Omary, D.A. Parry, M.A. Rogers and M.W. Wright (2006). "New consensus nomenclature for mammalian keratins." J Cell Biol **174**(2): 169-74.

Seago, S.V. and F.J. Ebling (1985). "The hair cycle on the human thigh and upper arm." Br J Dermatol **113**(1): 9-16.

Segall, A. (1918). "Ueber die Entwicklung und den Wechsel der Haare beim Meerschweinschen (Cavia Cobaya Schreb)." Arch f Mikrobiol Anat **91**: 218-291.

Sengel, P. (1976). Morphogenesis of skin. London, Oxford University Press.

Shimizu, H. and B.A. Morgan (2004). "Wnt signaling through the beta-catenin pathway is sufficient to maintain, but not restore, anagen-phase characteristics of dermal papilla cells." J Invest Dermatol **122**(2): 239-45.

Sieber-Blum, M. and M. Grim (2004). "The adult hair follicle: cradle for pluripotent neural crest stem cells." Birth Defects Res C Embryo Today **72**(2): 162-72.

Sieber-Blum, M., M. Grim, Y.F. Hu and V. Szeder (2004). "Pluripotent neural crest stem cells in the adult hair follicle." Dev Dyn **231**(2): 258-69.

Silver, A.F., H.B. Chase and C.T. Arsenault (1969). Early anagen initiated by plucking compared with early spontaneous anagen. Advances in Biology of Skin. W. Montagna and R.L. Dobson. London, Pergamon. **9:** 265-286.

Smith, E.A. and E. Fuchs (1998). "Defining the interactions between intermediate filaments and desmosomes." J Cell Biol **141**(5): 1229-41.

Smith, F.J., S.M. Morley and W.H. McLean (2002). "A novel connexin 30 mutation in Clouston syndrome." J Invest Dermatol **118**(3): 530-2.

Smith, M.R., H. Kung, S.K. Durum, N.H. Colburn and Y. Sun (1997). "TIMP-3 induces cell death by stabilizing TNF-alpha receptors on the surface of human colon carcinoma cells." Cytokine **9**(10): 770-80.

Soma, T., M. Ogo, J. Suzuki, T. Takahashi and T. Hibino (1998). "Analysis of apoptotic cell death in human hair follicles in vivo and in vitro." J Invest Dermatol **111**(6): 948-54.

Soma, T., M. Tajima and J. Kishimoto (2005). "Hair cycle-specific expression of versican in human hair follicles." J Dermatol Sci **39**(3): 147-154.

Sondell, B., L.E. Thornell, T. Stigbrand and T. Egelrud (1994). "Immunolocalization of stratum corneum chymotryptic enzyme in human skin and oral epithelium with monoclonal antibodies: evidence of a proteinase specifically expressed in keratinizing squamous epithelia." J Histochem Cytochem **42**(4): 459-65.

Stenn, K. (2005). "Exogen is an active, separately controlled phase of the hair growth cycle." J Am Acad Dermatol **52**(2): 374-5.

Stenn, K.S., S. Parimoo and S. Prouty (1998). Growth of the hair follicle: a cycling and regenerating biological system. Molecular Basis of Epithelial Appendage Morphogenesis. C.-M. Chuong. Austin, TX., RG Landes Company: 111-130.

Stenn, K.S. and R. Paus (2001). "Controls of hair follicle cycling." Physiol Rev **81**(1): 449-494.

Stephens, R.J., I.J. Beebe and T.C. Poulter (1973). "Innervation of the vibrissa of the californian sea lion, *Zalophus californianus*." Anat Rec **176**: 412-442.

Sudduth, S.L. and M.J. Koronkowski (1993). "Finasteride: the first 5 alpha-reductase inhibitor." Pharmacotherapy **13**(4): 309-25; discussion 325-9.

Sun, T.T., G. Cotsarelis and R.M. Lavker (1991). "Hair follicular stem cells: the bulge-activation hypothesis." J Invest Dermatol **96**(5): 77S-78S.

Sundberg, J.P. (1994). The balding (bal) mutation, chromosome 18. Handbook of Mouse Mutations with Skin and Hair Abnormalities: Animal Models and Biomedical Tools. J.P. Sundberg. Boca Raton, CRC Press: 187-191.

Tada, J. and K. Hashimoto (1997). "Ultrastructural localization of gap junction protein connexin 43 in normal human skin, basal cell carcinoma, and squamous cell carcinoma." J Cutan Pathol **24**(10): 628-35.

Tajima, M., C. Hamada, T. Arai, M. Miyazawa, R. Shibata and A. Ishino (2007). "Characteristic features of Japanese women's hair with aging and with progressing hair loss." J Dermatol Sci **45**: 93-103.

Tanaka, T., Y. Narisawa, N. Misago and K. Hashimoto (1998). "The innermost cells of the outer root sheath in human anagen hair follicles undergo specialized keratinization mediated by apoptosis." J Cutan Pathol **25**(6): 316-21.

Tang, L., S. Madani, H. Lui and J. Shapiro (2002). "Regeneration of a new hair follicle from the upper half of a human hair follicle in a nude mouse." J Invest Dermatol **119**(4): 983-4.

Taylor, G., M.S. Lehrer, P.J. Jensen, T.T. Sun and R.M. Lavker (2000). "Involvement of follicular stem cells in forming not only the follicle but also the epidermis." Cell **102**(4): 451-61.

Teubner, B., V. Michel, J. Pesch, J. Lautermann, M. Cohen-Salmon, G. Sohl, K. Jahnke, E. Winterhager, C. Herberhold, J.P. Hardelin, C. Petit and K. Willecke (2003). "Connexin30 (Gjb6)-deficiency causes severe hearing impairment and lack of endocochlear potential." Hum Mol Genet **12**(1): 13-21.

Thompson, D.L., R. Hoffman and C.L. DePew (1997). "Prolactin Administration to Seasonally Anestrous Mares: Reproductive, Metabolic, and Hair-Shedding Responses." J Anim Sci **75**: 1092-1099.

Thornton, M.J., I. Laing, K. Hamada, A.G. Messenger and V.A. Randall (1993). "Differences in testosterone metabolism by beard and scalp hair follicle dermal papilla cells." Clin Endocrinol (Oxf) **39**(6): 633-9.

Tobin, D.J., K. Foitzik, T. Reinheckel, L. Mecklenburg, V.A. Botchkarev, C. Peters and R. Paus (2002). "The lysosomal protease cathepsin L is an important regulator of keratinocyte and melanocyte differentiation during hair follicle morphogenesis and cycling." Am J Pathol **160**(5): 1807-21.

Tobin, D.J., A. Gunin, M. Magerl, B. Handijski and R. Paus (2003). "Plasticity and cytokinetic dynamics of the hair follicle mesenchyme: implications for hair growth control." J Invest Dermatol **120**(6): 895-904.

Toma, J.G., M. Akhavan, K.J. Fernandes, F. Barnabe-Heider, A. Sadikot, D.R. Kaplan and F.D. Miller (2001). "Isolation of multipotent adult stem cells from the dermis of mammalian skin." Nat Cell Biol **3**(9): 778-84.

Trautman, M.S., J. Kimelman and M. Bernfield (1991). "Developmental expression of syndecan, an integral membrane proteoglycan, correlates with cell differentiation." Development **111**(1): 213-20.

Trent, J.F. and R.S. Kirsner (1998). "Tissue engineered skin: Apligraf, a bi-layered living skin equivalent." Int J Clin Pract **52**(6): 408-13.

Tsuji, Y., S. Denda, T. Soma, L. Raftery, T. Momoi and T. Hibino (2003). "A potential suppressor of TGF-beta delays catagen progression in hair follicles." J Investig Dermatol Symp Proc **8**(1): 65-8.

Tumbar, T., G. Guasch, V. Greco, C. Blanpain, W.E. Lowry, M. Rendl and E. Fuchs (2004). "Defining the epithelial stem cell niche in skin." Science **303**(5656): 359-63.

Tunuguntla, R., D. Ripley, Q.X. Sang and N. Chegini (2003). "Expression of matrix metalloproteinase-26 and tissue inhibitors of metalloproteinases TIMP-3 and -4 in benign endometrium and endometrial cancer." Gynecol Oncol **89**(3): 453-9.

Uyttendaele, H., A.A. Panteleyev, D. de Berker, D.T. Tobin and A.M. Christiano (2004). "Activation of Notch1 in the hair follicle leads to cell-fate switch and Mohawk alopecia." Differentiation **72**(8): 396-409.

Vaalamo, M., T. Leivo and U. Saarialho-Kere (1999). "Differential expression of tissue inhibitors of metalloproteinases (TIMP-1, -2, -3, and -4) in normal and aberrant wound healing." Hum Pathol **30**(7): 795-802.

Van Neste, D. (2006). "Female patients complaining about hair loss: documentation of defective scalp hair dynamics with contrast-enhanced phototrichogram." Skin Res Tech **12**: 83-88.

Van Neste, D., T. Leroy and S. Conil (2007). "Exogen hair characterisation in human scalp." Skin Res Tech **In Press**.

Van Scott, E.J. and T.M. Ekel (1958). "Geometric relationships between the matrix of the hair bulb and its dermal papilla in normal and alopecic scalp." J Invest Dermatol **31**: 281–287.

Vandevelde, C. and W. Allaerts (1984). "Trichilemmal keratinisation: a causal factor in loosening the murine telogen club hair from the trichilemmal sac." J Anat **138 (Pt 4)**: 745-56.

Vasioukhin, V., E. Bowers, C. Bauer, L. Degenstein and E. Fuchs (2001). "Desmoplakin is essential in epidermal sheet formation." Nat Cell Biol **3**(12): 1076-85.

Vine, A.L., Y.M. Leung and J.S. Bertram (2005). "Transcriptional regulation of connexin 43 expression by retinoids and carotenoids: similarities and differences." Mol Carcinog **43**(2): 75-85.

Wang, H. (1943). "Morphogenetic functions of the epidermal and dermal components of the papilla in feather regeneration." Physiol Zool **16**: 325-350.

Wang, M.G., H. Yi, D. Guerini, C.B. Klee and O.W. McBride (1996). "Calcineurin A alpha (PPP3CA), calcineurin A beta (PPP3CB) and calcineurin B (PPP3R1) are located on human chromosomes 4, 10q21-->q22 and 2p16-->p15 respectively." Cytogenet Cell Genet **72**(2-3): 236-41.

Wang, Z., P. Wong, L. Langbein, J. Schweizer and P.A. Coulombe (2003). "Type II epithelial keratin 6hf (K6hf) is expressed in the companion layer, matrix, and medulla in anagen-stage hair follicles." J Invest Dermatol **121**(6): 1276-82.

Watson, S.A., P. Pisansarakit and G.P. Moore (1994). "Sheep vibrissa dermal papillae induce hair follicle formation in heterotypic skin equivalents." Br J Dermatol **131**(6): 827-35.

Watt, F.M. (1989). "Terminal differentiation of epidermal keratinocytes." Curr Opin Cell Biol **1**(6): 1107-15.

Weil, M., M.C. Raff and V.M. Braga (1999). "Caspase activation in the terminal differentiation of human epidermal keratinocytes." Curr Biol **9**(7): 361-4.

Weinberg, W.C., L.V. Goodman, C. George, D.L. Morgan, S. Ledbetter, S.H. Yuspa and U. Lichti (1993). "Reconstitution of Hair Follicle Development *In Vivo*: Determination of Follicle Formation, Hair Growth, and Hair Quality by Dermal Cells." J Invest Dermatol **100**: 229-236.

Whiting, D. (1992). "Treatment of female androgenetic alopecia with minoxidil 2%." Int J Dermatol **31**: 800-804.

Whiting, D.A. (1996a). "Chronic telogen effluvium." Dermatol Clin **14**(4): 723-31.

Whiting, D.A. (1996b). "Chronic telogen effluvium: increased scalp hair shedding in middle-aged women." J Am Acad Dermatol **35**(6): 899-906.

Whiting, D.A. (2001). "Possible mechanisms of miniaturization during androgenetic alopecia or pattern hair loss." J Am Acad Dermatol **45**(3 Suppl): S81-6.

Wick, M., C. Burger, S. Brusselbach, F.C. Lucibello and R. Muller (1994). "A novel member of human tissue inhibitor of metalloproteinases (TIMP) gene family is regulated during G1 progression, mitogenic stimulation, differentiation, and senescence." J Biol Chem **269**(29): 18953-60.

Wick, M., R. Haronen, D. Mumberg, C. Burger, B.R. Olsen, M.L. Budarf, S.S. Apte and R. Muller (1995). "Structure of the human TIMP-3 gene and its cell cycle-regulated promoter." Biochem J **311 (Pt 2)**: 549-54.

Williamson, D., M. Gonzalez and A.Y. Finlay (2001). "The effect of hair loss on quality of life." J Eur Acad Dermatol Venereol **15**(2): 137-9.

Winter, H., L. Langbein, S. Praetzel, M. Jacobs, M.A. Rogers, I.M. Leigh, N. Tidman and J. Schweizer (1998). "A novel human type II cytokeratin, K6hf, specifically expressed in the companion layer of the hair follicle." J Invest Dermatol **111**(6): 955-62.

Withers, A.P. (1987). An *in vitro* and *in vivo* study of sheep, rat and human hair follicle papilla cells, Ph.D. Thesis, University of Dundee.

Wojcik, S.M., S. Imakado, T. Seki, M.A. Longley, L. Petherbridge, D.S. Bundman, J.R. Bickenbach, J.A. Rothnagel and D.R. Roop (1999). "Expression of MK6a dominant-negative and C-terminal mutant transgenes in mice has distinct phenotypic consequences in the epidermis and hair follicle." Differentiation **65**(2): 97-112.

Wolfsberg, T.G., P. Primakoff, D.G. Myles and J.M. White (1995). "ADAM, a novel family of membrane proteins containing A Disintegrin And Metalloprotease domain: multipotential functions in cell-cell and cell-matrix interactions." J Cell Biol **131**(2): 275-8.

Wong, C.E., C. Paratore, M.T. Dours-Zimmermann, A. Rochat, T. Pietri, U. Suter, D.R. Zimmermann, S. Dufour, J.P. Thiery, D. Meijer, F. Beermann, Y. Barrandon and L. Sommer (2006). "Neural crest-derived cells with stem cell features can be traced back to multiple lineages in the adult skin." J Cell Biol **175**(6): 1005-1015.

Wright, E.A. (1965). "The growth of mouse vibrissae." Proc R Soc Med **58**: 804-806.

Wu, H., J.R. Stanley and G. Cotsarelis (2003). "Desmoglein Isotype Expression in the Hair Follicle and its Cysts Correlates with Type of Keratinization and Degree of Differentiation." J Invest Dermatol **120**: 1152-1157.

Wu, H., Z.H. Wang, A. Yan, S. Lyle, S. Fakharzadeh, J.K. Wahl, M.J. Wheelock, H. Ishikawa, J. Uitto, M. Amagai and J.R. Stanley (2000). "Protection against pemphigus foliaceus by desmoglein 3 in neonates." N Engl J Med **343**(1): 31-5.

Wu, J.J., T.Y. Zhu, Y.G. Lu, R.Q. Liu, Y. Mai, B. Cheng, Z.F. Lu, B.Y. Zhong and S.Q. Tang (2006). "Hair follicle reformation induced by dermal papilla cells from human scalp skin." Arch Dermatol Res **298**(4): 183-90.

Xiao, Y., M. Forsberg, J.T. Laitinen and M. Valtonen (1995). "Effects of melatonin implants in spring on testicular regression and moulting in adult male raccoon dogs (Nyctereutes procynoides)." J Reprod Fertil **105**(1): 9-15.

Xing, L. and K. Kobayashi (2001). "Ability of transplanted cultured epithelium to respond to dermal papillae." Tissue Eng **7**(5): 535-544.

Yang, C.L., T. Kurczab, G. Down, T. Kealey and K. Langlands (2005). "Gene expression profiling of the ageing rat vibrissa follicle." Br J Dermatol **153**(1): 22-8.

Ya-Xian, Z., T. Suetake and H. Tagami (1999). "Number of cell layer of the stratum corneum in normal skin-relationship to the anatomical location on the body, age, sex and physical parameters." Arch Dermatol Res **291**: 555-559.

Young, R.D. (1980). "Morphological and ultrastructural aspects of the dermal papilla during the growth cycle of the vibrissal follicle in the rat." J Anat **131**(Pt 2): 355-65.

Young, R.D. and R.F. Oliver (1976). "Morphological changes associated with the growth cycle of vibrissal follicles in the rat." J Embryol Exp Morphol **36**(3): 597-607.

Zebrowska, A., J. Narbutt, A. Sysa-Jedrzejowska, J. Kobos and E. Waszczykowska (2005). "The imbalance between metalloproteinases and their tissue inhibitors is involved in the pathogenesis of dermatitis herpetiformis." Mediators Inflamm **2005**(6): 373-9.

Zenz, R., R. Eferl, L. Kenner, L. Florin, L. Hummerich, D. Mehic, H. Scheuch, P. Angel, E. Tschachler and E.F. Wagner (2005). "Psoriasis-like skin disease and arthritis caused by inducible epidermal deletion of Jun proteins." Nature **437**(7057): 369-75.

Zhang, X.J., J.J. Chen, S. Yang, Y. Cui, X.Y. Xiong, P.P. He, P.L. Dong, S.J. Xu, Y.B. Li, Q. Zhou, Y. Wang and W. Huang (2003). "A mutation in the connexin 30 gene in Chinese Han patients with hidrotic ectodermal dysplasia." J Dermatol Sci **32**(1): 11-7.

Zheng, Y., X. Du, W. Wang, M. Boucher, S. Parimoo and K. Stenn (2005). "Organogenesis from dissociated cells: generation of mature cycling hair follicles from skin-derived cells." J Invest Dermatol **124**(5): 867-76.

Appendix 1

i) 1X Phosphate Buffered Saline:

40.00g NaCl
1.00g KCl
1.45g KH_2PO_4
9.03g $Na_2HPO_4.2H_2O$

pH 7.4

Solutions were made up to 5 litres in distilled water using the quantities above to give 1X PBS

ii) DEPC-PBS:

PBS was made up as above. Diethyl pyrocarbonate (Sigma) was added to a final concentration of 0.1%. Solutions were left in a fume hood overnight prior to autoclaving the following day.

iii) 10X Tris Buffered Saline:

60.55g Trizma Base
80.22g NaCl

pH 7.4

Solutions were made up to 1 litre in MillQ water using the quantities above to give 10X TBS.

10X Stock solutions were made. Stocks were diluted 1/10 in MillQ water prior to use.

iv) Karnovsky Fixative:

Karnovsky fixative composes of 2 solutions which were mixed, although were kept separate until required.

Solution A:
40mls 5% paraformaldehyde (Sigma)

Solution B:
10mls 25% EM grade Glutaraldehyde (Agar Aids)
50mls 0.2M Sodium phosphate buffer, pH 7.4 (made from 9.5mls 0.2M Monobasic Sodium Phosphate (Sigma) and 40.5mls 0.2M dibasic sodium phosphate (Sigma)

v) Geys Agar:

Geys solution was made at 2X concentration and filter sterilised. 2% Agar in distilled water was autoclaved. The solutions were then mixed 1:1 to give a final mix of 1% Agar in 1X Geys solution.

2X Geys solution

8g NaCl
0.37g KCl
0.17g $CaCl_2$
0.210g $MgCl_2$
0.150g Na_2HPO_4-$12H_2O$
0.30g KH_2PO_4
0.70g $MgSO_4$-$7H_2O$
1.0g Glucose
0.230g $NaHCO_3$

Made up to 500ml using distilled water

vi) 50x TAE buffer:

242 gm Tris base
57.1 ml Acetic acid
100ml 0.5M EDTA

pH to 8.5

Make up to 1 litre with distilled water. Use at 1x by diluting 1 in 50 in distilled water

vii) Loading Buffer for electrophoresis gels:

0.25% bromophenol blue
40% glycerol

Made up in sterilised water

Appendix 2

i) Gene list generated from GeneSpring Software:

Probe ID	Description	Fold Change from EE to LE
1398584_at	keratin complex 1, acidic, gene 5	-20.6
1368511_at	basic helix-loop-helix domain containing, class B3	-4.3
1369926_at	glutathione peroxidase 3	-3.6
1384392_at	cytochrome P450, family 26, subfamily b, polypeptide 1	-3.4
1374391_at	Similar to Sarcolipin (LOC367086), mRNA	-3.4
1369172_at	phosphodiesterase 1A, calmodulin-dependent	-3.3
1380057_at	phosphodiesterase 1A, calmodulin-dependent	-3.1
1367845_at	neurofilament 3, medium	-2.9
1378171_at	Neuropilin 2	-2.9
1379614_at	Protein phosphatase 3, catalytic subunit	-2.8
1378258_at	Coiled coil domain containing 3	-2.8
1392769_at	Transcribed locus	-2.8
1371161_at	protein phosphatase 1, regulatory (inhibitor) subunit 3B	-2.6
1376944_at	Prolactin receptor	-2.6
1382995_at	Neuropilin 2	-2.5
1373487_at	Spondin 1	-2.5
1387769_a_at	inhibitor of DNA binding 3	-2.5
1381070_at	Synaptoporin	-2.5
1384736_at	Transcribed locus	-2.5
1379075_at	O-acyltransferase (membrane bound) domain containing 2	-2.5
1384717_at	Development and Differentiation enhancing	-2.5
1370312_at	spondin 1	-2.4
1368989_at	Tissue inhibitor of metalloproteinase 3	-2.4
1369193_at	cyclin-dependent kinase inhibitor 2B (p15, inhibits CDK4)	-2.3
1374830_at	Coiled coil domain containing 3	-2.3
1389039_at	Neuropilin 2	-2.3
1392852_at	Cullin 3	-2.3
1397274_at	Transcribed locus, weakly similar to XP_576460.1 PREDICTED: similar to hypothetical protein PB402898.00.0 [Rattus norvegicus]	-2.3
1384655_at	kin of IRRE like 3 (Drosophila)	-2.3
1370135_at	caveolin 2	-2.2

1372256_at	Cysteine-rich protein 1	-2.2
1392785_at	Potassium channel tetramerisation domain containing 12	-2.2
1373710_at	Solute Carrier family 38, member 4	-2.2
1382535_at	Potassium channel tetramerisation domain containing 12	-2.2
1368260_at	aurora kinase B	-2.2
1384043_at	Protein phosphatase 2 regulatory subunit B, gamma isoform	-2.2
1390981_at	Similar to Fibrocystin L	-2.2
1388605_at	WAP four-disulfide core domain 3	-2.1
1377023_at	dual specificity phosphatase 2	-2.1
1383394_at	Similar to Dopachrome tautomerase	-2.1
1381986_at	neuron navigator 1	-2.1
1375059_at	similar to zinc finger protein 652 (predicted)	-2.1
1382657_at	bone morphogenetic protein 5 (predicted)	-2.1
1383404_at	Transcribed locus	-2.1
1376350_at	Similar to FMR2	-2
1393469_at	---	-2
1367846_at	S100 calcium-binding protein A4	-2
1370131_at	Caveolin	-2
1386889_at	stearoyl-Coenzyme A desaturase 2	-2
1375129_at	FGF Receptor 2	-2
1384329_at	Similar to Serine Protease PRSS22	2
1368052_at	tetraspanin 8	2
1368124_at	dual specificity phosphatase 5	2
1382336_at	similar to Juxtaposed with another zinc finger protein 1	2
1378261_at	Transcribed locus	2
1380493_at	---	2
1390477_at	Transcribed locus	2
1396422_at	Transcribed locus	2
1387052_at	glutamic pyruvic transaminase 1, soluble	2.1
1384503_at	kallikrein 8 (neuropsin/ovasin)	2.1
1380558_at	Similar to Homeobox protein DLX-3	2.1
1368661_at	solute carrier family 13, member 2	2.1
1386981_at	solute carrier family 16, member 1	2.1
1387092_at	FXYD domain-containing ion transport regulator 4	2.1
1391656_at	---	2.1
1372665_at	phosphoserine aminotransferase 1	2.1

1374870_at	Procollagen, type XXVII, alpha 1 /// Procollagen, type XXVII, alpha 1	2.1
1381966_at	AT rich interactive domain 1B (Swi1 like)	2.1
1374449_at	Solute carrier family 35, member E1	2.1
1372687_at	hypothetical protein LOC679258	2.1
1375134_at	Similar to CG31855-PA	2.1
1369020_at	solute carrier family 5 (sodium iodide symporter), member 5	2.2
1369665_a_at	interleukin 18	2.2
1386922_at	carbonic anhydrase 2	2.2
1387744_at	natriuretic peptide precursor type C	2.2
1385686_at	similar to Cornifin B	2.2
1377645_at	similar to hypothetical protein	2.2
1373010_at	LOC361776	2.2
1385612_at	similar to Keratin, type II cytoskeletal 6G	2.2
1383970_at	---	2.2
1396028_at	Transcribed locus	2.2
1368789_at	acid phosphatase, prostate	2.3
1383519_at	Hexokinase 2	2.3
1372523_at	glutamate-cysteine ligase, catalytic subunit	2.3
1370688_at	glutamate-cysteine ligase, catalytic subunit	2.3
1387239_a_at	peptidyl arginine deiminase, type IV	2.3
1393467_at	proprotein convertase subtilisin/kexin type 5	2.3
1381510_at	Transcribed locus	2.3
1392754_at	similar to cysteine-rich glycoprotein (predicted)	2.3
1368494_at	S100 calcium binding protein A8	2.3
1374691_at	sulfotransferase family 5A, member 1	2.3
1369381_a_at	solute carrier family 15, member 1	2.3
1374594_at	similar to RIKEN cDNA 1600029D21	2.3
1368773_at	FSH primary response hormone 1	2.3
1368527_at	prostaglandin-endoperoxide synthase 2	2.4
1369407_at	tumor necrosis factor receptor superfamily, member 11b (osteoprotegerin)	2.4
1367733_at	carbonic anhydrase 2	2.4
1390850_at	Adipose differentiation related protein	2.4
1367570_at	transgelin	2.4
1376617_at	Transcribed locus	2.4
1387993_at	cytochrome P450, family 2, subfamily b, polypeptide 13	2.5
1387178_a_at	cystathionine beta synthase	2.5

1387715_at	extracellular peptidase inhibitor	2.5
1388176_at	camello-like 5	2.5
1392483_at	Choline phosphotransferase 1	2.5
1369467_a_at	6-phosphofructo-2-kinase/fructose-2,6-biphosphatase 1	2.5
1368883_at	nephroblastoma overexpressed gene	2.6
1393887_at	choline phosphotransferase 1	2.7
1387125_at	S100 calcium binding protein A9	2.7
1383585_s_at	Sorting nexin 10	2.7
1376734_at	nephroblastoma overexpressed gene	2.8
1384907_at	similar to Dachshund homolog 1 (Dach1)	2.8
1368469_at	aquaporin 5	2.8
1378133_at	Transcribed locus	2.8
1379582_a_at	cyclin A2	2.8
1368205_at	complement factor I	2.8
1376445_at	interleukin 17B	2.8
1373088_at	hypothetical protein LOC682888	2.8
1390672_at	Reprimo-candidate mediator of the p53-dependent G2 arrest	2.9
1394503_at	Activin A receptor, type 1	2.9
1392773_at	proprotein convertase subtilisin/kexin type 5	3
1385483_at	similar to hypothetical protein A030011M19 (predicted)	3
1383968_at	---	3
1368577_at	gap junction membrane channel protein beta 6	3.1
1379709_at	keratin associated protein 14	3.1
1369660_at	defensin beta 1	3.4
1385752_at	neuronal PAS domain protein 3 (predicted)	3.4
1398253_at	kidney androgen regulated protein	3.5
1393841_at	similar to hypothetical protein FLJ31810 (predicted)	3.9
1394458_at	---	4
1369232_at	potassium channel, subfamily K, member 10	4
1383303_at	SA rat hypertension-associated gene	5.8
1380577_at	Leucine rich repeat (in FLII) interacting protein 2	6.1
1389573_at	ChaC, cation transport regulator-like 1 (E. coli)	7.5
1371280_at	high sulfur protein B2F	9.1
1394140_at	type I hair keratin KA25	9.3
1385844_at	keratin associated protein 6-2	9.7
1385010_at	type I hair keratin KA28	18

ii) Gene list generated from GeneTraffic software:

Probe ID	Description	Fold Change from EE to LE
1369172_at	phosphodiesterase 1A, calmodulin-dependent	-6.3
1379903_at	Protein Phosphatase 2 (family 2a) regulatory	-6.12
1368369_at	Prepronociceptin	-5.98
1376667_at	cytochrome P450, family 26, subfamily b, polypeptide 1	-5.67
1377246_at	similar to keratin 6L	-5.4
1369926_at	glutathione peroxidase 3	-5.16
1388329_at	Activin receptor IIB	-5.1
1383363_at	DIRAS family, GTP-binding RAS-like 2 (predicted)	-4.91
1384392_at	cytochrome P450, family 26, subfamily b, polypeptide 1	-4.45
1367660_at	fatty acid binding protein 3	-4.38
1368511_at	basic helix-loop-helix domain containing, class B3	-4.37
1377023_at	dual specificity phosphatase 2	-4.24
1374391_at	Similar to Sarcolipin	-4.08
1378171_at	Neuropilin 2	-3.83
1392852_at	Cullin 3 (predicted)	-3.79
1382218_at	hypothetical LOC298077	-3.71
1380057_at	phosphodiesterase 1A, calmodulin-dependent	-3.7
1367845_at	neurofilament 3, medium	-3.65
1378258_at	Coiled coil domain containing 3	-3.52
1388605_at	WAP four-disulfide core domain 3 (predicted)	-3.33
1392613_at	Transcribed locus /// Transcribed locus	-3.33
1382995_at	Neuropilin 2	-3.29
1373487_at	Spondin 1	-3.29
1370312_at	spondin 1	-3.23
1387769_a_at	inhibitor of DNA binding 3	-3.13
1371161_at	protein phosphatase 1, regulatory (inhibitor) subunit 3B	-3.08
1378623_at	Transcribed locus	-3.07
1368989_at	tissue inhibitor of metalloproteinase 3	-2.96
1380306_at	Transcribed locus	-2.94
1368350_at	protein tyrosine phosphatase, receptor-type, Z polypeptide 1	-2.85
1376944_at	Prolactin receptor	-2.77

1393157_at	Transcribed locus	-2.75
1397225_at	Transcribed locus	-2.74
1372153_at	type I keratin KA15	-2.72
1374830_at	Similar to Coiled-coil domain containing protein 3 precursor	-2.7
1384655_at	kin of IRRE like 3 (Drosophila)	-2.69
1392785_at	Potassium channel tetramerisation domain containing 12	-2.65
1381986_at	neuron navigator 1	-2.64
1389039_at	Neuropilin 2	-2.56
1371024_at	cut-like 1 (Drosophila)	-2.54
1388015_at	protein tyrosine phosphatase, receptor-type, Z polypeptide 1	-2.51
1379331_at	tenascin N	-2.49
1373710_at	Solute Carrier family 38 member 4	-2.47
1370255_at	surfactant associated protein C	-2.45
1382535_at	Potassium channel tetramerisation domain containing 12	-2.41
1381070_at	Synaptoporin	-2.38
1395586_at	eukaryotic translation elongation factor 1 alpha 1	-2.37
1370135_at	caveolin 2	-2.36
1375059_at	similar to zinc finger protein 652	-2.36
1370097_a_at	chemokine (C-X-C motif) receptor 4	-2.35
1376344_at	Cytochrome b reductase 1	-2.35
1383649_a_at	---	-2.34
1390141_at	methylenetetrahydrofolate dehydrogenase (NADP+ dependent) 1-like (predicted)	-2.34
1384852_at	RAB27A, member RAS oncogene family	-2.32
1387028_a_at	inhibitor of DNA binding 1	-2.31
1376736_at	hypothetical protein LOC683263	-2.31
1392542_at	non-kinase Cdc42 effector protein SPEC2	-2.3
1386889_at	stearoyl-Coenzyme A desaturase 2	-2.29
1369193_at	cyclin-dependent kinase inhibitor 2B (p15, inhibits CDK4)	-2.28
1376350_at	Similar to FMR2	-2.27
1368530_at	matrix metallopeptidase 12	-2.27
1391421_at	similar to Acyl-CoA dehydrogenase family member 8, mitochondrial precursor (ACAD-8) (predicted)	-2.27
1372256_at	Cysteine-rich protein 1	-2.26
1375138_at	tissue inhibitor of metalloproteinase 3	-2.26

1392996_at	cytoplasmic polyadenylation element binding protein 1 (predicted)	-2.25
1392612_at	Prolactin receptor	-2.24
1396129_at	chemokine (C-X-C motif) ligand 14	-2.24
1378254_at	similar to TBC1 domain family member 4	-2.22
1393469_at	---	-2.21
1378246_at	similar to T-cell activation protein phosphatase 2C (predicted)	-2.21
1367973_at	chemokine (C-C motif) ligand 2	-2.2
1379397_at	RAR-related orphan receptor alpha (predicted)	-2.2
1370212_at	homer homolog 3 (Drosophila)	-2.2
1380079_at	---	-2.19
1370964_at	argininosuccinate synthetase	-2.16
1395519_at	similar to B230212L03Rik protein	-2.16
1383394_at	Similar to Dopachrome tautomerase	-2.15
1375271_at	NIMA (never in mitosis gene a)- related kinase 9	-2.15
1387755_s_at	trans-golgi network protein 2	-2.15
1369504_at	transforming growth factor, beta receptor 1	-2.15
1389310_at	Transcribed locus	-2.15
1378462_at	Methylthioadenosine phosphorylase (predicted)	-2.14
1391953_at	msh homeobox homolog 2 (Drosophila)	-2.13
1374814_at	---	-2.12
1383468_at	Transcribed locus	-2.11
1383661_at	Heparan sulfate (glucosamine) 3-O-sulfotransferase 3B1 (predicted)	-2.1
1392714_at	serine (or cysteine) peptidase inhibitor, clade B (ovalbumin), member 11	-2.1
1387983_at	thyroid hormone receptor beta	-2.1
1372926_at	Tissue inhibitor of metalloproteinase 3	-2.08
1373972_at	neuron navigator 1	-2.08
1370855_at	cystatin C	-2.07
1378572_at	toll interacting protein (predicted)	-2.07
1392545_at	transcription factor AP-2 beta (predicted)	-2.07
1397274_at	---	-2.06
1388545_at	SPARC-related modular calcium binding protein 1	-2.06

1370746_at	protein kinase, cAMP dependent, catalytic, beta	-2.06
1367874_at	ras homolog gene family, member Q	-2.06
1373578_at	tripartite motif protein 2	-2.06
1367791_at	receptor (calcitonin) activity modifying protein 1	-2.05
1387845_at	potassium voltage-gated channel, subfamily G, member 3	-2.05
1386114_at	---	-2.05
1379614_at	Protein phosphatase 3, catalytic subunit	-2.05
1398246_s_at	Fc receptor, IgG, low affinity III	-2.04
1397813_at	Transcribed locus	-2.04
1375726_at	LIM domain only protein 7	-2.02
1393109_at	CDNA clone IMAGE:7302574	-2.02
1379036_at	DNA methyltransferase 2	-2.01
1377369_at	cytochrome b reductase 1	-2.01
1368962_at	neurexophilin 3	-2
1378480_at	Transcribed locus	-2
1381510_at	Transcribed locus	2
1387565_at	transient receptor potential cation channel, subfamily V, member 6	2
1370896_a_at	myosin, heavy polypeptide 11, smooth muscle	2
1392553_at	ADAMTS-like 5 (predicted)	2
1367974_at	annexin A3	2
1392483_at	Choline phosphotransferase 1	2.04
1391656_at	---	2.04
1368052_at	tetraspanin 8	2.04
1368379_at	scavenger receptor class B, member 2	2.04
1376785_at	Synaptonemal complex protein 3	2.04
1384273_at	carbohydrate kinase-like	2.04
1390549_at	adiponectin receptor 2	2.04
1383974_at	Transcribed locus	2.04
1384533_at	---	2.04
1392633_at	Transcribed locus	2.04
1368124_at	dual specificity phosphatase 5	2.08
1376352_at	Trinucleotide repeat containing 9 (predicted)	2.08
1389756_at	maternal embryonic leucine zipper kinase (predicted)	2.08
1389804_at	Transcribed locus	2.08
1390790_a_at	---	2.08

1386981_at	solute carrier family 16, member 1	2.13
1387092_at	FXYD domain-containing ion transport regulator 4	2.13
1387793_at	Transcribed locus, strongly similar to yippee-like 1	2.13
1370032_at	solute carrier family 9, isoform 3 regulator 1	2.13
1379582_a_at	cyclin A2	2.17
1370688_at	glutamate-cysteine ligase, catalytic subunit	2.17
1369407_at	tumor necrosis factor receptor superfamily, member 11b (osteoprotegerin)	2.17
1385686_at	similar to Cornifin B	2.17
1380558_at	Similar to homeobox protein DLX-3	2.17
1376178_at	DNA-damage inducible transcript 3	2.17
1383397_at	receptor-associated protein of the synapse (predicted)	2.17
1392547_at	hypothetical LOC302884	2.17
1368527_at	prostaglandin-endoperoxide synthase 2	2.22
1383519_at	Hexokinase 2	2.22
1390850_at	Adipose differentiation related protein	2.22
1372539_at	Castration induced prostatic apoptosis related protein 1	2.22
1368746_a_at	ATPase, H+/K+ transporting, nongastric, alpha polypeptide	2.22
1372915_at	Transcribed locus	2.22
1379076_at	Transcribed locus	2.22
1393935_at	hypothetical protein LOC680244	2.22
1386922_at	carbonic anhydrase 2	2.27
1387052_at	glutamic pyruvic transaminase 1, soluble	2.27
1368014_at	prostaglandin E synthase	2.27
1372602_at	similar to genethonin 1	2.27
1372665_at	phosphoserine aminotransferase 1	2.33
1368661_at	solute carrier family 13 (sodium-dependent dicarboxylate transporter), member 2	2.33
1369665_a_at	interleukin 18	2.33
1379275_at	sorting nexin 10	2.33
1390891_at	kinesin family member 11	2.33
1380775_at	M-phase phosphoprotein 1	2.33
1367733_at	carbonic anhydrase 2	2.33
1370201_at	calbindin 1	2.33

1393467_at	proprotein convertase subtilisin/kexin type 5	2.38
1384503_at	kallikrein 8 (neuropsin/ovasin)	2.38
1393660_at	Similar to N-acylsphingosine amidohydrolase 3	2.38
1379770_at	choline phosphotransferase 1	2.38
1368789_at	acid phosphatase, prostate	2.44
1372523_at	glutamate-cysteine ligase, catalytic subunit	2.44
1383165_at	Syncollin	2.44
1388133_at	cold shock domain containing C2, RNA binding	2.44
1387125_at	S100 calcium binding protein A9 (calgranulin B)	2.5
1392754_at	similar to cysteine-rich glycoprotein (predicted)	2.5
1368441_at	mesothelin	2.5
1385080_s_at	similar to gasdermin 1	2.5
1387972_at	mucin and cadherin like	2.5
1374710_at	Transcribed locus	2.5
1384329_at	Similar to Serine Protease PRSS22	2.56
1389179_at	cell death-inducing DNA fragmentation factor, alpha subunit-like effector A (predicted)	2.56
1387253_at	guanylate cyclase activator 2b	2.56
1372841_at	receptor accessory protein 6	2.56
1370026_at	crystallin, alpha B	2.56
1388985_at	Transcribed Sequences	2.56
1387239_a_at	peptidyl arginine deiminase, type IV	2.63
1392773_at	proprotein convertase subtilisin/kexin type 5	2.63
1369320_at	melanoma inhibitory activity 1	2.63
1387744_at	natriuretic peptide precursor type C	2.7
1369660_at	defensin beta 1	2.78
1390672_at	candidate mediator of the p53-dependent G2 arrest	2.78
1368883_at	nephroblastoma overexpressed gene	2.78
1378261_at	Transcribed locus	2.78
1384803_at	Transcribed Sequences	2.86
1388176_at	camello-like 5	2.94
1368613_at	stromal antigen 3	2.94
1376734_at	nephroblastoma overexpressed gene	3.03
1369020_at	solute carrier family 5 (sodium iodide symporter), member 5	3.03

1387993_at	cytochrome P450, family 2, subfamily b, polypeptide 13	3.03
1378133_at	Transcribed locus	3.03
1393841_at	similar to hypothetical protein FLJ31810 (predicted)	3.03
1376445_at	interleukin 17B	3.03
1393887_at	choline phosphotransferase 1	3.13
1384907_at	similar to Dachshund homolog 1 (Dach1)	3.13
1368469_at	aquaporin 5	3.13
1383585_s_at	Sorting nexin 10	3.13
1367894_at	similar to Insulin-induced gene 1 protein (INSIG-1) (Insulin-induced growth response protein CL-6)	3.13
1387715_at	extracellular peptidase inhibitor	3.23
1373088_at	hypothetical protein LOC682888	3.23
1385483_at	similar to hypothetical protein A030011M19 (predicted)	3.33
1368577_at	gap junction membrane channel protein beta 6	3.45
1378675_at	similar to transglutaminase E3 (predicted)	3.45
1376787_at	similar to hypothetical protein FLJ31810 (predicted)	3.45
1374248_at	myosin binding protein C, slow type	3.7
1383874_at	RGD1560812 (predicted)	3.7
1373324_at	dual specificity phosphatase 14 (predicted)	3.7
1387178_a_at	cystathionine beta synthase	4
1398253_at	kidney androgen regulated protein	4
1387082_at	fetuin beta	4
1368205_at	complement factor I	4.35
1388214_at	proprotein convertase subtilisin/kexin type 5	4.76
1394458_at	Transcribed Sequences	5
1376770_at	similar to EF hand domain containing 1 (predicted)	5
1385844_at	Keratin associated protein 6-2	7.14
1383303_at	SA rat hypertension-associated gene	7.69
1380577_at	Leucine rich repeat (in FLII) interacting protein 2	9.09
1389573_at	ChaC, cation transport regulator-like 1	12.5
1380524_at	type II keratin Kb26	14.29
1377659_at	Similar to myeloid leukemia factor 1	16.67
1380628_at	keratin complex 1, acidic, gene 4	20

1371280_at	high sulfur protein B2F	33.33
1385010_at	type I hair keratin KA28	33.33
1394140_at	type I hair keratin KA25	33.33
1388284_at	high sulfur protein B2F	33.33
1384627_at	Keratin associated protein 13-1	50

iii) Genes that were present in both GeneSpring and GeneTraffic gene lists, with groupings and comparative plucked profile:

Probe ID	Description	Fold Change from EE to LE	Category	Plucked Gene List
1367845_at	neurofilament 3, medium	-2.9	Structural	Yes
1381986_at	Neuron navigator 1	-2.1	Structural	Yes
1385686_at	Similar to Cornifin B	2.2	Structural	Yes
1371280_at	high sulfur protein B2F	9.1	Structural	No
1394140_at	type I hair keratin KA25	9.3	Structural	Yes
1385844_at	keratin associated protein 6-2	9.7	Structural	Yes
1385010_at	type I hair keratin KA28	18	Structural	Yes
1373487_at	Spondin 1	-2.5	Cell Adhesion and ECM	Yes
1368577_at	gap junction membrane channel protein beta 6	3.1	Cell Adhesion and ECM	No
1392754_at	similar to cysteine-rich glycoprotein (predicted)	2.3	Protease	Yes
1384329_at	Similar to Serine Protease PRSS22	2	Protease	Yes
1384503_at	Kallikrein 8 (neuropsin/ovasin)	2.1	Protease	No
1393467_at	proprotein convertase subtilisin/kexin type 5	2.3	Protease	No
1368205_at	complement factor I	2.8	Protease	No
1368989_at	Tissue inhibitor of metalloproteinase 3	-2.4	Protease Inhibitor	Yes
1388605_at	WAP four-disulfide core domain 3	-2.1	Protease Inhibitor	Yes
1387715_at	extracellular peptidase inhibitor	2.5	Protease Inhibitor	Yes
1369172_at	phosphodiesterase 1A, calmodulin-dependent	-3.3	Signal Transduction	Yes
1378171_at	Neuropilin 2	-2.9	Signal Transduction	Yes
1379614_at	Protein phosphatase 3, catalytic subunit	-2.8	Signal Transduction	Yes
1376944_at	Prolactin receptor	-2.6	Signal Transduction	Yes
1370135_at	Caveolin 2	-2.2	Signal Transduction	No
1377023_at	Dual specificity phosphatase 2	-2.1	Signal Transduction	Yes
1368052_at	Tetraspanin 8	2	Signal	No

			Transduction	
1368124_at	Dual specificity phosphatase 5	2	Signal Transduction	Yes
1369407_at	tumor necrosis factor receptor superfamily, member 11b (osteoprotegerin)	2.4	Signal Transduction	Yes
1369660_at	defensin beta 1	3.4	Signal Transduction	No
1380577_at	Leucine rich repeat (in FLII) interacting protein 2	6.1	Signal Transduction	Yes
1369665_a_at	Interleukin 18	2.2	Signalling	Yes
1387744_at	Natriuretic peptide precursor type C	2.2	Signalling	Yes
1376445_at	interleukin 17B	2.8	Signalling	No
1369193_at	cyclin-dependent kinase inhibitor 2B (p15, inhibits CDK4)	-2.3	Cell Cycle Arrest	No
1392852_at	Cullin 3	-2.3	Cell Cycle Arrest	Yes
1390672_at	Reprimo-candidate mediator of the p53-dependent G2 arrest	2.9	Cell Cycle Arrest	Yes
1379582_a_at	cyclin A2	2.8	Cell Cycle	Yes
1369926_at	glutathione peroxidase 3	-3.6	Enzyme	Yes
1384392_at	cytochrome P450, family 26, subfamily b, polypeptide 1	-3.4	Enzyme	Yes
1371161_at	protein phosphatase 1, regulatory (inhibitor) subunit 3B	-2.6	Enzyme	No
1383394_at	Similar to tyrosinase-related protein-2	-2.1	Enzyme	Yes
1387052_at	Glutamic pyruvic transaminase 1, soluble	2.1	Enzyme	Yes
1372665_at	Phosphoserine aminotransferase 1	2.1	Enzyme	Yes
1386922_at	Carbonic anhydrase 2	2.2	Enzyme	Yes
1368789_at	Acid phosphatase, prostate	2.3	Enzyme	Yes
1383519_at	Hexokinase 2	2.3	Enzyme	Yes
1372523_at	Glutamate-cysteine ligase, catalytic subunit	2.3	Enzyme	Yes
1387239_a_at	Peptidyl arginine deiminase, type IV	2.3	Enzyme	No
1368527_at	prostaglandin-endoperoxide synthase 2	2.4	Enzyme	No
1387993_at	cytochrome P450, family 2, subfamily b, polypeptide 13	2.5	Enzyme	No

1387178_a_at	cystathionine beta synthase	2.5	Enzyme	Yes
1388176_at	camello-like 5	2.5	Enzyme	Yes
1392483_at	Choline phosphotransferase 1	2.5	Enzyme	Yes
1383303_at	SA rat hypertension-associated gene	5.8	Enzyme	Yes
1368511_at	basic helix-loop-helix domain containing, class B3	-4.3	Transcription	Yes
1387769_a_at	Inhibitor of DNA binding 3	-2.5	Transcription	Yes
1375059_at	Similar to zinc finger protein 652	-2.1	Transcription	Yes
1380558_at	Similar to Homeobox protein DLX-3	2.1	Transcription	Yes
1384907_at	similar to Dachshund homolog 1 (Dach1)	2.8	Transcription	Yes
1374391_at	Similar to Sarcolipin (LOC367086), mRNA	-3.4	Transporter	Yes
1381070_at	Synaptoporin	-2.5	Transporter	Yes
1372256_at	Cysteine-rich protein 1	-2.2	Transporter	Yes
1392785_at	Potassium channel tetramerisation domain containing 12	-2.2	Transporter	Yes
1373710_at	Solute Carrier family 38, member 4	-2.2	Transporter	Yes
1368661_at	Solute carrier family 13, member 2	2.1	Transporter	No
1386981_at	Solute carrier family 16, member 1	2.1	Transporter	Yes
1387092_at	FXYD domain-containing ion transport regulator 4	2.1	Transporter	Yes
1369020_at	Solute carrier family 5 (sodium iodide symporter), member 5	2.2	Transporter	Yes
1368469_at	aquaporin 5	2.8	Transporter	Yes
1389573_at	ChaC, cation transport regulator-like 1 (E. coli)	7.5	Transporter	Yes
1378258_at	Coiled coil domain containing 3	-2.8	Other	Yes
1376350_at	Similar to FMR2	-2	Other	Yes
1390850_at	Adipose differentiation related protein	2.4	Other	Yes
1368883_at	nephroblastoma overexpressed gene	2.6	Other	Yes
1387125_at	S100 calcium binding protein A9	2.7	Other	No
1383585_s_at	Sorting nexin 10	2.7	Other	Yes
1398253_at	kidney androgen regulated protein	3.5	Other	Yes